
DECLARATION

I declare that the work described in this thesis is entirely my own work except where specifically stated in the text. This work has not been previously submitted for any degree at any institution.

RECOMBINANT HUMAN TROPOELASTIN: PRODUCTION, PROPERTIES AND INTERACTIONS

Bernadette Vrhovski

A thesis submitted in fulfilment
of the requirements for the degree of
Doctor of Philosophy

Department of Biochemistry,
University of Sydney

October 1997

DECLARATION

I declare that the work described in this thesis is entirely my own work except where specifically stated in the text. This work has not been previously submitted for any degree at any institution.

[Redaction]

human tropoelastin (SHEL) gene was constructed and cloned to produce four different expression systems; pSHEL, pSHEL_{26A}, pSHEL_{modified} and pSHEL_{LC}. A second isoform gene, SHEL_{26A}, encoding SHEL without the 26A domain, was produced by mutagenesis of SHEL. A further product of mutagenesis was an aberrant form of SHEL, SHEL_{modified}. SHEL_{modified} was successfully expressed at a high level as a GST fusion protein from pSHEL_{LC} and as the unfused protein from pSHEL_{modified}. Expression conditions for each of these two systems were optimised to maximise overexpression. The purification of GST-SHEL was affected by several factors, including significant protease destruction, limiting its intact release from the fusion protein. The purification procedure developed for unfused SHEL, however, was a relatively simple and fast method consisting of the selective solubilisation of SHEL with butanol. Degradation products were effectively removed using reverse-phase high performance liquid chromatography. SHEL_{26A} was produced in the same way. Highly purified products were verified by a range of techniques, including N-terminal sequencing and mass spectrometry, and the final yield routinely obtained was at least 50mg from one litre of bacterial culture, a significant improvement over other recombinant systems.

The proteolytic susceptibility of SHEL and SHEL_{26A} to human serum and other specific proteases was examined. Two major regions of susceptibility to serum and other serine proteases were precisely mapped by N-terminal sequencing. Enzymes likely to be responsible for serum degradation were found to include plasma kallikrein in addition to another serine protease with trypsin-like specificity, present at a much lower level.

SUMMARY

Potential protease inhibitors were identified and a peptide corresponding to a protease-susceptible site in SHEL was designed and found to be able to inhibit proteolysis. The process of coacervation was demonstrated to provide substantial protection from proteolytic degradation, particularly by kallikrein and thrombin. To enable the long-term study of tropoelastin and elastic fibre structure, function and biosynthesis, a recombinant system was developed to provide a source of human tropoelastin. Using synthetic gene precursors, a synthetic human tropoelastin (*SHEL*) gene was constructed and cloned to produce four different expression systems; pSHEL_C, pSHEL_D, pSHEL_E and pSHEL_F. A second isoform gene, *SHEL*Δ26A, encoding SHEL without the 26A domain, was produced by mutagenesis of *SHEL*. A further product of mutagenesis was an aberrant form of *SHEL*, *SHEL*Δ*modified*. SHEL was successfully expressed at a high level as a GST fusion protein from pSHEL_C and as the unfused protein from pSHEL_F. Expression conditions for each of these two systems were optimised to maximise overexpression. The purification of GST-SHEL was affected by several factors, including significant protease destruction, limiting its intact release from the fusion protein. The purification procedure developed for unfused SHEL, however, was a relatively simple and fast method consisting of the selective solubilisation of SHEL with butanol. Degradation products were effectively removed using reverse-phase high performance liquid chromatography. *SHEL*Δ26A was produced in the same way. Highly purified products were verified by a range of techniques, including N-terminal sequencing and mass spectrometry, and the final yield routinely obtained was at least 50mg from one litre of bacterial culture, a significant improvement over other recombinant systems.

The proteolytic susceptibility of SHEL and *SHEL*Δ26A to human serum and other specific proteases was examined. Two major regions of susceptibility to serum and other serine proteases were precisely mapped by N-terminal sequencing. Enzymes likely to be responsible for serum degradation were found to include plasma kallikrein in addition to another serine protease with trypsin-like specificity, present at a much lower level.

Potential protease inhibitors were evaluated and a peptide corresponding to a protease-susceptible site in SHEL was designed and found to be able to inhibit proteolysis. The process of coacervation was demonstrated to provide substantial protection from proteolytic degradation, particularly by kallikrein and thrombin.

Coacervation characteristics of SHEL and SHEL Δ 26A were assessed and found to be highly dependent on protein concentration, NaCl concentration and pH. The coacervation temperature of tropoelastin was, however, demonstrated to be dramatically altered by contaminating lipids and fatty acids. There was no detectable difference in the coacervation characteristics of SHEL and SHEL Δ 26A, and the aberrant SHEL Δ modified also displayed similar coacervation characteristics. Coacervation of each isoform at >10mg/ml was found to be finely tuned to occur at 37°C at 150mM NaCl concentration and pH 7-8, conditions which are found in the extracellular matrix.

Finally, I would like to thank my family for their love and support over the years and Peter Rose for his encouragement, love and for constantly reminding me of what's really important.

I gratefully acknowledge the receipt of an Australian Postgraduate Award for this project.

ACKNOWLEDGEMENTS

I would like to thank my supervisor, Dr Tony Weiss, for all his advice, encouragement and support over the last few years. His positive attitude helped me through the difficult times and provided me with added enthusiasm during the good. Many thanks to members of the Weiss laboratory, past and present, for all their advice and technical expertise, especially Suzanne Mithieux. In particular, a very big thank you to Steve Martin whose expert skill and tutelage provided me with an excellent foundation for my work.

I wish to thank Michael Swanton and Claire Brown at SUPAMAC for going out of their way to help me with HPLC experiments and Zia Ahmad for performing fatty acid analyses. Thank you to Steve Martin, Sharron Bannan and Lisa Riley for proofreading various sections of this thesis.

I would like to thank all the members of the lab over the years who have made the lab such a friendly, easy-going place to work, and especially Lisa Riley for her friendship.

Finally, I would like to thank my family for their love and support over the years and Peter Kerr for his encouragement, love and for constantly reminding me of what's really important.

I gratefully acknowledge the receipt of an Australian Postgraduate Award for this project.

ABBREVIATIONS

A ₆₀₀	absorbance at 600nm
APS	ammonium persulfate
BSA	bovine serum albumin
bp	base pairs
CD	circular dichroism
CIP	calf-intestinal alkaline phosphatase
CNBr	cyanogen bromide
EBP	elastin binding protein
EDTA	ethylene diamine tetra-acetic acid
GST	glutathione S-transferase
HLE	human leukocyte elastase
IPTG	isopropyl- β -D-thiogalactoside
kb	kilobases
kDa	kilodaltons
LB	Luria-Bertani media
LMT	low melting temperature
MAGP	microfibril-associated glycoprotein
MQW	Milli-Q water
NMR	nuclear magnetic resonance
PBS	phosphate buffered saline
pBS II SK ⁺	pBluescript II SK ⁺
pSHELA	<i>SHEL</i> cloned into pBS II SK ⁺ in the forward orientation
pSHELB	<i>SHEL</i> cloned into pBS II SK ⁺ in the reverse orientation
pSHEL C	<i>SHEL</i> cloned into pGEX-2T
pSHELD	<i>SHEL</i> cloned into pTrc99A
pSHELE	<i>SHEL</i> cloned into pND211
pSHELF	<i>SHEL</i> cloned into pET-3d
pSHEL Δ 26A	<i>SHEL</i> Δ 26A cloned into pET-3d
pSHEL Δ mod	<i>SHEL</i> Δ mod cloned into pET-3d
PVDF	polyvinylidene difluoride
RER	rough endoplasmic reticulum
RP-HPLC	reverse phase-high performance liquid chromatography
SDS	sodium dodecyl sulfate

SDS-PAGE	sodium dodecyl sulfate-polyacrylamide gel electrophoresis
S-GAL	peptide representing elastin binding domain of EBP
SHEL	synthetic human tropoelastin
SHEL	SHEL DNA sequence
SHELΔ26A	SHEL minus domain 26A
SHELΔ26A	SHELΔ26A DNA sequence
SHELΔmod	SHELΔ26A modified
SHELΔmod	SHELΔmod DNA sequence
SPS-peptide	serine protease site peptide
SVAS	supravalvular aortic stenosis
SUPAMAC	Sydney University and Prince Alfred Hospital Macromolecular Analysis Centre
TAE	Tris-acetate-EDTA
TB	terrific broth
TBE	Tris-borate-EDTA
TE	Tris-EDTA
TEMED	N, N, N', N'-tetramethylethylene diamine
TFA	trifluoroacetic acid
TTE	Tris-aurine-EDTA
X-Gal	β-D-galactopyranoside

PUBLICATIONS AND PRESENTATIONS

Declaration

Some parts of this thesis have been published:

Acknowledgements

Vrhovski, B., Jensen, S. and Weiss, A.S. (1997) Coacervation characteristics of recombinant human tropoelastin *Eur. J. Biochem.* (in press)

Chapter 1 General Introduction

Martin, S.L., Vrhovski, B. and Weiss, A.S. (1995) Total synthesis and expression in *Escherichia coli* of a gene encoding human tropoelastin *Gene* **154**: 159-166

1.1.2 Evolution and Phylogenetic Distribution

1.1.3 Diseases Affecting Elastic Fibres

1.1.4 Tropoelastin

Some parts of this thesis have been presented at conferences:

Weiss, A.S. and Vrhovski, B. (1997) Association behaviour of recombinant human tropoelastin. 21st Ann. Conference Matrix Biol. Soc. Aust. N Z.

Vrhovski, B. and Weiss, A.S. (1997) The coacervation characteristics of an isoform of human tropoelastin. Gordon Conference on Elastin and Elastic Tissue, New Hampshire, USA.

Vrhovski, B. and Weiss, A.S. (1996) Association behaviour of overexpressed recombinant human tropoelastin. 3rd Pan Pacific Connect. Tissue Soc. Sym, Hawaii, USA.

Vrhovski, B., and Weiss, A.S. (1995) Expression and coacervation properties of recombinant human tropoelastin, Gordon Conference on Elastin and Elastic Fibers, New Hampshire, USA.

Vrhovski, B. and Weiss, A.S. (1995) Recombinant human tropoelastin displays reversible temperature dependent coacervation effects (abstract) *Proc. Aust. Soc. Biochem. Mol. Biol.* **27**: Pos-1-163. 7th Fed. Asian Oceanian Biochem. Mol. Biol. Congress, Sydney, Aust.

Vrhovski, B. and Weiss, A.S. (1994) Recombinant human tropoelastin: molecular characteristics and coacervation (abstract) *Proc. Aust. Soc. Biochem. Mol. Biol.* **26**: Pos-2-31. 38th Ann. Conference, Gold Coast, Aust.

Martin, S.L., Vrhovski, B. and Weiss, A.S. (1994) Total design, synthesis and expression in *Escherichia coli* of a large gene encoding human tropoelastin (abstract) *Proc. Aust. Soc. Biochem. Mol. Biol.* **26**: Col-5-1. 38th Ann. Conference, Gold Coast, Aust.

1.6 Aims of This Work

Martin, S.L., Vrhovski, B. and Weiss, A.S. (1994) Total design, synthesis and expression in *Escherichia coli* of a gene for human tropoelastin. Miami Bio/Tech. Eur. Sym, Advances in Gene Technology: Molecular Biology and Human Genetic Disease, Monaco.

CONTENTS

2.2 Bacterial Strains and Growth	41
2.3 Microscopy	42
Declaration	41
Summary	ii
Acknowledgements	iv
Abbreviations	v
Publications and Presentations	vii
Chapter 1 General Introduction	1
1.1 Elastic Fibres	1
1.1.1 Composition and Distribution	1
1.1.2 Evolution and Phylogenetic Distribution	2
1.1.3 Diseases Affecting Elastic Fibres	3
1.1.4 Tropoelastin	5
1.2 Biosynthesis of Elastic Fibres	7
1.2.1 The Elastin Gene	7
1.2.1.1 Structure	7
1.2.1.2 Control of Expression	10
1.2.2 Alternative Splicing of the Elastin Gene	11
1.2.3 Isoforms of Tropoelastin	12
1.2.4 Secretion and Post-Translational Modification	13
1.2.5 The Role of Microfibrils	15
1.2.6 The Role of the Elastin Binding Protein	17
1.2.7 The Role of Coacervation	19
1.2.8 Cross-Linking	21
1.3 Degradation and Repair	24
1.3.1 Elastases and Elastolysis	24
1.3.2 Repair of Damaged Fibres	25
1.3.3 Proteolysis of Tropoelastin	25
1.4 Mechanism of Elasticity	27
1.4.1 Introduction	27
1.4.2 Random Chain Model	28
1.4.3 Preferred-Conformation Models	30
1.4.3.1 'Liquid Drop' Model	31
1.4.3.2 'Oiled Coil' Model	32
1.4.3.3 Fibrillar Model	32
1.4.4 Microscopic Evidence of Structure	34
1.4.5 Structural Studies on Soluble Elastins	35
1.5 Sources of Tropoelastin	37
1.5.1 Tissue Extracts	37
1.5.2 Recombinant Tropoelastins	38
1.6 Aims of This Work	39
3.4 Discussion	79
Chapter 2 General Materials and Methods	41
2.1 Chemicals	41

2.2 Bacterial Strains and Growth Media.....	41
2.3 Microscopy.....	42
2.4 Transformation.....	42
2.5 Cesium Chloride Plasmid Preparation.....	43
2.6 Quantitation of DNA.....	43
2.7 Sodium Dodecyl Sulfate-Polyacrylamide Gel Electrophoresis (SDS-PAGE).....	44
2.8 SDS-PAGE and Blotting for N-terminal Sequencing.....	45
2.9 N-terminal Sequencing.....	45
2.10 Scanning Densitometry.....	46
Chapter 3 Construction and Cloning of Synthetic Genes Encoding Two Isoforms of Tropoelastin: SHEL and SHELΔ26A.....	47
3.1 Introduction.....	47
3.2 Materials and Methods.....	50
3.2.1 Plasmids.....	50
3.2.2 Agarose Gel Electrophoresis.....	52
3.2.3 Restriction Enzymes.....	52
3.2.4 Purification of DNA Fragments.....	53
3.2.5 Alkaline Phosphatase Treatment of DNA.....	53
3.2.6 Plasmid Mini-Preparations.....	54
3.2.7 DNA Sequencing -Manual.....	54
3.2.8 DNA Sequencing -Automated.....	55
3.2.9 Construction of Full-Length <i>SHEL</i>	55
3.2.10 Construction of pSHEL C.....	56
3.2.11 Construction of pSHEL D.....	57
3.2.12 Construction of pSHEL E.....	57
3.2.13 Construction of pSHEL F.....	58
3.2.14 Construction of pSHEL Δ 26A.....	58
3.2.14.1 Mutagenesis.....	58
3.2.14.2 Restriction Enzyme Digestion and Ligation.....	60
3.3 Results.....	62
3.3.1 Construction of pSHEL A and pSHEL B.....	62
3.3.2 Construction of pSHEL C.....	64
3.3.3 Construction of pSHEL D.....	69
3.3.4 Construction of pSHEL E.....	71
3.3.5 Construction of pSHEL F.....	73
3.3.6 Constuction of pSHEL F Δ 26A.....	73
3.3.6.1 Mutagenesis and Creation of pSHEL F Δ modified.....	73
3.3.6.2 Restriction Enzyme Modification of pSHEL F and and pSHEL F Δ mod.....	77
3.4 Discussion.....	79
3.4.1 Construction of <i>SHEL</i>	79
3.4.2 Cloning of <i>SHEL</i> into Expression Vectors.....	80

3.4.3 Construction of SHEL Δ 26A Isoform.....	82
3.5 Conclusion.....	84
Chapter 4 Optimisation of Expression of GST-SHEL and SHEL Isoforms.....	85
4.1 Introduction.....	85
4.2 Materials and Methods.....	87
4.2.1 <i>E. coli</i> Strains.....	87
4.2.2 Bacterial Growth Media.....	87
4.2.3 Small-Scale Expression.....	87
4.2.4 Plasmid Stability Test.....	88
4.3 Results.....	89
4.3.1 Optimisation of pSHEL Δ C Expression.....	89
4.3.2 Expression of pSHEL Δ D.....	92
4.3.3 Expression of pSHEL Δ E.....	92
4.3.4 Optimisation of pSHEL Δ F Expression.....	95
4.3.5 Expression of pSHEL Δ F Δ mod and pSHEL Δ F Δ 26A.....	101
4.4 Discussion.....	103
4.4.1 Growth Curves.....	103
4.4.2 Expression of GST-SHEL.....	103
4.4.3 Expression of pSHEL Δ D and pSHEL Δ E.....	104
4.4.4 Expression of pSHEL Δ F, pSHEL Δ F Δ 26A and pSHEL Δ F Δ mod.....	104
4.5 Conclusion.....	107
Chapter 5 Purification of GST-SHEL and SHEL Isoforms.....	108
5.1 Introduction.....	108
5.2 Materials and Methods.....	110
5.2.1 Materials.....	110
5.2.2 Lysis of pSHEL Δ C Cultures.....	110
5.2.3 Glutathione Agarose Binding.....	110
5.2.4 Thrombin Cleavage.....	111
5.2.5 Lysis of pSHEL Δ F Cultures.....	112
5.2.6 Alcohol Solubilisation.....	112
5.2.7 RP-HPLC.....	113
5.2.8 Purification of SHEL Δ 26A and SHEL Δ mod.....	113
5.2.9 Spectrophotometric Determination of Yield.....	114
5.2.10 Mass Spectrometry.....	114
5.2.11 Endotoxin Determination.....	114
5.2.12 Circular Dichroism (CD).....	115
5.3 Results.....	115
5.3.1 Purification of GST-SHEL.....	115
5.3.1.1 Cell Lysis.....	115
5.3.1.2 Glutathione Agarose Binding.....	117
5.3.1.3 Thrombin Cleavage.....	117
5.3.2 Purification of SHEL.....	120

5.3.2.1	Cell Lysis.....	120
5.3.2.2	Alcohol Solubilisation.....	120
5.3.2.3	RP-HPLC Purification.....	124
5.3.3	Purification of SHEL Δ 26A.....	125
5.3.4	Purification of SHEL Δ mod.....	128
5.3.5	Source of Degradation Activity.....	128
5.3.6	Characterisation of Purified Proteins.....	131
5.3.6.1	N-terminal Protein Sequencing.....	131
5.3.6.2	Mass Spectrometry.....	131
5.3.6.3	Endotoxin Levels.....	132
5.3.6.4	Circular Dichroism.....	133
5.4	Discussion.....	135
5.4.1	GST-SHEL Purification.....	135
5.4.2	Purification of SHEL.....	137
5.4.3	Confirmation of Proteins.....	139
5.4.4	Circular Dichroism.....	140
5.5	Conclusion.....	141
Chapter 6 Proteolytic Susceptibility of Tropoelastin Isoforms To Human Serum and Individual Proteases.....		142
6.1	Introduction.....	142
6.2	Materials and Methods.....	144
6.2.1	Reagents.....	144
6.2.2	Serum Proteolysis of SHEL.....	144
6.2.3	Proteolytic Assays.....	145
6.2.4	N-terminal Sequencing.....	145
6.2.5	Peptide Preparation and Use.....	145
6.2.6	Proteolysis During Coacervation.....	146
6.3	Results.....	147
6.3.1	Degradation of SHEL by Serum.....	147
6.3.2	Effect of Protease Inhibitors on Serum Degradation.....	147
6.3.3	Degradation of SHEL with Specific Proteases.....	150
6.3.3.1	Human Thrombin.....	150
6.3.3.2	Human Plasma Kallikrein.....	152
6.3.3.3	Bovine Trypsin.....	152
6.3.3.4	Human Plasmin.....	155
6.3.3.5	Human Leukocyte Elastase (HLE).....	155
6.3.4	Mapping of Protease-Susceptible Sites.....	155
6.3.5	Effect of S-GAL and SPS-Peptide on Degradation.....	161
6.3.6	Effect of Coacervation on Degradation of SHEL.....	163
6.4	Discussion.....	165
6.4.1	Inhibitor Study of Serum Degradation of SHEL.....	165
6.4.2	Identification of Serum Proteolysis.....	166
6.4.3	Mapping of Protease Sensitive Sites.....	169

6.4.4 Protection from Degradation.....	170
6.4.5 Proteolysis of Coacervated Tropoelastin.....	173
6.4.6 Possible Consequences of Serum Degradation of Tropoelastin.....	174
6.5 Conclusion.....	176
Chapter 7 Factors Influencing The Coacervation Characteristics of Human	182
7.1 Tropoelastin Isoforms	177
7.1 Introduction.....	177
7.2 Materials and Methods.....	179
7.2.1 Coacervation.....	179
7.2.2 S-GAL Preparation and Use.....	180
7.2.3 Preparation of Lipid and Use in Coacervation.....	181
7.3 Results.....	182
7.3.1 Effect of Tropoelastin Concentration on Coacervation of SHEL....	182
7.3.2 Effect of NaCl Concentration on Coacervation of SHEL.....	185
7.3.3 Effect of pH on Coacervation of SHEL.....	185
7.3.4 Comparison of Effects.....	188
7.3.5 Coacervation of SHEL Δ 26A.....	190
7.3.6 Coacervation of SHEL Δ mod.....	190
7.3.7 Effect of S-GAL.....	194
7.3.8 Effect of Lipid Impurities.....	194
7.4 Discussion.....	200
7.4.1 Coacervation.....	200
7.4.2 Parameters Affecting SHEL Coacervation.....	200
7.4.3 Comparison of Coacervation of SHEL, SHEL Δ 26A and SHEL Δ mod.....	203
7.4.4 Effect of S-GAL on Coacervation.....	204
7.4.5 A Model for Tropoelastin Assembly <i>In Vivo</i>	206
7.4.6 Effect of Lipids on Coacervation.....	208
7.5 Conclusion.....	211
Chapter 8 General Discussion	212
8.1 Recombinant Tropoelastin Production.....	212
8.2 Proteolytic Susceptibility.....	214
8.3 Coacervation.....	216
8.4 Conclusion.....	218
References	219
Appendices	243
1 Sequencing Primers.....	243
2 DNA Sequence and Protein Translation of SHEL Δ mod.....	244
3 DNA Sequence and Protein Translation of SHEL Δ 26A.....	246
4 Overview of the purification protocol for SHEL.....	121
5 Stages of purification of SHEL.....	122

List of Tables	123
1.1 Diseases of the Elastic Fibre.....	4
1.2 Amino Acid Sequence of Selected Human Tropoelastin Domains.....	7
4.1 Effect of Different Additives on BL21(DE3)[pSHELF] Colony Formation.....	95
5.1 N-terminal Sequences.....	131
5.2 Mass Spectrometry Measurements.....	132
5.3 Endotoxin Levels in Selected Preparations of SHEL.....	133
6.1 N-terminal Sequences of Protease-Produced Tropoelastin Peptides.....	158
7.1 Fatty Acid Analysis of Lipid Isolated From Recombinant Tropoelastin.....	151
6.4 Preparations.....	197
6.5 Effect of bovine trypsin on SHEL and SHELΔ26A.....	154
6.6 Effect of plasmin on SHEL and SHELΔ26A.....	156
List of Figures	157

1.1 Structure of the human tropoelastin cDNA.....	9
1.2 Model of the elastin binding (EBP) complex.....	18
1.3 Structure and route of formation of elastin cross-links.....	22
1.4 Proposed elastin structural models.....	29
3.1 Assembly and cloning of the SHEL gene.....	49
3.2 Main features of expression plasmids.....	51
3.3 Construction scheme for pSHELFΔ26A.....	61
3.4 Screening and restriction mapping of pSHELA and pSHELB.....	63
3.5 Release of individual blocks from pSHELB.....	65
3.6 The nucleotide and encoded protein sequence of the synthetic gene (SHEL) for human tropoelastin.....	66
3.7 Screening and restriction mapping of pSHEL C.....	68
3.8 Screening and restriction mapping of pSHELD.....	70
3.9 Screening and restriction mapping of pSHELE.....	72
3.10 Screening and restriction mapping of pSHELF.....	74
3.11 Comparison of SHEL and SHELδmod protein sequence.....	76
3.12 Screening for pSHELFΔ26A.....	78
4.1 Growth curves for pSHEL C in XL1-Blue.....	90
4.2 pSHEL C expression in various <i>E. coli</i> strains.....	91
4.3 Growth curves for pSHELD in various <i>E. coli</i> strains.....	93
4.4 Expression of pSHELE in DH5α.....	94
4.5 Expression of pSHELF in various media.....	96
4.6 Effect of IPTG concentration on pSHELF expression.....	98
4.7 Time course of pSHELF expression in 2TY.....	99
4.8 Constitutive expression of pSHELF in BL21(DE3).....	100
4.9 Comparative expression of SHEL, SHELΔ26A and SHELΔmod.....	102
5.1 Lysis of DH5α expressing GST-SHEL.....	116
5.2 Binding of GST-SHEL to glutathione agarose.....	118
5.3 Thrombin cleavage of soluble cell lysate containing GST-SHEL.....	119
5.4 Overview of the purification protocol for SHEL.....	121
5.5 Stages of purification of SHEL.....	122

5.6 Purified SHEL after removal of alcohol.....	123
5.7 RP-HPLC purification of SHEL.....	126
5.8 Stages in the purification of SHEL Δ 26A.....	127
5.9 Stages in the purification of SHEL Δ mod.....	129
5.10 Degradation of SHEL, SHEL Δ 26A and SHEL Δ mod by <i>E. coli</i> lysate.....	130
5.11 Circular dichroism spectrum of SHEL.....	134
6.1 Degradation of SHEL with serum.....	148
6.2 Effect of protease inhibitors on serum degradation of SHEL.....	149
6.3 Effect of thrombin on SHEL and SHEL Δ 26A.....	151
6.4 Effect of kallikrein on SHEL and SHEL Δ 26A.....	153
6.5 Effect of bovine trypsin on SHEL and SHEL Δ 26A.....	154
6.6 Effect of plasmin on SHEL and SHEL Δ 26A.....	156
6.7 Effect of HLE on SHEL and SHEL Δ 26A.....	157
6.8 Schematic diagram showing the relative positions of protease sites identified by N-terminal sequencing for serum, kallikrein and thrombin...	159
6.9 Typical effect of S-GAL and the SPS-peptide on degradation of SHEL.....	162
6.10 Effect of coacervation on the degradation of SHEL by proteases.....	164
7.1 Coacervation of 40mg/ml SHEL.....	183
7.2 Effect of SHEL concentration on coacervation.....	184
7.3 Effects of salts on coacervation of SHEL.....	186
7.4 Effect of pH on coacervation of SHEL.....	187
7.5 Comparison of different parameters on coacervation of SHEL.....	189
7.6 Comparison of different parameters on coacervation of SHEL Δ 26A.....	191
7.7 Comparison of the concentration dependence of SHEL and SHEL Δ 26A on coacervation temperature.....	192
7.8 Comparison of different parameters on coacervation of SHEL Δ mod.....	193
7.9 Effect of S-GAL on coacervation of SHEL.....	195
7.10 Effect of impurities on coacervation.....	196
7.11 Effect of lipid addition on coacervation of SHEL Δ 26A.....	199
7.12 Proposed model for tropoelastin assembly.....	207

CHAPTER 1

GENERAL INTRODUCTION

1.1 ELASTIC FIBRES

1.1.1 Composition and Distribution

Elastic fibres are found in the extracellular matrix of connective tissue, providing elasticity and resilience to tissues which require the ability to deform repetitively and reversibly. Fibres are organised into three distinct morphologies: small and rope-like in lung, skin and ligament; thin concentric sheets in aorta and in a large three dimensional honeycomb structure in elastic cartilage (Prosser and Mecham, 1988). Ultrastructurally, elastic fibres are complex structures composed of two major components (Ross and Bornstein, 1969): an amorphous component, consisting of the extensively cross-linked protein elastin which makes up the bulk (90%) of the fibre; and a fibrillar component, the microfibrils, which are rich in acidic glycoproteins and are organized into 8-16nm fibrils of beaded appearance (Cleary, 1987). Microfibrils themselves are made up of at least five distinct proteins (Gibson *et al.*, 1989) including two forms of the 350kDa glycoprotein fibrillin (Zhang *et al.*, 1994; Sakai *et al.*, 1986) and two distinct but related microfibril associated glycoproteins, MAGP-1 (Gibson *et al.*, 1991) and MAGP-2 (Gibson *et al.*, 1996). Other components are also thought to be present in the elastic fibre including lysyl oxidase, the enzyme which initiates elastin cross-linking (Kagan *et al.*, 1986), and the elastin binding protein (EBP) or receptor (Mecham and Heuser, 1991).

Elastin is an extremely insoluble protein due to the extensive cross-linking at Lys residues. It is also the most hydrophobic protein known. Although there is some species variation (see below), elastin from higher vertebrates including humans contains over 30% Gly and approximately 75% of the entire sequence is made up of just four hydrophobic amino acids (Gly, Val, Ala, Pro). Tissues rich in elastin include aorta and major vascular vessels (28-32% dry weight), lung (3-7%) elastic ligaments (50%), tendon (4%) and

skin (2-3%) (Uitto, 1979). However, however, are much more highly conserved (Boyd *et al.*, 1991).

1.1.2 Evolution and Phylogenetic Distribution

1.1.3 Diseases Affecting Elastic Fibres

Elastin is found in all vertebrates studied except the primitive cyclosoemes but has not been identified in any invertebrates (Sage and Gray, 1979). The morphology of fibres is different amongst the various phyla and individual species studied. Fibres are most dense in mammalian aorta while in lower vertebrates they tend to be in a more open, loose arrangement (Sage and Gray, 1980). There is a clear difference in amino acid composition in different species with elastin from higher vertebrates being distinctly more hydrophobic. The most hydrophilic elastin is found in teleost fish where Ala and Val are less abundant and hydrophilic amino acids Asp, Asn, Glu, Gln, Ser, His and Met are increased compared with higher vertebrate elastin which has little or none of these (Sage and Gray, 1979). Phylogenetic analysis suggests that the first appearance of elastin coincided with the formation of a closed circulatory system and is an adaptive response to the high pressure and pulsatile blood flow inside arteries (Sage and Gray, 1977). The demonstration that the production of heat as resistance to stretching is directly related to elastin hydrophobicity is consistent with this proposal (Sage, 1982). There is some speculation given the similarity between collagen and elastin hydrophobic domains, particularly in terms of Gly content, that elastin may have a distant evolutionary relationship with collagen (Rosenbloom, 1984).

Mammalian tropoelastin, the soluble precursor to elastin (Section 1.1.4) is a moderately conserved protein with a unit evolutionary period of 5.8 million years (Boyd *et al.*, 1991). A large amount of divergence is tolerated in the hydrophobic domains if the overall hydrophobicity is maintained.

The cross-linking domains, however, are much more highly conserved (Boyd *et al.*, 1991).

1.1.3 Diseases Affecting Elastic Fibres

Various acquired and inherited diseases are known to affect the structure, distribution and abundance of elastic fibres (Table 1.1). The organs most obviously affected are those rich in elastin (Section 1.1.1). Due to the complexity of the elastic fibre and the interplay of an ensemble of molecules in fibre formation and structure, most of these diseases do not involve elastin as the primary defect yet severely affect the elastic fibre integrity.

Only supravalvular aortic stenosis (SVAS) and Williams syndrome have been directly linked with alterations in the elastin gene. Three types of mutations have been identified in SVAS. One is a large 30kb deletion within the gene involving exons 2-27 (Olson *et al.*, 1995). Another involves a deletion of the 3'-end of the gene resulting in a truncated protein missing the C-terminus from exon 28 onward (Ewart *et al.*, 1994; Curran *et al.*, 1993). A third type involves various point mutations, most of which result in the loss of the conserved C-terminus either through the introduction of early stop codons or through frameshifts (Li *et al.*, 1997). Williams syndrome is a contiguous gene disorder which results from a large (e.g. 114kb) deletion involving an entire elastin allele (Lowery *et al.*, 1995; Ewart *et al.*, 1993) in conjunction with other adjacent genes, including LIM-kinase, probably responsible for the neurological defects (Tassabehji *et al.*, 1996).

Disease

supravalvular aortic
stenosis
(SVAS)

Williams syndrome

Bicuspid aortic valve
syndrome

pericardial effusion

cutis laxa (inherited)

Marfan syndrome

Menkes syndrome

emphysema

atherosclerosis

* Compiled from

Table 1.1: Diseases of the Elastic Fibre

Disease	Features*	Aetiology
supravalvular aortic stenosis (SVAS)	narrowing of arteries, reduced elastin content, architecture of aorta disrupted	mutations in elastin gene (Li <i>et al.</i> , 1997; Olson <i>et al.</i> , 1995; Ewart <i>et al.</i> , 1994)
Williams syndrome	SVAS, mental retardation, premature ageing of skin, lax joints	deletion of elastin gene allele and adjacent loci (Lowery <i>et al.</i> , 1995)
Buschke-Ollendorff syndrome	increased thick elastic fibres, decrease in microfibrils, skin lesions, bone dysplasia	unknown but genetic (Giro <i>et al.</i> , 1992)
pseudoxanthoma elasticum	inelastic skin, cardiovascular defects, fragmentation, clumping and calcification of elastic fibres, increase in glycosaminoglycans	unknown, elastin gene defect excluded (Raybould <i>et al.</i> , 1994)
cutis laxa (inherited)	X-linked and autosomally inherited forms, loose sagging skin, increased elastic fibre fragmentation, decreased lysyl oxidase activity	uncertain, tropoelastin mRNA stability (Zhang <i>et al.</i> , 1995) or copper transport defect proposed (Levinson <i>et al.</i> , 1993)
Marfan syndrome	widespread skeletal, ocular and cardiovascular defects, loose skin, increased fragmentation of elastin	mutations in fibrillin gene (Dietz and Pyeritz, 1995)
Menkes syndrome	X-linked, brittle hair, tortuous blood vessels, elastic fibre fragmentation, neurological defects	defect in copper-transport ATPase Mc-1 gene (Vulpe <i>et al.</i> , 1993)
emphysema	increased compliance of lung, loss of elastin in lung	unbalanced protease/antiprotease activity suspected (Pierce <i>et al.</i> , 1995)
atherosclerosis	fragmentation of elastin in arteries, increased stiffness of arteries, increased lipid and calcium accumulation in elastin fibres	not certain, complex (Sandberg <i>et al.</i> , 1981)

* Compiled from Uitto and Ryhänen, 1987; Sandberg *et al.*, 1981; Uitto *et al.*, 1991; Christiano and Uitto, 1994.

Abnormal accumulation of elastin fibres is seen in pseudoxanthoma elasticum and Buschke-Ollendorff syndrome, while an increase in fragmentation and loss of fibres is observed in cutis laxa, Marfan syndrome and Menkes disease (Uitto and Ryhänen, 1987). Acquired diseases include emphysema where an increased degradation of elastic fibres is seen in the lung, and atherosclerosis where a loss of elasticity in major blood vessels is accompanied by calcium and lipid deposition (Sandberg *et al.*, 1981). Some of these diseases have been linked to errors in copper metabolism, and hence lysyl oxidase (Section 1.2.8), or microfibrillar proteins (Table 1.1). Thus, an alteration in one of many key molecules involved in elastic fibre synthesis can result in severe damage to the entire fibre and organ system affected. A more complete understanding of elastic fibre biosynthesis and function is important to help shed light on these diseases and lead to possible therapies.

1.1.4 Tropoelastin

Due to the insolubility of elastin, research into the process of elastic fibre formation was hampered until the discovery of the soluble precursor, tropoelastin. Tropoelastin was first isolated from copper-deficient animals and even today a major source of tropoelastin is tissues from animals such as piglets and chicks raised on copper-deficient diets or treated with lathyrogens (Rich and Foster, 1984; Rich and Foster, 1982; Rucker, 1982; Sandberg and Wolt, 1982) both of which reduce the activity of lysyl oxidase thus inhibiting the cross-linking reaction (Section 1.2.8).

The amino acid sequence of tropoelastins from various sources have been determined using molecular biological techniques to isolate and sequence elastin genes. Human (Indik *et al.*, 1987a, b), chick (Bressan *et al.*, 1987),

bovine (Yeh *et al.*, 1989; Raju and Anwar, 1987) and rat (Pierce *et al.*, 1990) tropoelastin genes have all been sequenced and the amino acid sequence determined. All of these tropoelastins were found to have a significant homology at both DNA and amino acid level. Previously, large segments of the porcine tropoelastin sequence were determined using tryptic peptides (Sandberg and Davidson, 1984). Two major types of domains are found in tropoelastin: (1) hydrophobic domains rich in polar amino acids especially Gly, Val, Pro and Ala, and often occurring in repeats of three to six peptides such as GVGVP, GGVP and GVGVP; (2) hydrophilic domains typically rich in Lys and Ala involved in cross-linking. These domains often consist of stretches of Lys separated by two or three Ala residues such as AAKAAKAA. Other hydrophilic domains do not contain the polyAla tract but ~~instead~~ have Lys near a Pro instead (Indik *et al.*, 1989, 1987b). For the most part these hydrophobic and hydrophilic domains alternate. The amino acid sequence of a typical hydrophobic and cross-linking domain are shown in Table 1.2.

Table 1.2 Amino Acid Sequence of Selected Human Tropoelastin Domains

Domain	Sequence
Hydrophobic Domain (Exon 24)	GLVPGVGVAPGVGVAPGVGVAPGVGLAPGVGVAPGVG VAPGVGVAPGIGPPGVA
Cross-link Domain (Exon 19)	GVVSPEAAAKAAAKAAY
26A	GADEGVRRSLSPELREGGDPSSSQHLPSTPSSPR
C-Terminus	GGACLGKACGRKRK

Evidence suggests that only a single elastin gene is present in the mammalian genome. The C-terminus of tropoelastin is highly basic and is very strongly conserved (>70%) among all species. It contains the only two Cys residues in the

protein and terminates with a positively charged RKRK sequence (Table 1.2) both of which are strictly conserved. Tropoelastin is secreted with a 26 amino acid signal peptide as an approximately 72kDa protein in the human (Indik *et al.*, 1987b), although there is some variation due to different tropoelastin isoforms (Section 1.2.2). In addition, human tropoelastin contains an unusual highly hydrophilic domain, exon 26A, that does not fall into any other category and whose function is unknown (Table 1.2). Exon 26A is enriched for Ser residues (8 out of a total of 14 in tropoelastin) and contains numerous charged residues (Glu, Asp, Arg) and the only His in tropoelastin (Indik *et al.*, 1987a). This domain has not been identified in any other species and very little is known about its role. There is some evidence that the absence of 26A will result in a tropoelastin isoform that is a less efficient substrate for lysyl oxidase and that this is not solely due to the hydrophilicity of 26A (Bedell-Hogan *et al.*, 1993). It has been speculated that this domain may function in antibody or sugar binding since it has a high surface probability and antigenicity index (Debelle *et al.*, 1992). Others have suggested that its presence may be increased in aged or diseased elastic fibres and may be a marker of damage (Indik *et al.*, 1989). The effect of this domain on tropoelastin and elastin physical properties is not known.

1.2 BIOSYNTHESIS OF ELASTIC FIBRES

1.2.1 The Elastin Gene

1.2.1.1 Structure

Evidence suggests that only a single elastin gene is present in the mammalian genome (Olliver *et al.*, 1987). The human gene has been localised to chromosome 7q11.1-21.1 (Fazio *et al.*, 1991), spanning 45kb (Bashir *et*

al., 1989). The human gene has 34 exons compared with 36 in the bovine (Bashir *et al.*, 1989; Yeh *et al.*, 1989) with an intron:exon ratio of 20:1, indicating that relatively small exons are interspersed within large introns (Bashir *et al.*, 1989; Cicila *et al.*, 1985). *Alu* repeats are found in the human elastin gene at a frequency four times higher than elsewhere in the genome (Indik *et al.*, 1987b) raising the possibility of instability in this gene in the general population (Rosenbloom *et al.*, 1993) and possibly contributing to diseases such as SVAS (Olson *et al.*, 1995).

Analysis of the structure of the gene in various species shows that hydrophobic and cross-linking domains of tropoelastin are encoded by separate exons that alternate (Fig. 1.1), reflecting the protein structure (Pierce *et al.*, 1990; Bashir *et al.*, 1989; Indik *et al.*, 1987a; Cicila *et al.*, 1985). Some variation exists in the presence of exon homologues amongst species. For example, bovine exons 34 and 35 are absent from the human gene (Bashir *et al.*, 1989) while the human gene has the introduction of an unusual hydrophilic-encoding exon 26A, not described in any other species (Bashir *et al.*, 1989; Indik *et al.*, 1987a). Exon 36, is extremely highly conserved amongst species and codes for the basic C-terminus as well as a large 3'-untranslated region (Indik *et al.*, 1987b) suggesting the possibility of regulatory elements in this region (Parks and Deak, 1990).

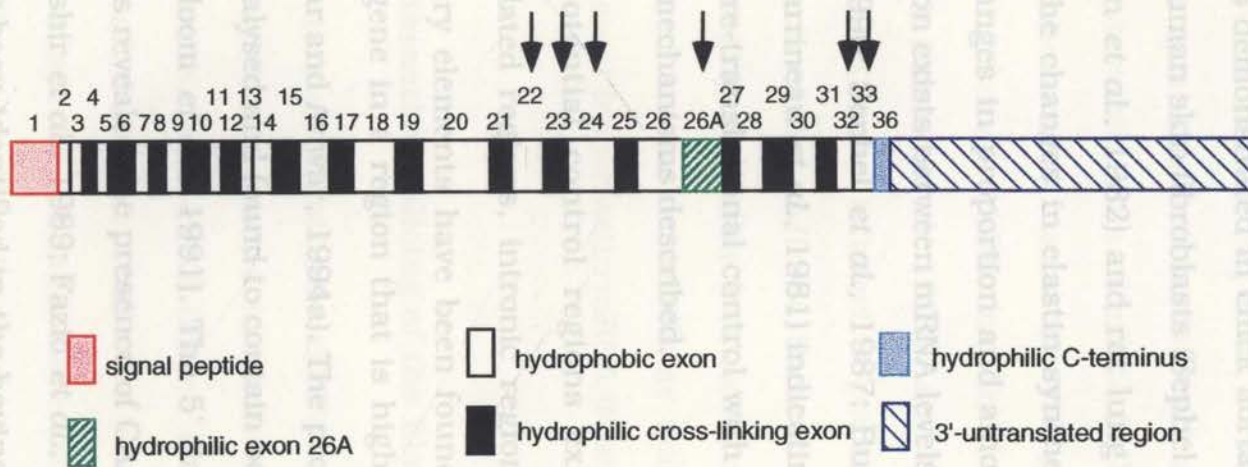


FIGURE 1.1 Structure of the human tropoelastin cDNA. Most of the gene consists of exons encoding hydrophobic and cross-linking domains which alternate. Exon 26A is an unusual hydrophilic exon of unknown function which does not encode any Lys residues and is not therefore involved in cross-linking. A large 3'-untranslated region is present in exon 36. Exons subject to alternate removal by splicing are marked with an arrow (adapted from Bashir *et al.*, 1989).

1.2.1.2 Control of Expression

Expression of tropoelastin mRNA and elastic fibre synthesis is highest in early development and occurs primarily in a defined period (Parks *et al.*, 1988), as demonstrated in chick aorta (Pollock *et al.*, 1990; Burnett *et al.*, 1982), human skin fibroblasts (Sephel *et al.*, 1987), sheep nuchal ligament (Davidson *et al.*, 1982) and rat lung (Myers *et al.*, 1983; Dubick *et al.*, 1981). The changes in elastin synthesis appear to be a consequence of both changes in proportion and amount of elastin mRNA and a strong correlation exists between mRNA levels and tropoelastin synthesis (Pollock *et al.*, 1990; Sephel *et al.*, 1987; Burnett *et al.*, 1982; Davidson *et al.*, 1982; Barrineau *et al.*, 1981) indicating tropoelastin expression is mainly under pre-translational control with both pre- and post-transcriptional control mechanisms described.

Extracellular matrix space may inhibit the further production of tropoelastin mRNA (Foster and Curtiss, 1990).

Many potential control regions exist in the elastin gene including untranslated regions, intronic regions and promoter regions. Negative regulatory elements have been found in the first intronic region in the bovine gene in a region that is highly conserved with the human gene (Manohar and Anwar, 1994a). The promoter region of the human gene has been analysed and found to contain both up and down-regulatory elements (Rosenbloom *et al.*, 1991). The 5' flanking region of the human elastin gene has revealed the presence of CAAT promoter sequences but no TATA box (Bashir *et al.*, 1989; Fazio *et al.*, 1990) although a possible TATA box has now been identified in the bovine gene (Manohar and Anwar, 1994b). The promoter region is GC-rich and multiple binding sites for Sp1 and AP2 transcription factors have been found in the human promoter region (Bashir *et al.*, 1989; Fazio *et al.*, 1990). Up to eight different transcription start sites have been identified (Bashir *et al.*, 1989; Rosenbloom *et al.*, 1991; Rosenbloom *et al.*, 1993) indicating that the elastin gene is under a

complex control mechanism. The second is the excision of a portion of an exon where alternative 5' donor and 3' acceptor sites are used, as is the case for human exon 26A (Indik *et al.*, 1987a). No obvious sequence differences exist between consensus intron/exon boundaries of alternatively and constitutively spliced exons in the human or bovine gene (Indik *et al.*, 1987a; Yeh *et al.*, 1987) but specific sequence elements which could contribute to alternative splicing have been identified in the rat gene (Pierce *et al.*, 1992b). Growth factors and hormones such as transforming growth factor β (Katchman *et al.*, 1994; Kähäri *et al.*, 1992), insulin-like growth factor I (Wolfe *et al.*, 1993) vitamin D (Pierce *et al.*, 1992a) and interleukin-1 β (Mauviel *et al.*, 1993) have all been shown to affect tropoelastin synthesis at either the mRNA or promoter level. In addition, there is evidence that tropoelastin may be under negative feedback autoregulation whereby accumulation of tropoelastin in the extracellular matrix space may inhibit the further production of tropoelastin mRNA (Foster and Curtiss, 1990).

Exon 23 is a cross-linking domain while exons 22, 24, 32 and 33 are hydrophobic domains. Exon 26A is the unusual hydrophilic domain

1.2.2 Alternative Splicing of the Elastin Gene

The isolation of tropoelastin cDNAs indicates that significant variation is present within a species in nucleotide sequence and size of both the isolated mRNA and cDNA (Pierce *et al.*, 1990; Baule and Foster, 1988; Fazio *et al.*, 1988a). cDNAs were found to differ only in the presence or absence of specific domains corresponding to entire exons or segments of exons. These variable cDNAs were shown to be the result of alternative splicing of tropoelastin mRNA. Exon/intron borders in the elastin gene appear to always split codons in the same way so that alternative splicing can occur in a cassette-like fashion allowing the reading frame to be maintained (Rosenbloom *et al.*, 1993). Two types of alternative splicing have been demonstrated. The first is complete excision of an entire exon, (Rich and Foster, 1993) and no obvious differences were seen in polypeptides

as seen with human exons 22, 23 and 32. The second is the excision of a portion of an exon where alternative 5' donor and 3' acceptor sites are used, as is the case for human exon 26A (Indik *et al.*, 1987a). No obvious sequence differences exist between consensus intron/exon boundaries of alternatively and constitutively spliced exons in the human or bovine gene (Indik *et al.*, 1987a; Yeh *et al.*, 1987) but specific sequence elements which could contribute to alternative splicing have been identified in the rat gene (Pierce *et al.*, 1992b).

1.2.3 Isoforms of Tropoelastin

At least 11 human tropoelastin splice variants have been identified with six exons shown to be subject to alternative splicing; exons 22, 23, 24, 26A, 32 and 33 (Boyd *et al.*, 1991; Fazio *et al.*, 1988a,b; Indik *et al.*, 1987a). Exon 23 is a cross-linking domain while exons 22, 24, 32 and 33 are hydrophobic domains. Exon 26A is the unusual hydrophilic domain which does not directly participate in cross-linking.

The roles of the different isoforms of tropoelastin ^{have} ~~has~~ not yet been established. Alternative splicing is developmentally regulated with age-related changes in isoform ratio and splice site usage demonstrated in the rat (Heim *et al.*, 1991), cow (Yeh *et al.*, 1989; Parks *et al.*, 1988; Wrenn *et al.*, 1987) and chick (Baule and Foster, 1988; Barrineau *et al.*, 1981). A higher splicing out frequency of all alternatively spliced exons is seen in tissue from adult cows compared with foetal and neonatal tissue (Yeh *et al.*, 1989).

Tissue-specificity has not been clearly demonstrated, however, with only minimal differences between tissues found. In rat heart, lung and aorta mRNA of the same sizes were found in abundance in all three tissues (Rich and Foster, 1989) and no obvious differences were seen in polypeptides

from cell-free translation of bovine foetal ligament, lung, ear or aorta mRNA (Parks *et al.*, 1988). *In situ* hybridisation also showed that each of the different isoforms were present in all bovine elastogenic tissue studied (Parks *et al.*, 1992). However, in the rat some tissue-specific splicing has been demonstrated with exon 33 spliced at 9-12% frequency in the aorta and lung compared with just 2% in skin (Heim *et al.*, 1991). Similarly, changes in splice usage with age in chick aorta were not paralleled in chick lung (Barrineau *et al.*, 1981). In addition, expressed protein containing human exon 26A has so far been identified from foetal aortic cells but not from skin fibroblasts (Fazio *et al.*, 1988a; Indik *et al.*, 1987a). In all species and tissues, exon 33 appears to be the most frequently spliced (Parks *et al.*, 1992; Heim *et al.*, 1991; Yeh *et al.*, 1989).

1.2.4 Secretion and Post-Translational Modification

Smooth muscle cells, endothelial and microvascular cells, chondrocytes and fibroblasts have all been demonstrated to synthesise elastin (Uitto *et al.*, 1991). Translation of mRNA takes place on ribosomes on rough endoplasmic reticulum (RER). Chains of approximately 72kDa are released into the lumen of the RER where the 26 amino acid signal peptide is cleaved (Saunders and Grant, 1984). Tropoelastin is secreted to the plasma membrane via secretory vesicles (Saunders and Grant, 1985; Damiano *et al.*, 1981) and it is possible to accumulate tropoelastin in the RER and Golgi apparatus experimentally using inhibitors of protein secretion (Davis and Mecham, 1996a). Inhibition of secretion of tropoelastin results in intracellular degradation of the accumulated tropoelastin (Ikeda *et al.*, 1997; Davis and Mecham, 1996a) and cysteine proteases have been shown to be responsible for the degradation seen when tropoelastin accumulates to a significant level in the RER; a process which has been speculated to

be a clearance mechanism for aberrant tropoelastin (Davis and Mecham, 1996a). Newly synthesised tropoelastin has been estimated to take 1hr to be secreted into the extracellular space in smooth muscle cells (Kao *et al.*, 1982) and as little as 20-30min in chick embryo artery cells (Saunders and Grant, 1985; Rosenbloom and Cywinski, 1976a).

Tropoelastin undergoes very little post-translational modification and there is no evidence for glycosylation. Hydroxylation of Pro residues occurs to a variable degree with 3-20% total Pro hydroxylated by the enzyme prolyl hydroxylase (Uitto *et al.*, 1991; Uitto *et al.*, 1976). It appears that Pro hydroxylation is not necessary for elastic fibre synthesis and that overhydroxylation may be detrimental. Inhibition of prolyl hydroxylase does not affect tropoelastin secretion (Narayanan *et al.*, 1977; Rosenbloom and Cywinski, 1976b; Uitto *et al.*, 1976) but overhydroxylation caused by the addition of ascorbate, a cofactor of prolyl hydroxylase, to cell cultures resulted in a decrease in elastin production (Davidson *et al.*, 1997; Barone *et al.*, 1985; Tinker and Rucker, 1985; Faris *et al.*, 1984). Overhydroxylation may result in destabilisation of tropoelastin secondary structure thus inhibiting coacervation and decreasing the ability of tropoelastin to form fibres at physiological temperature (Urry *et al.*, 1979). Cross-linking and the formation of insoluble elastin is consequently also reduced (Section 1.2.7 and 1.2.8). Hydroxylation may therefore simply be a by-product of collagen hydroxylation which occurs in the same cellular compartment. More recently, however, it has been proposed that the effect of ascorbate may be due to transcriptional regulation of elastin mRNA levels, although the mechanism is not known (Davidson *et al.*, 1997).

and molecular modelling has predicted the formation of a hairpin loop forming a positively charged pocket with the C-terminal RRK sequence at the end (Brown *et al.*, 1992). It was speculated that this pocket could provide a non-covalent binding site for the highly acidic microfibrils. It has now been confirmed experimentally that tropoelastin will indeed bind to the microfibrillar protein MAGP-1 (Bashir *et al.*, 1994; Brown-Augsburger *et al.*, 1994) and the binding has been localised to the C-terminus of

1.2.5 The Role of Microfibrils

Deposition of tropoelastin into the extracellular space occurs only at defined regions on the cell surface and tropoelastin is rapidly incorporated into the forming elastic fibre without further proteolysis (Bressan and Prockop, 1977). Before any elastin is deposited, microfibrils are secreted into the extracellular space close to the cell surface marking the first step in elastogenesis (Cleary, 1987). In early elastogenesis elastic fibres are thus exclusively made of microfibrils. The relative elastin content increases as elastin is laid down in small clumps which gradually fuse to form amorphous fibres (Mecham, 1991).

Since elastin is laid down in the same orientation as the microfibrils, it is suggested that the microfibrils are a scaffold upon which elastin is deposited and thus directs the form of the growing fibre (Ross and Bornstein, 1969). It is also suggested that the microfibrils serve to align the tropoelastin molecules into the correct orientation for subsequent cross-linking (Mecham, 1991). The highly conserved C-terminus of tropoelastin is necessary for correct elastic fibre formation and when missing severely alters fibre integrity, as noted in lamb ductus arteriosus where a truncated tropoelastin is present and does not form fibres (Hinek and Rabinovitch, 1993) and similarly in SVAS (Section 1.1.3). The two Cys residues confined to the C-terminus of tropoelastin have been demonstrated to form an intrachain disulfide bond and molecular modelling has predicted the formation of a hairpin loop forming a positively charged pocket with the C-terminal RKRK sequence at the end (Brown *et al.*, 1992). It was speculated that this pocket could provide a non-covalent binding site for the highly acidic microfibrils. It has now been confirmed experimentally that tropoelastin will indeed bind to the microfibrillar protein MAGP-1 (Bashir *et al.*, 1994; Brown-Augsburger *et al.*, 1994) and the binding has been localised to the C-terminus of

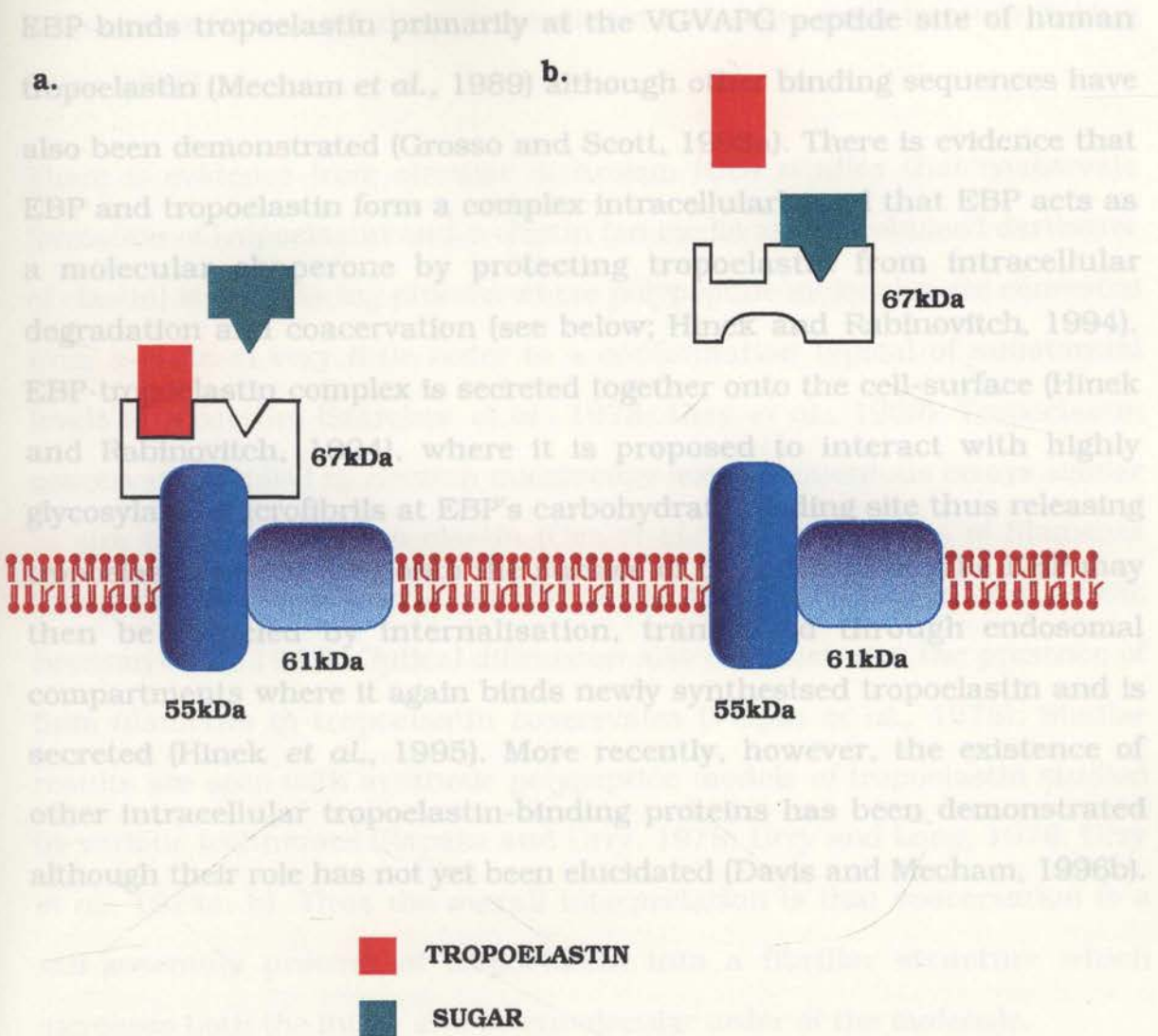
tropoelastin (Brown-Augsburger *et al.*, 1996; 1994) and the N-terminal half of MAGP-1 (Brown-Augsburger *et al.*, 1996). Both proteins appear to require an intact secondary structure which has been cited as evidence that binding is not simply ionic (Brown-Augsburger *et al.*, 1994). Transglutaminase mediated cross-linking of MAGP-1 to tropoelastin might then covalently lock this association (Mecham *et al.*, 1995; Brown-Augsburger *et al.*, 1994). Blocking MAGP-1 or the C-terminus of tropoelastin with antibodies reduces elastin accumulation in the extracellular matrix (Mecham *et al.*, 1995; Brown-Augsburger *et al.*, 1994) indicating that the interaction between tropoelastin and MAGP-1 is an important step in fibrillogenesis.

It is still unknown how the other microfibrillar proteins contribute to fibrillogenesis. Mutations in fibrillin-1, for example, result in Marfan syndrome characterised by widespread connective tissue abnormalities and an increase in elastin fragmentation (Section 1.1.3). A large number of different fibrillin-1 gene mutations have been identified, most of them unique and most involving single amino acid substitutions in various domains, yet all capable of causing Marfan syndrome (Dietz and Pyeritz, 1995). Mutations in the second fibrillin gene causes a related disorder, congenital contractural arachnodactyly (Lee *et al.*, 1991). Fibrillin is thought to be the major component of microfibrils which align in a head-to-tail fashion as parallel bundles of 6-8 molecules to form most of the microfibrillar structure (Gibson *et al.*, 1996). It is unknown whether tropoelastin binds directly to fibrillin. It has been speculated that MAGP-1, which has been localised to the bead region of the microfibril (Henderson *et al.*, 1996), may stabilise the end-to-end or lateral aggregation of fibrillin by disulfide bonding (Gibson *et al.*, 1996) or possibly by transglutaminase cross-linking (Mecham *et al.*, 1995) thereby providing an anchor for tropoelastin to fibrillin.

1.2.6 The Role of the Elastin Binding Protein

The mechanism behind the specific targeting of the tropoelastin molecule to sites of fibre formation on the cell surface is gradually being elucidated. Initially, the conserved C-terminus of tropoelastin was speculated as being involved in membrane binding as a targeting mechanism but this has been shown not to be the case (Grosso and Mecham, 1988). It is now clear that an elastin associating protein such as the elastin binding protein (EBP), or receptor, is involved in this targeting (Hinek *et al.*, 1988). Tropoelastin binds to a receptor complex consisting of at least three proteins: 61 and 55kDa membrane binding proteins and a peripheral 67kDa elastin binding component (Mecham *et al.*, 1989). The 67kDa domain is related to an alternatively spliced form of β -galactosidase and has at least two binding sites: one for tropoelastin and a carbohydrate binding domain (Hinek *et al.*, 1993). Binding of a carbohydrate such as lactose or galactose greatly reduces affinity of EBP for tropoelastin and to the membrane anchor. Upon carbohydrate binding, any tropoelastin bound to EBP is released and at the same time EBP is released from its anchor on the membrane bound protein (Mecham *et al.*, 1991; Figure 1.2).

Figure 1.2. Model of the elastin binding protein (EBP) complex. The EBP complex consists of two membrane bound proteins of 61 and 55kDa and a 67kDa peripheral subunit which binds tropoelastin and sugars through two separate sites. Tropoelastin binds to the inner EBP complex (a). When a sugar moiety binds to the EBP (such as from a glycosylated microbead), the 67kDa subunit loses its affinity for both tropoelastin and the membrane bound protein (b) releasing tropoelastin onto the growing elastic fibre (adapted from Mecham, 1991).



1.2.7 Role of Coacervation

Tropoelastin is completely soluble in cold aqueous solutions of less than 20°C. However, on raising the temperature towards the physiological range the solution becomes cloudy as the tropoelastin molecules aggregate by

Figure 1.2. Model of the elastin binding protein (EBP) complex. The EBP complex consists of two membrane bound proteins of 61 and 55kDa and a 67kDa peripheral subunit which binds tropoelastin and sugars through two separate sites. Tropoelastin binds to the intact EBP complex (a). When a sugar moiety binds to the EBP (such as from a glycosylated microfibril), the 67kDa subunit loses its affinity for both tropoelastin and the membrane-bound protein (b) releasing tropoelastin onto the growing elastic fibre (adapted from Mecham, 1991).

a liquid-liquid phase separation occurs. The bottom layer forms a sticky visco-elastic phase containing highly concentrated tropoelastin and approximately 60% water while the top layer is an aqueous equilibrium solution (Urry, 1988). Coacervation of tropoelastin is considered to be an important step in fibrillogenesis and it has been suggested that coacervation

EBP binds tropoelastin primarily at the VGVAPG peptide site of human tropoelastin (Mecham *et al.*, 1989) although other binding sequences have also been demonstrated (Grosso and Scott, 1993a). There is evidence that EBP and tropoelastin form a complex intracellularly and that EBP acts as a molecular chaperone by protecting tropoelastin from intracellular degradation and coacervation (see below; Hinek and Rabinovitch, 1994). EBP-tropoelastin complex is secreted together onto the cell-surface (Hinek and Rabinovitch, 1994), where it is proposed to interact with highly glycosylated microfibrils at EBP's carbohydrate binding site thus releasing tropoelastin specifically onto the surface of the microfibril. The EBP may then be recycled by internalisation, transferred through endosomal compartments where it again binds newly synthesised tropoelastin and is secreted (Hinek *et al.*, 1995). More recently, however, the existence of other intracellular tropoelastin-binding proteins has been demonstrated although their role has not yet been elucidated (Davis and Mecham, 1996b).

1.2.7 Role of Coacervation

Tropoelastin is completely soluble in cold aqueous solutions of less than 20°C. However, on raising the temperature towards the physiological range the solution becomes cloudy as the tropoelastin molecules aggregate by interactions between hydrophobic domains in a process referred to as coacervation. The process is thermodynamically controlled and can be reversed by cooling the solution. If coacervated solutions are left to settle, a liquid-liquid phase separation occurs. The bottom layer forms a sticky visco-elastic phase containing highly concentrated tropoelastin and approximately 60% water while the top layer is an aqueous equilibrium solution (Urry, 1988). Coacervation of tropoelastin is considered to be an important step in fibrillogenesis and it has been suggested that coacervation

both concentrates and aligns tropoelastin molecules prior to cross-linking (Urry, 1978).

After secretion into the extracellular space, tropoelastin is rapidly There is evidence from circular dichroism (CD) studies that coacervate formation of tropoelastin and α -elastin (an oxalic acid-solubilised derivative of elastin) is an ordering process where polypeptide molecules are converted from a state of very little order to a conformation typical of substantial levels of structure (Starcher *et al.*, 1973; Urry *et al.*, 1969). Tropoelastin coacervates studied by electron microscopy reveal filamentous arrays similar in size to filaments from elastin (Cox *et al.*, 1974). Bundles of filaments thought to be due to lateral association are also seen (Bressan *et al.*, 1986; Bressan *et al.*, 1983). Optical diffraction also demonstrates the presence of 5nm filaments in tropoelastin coacervates (Volpin *et al.*, 1976). Similar results are seen with synthetic polypeptide models of tropoelastin studied by various techniques (Rapaka and Urry, 1978; Urry and Long, 1976; Urry *et al.*, 1974a, b). Thus the overall interpretation is that coacervation is a self-assembly process of tropoelastin into a fibrillar structure which increases both the intra- and intermolecular order of the molecule.

Overhydroxylation of Pro residues increases its hydrophilicity and may therefore reduce the ability of tropoelastin to coacervate providing an explanation for the reduced elastic fibre formation seen in the presence of ascorbate (Barone *et al.*, 1985). Cross-linking of tropoelastin by lysyl oxidase is greatly reduced at low temperatures when tropoelastin is not coacervated (Narayanan *et al.*, 1978) despite the level of lysyl oxidase activity being unaffected (Narayanan *et al.*, 1977). This indicates that coacervation is crucial for adequate cross-linking. It is not known, however, if coacervation favours cross-linking by intermolecular alignment of individual molecules, by changes in conformation or hydrophobicity of tropoelastin or simply by concentrating the molecules.

1.2.8 Cross-Linking

After secretion into the extracellular space, tropoelastin is rapidly insolubilised by cross-link formation without any further modifications or proteolytic processing (Bressan and Prockop, 1977). The initial reaction is an oxidative deamination of Lys residues by the enzyme lysyl oxidase to produce allysine, also known as α -amino adipic δ -semialdehyde (Figure 1.3). All subsequent reactions are spontaneous and involve the condensation of Lys and allysine residues to produce cross-links such as allysine aldol, lysinonorleucine, merodesmosine and the tetrafunctional cross-links unique to elastin, desmosine and isodesmosine (Reiser *et al.*, 1992). The structures and likely route of formation of these cross-links are shown in Figure 1.3.

Lysyl oxidase is a copper-dependent enzyme, highly thermostable and with a broad pH optimum. It initiates cross-link formation in both collagen and elastin (Kagan and Sullivan, 1982). When lysyl oxidase is inhibited cross-linking is greatly reduced and tropoelastin accumulates in tissues demonstrating the vital importance of this enzyme in elastogenesis (Tinker *et al.*, 1990). Nutritional deprivation of copper in humans and animals can lead to haemorrhage and aortic aneurysms (Tinker and Rucker, 1985). This is the basis for most tropoelastin purification protocols; animals are either fed copper deficient diets reducing lysyl oxidase activity (Rucker, 1982; Sandberg and Wolt, 1982) or lysyl oxidase is inhibited irreversibly by lathyrogens such as β -aminopropionitrile (Rich and Foster, 1982; Foster *et al.*, 1975). The affinity of lysyl oxidase is highest for insoluble forms of tropoelastin and collagen rather than monomers in solution emphasising the importance of tropoelastin coacervation to subsequent biosynthetic events (Section 1.2.7). Lysyl oxidase has been localised immunologically to the mature elastic fibre, indicating that it may be incorporated into the growing fibre (Kagan *et al.*, 1986).

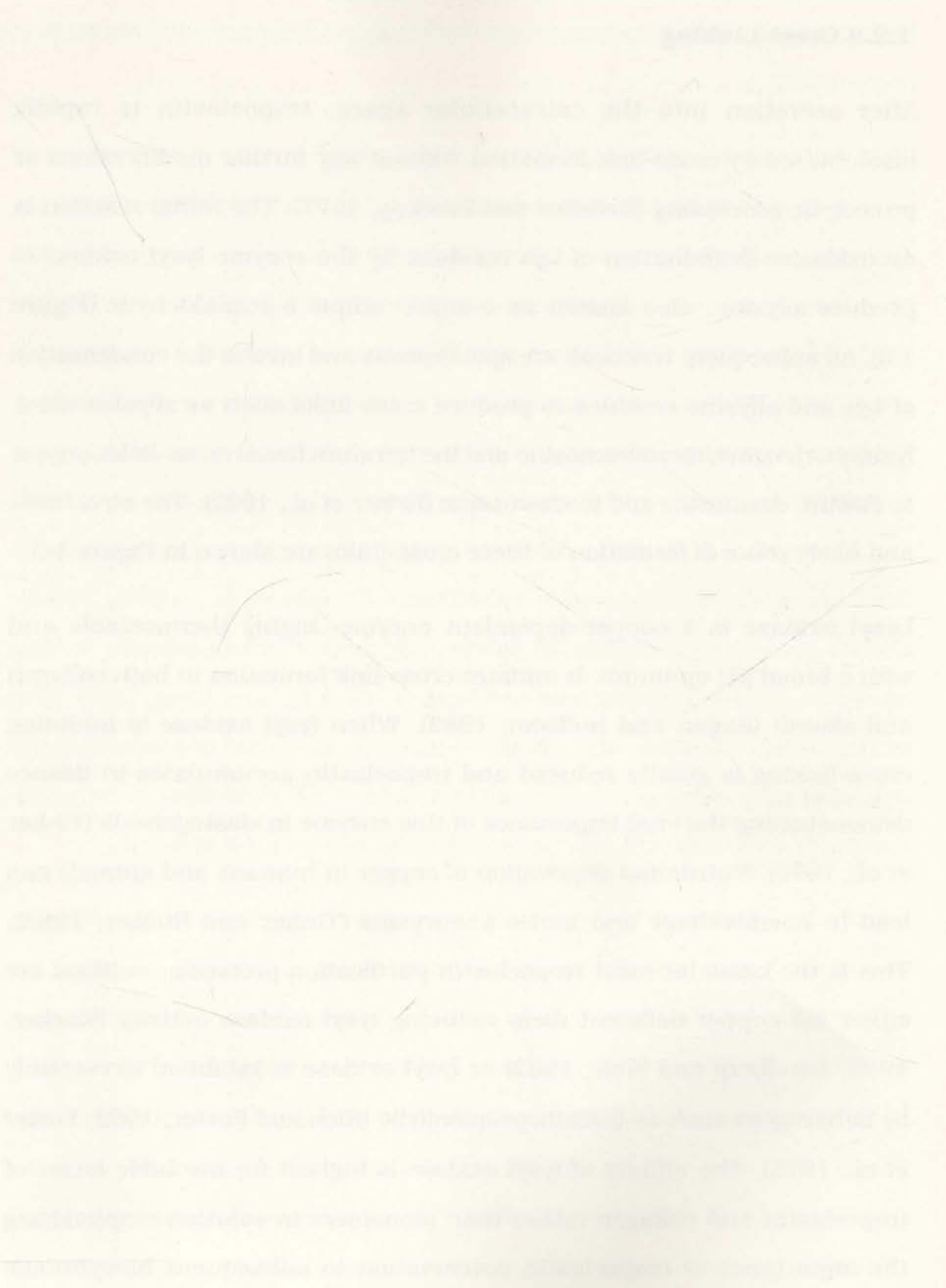


Figure 1.3 Structure and route of formation of elastin cross-links. The reaction catalysed by lysyl oxidase (shaded) converts lysine to allsine. The subsequent spontaneous condensations between lysine and allsine produces the other cross-links with the tetrafunctional desmosine and isodesmosine thought to result from two different pathways.

Most of the Lys residues in tropoelastin are incorporated into cross-links. Desmosines and isodesmosines are formed from four Lys residues (Partridge *et al.*, 1964) but only link two tropoelastin chains (Foster *et al.*, 1974). Three allysines and one Lys residue contribute to each desmosine and isodesmosine. It is thought that the presence of an aromatic residue (Tyr or Phe) on the C-terminal side of Lys prevents oxidation by lysyl oxidase (Foster *et al.*, 1974) favouring lysinonorleucine formation and thus directing desmosine and isodesmosine formation (Reiser *et al.*, 1992).

Lys residues in Ala-rich regions are always in groups of two or three separated by either two or three Ala residues. These regions are α -helical (Foster *et al.*, 1976) and the separation of Lys by two or three Ala places the Lys residues near one another on the same side of the helix, resulting in a conformation favourable to desmosine and isodesmosine formation. Only two exons, 19 and 25, contain three Lys residues instead of two. These exons are significant in that three separate tropoelastin chains are joined using these domains. Exons 19 and 25 of two antiparallel chains are joined by a desmosine and exon 10 from a third tropoelastin chain bridges them through two lysinonorleucine cross-links utilising the remaining two Lys residues (Brown-Augsburger *et al.*, 1995; Mecham *et al.*, 1995). This is the first demonstration of specific cross-links joining more than two chains. The Lys residues in Pro-containing domains which dominate the N-terminal half of tropoelastin are unlikely to be α -helical and hence unlikely to form desmosine or isodesmosine although their specific structures and interactions have not been determined.

lipids and cholesterol (Kagan *et al.*, 1977). Increased elastolytic activity has also been observed in skin disorders such as cutis laxa (Fornieri *et al.*, 1994). Increased elastolysis and degradation of elastin is also a feature of normal ageing (Braverman and Fonferko, 1982; Hall, 1976) suggesting elastolytic enzymes may produce damage slowly and may accumulate over

1.3 DEGRADATION AND REPAIR (1982).

1.3.1 Elastases and Elastolysis

Insoluble elastin has a very slow turnover in normal tissues. In adult rat lung, turnover was estimated to be several years, approaching the lifetime of the organism (Dubick *et al.*, 1981). One of the reasons for this may be the high resistance of elastin to proteolytic degradation. The group of proteases able to degrade insoluble elastin are collectively known as elastases and are generally active on a large number of substrates beside elastin. Serine elastases, which include pancreatic elastase, polymorphonuclear leukocyte elastase (also known as neutrophil elastase) and Cathepsin G are the most abundant elastases in mammals (Stone *et al.*, 1982). Blood monocytes also contain elastolytic metalloproteinases called matrix metalloproteinases which include 92 and 72kDa gelatinases, matrilysin and macrophage elastase (Shapiro, 1994). Blood monocytes produce serine elastases but after differentiation to macrophages lose this ability and produce matrix metalloproteinases instead (Shapiro, 1994). An important regulator of elastase function, particularly in lung, is α_1 -proteinase inhibitor (Shapiro, 1994; Werb *et al.*, 1982).

Elastin degradation is important in many physiological processes such as growth, wound healing, pregnancy and tissue remodelling (Werb *et al.*, 1982). However, inappropriate and uncontrolled elastolysis can be destructive, contributing to disorders such as emphysema in the lung and atherosclerosis in arteries. Elastolysis in arteries can be enhanced by lipids and cholesterol (Kagan *et al.*, 1977). Increased elastolytic activity has also been observed in skin disorders such as cutis laxa (Fornieri *et al.*, 1994). Increased elastolysis and degradation of elastin is also a feature of normal ageing (Braverman and Fonferko, 1982; Hall, 1976) suggesting that elastolytic enzymes may produce damage slowly and may accumulate over

a lifetime (Braverman and Fonferko, 1982).

Specific degradation has also been noted in cell culture of smooth muscle

1.3.2 Repair of Damaged Fibres

Even highly purified tropoelastin has been reported to degrade into approximately five discrete bands on prolonged storage, leading to a hypothesis that it is co-purified with an intrinsic protease which promotes its gradual breakdown (Mecham and Foster, 1977; Mecham *et al.*, 1977; Mecham *et al.*, 1979). Mammalian serum contains proteases which are capable of degrading tropoelastin (Romero *et al.*, 1986). Serum has also been shown to induce elastase activity in smooth muscle cells leading to degradation of elastin (Kobayashi *et al.*, 1994). Serine protease inhibitors reduce the degradation of tropoelastin caused by serum (Romero *et al.*, 1986). Tropoelastin gene expression does, however, appear to be stimulated after injury in adult smooth muscle cells suggesting that new tropoelastin may have a role in repair (Belknap *et al.*, 1996). A new form of cross-link incorporating a Schiff base was hypothesised to occur in repaired elastin resulting in an altered structure likely to weaken the overall structure (Stone *et al.*, 1988). This may explain the observation that in the repair of lung tissue occurring after experimentally induced emphysema, elastin levels can return to normal but the new elastic fibres are highly disorganised and not fully functional (Soskel and Sandberg, 1987; Rucker and Dubick, 1984).

Other workers have postulated that serine proteases modulate tropoelastin mRNA levels by suggesting that soluble tropoelastin accumulation acts as a negative transcription (McGowan *et al.*, 1996).

1.3.3 Proteolysis of Tropoelastin

Soluble peptides produced by degradation of elastin with elastase have been demonstrated to down-regulate mRNA levels when added to undigested elastin-producing cultures, while increasing mRNA levels in damaged cultures thus serving to localise repair to damaged tissues (Foster and Christner *et al.*, 1978). Purification of tropoelastin from tissues usually results in extensive degradation which can be substantially reduced by

using protease inhibitors, particularly of serine proteases (Franzblau *et al.*, 1989; Rich and Foster, 1984; Rucker, 1982; Sandberg and Wolt, 1982). Specific degradation has also been noted in cell culture of smooth muscle cells which was attributed to a metalloprotease (Hayashi *et al.*, 1995). Even highly purified tropoelastin has been reported to degrade into approximately five discrete bands on prolonged storage, leading to a hypothesis that it is co-purified with an intrinsic protease which promotes its gradual breakdown (Mecham and Foster, 1977; Mecham *et al.*, 1977; Mecham *et al.*, 1976). Mammalian serum contains proteases which are capable of degrading tropoelastin (Romero *et al.*, 1986). Serum has also been shown to induce elastase activity in smooth muscle cells leading to degradation of elastin (Kobayashi *et al.*, 1994). Serine protease inhibitors can reduce the degradation of tropoelastin caused by serum (Romero *et al.*, 1986).

There have been some differing hypotheses put forward as to the possible role and consequences of tropoelastin degradation. Franzblau *et al.* (1989) suggested that the extensive degradation seen in purified tropoelastin was not an artifact of purification but was part of normal elastogenesis due to discrete cleavage from the C-terminus preferentially at Tyr residues, thus removing any incorrectly cross-linked fibres. However, this is in conflict with evidence showing tropoelastin to be incorporated into the fibre without any degradation (Bressan and Prockop, 1977). Other workers have postulated that serine proteases modulate tropoelastin mRNA levels by suggesting that soluble tropoelastin accumulation acts as a negative feedback control mechanism for transcription (McGowan *et al.*, 1996). Soluble peptides produced by degradation of elastin with elastase have been demonstrated to down-regulate mRNA levels when added to undigested elastin-producing cultures, while increasing mRNA levels in damaged cultures thus serving to localise repair to damaged tissues (Foster and

Curtiss, 1990; Foster *et al.*, 1990). Soluble elastin peptides are chemoattractants for monocytes and fibroblasts suggesting that protease degradation products derived from cross-linked material have a role in cell migration and inflammation (Wachi *et al.*, 1995; Bisaccia *et al.*, 1994; Grosso and Scott, 1993a;b). Thus, the proteolytic degradation of tropoelastin and elastin may have important consequences for normal elastogenesis and repair processes.

1.4 MECHANISM OF ELASTICITY

1.4.1 Introduction

Various structural models have been proposed to explain the function of elastin and its ability to recoil after being stretched. There is good evidence to suggest that the basis of the elasticity of elastin is entropic - i.e. stretching decreases the entropy of the system and that recoil is driven by a spontaneous return to maximum entropy (Gosline 1978a; Dorrington and McCrum, 1977; Weis-Fogh and Andersen, 1970). It is the mechanism by which this occurs that is speculative. There are two groups of structure-function models proposed - those where elastin is considered to be isotropic and devoid of structure and those which consider elastin to be anisotropic containing regions of order. The following is a summary of the major models proposed.

1.4.2 Random Chain Model

The random chain model (Hoeve and Flory, 1974) considers elastin to be like a typical rubber. It consists of random, flexible chains that are kinetically free and in constant motion due to thermal agitation (Figure 1.4a). The chains are linked together by permanent random cross-links producing an amorphous rubber-like matrix. Elasticity arises due to an increase in order when these random chains are stretched. The return to maximum entropy is the driving force to return the chains to random conformation when the stretching force is removed.

There is ample evidence to support the random chain model. The amino acid sequence of elastin is conducive to random chains - they are rich in Gly and small amino acids which provide least restriction to kinetic freedom of the chain and Pro, a helix breaker, may also help to keep the chains free (Gosline, 1980). Single elastin fibres have been studied by polarised light microscopy and found to exhibit no birefringence indicating isotropic (random) conformation and no evidence was found of the presence of filaments or fibrils (Aaron and Gosline, 1980). The mechanical state of elastin was found to be typical of an amorphous polymer in viscoelastic transition phase in agreement with rubber elasticity theory (Dorrington *et al.*, 1975). Elastin goes through a glass transition typical of rubbers (Gosline and French, 1979). Raman spectroscopy has demonstrated that elastin purified from bovine *ligamentum nuchae* was substantially disordered (Prescott *et al.*, 1987). Nuclear magnetic resonance (NMR) studies on elastin also indicated that the backbone is highly mobile, indicating kinetically free chains (Torchia and Piez, 1973).

Random coil model, consisting of random cross-links holding together a liquid model, consisting of alternating hydrophobic and hydrophilic regions. Fibrillar model, consisting of a helical cross-linking regions and a lower order, the β -spiral, formed by the repeating hydrophobic domains. The β -spiral can associate to form larger filaments which along with the cross-links hold several strands together (adapted from Bailey and Etherington, 1980).

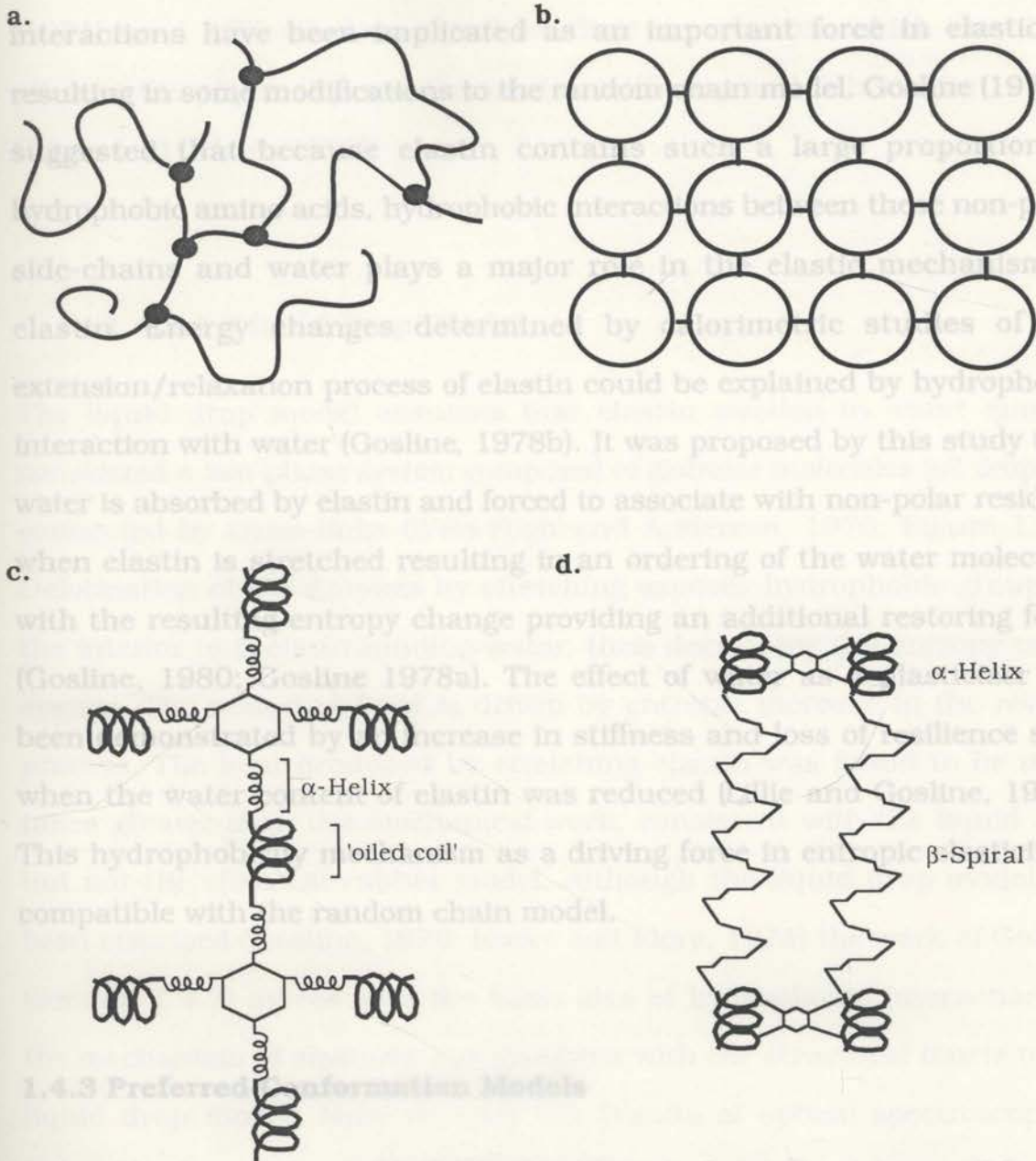


Figure 1.4 Proposed elastin structural models. Four models are described in the text. **a.** Random coil model, consisting of random chains held together by cross-links **b.** Liquid-drop model, consisting of globular tropoelastin molecules linked by cross-links **c.** Oiled-coil model, consisting of alternating α -helical cross-linking domains joining two or more chains and an 'oiled coil' formed by the hydrophobic domains **d.** Fibrillar model, consisting of α -helical cross-linking regions and a loose helix, the β -spiral, formed by the repeating hydrophobic domains. The β -spirals can associate to form larger filaments which along with the cross-links hold several chains together (adapted from Bailey and Etherington, 1980).

ability of tropoelastin to serve as a substrate for lysyl oxidase preferentially in the coacervate state indicates a degree of order, as does its interaction

A major difference between elastin and true rubbers is that elastin is not self-lubricating and is only elastic when swollen in water. Thus, hydrophobic interactions have been implicated as an important force in elasticity, resulting in some modifications to the random chain model. Gosline (1978a) suggested that because elastin contains such a large proportion of hydrophobic amino acids, hydrophobic interactions between these non-polar side-chains and water plays a major role in the elastic mechanism of elastin. Energy changes determined by calorimetric studies of the extension/relaxation process of elastin could be explained by hydrophobic interaction with water (Gosline, 1978b). It was proposed by this study that water is absorbed by elastin and forced to associate with non-polar residues when elastin is stretched resulting in an ordering of the water molecules with the resulting entropy change providing an additional restoring force (Gosline, 1980; Gosline 1978a). The effect of water as a plasticiser has been demonstrated by an increase in stiffness and loss of resilience seen when the water content of elastin was reduced (Lillie and Gosline, 1990). This hydrophobicity mechanism as a driving force in entropic elasticity is compatible with the random chain model.

1.4.3 Preferred-Conformation Models

Although most of the early physical studies performed are compatible with the random chain model, several features of elastin cannot readily be reconciled with this model. The ability of tropoelastin to coacervate and form fibrous structures (Section 1.2.7) is largely ignored (Bailey and Etherington, 1980). The fibrous nature of elastin seen by electron microscopy also does is not easily accommodated by a random chain model. The ability of tropoelastin to serve as a substrate for lysyl oxidase preferentially in the coacervate state indicates a degree of order, as does its interaction

with MAGP-1 (Section 1.2.5). Problems have also been noted in the choice of solvents used for physical experiments. For example, Hovee and Flory (1974) used 30% ethylene glycol for their experiments which may have affected the physical properties of elastin (Bailey and Etherington, 1980; Volpin and Ciferri, 1970).

1.4.3.1 'Liquid Drop' Model

The liquid drop model assumes that elastin swollen in water may be considered a two-phase system composed of globular molecules (oil droplets) connected by cross-links (Weis-Fogh and Andersen, 1970; Figure 1.4b). Deformation of the droplets by stretching exposes hydrophobic groups in the interior to the surrounding water, thus decreasing the entropy of the system. The restoring force is driven by entropic increase in the reverse process. The heat produced by stretching elastin was found to be many times greater than the mechanical work, consistent with the liquid drop but not the classical rubber model. Although the liquid drop model has been criticised (Gosline, 1976; Hovee and Flory, 1974) the work of Gosline (Section 1.4.2) agrees with the basic idea of hydrophobic interactions in the mechanism of elasticity but disagrees with the structural tenets of the liquid drop model. More recently the results of optical spectroscopy of elastin and κ -elastin (a potassium hydroxide-solubilised form of elastin) were used to propose that elastin architecture is like that proposed by the liquid drop model i.e. globular molecules linked by cross-links, but the hydrophobic mechanism of elasticity was rejected due to the apparent high mobility of the hydrophobic regions (Debelle *et al.*, 1995). However, these results also contradicted the random chain and fibrillar models (Section 1.4.3.3).

1.4.3.2 'Oiled Coil' Model

An alternative model based on the liquid-drop model was proposed by Gray *et al.* (1973), termed the 'oiled coil' (Figure 1.4c). Rather than the globular units of the liquid-drop model, this structural model was based on fibrillar units of alternating α -helical cross-linking domains and a broad coil (the oiled coil) consisting of the hydrophobic repeat units enriched for Gly, Val and Pro. The Gly residues are on the exterior of the coil and the hydrophobic Val and Pro residues on the interior. Upon extension the hydrophobic interior of the coil is exposed to water and, as in the other hydrophobic models, results in an entropic change which provides the restoring force when released. Being a fixed configuration model incompatible with the high mobility expected for random chains, the oiled coil model has been largely rejected for similar reasons to the liquid-drop model (Gosline, 1976; Hovee and Flory, 1974).

1.4.3.3 Fibrillar Model

The fibrillar model (Figure 1.4d), first proposed by Urry (1974), is based on extensive studies of the repeating hydrophobic segments of tropoelastin including: the hexapeptide APGVGV, the pentapeptide VPGVG and the tetrapeptide VPGG. These polypeptide repeats have been shown by techniques such as CD and NMR to be able to form a stable conformation known as the type II β -turn (Urry and Long, 1976; Urry *et al.*, 1974b). When the temperature is raised these β -turns will optimise intramolecular hydrophobic interactions by forming a loose helix, the β -spiral, with the β -turns acting as spacers between turns of the helix. Several β -spirals then associate to optimise hydrophobic interactions between molecules, forming twisted filaments (Urry, 1982). These interactions occur during

the coacervation process. β -spirals are dynamic structures with preferred rather than fixed conformations and similarly it is proposed that the interchain hydrophobic interactions are dynamic also (Urry and Long, 1977). The overall structure of elastin is therefore proposed in this model to consist of alternating β -spirals formed by the hydrophobic domains and α -helical cross-linking domains with the individual chains being held together by both cross-links and hydrophobic interactions (Urry, 1974).

In the fibrillar model, the entropic elasticity is explained by the librational entropy mechanism. The β -spirals are a loose coil and are filled with water molecules contiguous with the surrounding bulk water. The peptide segments between β -turns are dynamic and undergo low-amplitude, high-frequency rocking motions known as librations. When the spiral is stretched, the librations decrease in amplitude and introduce order to the protein. The entropy is decreased and provides the restoring elastic force. A more specific function is proposed for the penta- and hexapeptide segments in the β -spiral. The pentapeptide β -spiral is elastomeric while the hexapeptide β -spirals, which are more rigid, are proposed to function as interlocking and aligning segments (Urry, 1974).

This model is supported by a significant amount of experimental data, the majority of which have used polypeptide models of the repeat regions (see above). As already outlined in Section 1.2.7, coacervation of α -elastin, tropoelastin and the polypeptide models results in an increase in order with type II β -turns the predominant secondary structure, particularly in the hydrophobic polypeptides (Castiglione Morelli *et al.*, 1993; Megret *et al.*, 1993; Tamburro *et al.*, 1990; Bressan *et al.*, 1986; Bressan *et al.*, 1983; Urry and Long, 1976; Cox *et al.*, 1974). Coacervation also results in fibre formation (Bressan *et al.*, 1986; Bressan *et al.*, 1983; Cox *et al.*, 1974) and the viscous coacervate can readily be drawn into fibres (Partridge

and Whiting, 1977). When synthetically cross-linked, the polypentapeptide exhibits an elastic modulus similar to elastin and an increase in elastic force with increasing temperature over the temperature range that coacervation and conformational changes occur (Urry *et al.*, 1985). This demonstrates that elastic force only develops as structure and order increase, the exact opposite of the behaviour expected of random chains.

The results from electron microscopy of elastin and tropoelastin coacervates have been criticised as artifactual due to the harsh chemical techniques used to fix and prepare samples. More recent work, however, has utilised

1.4.4 Microscopic Evidence of Structure

Microscopic studies of elastic fibres strongly suggest the presence of structure, in particular a filamentous or fibrillar structure. Transmission and scanning electron microscopy of purified elastin showed elastin to consist of interwoven and twisted fibrils (Gotte, 1977). 100nm diameter fibrils were seen at low resolution but at high resolution individual filaments of 3nm diameter were observed (Gotte, 1977). When stretched, filaments showed a 5nm centre-to-centre distance and appeared to have a globular structure. A parallel array of primary filaments with similar centre-to-centre distance were seen in undegraded elastin from bovine *ligamentum nuchae* (Serafini-Fracassini *et al.*, 1976). Extensive inter-filament cross-linking was ruled out since fibres were easily separated by sonication indicating that cross-linking may be confined to the primary filament and hydrophobic interactions may hold the structural units together. More recently a variety of structures of different magnitude, including filaments, fibrils, fibres, networks and dendritic leaf forms were all identified in elastin samples by scanning and transmission electron microscopy indicating elastin may be made up of repeating self-similar structures on many levels (Tamburro *et al.*, 1995).

The same type of filamentous organization is seen in tropoelastin coacervates

(Cox *et al.*, 1974). Lateral association of 5nm filaments and a second type consisting of 100-150nm banded filaments were seen in tropoelastin coacervates (Bressan *et al.*, 1986; Bressan *et al.*, 1983). Optical diffraction of tropoelastin and α -elastin coacervates also demonstrated the presence of filaments with the same centre-to-centre diameter aligned in parallel arrays (Volpin *et al.*, 1976).

The results from electron microscopy of elastin and tropoelastin coacervates have been criticised as artifactual due to the harsh chemical techniques used to fix and prepare samples. More recent work, however, has utilised quick-freeze deep-etch electron microscopy which minimises such artifacts because no such treatments are involved. Using this technique, the elastin component of bovine ear cartilage is seen to be densely packed with a random network of fine filaments of 7nm average diameter (Mecham and Heuser, 1990) in good agreement with previous data. In the relaxed state it appears that the filaments are arranged randomly but when the elastin fibre is stretched filaments are oriented in the direction of the applied force showing the filamentous structure quite clearly (Mecham and Heuser, 1991). This same study found purified tropoelastin monomers seen by freeze-fracture and rotary shadowing to be globular with 5-7nm diameter, suggesting that these globules join together in three dimensions to form the filamentous structures of the same diameter.

1.4.5 Structural Studies on Soluble Elastins

Soluble forms of elastin include tropoelastin and elastin solubilised by oxalic acid (α -elastin) or potassium hydroxide (κ -elastin). The elastin derivatives are a heterogeneous mixture of partially cross-linked peptides with a wide molecular weight range. However, they are much easier to

obtain than tropoelastin and have therefore been studied in preference to the more logical elastin precursor, tropoelastin. CD studies of α -elastin in aqueous solution have shown a large negative peak at 200nm compatible with high levels of disordered regions but also a negative shoulder at 220nm which is thought to result from α -helix (Tamburro *et al.*, 1977; Starcher *et al.*, 1973; Urry *et al.*, 1969) now assigned to cross-link regions. When α -elastin was studied by CD at increasing temperatures an increase in order was seen compatible with the appearance of both α -helix and β -bends (Tamburro *et al.*, 1977) in agreement with CD studies of coacervates. Thus, CD data of soluble α -elastin points not to a totally disordered protein but to a partially ordered one which increases in structure with heating and coacervation.

It may be possible to study soluble elastin, particularly tropoelastin, to help shed light on the overall structure of elastin.

Tropoelastin, being much harder to isolate, has not been studied in as much detail as solubilised elastin and some conflicting data exists. CD spectra of chick tropoelastin showed it to be partially ordered and not completely random (Rucker *et al.*, 1973). However, zone velocity centrifugation established tropoelastin to be a random coil, quite different in properties from globular proteins (Schein *et al.*, 1977). These experiments were carried out in a sucrose gradient which was suggested to affect the hydration of tropoelastin as sucrose is a very poor solvent for tropoelastin (discussion following Schein *et al.*, 1977).

More recently the secondary structure for tropoelastin was predicted to contain ten α -helices separated by more ambiguous structures, mainly predicted to be β -sheet (Debelle *et al.*, 1992). The α -helices corresponded to the cross-linking regions and the β -sheet regions to the hydrophobic regions. CD spectra of bovine tropoelastin found it to be typical of disordered proteins but could also be assigned to short and distorted β -barrels, with total secondary structure calculated as 10% α -helix, 30% β -sheet, 20%

β -turn and 40% coil in broad agreement with predictions (Debelle and Alix, 1995). Various optical spectroscopic techniques used to study κ -elastin revealed it to have different local conformation to elastin suggesting that may not be a good model for elastin (Debelle *et al.*, 1995). CD studies of κ -elastin suggested that its global conformation was similar to tropoelastin being mainly disordered but possibly containing short, distorted β -barrels (Debelle *et al.*, 1995). From this study, it was suggested that elastin is made up of a three-dimensional arrangement of globular tropoelastin molecules connected by cross-links, akin to the liquid-drop model architecture with α -helical cross-linking regions and hydrophobic elastic regions made up of short and distorted highly mobile β -barrels (Debelle *et al.*, 1995). Thus, it may be possible to study soluble elastin, particularly tropoelastin, to help shed light on the overall structure of elastin.

1.5 SOURCES OF TROPOELASTIN

1.5.1 Tissue Extracts

When tropoelastin was first studied the only way to obtain it was from animal tissues and this is today still routinely used to obtain tropoelastin. Chicks and piglets are the most commonly used sources. Since tropoelastin is rapidly cross-linked *in vivo* it does not exist in any appreciable quantities in normal animal tissue. To increase yields, it is therefore necessary to inhibit cross-linking by feeding either copper-deficient diets or lathyrogens, such as β -aminopropionitrile, to young animals. These techniques are very labour and time intensive. Copper-starvation requires careful monitoring of every aspect of diet in special animal raising facilities and many weeks may be needed to raise animals to a significant level of deficiency (Sandberg and Wolt, 1982). Both copper-deficiency and lathyrogens, even with extreme

care, may result in some discomfort to animals as they are often showing signs of deficiency and illness prior to sacrifice (Rich and Foster, 1982; Sandberg and Wolt, 1982). In addition to these problems, yields of tropoelastin from animals are low and many animals are required to obtain sufficient tropoelastin for study. Only 2mg tropoelastin is typically obtained from a gram of copper-deficient pig aorta (Smith *et al.*, 1972) while 500-700 chicks were required to obtain 30mg tropoelastin (Rucker, 1982). With lathyrogens up to 2000 chicks were used to prepare 65mg tropoelastin (Foster *et al.*, 1975) although various improvements reduced this to 200 chicks for 40mg (Rich and Foster, 1982). Numerous steps are required to extract tropoelastin from tissues, including mincing, extensive salt solubilisation, coacervation, alcohol fractionation, ion-exchange and gel-filtration. In addition, use of enzyme inhibitors greatly improved quality and quantity of yield (Narayanan and Page, 1974; Sandberg *et al.*, 1974). Obviously, these methods limit tropoelastin available for study to animal forms and alternative methods are needed to study human tropoelastin.

1.5.2 Recombinant Tropoelastins

The production of recombinant tropoelastin in bacterial systems has greatly simplified the availability of tropoelastin. In addition, it provides a valuable means for obtaining human tropoelastin. Modified bovine tropoelastin, consisting of exons 15-36, has been expressed in *Escherichia coli* as a Protein-A fusion (Grosso *et al.*, 1991). Purification was greatly simplified compared with tissue extraction methods but relatively low yields of 2-10mg/L culture were obtained. Purification involved a hazardous cyanogen bromide (CNBr) cleavage which, due to the highly acidic reaction conditions,

has the potential for damage to the polypeptide. The final product, although useful, was not a physiologically relevant form of tropoelastin. A human tropoelastin cDNA has also been expressed in bacteria as a fusion with influenza NS1 protein (Indik *et al.*, 1990). This isoform of tropoelastin, containing exon 26A and the signal peptide, was the first form of human tropoelastin to be obtained for study. Other isoforms have now also been expressed in recombinant form (Bedell-Hogan *et al.*, 1993). Tropoelastin was expressed in *E. coli* for six to seven hours producing insoluble recombinant tropoelastin (Indik *et al.*, 1990). CNBr was again necessary for purification with the resulting yield a relatively modest 2-4mg/L culture.

Recombinant forms of tropoelastin have proved to be viable alternatives to tissue-derived tropoelastin. Recombinant tropoelastin reacts with elastin antibodies, is a chemotactic agent (Indik *et al.*, 1990) and is a substrate for lysyl oxidase (Bedell-Hogan *et al.*, 1993). In all recombinant systems used so far, purified tropoelastin showed distinct degradation products which were sufficiently severe in one case that unfused tropoelastin could not be produced at all (Indik *et al.*, 1990). Recombinant systems clearly have great potential as sources of tropoelastin although there is great room for significant improvement upon existing expression and purification systems.

1.6 AIMS OF THIS WORK

The aims of the present work are:

1. to assist in the long-term study of tropoelastin properties, functional interactions and biosynthesis by developing an improved recombinant expression and purification system for different isoforms of human tropoelastin.

2. to use the recombinant tropoelastins to shed some light on the structural and functional aspects of elastin biosynthesis and interactions.

CHAPTER 2

GENERAL MATERIALS AND METHODS

CHAPTER 2

GENERAL MATERIALS AND METHODS

2.1 Chemicals

Ampicillin, 5-bromo-4-chloro-3-indoyl β -D-galactopyranoside (X-Gal), isopropyl- β -D-thiogalactoside (IPTG) and ethidium bromide were from Progen Industries (Australia). Acrylamide, bisacrylamide, ammonium persulfate (APS) and N, N, N', N'-tetramethylethylenediamine (TEMED) were from Boehringer Mannheim (Germany). All other chemicals used were of analytical reagent grade. TE is 10mM Tris-HCl, pH 8.0, 1mM EDTA and was sterilised by autoclaving before use.

2.2 Bacterial Strains and Growth Media

All bacterial strains used were from existing laboratory stocks except BMH17-18 *mutS* (Clontech, USA). Strains and their genotypes are given (Sambrook *et al.*, 1989).

XL1-Blue: *supE44 hsdR17 recA1 endA1 gyrA46 thi relA1 lac F'[proAB⁺ lac^f lacZ Δ M15 Tn10(*tef*)]*

DH5 α : *supE44 Δ lacU1 69 (ϕ 80 lacZ Δ M15) hsdR17 recA1 endA1 gyrA96 thi-1 relA1*

HMS174: *recA1 hsdR rif*

BL21(DE3): *hsdS gal (λ clts857 ind1Sam7 nin5 lacUV5-T7 gene1)*

BMH17-18 *mutS*: *thi supE Δ (lac-proAB) [mutS::Tn10] [F' proAB lac^fZ Δ M15]*

Bacto tryptone and bacto yeast extract were obtained from Difco Laboratories (USA) and agar from Life Technologies (USA). Luria-Bertani media (LB) consisted of 1%[w/v] bacto tryptone, 0.5%[w/v] bacto yeast extract, 0.5%[w/v] NaCl and supplemented where appropriate with ampicillin

(50 μ g/ml). 2TY media consisted of 1.6%[w/v] bacto tryptone, 1%[w/v] bacto yeast extract, and 0.5%[w/v] NaCl with 50 μ g/ml ampicillin. All media were sterilised before use by autoclaving and cooled to < 50°C before adding ampicillin. Plates (25ml) were made from LB containing 1.5% agar which was added before autoclaving. Media was allowed to cool before ampicillin, IPTG or X-Gal were added and plates poured.

2.5 Cesium Chloride Plasmid Preparation

Bacteria were stored in 25% glycerol at -80°C for long term storage and revived by streaking onto LB plates and incubating at 37°C overnight. BMH17-18 *mutS* cells were maintained on LB plates and media containing 10 μ g/ml tetracycline. Plasmid-containing bacteria were maintained on LB plates containing 75 μ g/ml ampicillin and grown in ampicillin-containing media (50 μ g/ml).

2.3 Microscopy

5 μ l culture was diluted with 5 μ l sterile water, placed on a slide and covered with a cover slip. A drop of immersion oil was placed on top and cells observed at 1000x magnification with phase contrast using an Olympus BH-2 microscope.

2.4 Transformation

Transformation of competent bacteria by electroporation was performed using a Gene Pulser apparatus (Bio-Rad, USA) according to a protocol supplied by the manufacturer. Electrocompetent cells were made according to a protocol supplied by Bio-Rad except for BMH17-18 *mutS* which were made following an alternative standard protocol supplied by Clontech.

Competent cells were stored in aliquots at -80°C . After electroporation cells were grown for one hour at 37°C at 280rpm in 1ml LB and aliquots were plated at various dilutions. Transformants were selected by growth at 37°C overnight on LB plates supplemented with $75\mu\text{g}/\text{ml}$ ampicillin.

2.7 Sodium Dodecyl Sulfate- Polyacrylamide Gel Electrophoresis (SDS-PAGE)

2.5 Cesium Chloride Plasmid Preparation

Bacteria were grown in 500ml LB+ampicillin media at 37°C overnight with shaking at 280rpm. Plasmid extraction was performed following the large scale alkaline lysis protocol in Sambrook *et al.* (1989) except that lysozyme was omitted. DNA was dissolved in 7ml TE and $0.96\text{g}/\text{ml}$ cesium chloride (Boehringer Mannheim, Germany) and $0.8\text{mg}/\text{ml}$ ethidium bromide added. The solution was placed in a Quick-Seal centrifuge tube (Beckman Instruments, USA), overlaid with paraffin oil and heat sealed. A cesium chloride gradient was established by centrifuging at 40 000rpm in a 70.1Ti rotor for approximately 60hr in an ultracentrifuge (L8-70 or L8-80M Beckman, USA). The band corresponding to plasmid DNA was visualised under long-wave UV light and removed with a sterile needle. Ethidium bromide was removed by repeated extraction with an equal volume of butanol saturated with 5M NaCl in TE. DNA was ethanol precipitated (Sambrook *et al.*, 1989) and redissolved in TE for storage at -20°C .

2.6 Quantitation of DNA

Cesium chloride purified DNA was quantitated by spectrophotometry using the relationship $A_{260}=1$ at $50\mu\text{g}/\text{ml}$ DNA. Purity was determined by an $A_{260}:A_{280}$ ratio which was between 1.8 and 2.0 if the DNA was sufficiently pure (Ausubel *et al.*, 1987). Smaller DNA samples were quantitated by

electrophoresis alongside samples of known quantity of DNA and the amount of DNA was estimated visually after gel photography.

2.6 SDS-PAGE and Blotting for Amino Acid Analysis and N-terminal

2.7 Sodium Dodecyl Sulfate- Polyacrylamide Gel Electrophoresis (SDS-PAGE)

Gels were poured using fresh acrylamide stocks and half the usual amounts

Samples of bacterial culture (1ml) for SDS-PAGE analysis were centrifuged in a microfuge for 30s to harvest cells and resuspended in 200 μ l 1x loading buffer (1%[w/v] SDS, 3%[v/v] glycerol, 0.5%[v/v] β -mercaptoethanol, 12.5mM Tris-HCl pH 6.8, 0.0025%[w/v] Coomassie blue-G). For other samples to be analysed by SDS-PAGE, 4x loading buffer was added to a final concentration of 1x. Aliquots for analysis were removed and boiled for 4min to denature protein prior to electrophoresis.

Denaturing gels containing acrylamide at concentrations from 8 to 15% were prepared according to the method of Laemmli (1970). 0.75ml 1% APS and 20 μ l TEMED was added and the solution poured into a Tall Mighty

Small apparatus (with 1.5mm spacers) or a Mighty Small apparatus (with 0.75mm spacers) both from Hoefer Scientific, USA. A 4% stacking gel was overlaid onto the separating gel and samples loaded alongside size markers (Mark 12, Novex, USA). Gels were run in 25mM Tris-HCl, 192mM glycine, 0.1%(w/v) SDS, pH approximately 8.3, at 30mA until tracking dye had reached the bottom of the gel. Gels were fixed in 50%(v/v) methanol for 30-60min and stained in 45%(v/v) methanol, 10%(v/v) acetic acid, 0.125%(w/v) Coomassie blue-R (Sigma Chemical Company, USA) for three hours with gentle agitation. Gels were destained in 25%(v/v) methanol, 10%(v/v) acetic acid with a destain bag (Mo-Bi-Tec GmbH, Germany). Gels were dried using gel drying solution, cellophane and drier from Novex (USA) overnight at 25°C. Alternatively, a drying solution consisting of 20%

methanol, 2% glycerol was used.

2.8 SDS-PAGE and Blotting for Amino Acid Analysis and N-terminal Sequencing

Gels were poured using fresh acrylamide stocks and half the usual amounts of APS and TEMED. Gels were allowed to set for 16-24hrs. For simple protein profiles, gels were pre-run at room temperature for four hours at 20mA using 150mM Tris-HCl, pH 8.8 buffer with 10 μ l/L thioglycollic acid in the upper buffer chamber. Samples were loaded and run at 4°C with fresh buffer for approximately three hours. For more complex profiles gels were pre-run at room temperature in the usual Tris-glycine buffer (Section 2.7), fresh buffer added and the gel allowed to equilibrate to room temperature before samples were added and run at 20mA with 10 μ l/L thioglycollic acid added to the upper chamber. Pre-stained standards (Kaleidoscope; Bio-Rad, USA) were used to monitor extent of migration.

Gels were blotted onto polyvinylidene difluoride (PVDF) membrane (ProBlott, Applied Biosystems, USA), treated according to manufacturer's instructions, overnight at 70mA using 10mM CAPS pH 11.0, 10% methanol, 10 μ l/L thioglycollic acid buffer at 4°C with stirring. Blotting was performed using a Hoefer Transblot apparatus and was used according to manufacturer's instructions. The membrane was stained with 0.1% Coomassie blue-R in 50% methanol and destained in 50% methanol, 10% acetic acid. The membrane was washed with water overnight before being air-dried. Bands were excised with a clean scalpel.

2.9 N-Terminal Sequencing

Samples were blotted onto PVDF as described in Section 2.8. Bands were excised with a clean scalpel and sequenced by Sydney University and Prince Alfred Hospital Macromolecular Analysis Centre (SUPAMAC) using Applied Biosystems hardware and protocols. Alternatively, samples ^{were} ~~where~~ sent to the Biomolecular Resource Facility (Australian National University, Canberra).

2.10 Scanning Densitometry

Scanning densitometry of stained gels was performed using the Molecular Dynamics Personal Densitometer. Images were analysed and quantitated using ImageQuant software (Version 3.2, Molecular Dynamics, USA).

CHAPTER 3

**CONSTRUCTION AND CLONING OF
SYNTHETIC GENES ENCODING TWO
ISOFORMS OF TROPOELASTIN:
SHEL AND SHEL Δ 26A**

3.1 INTRODUCTION

Despite the availability of cDNA clones, large quantities of pure tropoelastin have not been prepared using recombinant techniques. Previous recombinant work with tropoelastin by Indik *et al.* (1990) and Grosso *et al.* (1991) achieved only modest expression of between 2 and 10mg from a litre of bacterial culture. One contribution to this may be the significant number of 'rare' *E. coli* codons encoded by the repetitive tropoelastin sequence (Martin *et al.*, 1995). Highly expressed genes demonstrate a major bias towards a subset of codons which varies between organisms, resulting in some codons being used in these genes at very low levels or not at all (Sharp *et al.*, 1986; Bennetzen and Hall, 1982). 35% of the natural human tropoelastin gene sequence contains low-usage *E. coli* codons, defined as being used at a frequency of 10% or less in highly expressed *E. coli* genes, which may hamper its expression potential in this host (Martin *et al.*, 1995). Other workers have shown that the use of rare codons in a highly-expressing recombinant system may result in lowered protein yields, heterogeneity or in-frame translational deletions in the final product (Rosenberg *et al.*, 1993; Kane *et al.*, 1992; Makoff *et al.*, 1989). Although clusters of rare codons produce the most problems, the overall number may also cause translational errors (Kane, 1995). It has therefore been recommended that synthetic genes be constructed if a gene contains a large proportion of low-usage *E. coli* codons, such as is the case for tropoelastin, to remove the possibility of such expression problems (Kane, 1995; Das, 1990).

The synthetic tropoelastin gene sequence (*SHEL*) used in this work was designed by optimising the codon usage for *E. coli* expression without changing the amino acid sequence. Convenient restriction sites were also added to facilitate cloning and future manipulation. The gene is based on

cHEL2, a natural tropoelastin cDNA sequence obtained from human foetal aorta (Indik *et al.*, 1987a). *SHEL* contains exon 26A but unlike cHEL2, does not contain the signal peptide. Figure 3.1 shows the cloning strategy used in the construction of *SHEL*. 50 oligonucleotides were designed, synthesised and annealed in our laboratory as in Figure 3.1 to produce the gene sequence. Oligonucleotide blocks were cloned into manageable sizes in pBS II SK⁺ vectors and confirmed by sequencing to produce pSHEL1-8. The 'blocks' from pSHEL1-8 were then cloned into larger precursors, pSHEL α , β and γ , by combining three (α, β) or two (γ) blocks. Preliminary cloning work was performed in our laboratory by Dr Stephen Martin. The precursor plasmids pSHEL α , β and γ were the starting point for the work described in this chapter.

This chapter describes the construction and cloning of two tropoelastin isoforms. The construction of the full-length *SHEL* gene from the precursors and its subsequent cloning into a variety of different expression vectors is described. The production of a second isoform, *SHEL* Δ 26A, using site-directed mutagenesis of *SHEL* to remove exon 26A is also described. This latter isoform involved a two-step procedure consisting of mutagenesis, which resulted in the formation of an aberrant mutant product *SHEL* Δ modified (*SHEL* Δ mod) and the subsequent manipulation of *SHEL* Δ mod to produce the desired *SHEL* Δ 26A.

*Figure 3.1 Assembly and cloning of the SHEL gene. Inset: Scheme for the assembly of pSHEL1 from individual oligos (numbered). The phosphorylated ends of the oligos are shown as small filled circles. A similar technique, utilizing the appropriate restriction sites was used for the remaining blocks, to form pSHEL2 to 8. Main figure: Scheme for the assembly and cloning of the SHEL gene from the intermediate plasmids pSHEL1-8. SHEL gene fragments were released from plasmids pSHEL1-8 by digestion with the appropriate restriction enzymes as shown. Two (pSHEL γ) or three (pSHEL α, β) blocks were ligated into pBlueScript II SK⁺ to produce the precursor plasmids pSHEL α, β and γ . The SHEL gene fragments from each of these three precursor plasmids were excised and purified to produce the full length SHEL gene as described in Section 3.2.9. B, BamHI; H, HindIII; K, KpnI; N, NotI; P, PstI; S, SacI; Sp, SpeI (from Martin *et al.*, 1995).*

3.2 MATERIALS AND METHODS

3.2.1 Plasmids

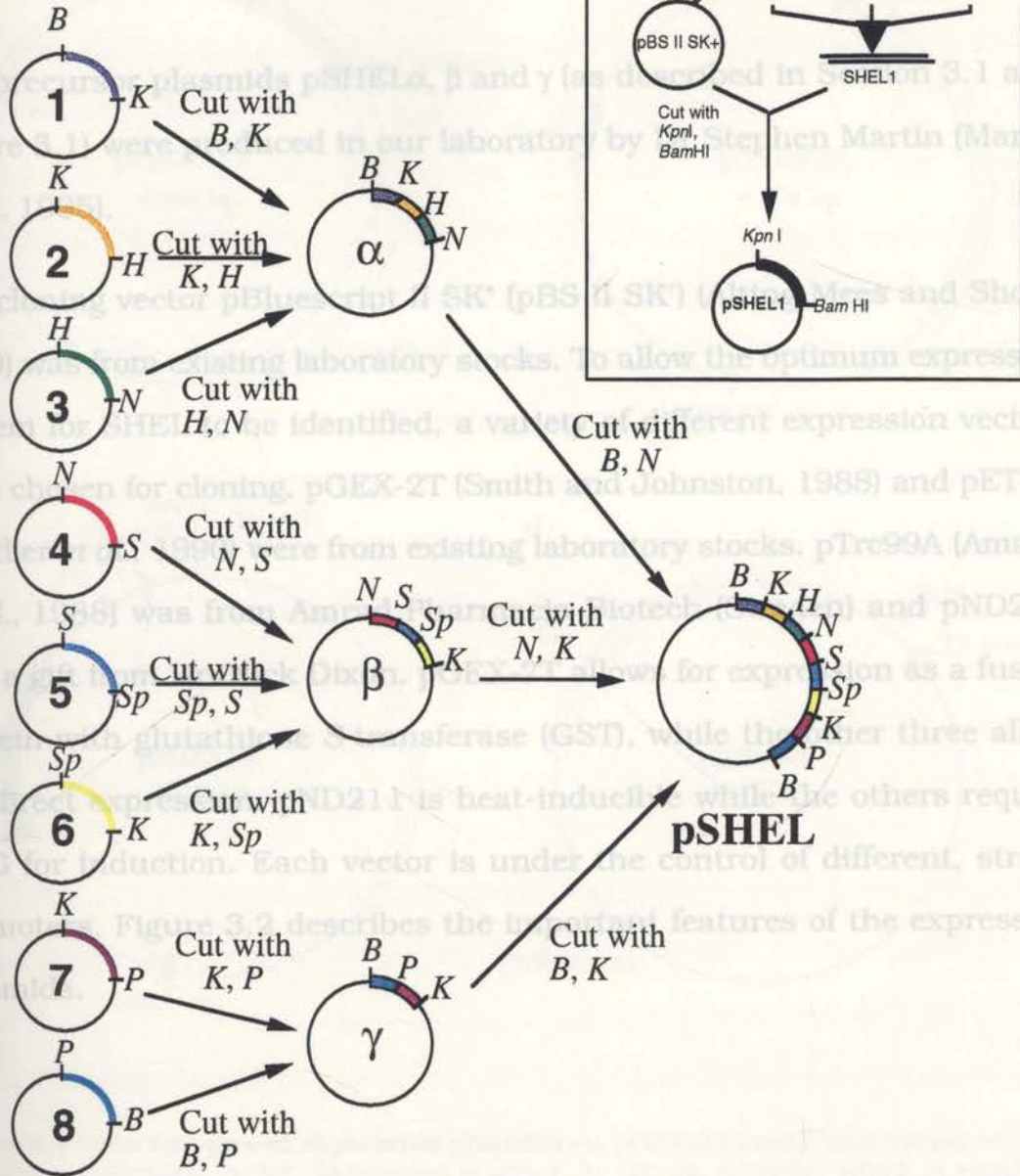


Figure 3.1 Assembly and cloning of the SHEL gene. Inset: Scheme for the assembly of pSHEL1 from individual oligos (numbered). The phosphorylated ends of the oligos are shown as small filled circles. A similar technique, utilizing the appropriate restriction sites was used for the remaining blocks, to form pSHEL2 to 8. **Main figure:** Scheme for the assembly and cloning of the SHEL gene from the intermediate plasmids pSHEL1-8. SHEL gene fragments were released from plasmids pSHEL1-8 by digestion with the appropriate restriction enzymes as shown. Two (pSHEL γ) or three (pSHEL α , β) blocks were ligated into pBluescript II SK+ to produce the precursor plasmids pSHEL α , β and γ . The SHEL gene fragments from each of these three precursor plasmids were excised and purified to produce the full length SHEL gene as described in Section 3.2.9. B, *Bam*HI; H, *Hind*III; K, *Kpn*I; N, *Not*I; P, *Pst*I; S, *Sac*I; Sp, *Spe*I (from Martin *et al.*, 1995).

3.2 MATERIALS AND METHODS

3.2.1 Plasmids

The precursor plasmids pSHEL α , β and γ (as described in Section 3.1 and Figure 3.1) were produced in our laboratory by Dr Stephen Martin (Martin *et al.*, 1995).

The cloning vector pBluescript II SK⁺ (pBS II SK⁺) (Alting-Mees and Short, 1989) was from existing laboratory stocks. To allow the optimum expression system for SHEL to be identified, a variety of different expression vectors were chosen for cloning. pGEX-2T (Smith and Johnston, 1988) and pET-3d (Studier *et al.*, 1990) were from existing laboratory stocks. pTrc99A (Amann *et al.*, 1988) was from Amrad Pharmacia Biotech (Sweden) and pND211 was a gift from Dr. Nick Dixon. pGEX-2T allows for expression as a fusion protein with glutathione S-transferase (GST), while the other three allow for direct expression. pND211 is heat-inducible while the others require IPTG for induction. Each vector is under the control of different, strong promoters. Figure 3.2 describes the important features of the expression plasmids.

Figure 3.2 Main features of expression plasmids. a. pGEX-2T (Smith and Johnston, 1988) is a fusion expression vector. Expression is driven by the *lac* promoter which is coupled to the complete coding sequence for *Schistosoma japonicum* GST (Sj26). A multiple cloning site (MCS) containing *Bam*HI is present at the 3' end of Sj26 to allow production of the desired protein as fusions with GST. A thrombin recognition site is also encoded at the junction between Sj26 and the MCS to allow removal of GST after induction. The vector contains the gene for the *lac* repressor (*lac*R) and part of *lac*Z making it IPTG inducible. The ampicillin resistance gene (*bla*) and origin of replication (*ori*) are shown. b. pTrc99A expression (Amann *et al.*, 1988) is controlled by the IPTG-inducible *trc* promoter coupled to an MCS containing *Nco*I to allow for direct expression of recombinant proteins. *lac*R, *bla* and the pBR322 *ori* are shown. c. pND211 (N. Dixon, personal communication) is based on the pCB30 vector (Elwyn *et al.*, 1969). pND211 expression is controlled by both the leftward and rightward λ bacteriophage promoters (P_L and P_R) in tandem. The λ gene *cI857* encodes the heat-labile λ repressor which represses expression at 30°C but allows induction when cells are grown at 42°C. An *Nco*I site used for cloning, flanked by *Bam*HI sites, is shown. *bla* and the ColE1 *ori* are shown. d. pET-3d (Studier *et al.*, 1990) expression is directed by the T7 promoter, which is IPTG inducible in DE3 lysogen strains of *E. coli*. An *Nco*I site allows for direct expression of recombinant proteins. *bla* and the pBR322 *ori* are shown.

3.2.2 Agarose Gel Electrophoresis

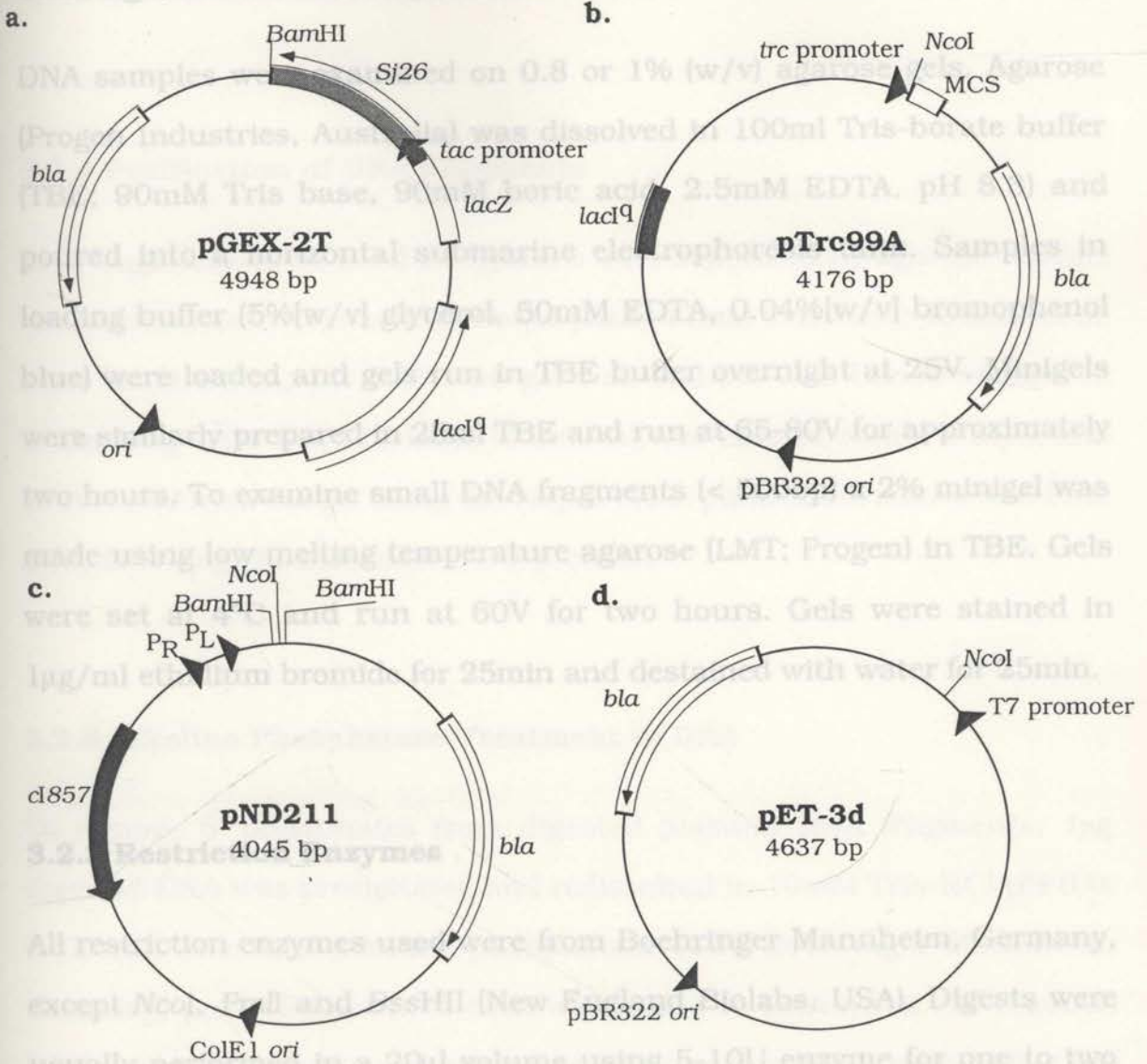


Figure 3.2 Main features of expression plasmids. **a.** pGEX-2T (Smith and Johnston, 1988) is a fusion expression vector. Expression is driven by the *tac* promoter which is coupled to the complete coding sequence for *Schistosoma japonicum* GST (*Sj26*). A multiple cloning site (MCS) containing *Bam*HI is present at the 3' end of *Sj26* to allow production of the desired protein as fusions with GST. A thrombin recognition site is also encoded at the junction between *Sj26* and the MCS to allow removal of GST after induction. The vector contains the gene for the *lac* repressor (*lacI^q*) and part of *lacZ* making it IPTG inducible. The ampicillin resistance gene (*bla*) and origin of replication (*ori*) are shown. **b.** pTrc99A expression (Amman *et al.*, 1988) is controlled by the IPTG-inducible *trc* promoter coupled to an MCS containing *Nco*I to allow for direct expression of recombinant proteins. *lacI^q*, *bla* and the *pBR322 ori* are shown. **c.** pND211 (N.Dixon, personal communication) is based on the pCE30 vector (Elvin *et al.*, 1990). pND211 expression is controlled by both the leftward and rightward λ bacteriophage promoters (*P_L* and *P_R*) in tandem. The λ gene *cI857* encodes the heat-labile λ repressor which represses expression at 30°C but allows induction when cells are grown at 42°C. An *Nco*I site used for cloning, flanked by *Bam*HI sites, is shown. *bla* and the *ColE1 ori* are shown. **d.** pET-3d (Studier *et al.*, 1990) expression is directed by the *T7* promoter, which is IPTG inducible in DE3 lysogen strains of *E. coli*. An *Nco*I site allows for direct expression of recombinant proteins. *bla* and the *pBR322 ori* are shown.

3.2.2 Agarose Gel Electrophoresis

DNA samples were examined on 0.8 or 1% (w/v) agarose gels. Agarose (Progen Industries, Australia) was dissolved in 100ml Tris-borate buffer (TBE; 90mM Tris base, 90mM boric acid, 2.5mM EDTA, pH 8.3) and poured into a horizontal submarine electrophoresis tank. Samples in loading buffer (5% [w/v] glycerol, 50mM EDTA, 0.04% [w/v] bromophenol blue) were loaded and gels run in TBE buffer overnight at 25V. Minigels were similarly prepared in 25ml TBE and run at 65-80V for approximately two hours. To examine small DNA fragments (< 500bp) a 2% minigel was made using low melting temperature agarose (LMT; Progen) in TBE. Gels were set at 4°C and run at 60V for two hours. Gels were stained in 1µg/ml ethidium bromide for 25min and destained with water for 25min.

3.2.5 Alkaline Phosphatase Treatment of DNA

3.2.3 Restriction Enzymes

To remove 5' phosphates from digested plasmid DNA fragments, 1µg digested DNA was precipitated and redissolved in 10mM Tris-HCl pH 8.0. All restriction enzymes used were from Boehringer Mannheim, Germany, except *NcoI*, *PmlI* and *BssHII* (New England Biolabs, USA). Digests were usually performed in a 20µl volume using 5-10U enzyme for one to two hours (unless otherwise stated) at 37°C using reaction buffer supplied by the manufacturer, except for *BssHII* which was performed at 50°C. 100µg/ml bovine serum albumin (BSA; Boehringer Mannheim, Germany) was added to reactions with *KpnI* and *PmlI*. For double digests with incompatible buffers, the DNA was digested first with one enzyme (usually the one requiring lower NaCl), the enzyme inactivated by heating at 65°C for 15min, DNA precipitated with ethanol (Sambrook *et al.*, 1989) and redissolved in 1x reaction buffer for the second enzyme digest. Size estimation of fragments was performed by measuring distance migrated from wells compared with size markers using the program Exline created

by Mr Dennis Leonard (Department of Biochemistry, University of Sydney).

A single colony was inoculated into 3ml LB+ampicillin media in 10ml screw-topped tubes and grown overnight with shaking at 37°C. Plasmids

3.2.4 Purification of DNA Fragments

DNA fragments to be used in ligations were separated by agarose minigel electrophoresis in Tris-acetate buffer (TAE; 40mM Tris base, 40mM acetic acid, 2mM EDTA, pH 8.5). The gel was stained and bands visualised under long-wave UV. The band of interest was excised with a scalpel and DNA eluted from the gel using the Prep-A-Gene purification matrix (Bio-Rad, USA) following the manufacturer's protocol.

3.2.5 Alkaline Phosphatase Treatment of DNA

To remove 5' phosphates from digested plasmid DNA fragments, 1µg digested DNA was precipitated and redissolved in 10mM Tris-HCl pH 8.0. 0.1U calf-intestinal alkaline phosphatase (CIP; Boehringer Mannheim, Germany) per 100pmol DNA ends was added to DNA in 1x CIP reaction buffer supplied by the manufacturer and supplemented with 100µg/ml BSA. The reaction was allowed to proceed for 30min at 37°C and was stopped by adding 0.5M EDTA, pH 8. The enzyme was inactivated by heating at 75°C for 10min. DNA was extracted with phenol/chloroform/isoamyl alcohol (Amresco, USA) and precipitated by the addition of 0.1 volumes 3M sodium acetate, pH 7.0 and two volumes ethanol (Sambrook *et al.*, 1989). The success of the reaction was tested by performing self-ligations on equivalent amounts of treated and untreated DNA; a ten to twenty-fold reduction in the number of colonies was routinely obtained.

3.2.6 Plasmid Mini-Preparations

A single colony was inoculated into 3ml LB+ampicillin media in 10ml screw-topped tubes and grown overnight with shaking at 37°C. Plasmids were extracted following the alkaline lysis protocol in Sambrook *et al.* (1989). When using HMS174 cells, two extractions with phenol/chloroform/isoamyl alcohol were performed to remove nucleases prior to ethanol precipitation. Plasmids were stored at -20°C in TE or sterile MilliQ water (MQW; Millipore, USA). Alternatively, plasmid preparations were performed using the Insta-Prep Kit (5 Prime to 3 Prime Inc., USA) or QIAprep Spin Plasmid Kit (Qiagen GmbH, Germany) according to the supplied protocol.

3.2.7 DNA Sequencing -Manual

5µg cesium chloride (Section 2.5) or QIAprep purified DNA was used for each reaction. Samples were sequenced using internal SHEL primers (Appendix I) (Dr Stephen Martin; Department of Biochemistry, University of Sydney) and manufactured by SUPAMAC. Reactions were performed using the Sequenase Version 2.0 kit (USB, USA) according to the manufacturer's instructions. [³⁵S]dATPαS was supplied by Amersham International plc, UK. A 6% acrylamide gel containing 8M urea and 0.8x Tris-aurine buffer (TTE; 1x: 90mM Tris base, 29mM taurine, 0.5mM EDTA) was prepared and 1ml 10% APS and 30µl TEMED added. The gel was poured between two plates: one rendered sticky by treatment with 300µl γ-methacryloxypropyl-trimethoxy-silane and 100µl ethanol mixed with 300µl glacial acetic acid and 3ml water; the other non-sticky by treatment with 5ml dimethyldichloro silane. The gel was pre-run for 45min at 55W on a Model 2 sequencing gel apparatus (BRL, USA) using 0.8x

TTE as buffer. Samples were run for three and a half hours at 45W. After electrophoresis was complete, the plates were separated and the gel retained on the sticky plate. Gels were soaked in 10% acetic acid for 10min to fix the DNA, followed by 20% ethanol for 10min to remove urea. The gel was dried at 80°C and allowed to cool before being exposed to autoradiographic film (Hyperfilm-MP; Amersham International plc, UK) for 24-48hr. The film was developed using an Ecomat 2400 automatic developer (Nishimoto Sangyo Co., Ltd, Japan).

3.2.8 DNA Sequencing - Automated

Automated sequencing was performed by either Sequi-Net (Department of Biochemistry, Colorado State University, USA) or by SUPAMAC. DNA was supplied after purification by either cesium chloride gradient or Qiagen Tip 20 (Qiagen GmbH, Germany) and sequenced using the same primers as for manual sequencing.

3.2.10 Construction of pSHEL α

3.2.9 Construction of Full-Length SHEL

Cesium-chloride purified stocks of the three precursor plasmids pSHEL α , β and γ were digested with the appropriate pairs of restriction enzymes as shown in Figure 3.1. The SHEL gene fragments were purified from agarose gels (Section 3.2.4). pBS II SK⁺ was digested with *Bam*HI and treated with CIP (Section 3.2.5). 50ng of each SHEL fragment and 100ng pBS II SK⁺ were ligated together at 16°C for one hour using the DNA Ligation System (Amersham, U.K.) according to the supplied protocol. Controls containing vector only and insert only were included. The enzyme was inactivated by heating at 65°C for 10min. Due to the large reaction volume, the mixture

was ethanol precipitated and redissolved in 20 μ l MQW before 2 μ l was used to transform *E. coli* XL1-Blue cells by electroporation (Section 2.4). Transformants were selected on LB plates containing ampicillin (75 μ g/ml), IPTG (0.1mM) and X-Gal (80 μ g/ml).

To screen for the presence of the correct insert, plasmid mini-preparations were performed (Section 3.2.6). Plasmids were screened by digestion with *Hind*III and analysed by 1% agarose gel electrophoresis. Constructs were designated pSHELA or pSHELB depending on the orientation of the *SHEL* insert. Further enzyme digests using *Bgl*II, *Bam*HI, *Nco*I and *Kpn*I were performed to confirm constructs. Double digests of pSHELB (400ng per reaction) were performed with appropriate pairs of enzymes to release each individual block to confirm sizes. These were analysed on 2% LMT agarose gels. A confirmed clone of pSHELB was used to prepare DNA by a cesium chloride gradient (Section 2.5) for further use.

3.2.10 Construction of pSHELC

5 μ g pSHELB was digested with *Bam*HI in a 100 μ l volume. The 2.2kb *SHEL* fragment was isolated from a gel slice (Section 3.2.4) and 200ng ligated with 100ng pGEX-2T which had been cut with *Bam*HI and CIP-treated (Section 3.2.5). Ligation was performed at 16 $^{\circ}$ C as in Section 3.2.9 with the appropriate controls. 2 μ l was electroporated into *E. coli* XL1-Blue (Section 2.4) and colonies selected by growth on LB+ampicillin (75 μ g/ml) plates.

Plasmids were isolated by mini-preparations (Section 3.2.6) and screened for the presence and correct orientation of insert by digestion with *Pst*I and analysis on 1% agarose gels. A candidate clone was further analysed by restriction digestion with *Bam*HI, *Nco*I, *Kpn*I, *Hind*III, *Not*I, *Sac*I, *Spe*I

and *Bgl*I to confirm the construct.

3.2.11 Construction of pSHELD

Putative pSHELE clones were further analysed by restriction digestion. 5µg pSHELB was digested with *Nco*I in a total volume of 100µl. The DNA was precipitated and redigested in a 100µl volume with *Bam*HI. The 2.2kb *Nco*I-*Bam*HI *SHEL* fragment was purified from an agarose gel slice (Section 3.2.4). 2µg pTrc99A vector was similarly digested in a 40µl total volume and gel-purified. 100ng pTrc99A was ligated to 50ng *SHEL* fragment as in Section 3.2.9, along with appropriate controls, and electroporated into *E. coli* XL1-Blue (Section 2.4). Transformants were selected on LB+ampicillin (75µg/ml) plates.

Plasmids were purified (Section 3.2.6) from transformants and DNA was digested with *Hind*III to screen for the correct construct. A candidate clone was further assessed by restriction enzyme digestion with *Nco*I, *Bam*HI, *Sac*I, *Hind*III, *Bgl*I, and double digestion with *Nco*I/*Bam*HI.

3.2.12 Construction of pSHELE

2.5µg pND211 was digested with *Nco*I in a 50µl volume and dephosphorylated (Section 3.2.5). 200ng *Nco*I-*Bam*HI *SHEL* fragment (Section 3.2.11) was ligated to 100ng pND211 using 1U DNA ligase (Boehringer Mannheim, Germany) in a 10µl volume at 16°C for eight hours. Since the second *Nco*I site of pND211 is incompatible with the *Bam*HI end of *SHEL*, this end was filled in by adding deoxynucleotide mix to 2mM final concentration, 1U Klenow and 2U DNA ligase (Boehringer Mannheim, Germany) and ligating overnight at 16°C. The reaction was inactivated by heating at 65°C for 20min, diluted twofold with MQW and 2µl electroporated into *E. coli* DH5α (Section 2.4). Transformants were selected by growth on LB+ampicillin

(75µg/ml) plates at 30°C for 48hr. Plasmids were isolated by mini-preparations and screened for correct insert orientation by *Pst*I digestion. Putative pSHELE clones were further analysed by restriction digestion with *Nco*I, *Bam*HI, *Hind*III, *Sac*I and *Pst*I.

3.2.13 Construction of pSHELF

50ng *Nco*I-*Bam*HI SHEL fragment (Section 3.2.11) was ligated with 100ng pET-3d, previously digested with *Nco*I and *Bam*HI, as in Section 3.2.9. 2µl DNA was used to transform *E. coli* HMS174 by electroporation and transformants selected by growth on LB+ampicillin (75µg/ml) plates.

Colonies were grown overnight and plasmid DNA extracted (Section 3.2.6). DNA was digested with *Bam*HI to screen for the correct construct. A candidate clone was partially sequenced using SHEL internal primers 1R and 8F (Section 3.2.7; Appendix 1) to confirm the integrity of the junctions of the insert.

3.2.14 Construction of pSHELF Δ 26A

3.2.14.1 Mutagenesis

The Transformer Mutagenesis Kit (Clontech, USA) was used with pSHELF in accordance with the supplied protocol to remove DNA corresponding to exon 26A. The sequence of the mutagenic primer used (manufactured by Beckman, Australia) was:

5' CGG GTT TCG GTG CTG TTC CGG GCG CGC TGG 3'

which flanked either side of exon 26A by 15bp resulting in its precise

deletion. A second selection primer, which mutates a unique restriction site to another restriction site is normally used in the protocol but was not in this case since deletion of exon 26A also resulted in the deletion of a unique restriction site, *PmlI*. This enzyme was therefore used to digest the mutation reaction to linearise any unmutated parental plasmid and consequently to enrich for mutant plasmid in accordance with the manufacturer's instructions. The reaction mixture was used to transform competent BMH17-18 *mutS* *E. coli*, defective in mismatch repair, by electroporation (Section 2.4) and the entire transformed culture was grown overnight in 5ml LB+ampicillin. Mixed plasmid DNA, containing both mutated and parental plasmids, was isolated from the culture using the Qiagen Spin Plasmid isolation kit and the plasmid DNA was digested with *PmlI* to linearise the parental plasmid. The plasmid DNA, now enriched for mutated plasmid, was used to transform *E. coli* HMS174 by electroporation (Section 2.4) and transformants selected on LB plates containing 75µg/ml ampicillin. Colonies were grown overnight and plasmid mini-preparations performed (Chapter 3.2.6). Constructs were screened using *PmlI* and those which were insensitive to digestion were further screened by *KpnI/PstI* double digestion. Candidate clones were sequenced manually using 6F and 7R primers (Appendix 1) to confirm sequence integrity either side of the deleted region (Section 3.2.7). Automated sequencing (Section 3.2.8) using primers 1R, 3F, 3R, 5R, 6F, 7R, pET forward and pET reverse (Appendix 1) was performed to verify the rest of the sequence. A number of undesired mutations were discovered (see Results) necessitating further manipulations to the DNA, now named pSHELFAmod.

3.2.14.2 Restriction Enzyme Digestion and Ligation

Sequencing confirmed the region immediately surrounding the deletion was correct. *Pst*I and *Bss*HII restriction sites surrounding the correct region of pSHELFA Δ mod were used to remove the desired segment and re-insert it into the corresponding site of pSHELFA. Figure 3.3 describes the construction scheme. 6.5 μ g pSHELFA and 7.5 μ g pSHELFA Δ mod were digested with *Bss*HII, precipitated and digested with *Pst*I. The appropriate three fragments (Figure 3.3) were gel-purified (Section 3.2.4) and ligated using 1U DNA ligase (Boehringer Mannheim, Germany) overnight at 16°C. DNA was transformed into *E. coli* XL1-Blue (Section 2.4) and transformants selected on plates containing 75 μ g/ml ampicillin.

Plasmids were isolated by mini-preparations (Section 3.2.6) and screened using *Bgl*II digestion. A candidate clone was further analysed by restriction enzyme digestion and automated sequencing was then performed (Section 3.2.8) using primers 1R, 3F, 3R, 5R, 6F, 7R, and T7 forward (Appendix 1) to confirm the entire sequence. The correct sequence was designated pSHELFA Δ 26A.



Figure 3.3 Construction scheme for pSHELFA Δ 26A. pSHELFA and the aberrant pSHELFA Δ mod were both digested with *Spe*I and *Bss*HII. *Bss*HII cuts both plasmids twice and *Spe*I once resulting in three fragments. The 5424 and 946bp fragments from pSHELFA and the small 388bp fragment from pSHELFA Δ mod were purified from agarose gels. The 5424bp fragment was CIP treated to reduce recircularisation and the three fragments ligated overnight at 16°C using DNA ligase. The final product, pSHELFA Δ 26A contained the desired deletion of exon 26A from the SHEL gene with no other mutations.

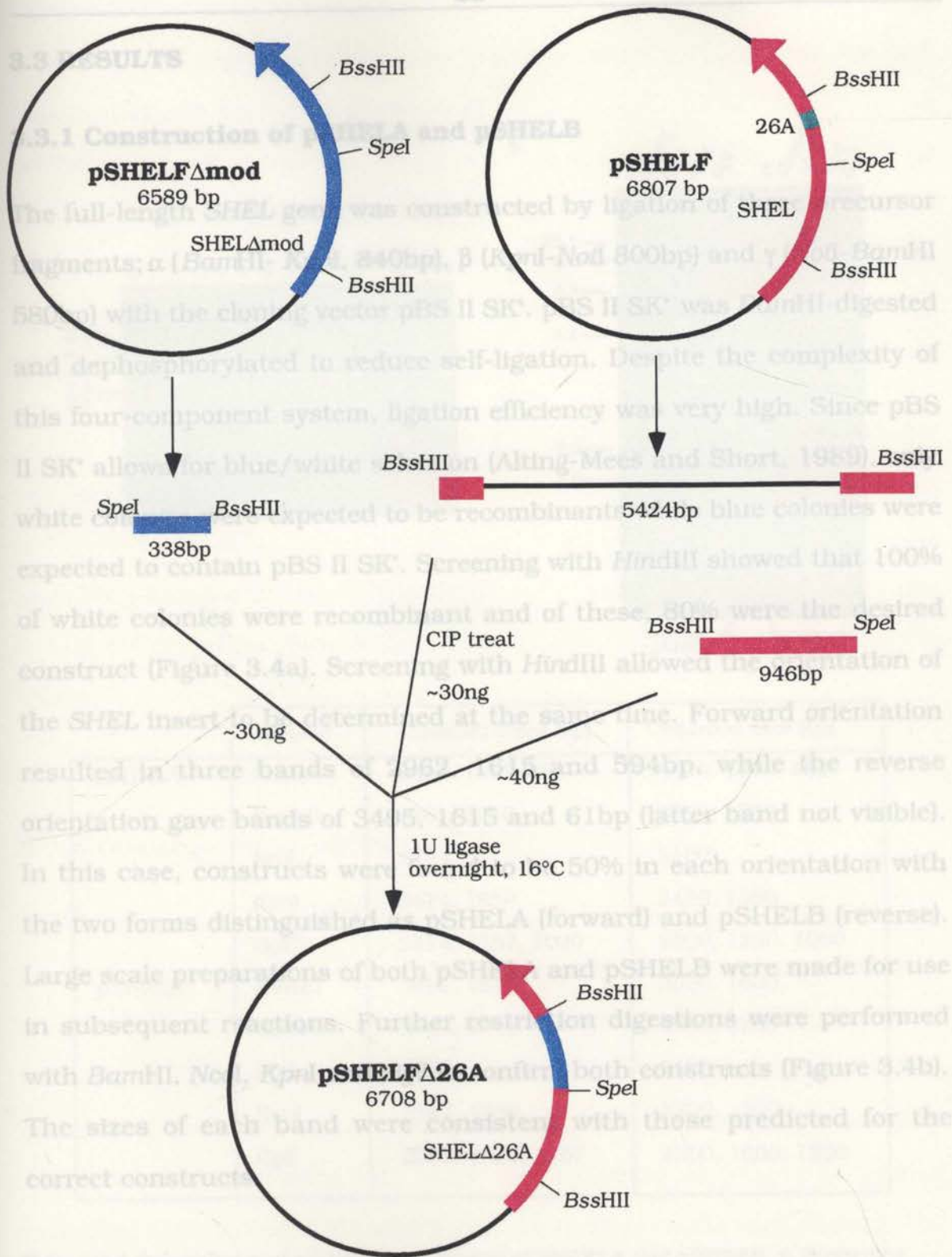


Figure 3.3 Construction scheme for pSHELF Δ 26A. pSHELF and the aberrant pSHELF Δ mod were both digested with *SpeI* and *BssHII*. *BssHII* cuts both plasmids twice and *SpeI* once resulting in three fragments. The 5424 and 946bp fragments from pSHELF and the small 338bp fragment from pSHELF Δ mod were purified from agarose gels. The 5424bp fragment was CIP treated to reduce recircularisation and the three fragments ligated overnight at 16°C using DNA ligase. The final product, pSHELF Δ 26A contained the desired deletion of exon 26A from the SHEL gene with no other mutations.

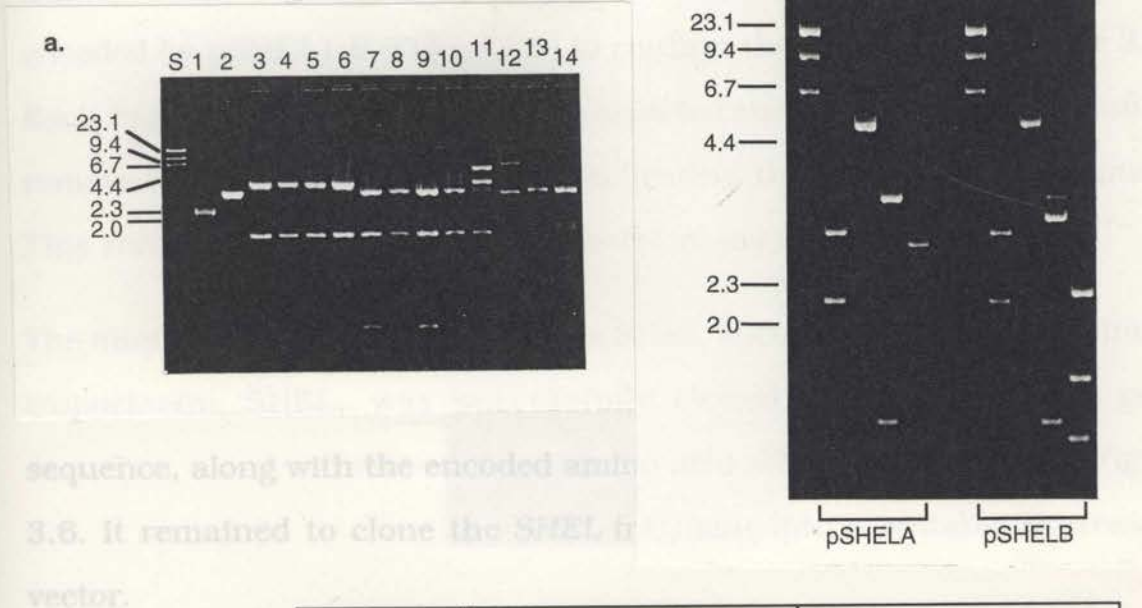
3.3 RESULTS

3.3.1 Construction of pSHELA and pSHEL B

The full-length *SHEL* gene was constructed by ligation of three precursor fragments; α (*Bam*HI- *Kpn*I, 840bp), β (*Kpn*I-*Not*I 800bp) and γ (*Not*I-*Bam*HI 580bp) with the cloning vector pBS II SK⁺. pBS II SK⁺ was *Bam*HI-digested and dephosphorylated to reduce self-ligation. Despite the complexity of this four-component system, ligation efficiency was very high. Since pBS II SK⁺ allows for blue/white selection (Alting-Mees and Short, 1989), only white colonies were expected to be recombinants while blue colonies were expected to contain pBS II SK⁺. Screening with *Hind*III showed that 100% of white colonies were recombinant and of these, 80% were the desired construct (Figure 3.4a). Screening with *Hind*III allowed the orientation of the *SHEL* insert to be determined at the same time. Forward orientation resulted in three bands of 2962, 1615 and 594bp, while the reverse orientation gave bands of 3495, 1615 and 61bp (latter band not visible). In this case, constructs were found to be 50% in each orientation with the two forms distinguished as pSHELA (forward) and pSHEL B (reverse). Large scale preparations of both pSHELA and pSHEL B were made for use in subsequent reactions. Further restriction digestions were performed with *Bam*HI, *Nco*I, *Kpn*I and *Bgl*I to confirm both constructs (Figure 3.4b). The sizes of each band were consistent with those predicted for the correct constructs.

Figure 3.4 Screening and restriction mapping of pSHELA and pSHEL B. a. Screening for pSHELA and pSHEL B using *Hind*III. Lane 1 contains pBS II SK⁺ control and lane 2 pBS II SK⁺ cut with *Hind*III. Lanes 3-6 correspond to pSHEL B and lanes 7-10 to pSHELA. Lanes 11 and 12 are aberrant clones while lanes 13 and 14 (both blue colonies) correspond to recircularised pBS II SK⁺. b. A clone of pSHELA and pSHEL B was digested with the enzymes indicated. The fragments generated were found to correlate closely with the predicted sizes. λ /*Hind*III size markers (S) are shown in kb.

it was noticed that two of the eight putative constructs had lost the *Nof* recognition site (not shown). Further performed to ensure that all other res intact. Double digests were performed



	Enzyme	Expected Sizes (bp)	Observed Size (bp)
pSHELA	<i>Hind</i> III	2962, 1615, 594	3000, 1600, 600
	<i>Bam</i> HI	2961, 2210	2950, 2200
	<i>Nco</i> I	5171	5100
	<i>Kpn</i> I	3474, 1359	3450, 1350
	<i>Bgl</i> II	2814, 1267, 1090	2800, 1250, 1050
pSHELB	<i>Hind</i> III	3496, 1615	3500, 1600
	<i>Bam</i> HI	2961, 2210	2950, 2200
	<i>Nco</i> I	5171	5100
	<i>Kpn</i> I	3167, 1359	3200, 1350
	<i>Bgl</i> II	2283, 1621, 1267	2300, 1600, 1250

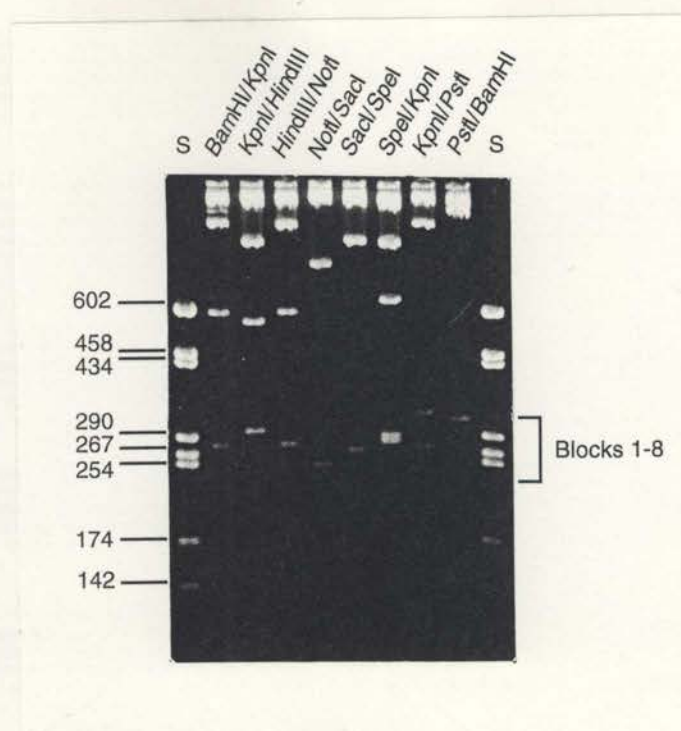
Figure 3.4 Screening and restriction mapping of pSHELA and pSHELB. **a.** Screening for pSHELA and pSHELB using *Hind*III. Lane 1 contains pBS II SK⁺ control and lane 2 pBS II SK⁺ cut with *Hind*III. Lanes 3-6 correspond to pSHELA. Lanes 7-10 correspond to pSHELB and lanes 11-14 (both blue colonies) correspond to recircularised pBS II SK⁺. **b.** A clone of pSHELA and pSHELB was digested with the enzymes indicated. The fragments generated were found to correlate closely with the predicted sizes. λ /*Hind*III size markers (S) are shown in kb.

It was noticed that two of the eight putative constructs had lost the *NotI* recognition site (not shown). Further digestion of a pSHEL B clone was performed to ensure that all other restriction sites used in cloning were intact. Double digests were performed to release each individual block, as encoded by pSHEL1-8 (Figure 3.1) to confirm the size of each (Figure 3.5). Each fragment was found to be of the expected size and could be successfully removed by restriction digestion, indicating that the sites were intact. This verified clone of pSHEL B was therefore used in further cloning.

The intact synthetic tropoelastin gene *SHEL*, encoding an isoform of human tropoelastin, *SHEL*, was successfully cloned. The intact *SHEL* gene sequence, along with the encoded amino acid sequence is shown in Figure 3.6. It remained to clone the *SHEL* fragment into a suitable expression vector.

3.3.2 Construction of pSHEL C

SHEL, removed from pSHEL B with *Bam*HI, was ligated into the *Bam*HI site of the expression vector pGEX-2T. Plasmid DNA from transformants was screened using *Pst*I which allowed *SHEL*-containing clones to be identified and, importantly, distinguished reverse and forward orientations of the *SHEL* insert which was vital for subsequent expression. Approximately 15% contamination with pBS II SK⁺ was expected as judged by plating transformations onto IPTG and X-Gal containing media (not shown). *Pst*I screening showed that 1 out of 10 colonies contained pBS II SK⁺ and 2 out of 10 colonies contained *SHEL* insert, with one forward (5.9, 1.3kb) and one reverse (3.2, 4.0kb) orientation identified (Figure 3.7a).

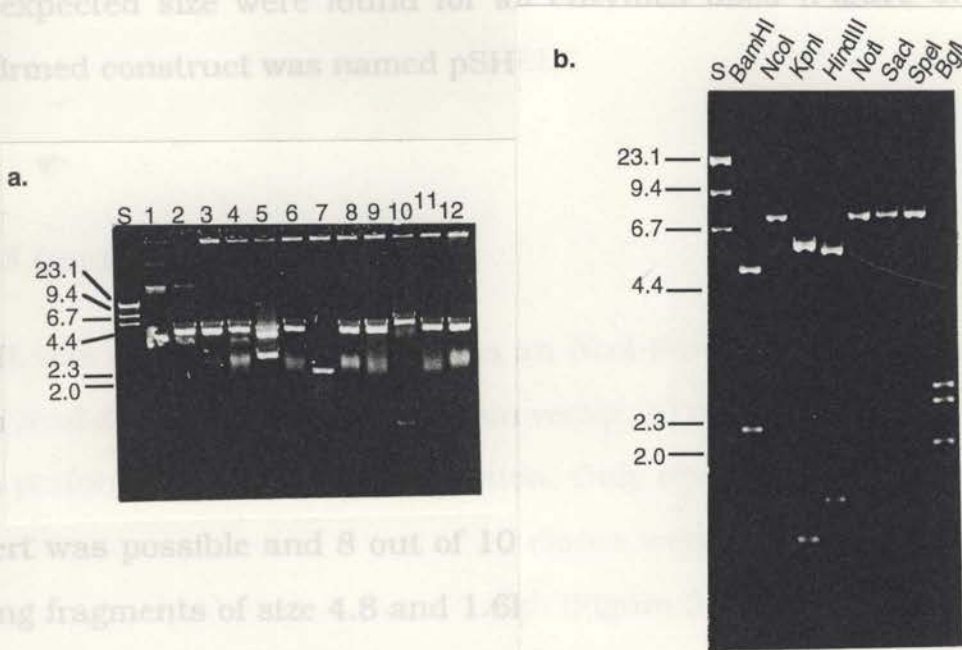


Block No.	Enzymes	Expected Size (bp)	Observed Size (bp)
1	<i>Bam</i> HI/ <i>Kpn</i> I	276	278
2	<i>Kpn</i> I/ <i>Hind</i> III	288	295
3	<i>Hind</i> III/ <i>Not</i> I	271	278
4	<i>Not</i> I/ <i>Sac</i> I	250	250
5	<i>Sac</i> I/ <i>Spe</i> I	261	267
6	<i>Spe</i> I/ <i>Kpn</i> I	289	288
7	<i>Kpn</i> I/ <i>Pst</i> I	269	270
8	<i>Pst</i> I/ <i>Bam</i> HI	306	310

Figure 3.5 Release of individual blocks from pSHELB. Individual blocks were released from pSHELB by double digestion using the enzymes indicated. The size of each block was compared with pBS II SK⁺ / *Hae*III size markers (S, shown in bp) and found to correlate closely with the predicted block size.

BamHI 1 NcoI A G C T G C T T A T A A C T T G T C A C T A A A G T A C T T 120
 GATCCATGGGTGGCGTTCCGGGTGCTATCCGGGTGGCGTTCGGGTGGTATTCTACCCAGGCGGGGTCTGGTGCACCTGGGCGGTGGCGCTGGCCCCGGTGGTAAACCGCTGA
 GTACCCACCGCAAGGCCACGATAGGCCACCGCAAGGCCACCCACATAGATGGTCCGCGCCAGAGCCACGTCACCCGCCACCGGACCCGGGCCACCATTGGCGACT 26 27
 S M G G V P G A I P G G V P G G V F Y P G A G L G A L G G G A L G P G G K P L K
 G A C A G T G C T G G C C C A T G G T A G T T A C T 240
 AACCGTTCAGGCGGTTCGGCAGGTGCTGGTCTGGTGCAGGTCTGGGCGGTTCGCCGTTACCTTCGGGTGCTCTGGTTCGGGTGGCGTTGCAGACGACGTCTGCCTACA
 TTGGCCAAGTCCCGACCGCTCCACGACCCAGCCAGTCCAGACCCCGCAAGGCCGCCAATGGAAGGCCACGAGACCAAGGCCACCGCAACGCTCTGGCTGCAGCAGCATGT 28
 P V P G G L A G A G L G A G L G A F P A V T F P G A L V P G G V A D A A A A Y K
 T T T C T G T T T C A T C T A A G A T G G T T T A C A G G T G G G 4
 AAGCGCAAGGCGAGTTCGGGTCTGGGCGGGTACAGGTGTGGCGGTCTGGTGTATCTGGCGCAGTGTTCGGCAGCCGGTGCAGGTGTAACCGGGCAAAGTTCAGGTG 360
 TTGCGGTTTCCTGTCACGCCAGCCCGCCATGGTCCACAACCCGACCCACATAGACGACCGGTCAACAAGGCGTCCGGCCACGTCACATTTCGGCCGTTTCAGGTCCAC
 A A K A G A G L G G V P G V G G L G V S A G A V V P Q P G A G V K P G K V P G V 29
 G G A T A C G C A A T G C G G G C T A C T A A G C T T 5 6
 TTGGTCTCGCGGCGTATACCGGGTGGTGTCTGCGGGCGCGCTTCCAGGTGTTGGTACTGCGGGCGTTCGACCGGTGCAGGTGTTAAACCGAAGCCACAGGTGTAGCGG
 AACGACAGCGCCGCATATGGGCCACCAAGACGGCCCGCGCAAGGGTCCACAACACATGACGGCCCGCAAGGCTGGCCACGTCACAATTGGCTTCGGTGTCCACATCCGC 30 31
 G L P G V Y P G G V L P G A R F P G V G V L P G V P T G A G V K P K A P G V G G
 A T T T A A A A C T G A A T A C A G T C G C C G T A C A 7
 GCGGTTTCGGGGTATCCCGGGTGTGGCCGTTTCGGTGGTCCGACGAGCGGTTCCGCTGGGTACCCGATCAAAGCGCCGAAGCTTCAGGTGGCTACGGTCTGCCATACACCACCG 600
 CGCGCAAGGCCCATAGGCCCAACCGGGCAAGCCACAGGCGTGGTCCGAAGCGACCAATGGGCTAGTTTCGGCGCTTCGAAGTCCACCGATGCCAGACCGCATGGTGGC 32
 A F A G I P G V G P F G G P Q P G V P L G Y P I K A P K L P G G Y G L P Y T T G
 G C T T G C A A G T A C G T T A G A G C C A A A G A T A 8
 GTAAACTCCGCTACGGCTACGGTCCGGGTGGCGTAGCAGGTGCTGCGGGTAAAGCAGGCTACCAACCGGTACTGGTGTGGTCCGAGGTGTCGCGCAGCTGCGCGAAGCCAGCAG 720
 CATTGACGGCATGCCAGTCCAGGCCACCGCATCGTCCAGACGCCCATTCGTCCTAGGGTGGCCATGACCAACAACCGCGTCCGACGACCGCGTCCGCTCGTC 33
 K L P Y G Y G P G G V A G A A G K A G Y P T G T G V G P Q A A A A A A K A A A
 G T T A C A C C T T T A G T T C G T G A T T A T A C T G A T A 9
 CAAAATTCGGCGCGGGTGCAGCGGGTGTCTGCGGGCGTAGGTGGTGGCTCCGGGTTCAGGTGCGATCCCGGCATCGGTGGTATCGCAGGCGTAGTACTCCGGCGGGCG 840
 GTTTAAGCCGCGCCACGTCGCCCCAAGACCGCCCATCCACACGACCGCAAGGCCACAAGTCCAGCTAGGGCCGTAGCCACCATAGCTCCGCATCCATGAGGCCCGCCCGC 34
 K F G A G A A G V L P G V G G A G V P G V P G A I P G I G G I A G V G T P A A A
 A A A C T G C G T A T T T A G T G T C A A T T C A A C A T 10 11
 CTGCGGCTGCGCAGCTCGCGGAAAGCAGCTAAATACGGTCCGGCAGGCGCTGGTTCGGGTGGTCCAGGCTTCGGCGGGTGTAGGCGTTCGGGTGCTGGTGTCCGGCGG
 GACGCCGACCGGTGCGACCGCGTTCGCTGATTTATGCCACGCGCTGCTCGGACCAAGGCCACCAAGTCCGAAGCCAGCCCAACAATCCGCAAGGCCACGACCAAGGCCCGC 960
 A A A A A A K A A K Y G A A A G L V P G G P G F G P G V V G V P G A G V P G V 35 36
 T C A T G T A C A T G A T G G A A A T A A G A C 12
 TAGGTGTTCCAGGTGCGGGCATCCCGGTTGACCGGGTGCAGGTATCCCGGGCGTCCGGTTCAGGTGTTGTATCCCGGAAAGCGGAGCTAAGGCTGCTGCGAAAGTGCAGAAATACG 1080
 ATCCCAAGGTCCACGCGCTAGGGCCAAATGGCCACGTCATAGGGCCCGGACGCGCAAGGTCACAACATAGGGCCCTTCGCGCTGATTCGACGACGCTTTCGACGCTTTATGC 37
 G V P G A G I P V V P G A G I P G A A V P G V V S P E A A A K A A A K A A K Y G
 G G C A C A A T T T G T A T G C T C C T T C A C A T T A C A C T A G C 13 14
 GAGTCTGTCGGGCGTGGTGTGGTGGCATCCCGACCTACGGTGTAGGTGCAGGCGGTTCCAGGTTTCGGCGTGTGGTGGTGGTATCCCGGGTGTAGTGGTTCGCTGTGTTG 1200
 CTCGAGCAGGCCCGCAACCAACACCGTAGGGCTGGATGCCATCCACGTCGCGCAAGGGTCCAAAGCCGCAACCAACACCGTAGGGCCACATCGACCAAGGCCAGACAAAC 38 39
 A R P G V G V G G I P T Y G V G A G G F P G F G V G V G G I P G V A G V P S V G
 A T T C A C A T C G A T C T C T A T C C G T C A G G C A A T 15
 GTGGCGTACCGGGTGTGGTGGCGTTCAGGTATCTCCCGAAGCGCAGGACGCTGCGGCAGCTAAAGCAGCAAGTACGGCGTGGTACTCCGGCGGCGAGCAGTGCFAAAG 1320
 CACCGCATGGCCCAACCCAGCGAGTCCACATCCATAGAGGGGCTTCGCGTCCGTCGACGCGCTGATTTCTGCTGCTTCATGCCGCAACCATGAGGCCCGCTGCTGCAGCATTC 40
 G V P G V G A G V P G V G I S P E A Q A A A A A K A A K Y G V G T P A A A A A K A
 C C C C T T T T C C G T T A G T T C G T A T C T T T A G 16
 CAGCGGCTAAAGCAGCGAGTTCGGACTAGTTCGGGCGTAGGTGTTGCGCAGGTGTGGCGTAGCAGCGGTTGGTGTGCTCCGGCGTAGGTCTGGCACCGGGTGTGGCGTTG 1440
 GTCGCCGATTCGTCGCGTCAAGCTGATCAAGGCCCGCATCCACAACCGGTCCACAACCGCATCGTGGCCCAACCAACAGGCGCCCATCCAGACCGTGGCCCAACCGCAAC 41 42 43
 A A K A A Q F G L V P G V G V A P G V G V A P G V G V A P G V G L A P G V G V A
 T T A T G T T C G T C C T T A A A A C C G C C C A T 17 18
 CAGCAGGTAGGTGTTGGCGGGCGTGGTGTAGCACCGGGTATCCGTCGGGTGGCGTTCGGGCTGCTGCGAAATCTGCTGCAAGGTGTGCTGCGAAAGCGCAGCTGCTGCAGCAG 1560
 GTGGTCCACATCCACAACCGCGCCGCAACACATCGTGGCCATAGCCAGGCCACCGCAAGCGCAGCAGCTTTAGACGAGCGCTTCAACGACGCTTTCGCGTCGACGACGCTGCT 42 43
 P G V G V A P G V G V A P G I G P G G V A A A A K S A A K V A A K A Q L R A A A

The clone containing SHEL in the forward orientation was subjected to further restriction enzyme digestion with a range of enzymes. Bands of the expected size were found for all enzymes used (Figure 3.7b). The confirmed construct was named pSHEL.



Enzyme	Expected Size (bp)	Observed Size (bp)
<i>Pst</i> I	5881, 1277	5900, 1277
<i>Bam</i> HI	4948, 2210	5000, 2200
<i>Nco</i> I	7215	7200
<i>Kpn</i> I	5799, 1359	5800, 1800
<i>Hind</i> III	5543, 1615	5600, 1675
<i>Not</i> I	7215	7200
<i>Sac</i> I	7215	7200
<i>Spe</i> I	7215	7200
<i>Bgl</i> II	2643, 2462, 2053	2675, 2500, 2050

Figure 3.7 Screening and restriction mapping of pSHEL. **a.** Screening for pSHEL using *Pst*I. Lane 1 is uncut pGEX-2T control and lane 2 pGEX-2T cut with *Pst*I. Of the clones screened, lane 5 contains SHEL in the inverted orientation in pGEX-2T with fragments of size 3181 and 3977bp, lane 7 is recircularised pBS II SK⁺ of fragment size 2961bp and lane 10 contains pSHEL. The other clones are recircularised pGEX-2T. **b.** pSHEL was digested with the enzymes indicated. Each of the fragments generated corresponded closely with the predicted sizes as shown above. λ /*Hind*III size markers (S) are shown in kb.

The clone containing *SHEL* in the forward orientation was subjected to further restriction enzyme digestion with a range of enzymes. Bands of the expected size were found for all enzymes used (Figure 3.7b). The confirmed construct was named pSHELc.

3.3.3 Construction of pSHELD

SHEL was excised from pSHELb as an *NcoI*-*Bam*HI fragment and ligated with *NcoI*-*Bam*HI digested expression vector, pTrc99A. Screening of clones was performed using *Hind*III digestion. Only one orientation of the *SHEL* insert was possible and 8 out of 10 clones were found to contain *SHEL*, giving fragments of size 4.8 and 1.6kb (Figure 3.8a). A positive clone was further screened by digestion with a range of enzymes. The correct fragment sizes were seen for each digestion (Figure 3.8b) confirming a correct construct which was named pSHELD.

Enzyme	Size (bp)	Observed Size (bp)
<i>NcoI</i>	6356	6500
<i>Bam</i> HI	6356	6500
<i>NcoI/Bam</i> HI	4176, 2210	4200, 2200
<i>Sac</i> I	6356	6500
<i>Hind</i> III	4690, 1616	4650, 1600
<i>Bgl</i> II	3771, 2585	3800, 2550

Figure 3.8 Screening and restriction mapping of pSHELD. a. Screening for pSHELD with *Hind*III. Lane 1 contains control pTrc99A cut with *Hind*III. Lanes 4, 5, 7, 8, 9, 10 and 11 are pSHELD while the other lanes contain pTrc99A. b. A candidate pSHELD clone was digested with the enzymes indicated. Each of the fragments generated corresponded closely with the sizes predicted. λ /*Hind*III size markers (S) are shown in kb.

3.3.4 Construction of pSHELE

Due to the more complex ligation of *NcoI*-*Bam*HI *SHEL* fragment into a single *NcoI* site of pND211 which involved an end-filling step, it was expected that ligation efficiency would be low. CIP treatment of pND211 was highly effective in reducing the number of background colonies by over 99% (not shown). Despite this, the number of transformants from *SHEL*-pND211 ligation was fivefold lower than for pND211 controls. 2 out of 35 transformants were found to contain insert after *Pst*I screening, both in the forward orientation (Figure 3.9a). 3267 and 2988bp fragment sizes were expected but the smaller fragment size was slightly different in the two putative clones necessitating further digestions to confirm if either was correct. *Hind*III digestion of the first clone (c16) indicated that one site was missing as 2.7 and 1.3kb fragments were not present (Figure 3.9b). This pattern was consistent with a deletion at the 3' end of *SHEL* and also correlated with the smaller than expected sizes of fragments generated by *Pst*I and *Bam*HI. *NcoI* digestion also appeared not to be taking place at either site.

The second clone (c17) gave the correct fragment sizes with *Hind*III and *Bam*HI but again failed to cut with *NcoI* (Figure 3.9c). Preliminary results indicated that the ATG start codon contained within the first *NcoI* sequence was intact, however, (Chapter 4) and c17 named pSHELE. No further clones could be isolated even from a fresh ligation and the search for a fully intact pSHELE clone was abandoned.

Figure 3.9 Screening and restriction mapping of pSHELE clones. **a.** Screening for pSHELE with *Pst*I. Lane 1 contains control pND211 digested with *Pst*I. Of the others, only lanes 7 and 8 are putative positive constructs, both with fragments resembling the predicted fragments for pSHELE while the others appear to be recircularised pND211. However, of the two putative pSHELE clones the lower fragments are different size in the two constructs. From the resolution provided by this gel, it is not possible to tell which of the two is the correct pSHELE fragment. **b.** The putative clone from lane 6 in Figure 3.9a (c16) was digested with the enzymes indicated. c16 shows the incorrect pattern for *Hind*III with the expected 2701 and 1349bp fragments absent and an approximately 4100bp fragment present, consistent with a missing *Hind*III site at the 3' end of *SHEL*. *Nco*I did not cut the plasmid at either expected site. *Bam*HI fragments are also smaller than expected with the expected 2228bp fragment estimated at 2050bp. **c.** The second putative clone from lane 7 in Figure 3.9a (c17) gave the expected pattern for *Hind*III as well as correct fragment sizes with the other enzymes also. *Sac*I has not cut to completion on this gel. However, *Nco*I did not cut this construct either while able to cut control pND211 plasmids successfully (not shown). λ /*Hind*III size markers (S) are shown in kb.

3.3.5 Construction of pSHELF

NcoI-*Bam*HI SHELF

Screening of clones

which cuts the ex

12 clones were fou

double digests w

one putative correct clone chosen for sequencing to confirm the integrity

of functions. Sequencing with

expression vector.

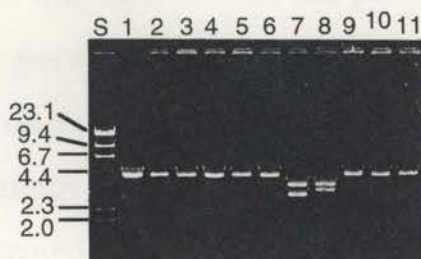
restriction digestion

6.8kb. 10 out of

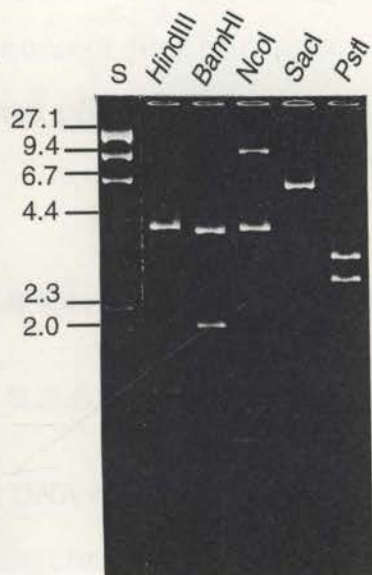
10a). *NcoI*-*Bam*HI

Figure 3.10b) and

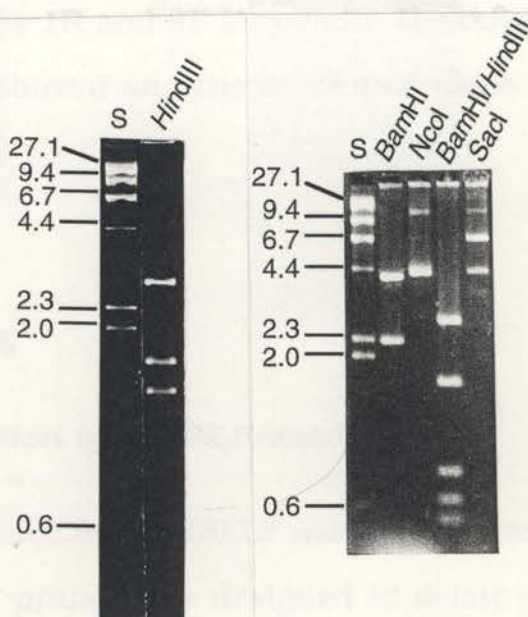
a.



b.



c.



Enzyme	Expected Sizes (bp)	Calculated Sizes (bp)	
		c16	c17
<i>Pst</i> I	3267, 2988	3300, 2800	3300, 3100
<i>Hind</i> III	2701, 1615, 1349, 465, 125	4150, 1600 500	2700, 1600 1300
<i>Bam</i> HI	4002, 2228	4000, 2050	4000, 2200
<i>Nco</i> I	4045, 2210	did not cut	did not cut
<i>Sac</i> I	6255	6000	6500
<i>Bam</i> HI/ <i>Hind</i> III	2645, 1615, 767, 582, 465, 125	not done	2600, 1600, 800 600, 500

that any DNA not susceptible to *Pvu*II would be a candidate 26A deletion clone.

3.3.5 Construction of pSHELF

NcoI-*Bam*HI *SHEL* fragment was ligated with the pET-3d expression vector. Screening of clones was performed using *Bam*HI restriction digestion which cuts the construct once to give a fragment of size 6.8kb. 10 out of 12 clones were found to contain the *SHEL* insert (Figure 3.10a). *NcoI*-*Bam*HI double digests were performed to confirm constructs (Figure 3.10b) and one putative correct clone chosen for sequencing to confirm the integrity of junctions. Sequencing with primers 1R and 8F (Appendix 1) confirmed the correct junction sequence (not shown) and the confirmed clone was named pSHELF.

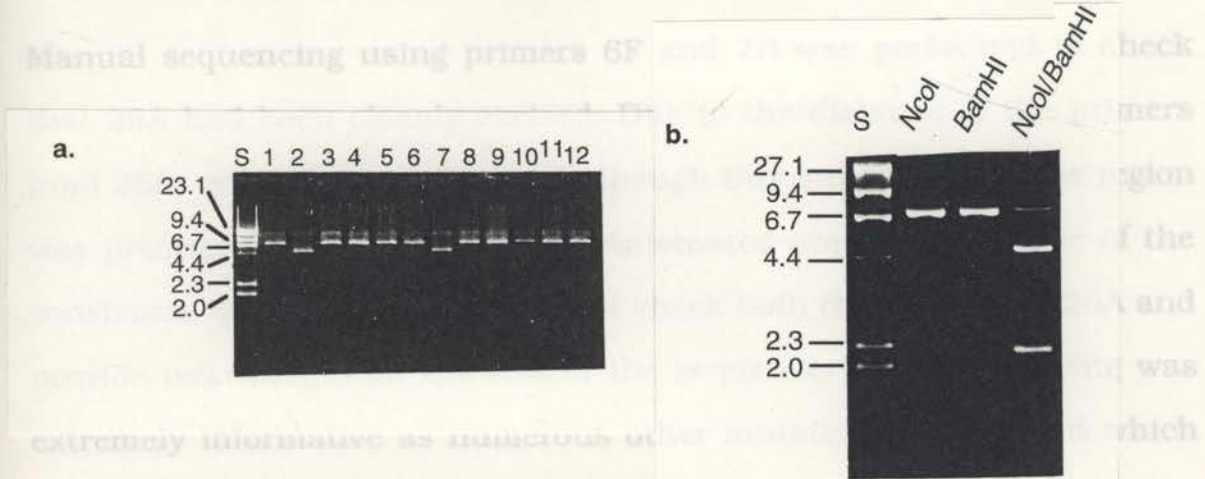
3.3.6 Construction of pSHELF Δ 26A

3.3.6.1 Mutagenesis and Creation of pSHELF Δ modified

The DNA encoding exon 26A was removed from pSHELF using a site-directed mutagenesis procedure. The single primer was designed to delete exon 26A and at the same time removed a unique restriction site, *Pml*I, contained within 26A thus removing the need to use a second selection primer in the mutagenesis reaction. The mutagenesis reaction was carried out alongside a control mutagenesis reaction (using plasmid DNA and primers supplied by the manufacturer) which indicated that 65% of the colonies screened contained the desired mutation (not shown) compared with the manufacturer's specification of 75% thus suggesting that the techniques used were successful. After the final transformation of HMS174 with DNA from the mutagenesis reaction, clones were screened with *Pml*I. Since this site should be removed by successful mutagenesis, it was expected that any DNA not susceptible to *Pml*I would be a candidate 26A deletion clone.

Three putative clones were identified with this method (not shown). These were then double-digested with *Pst*I and *Kpn*I which defined the ends of the block containing 26A. Two of these were found to contain a 170bp fragment indicative of the successful 99bp deletion of 26A instead of the 269bp fragment from unmutated SHEL (not shown).

Manual sequencing using primers 6F and 7R was performed to check



Enzyme	Expected Size (bp)	Observed Size (bp)
<i>Bam</i> HI	6807	6800
<i>Nco</i> I	6807	6800
<i>Nco</i> I/ <i>Bam</i> HI	4597, 2210	4600, 2200

Figure 3.10 Screening and restriction mapping of pSHELf. **a.** Twelve potential clones were screened with *Bam*HI which cuts pET-3d and the pSHELf construct once. Only lanes 2 and 7 contained pET-3d at 4637bp while all the others were consistent with pSHELf. **b.** A candidate pSHELf clone was further analysed with the enzymes shown and resulting fragments corresponded to the sizes expected. λ /*Hind*III size markers are shown in kb (S).

Three putative clones were identified with this method (not shown). These were then double-digested with *Pst*I and *Kpn*I which defined the ends of the block containing 26A. Two of these were found to contain a 170bp fragment indicative of the successful 99bp deletion of 26A instead of the 269bp fragment from unmutated *SHEL* (not shown).

Manual sequencing using primers 6F and 7R was performed to check that 26A had been cleanly excised. Due to the distance of the primers from 26A, only 7R was informative though this indicated that the region was precisely deleted (not shown). Automated sequencing of one of the constructs was therefore employed to check both the excision of 26A and provide information on the rest of the sequence. DNA sequencing was extremely informative as numerous other mutations were found which affected the amino acid sequence outside the targeted region. The interpolated amino acid sequence of this construct compared with *SHEL* is shown (Figure 3.11) and the complete DNA and protein sequence is shown in Appendix 2. The most dramatic mutation was a large 44 amino acid deletion near the N-terminus which was substituted by a three amino acid sequence, FGA. Most of the other changes involved deletion of two to four amino acids and substitution with various related sequences; FGAV, GFGAV, FGA and GFGA which correspond to the amino acids encoded by the deletion primer sequence. Two additional mutations were found - the substitution of Ile at position 7 with Val and a deletion of an Ala just outside the 3' end of 26A. 26A, however, was found to be precisely excised. This aberrant construct was named pSHEL Δ mod.

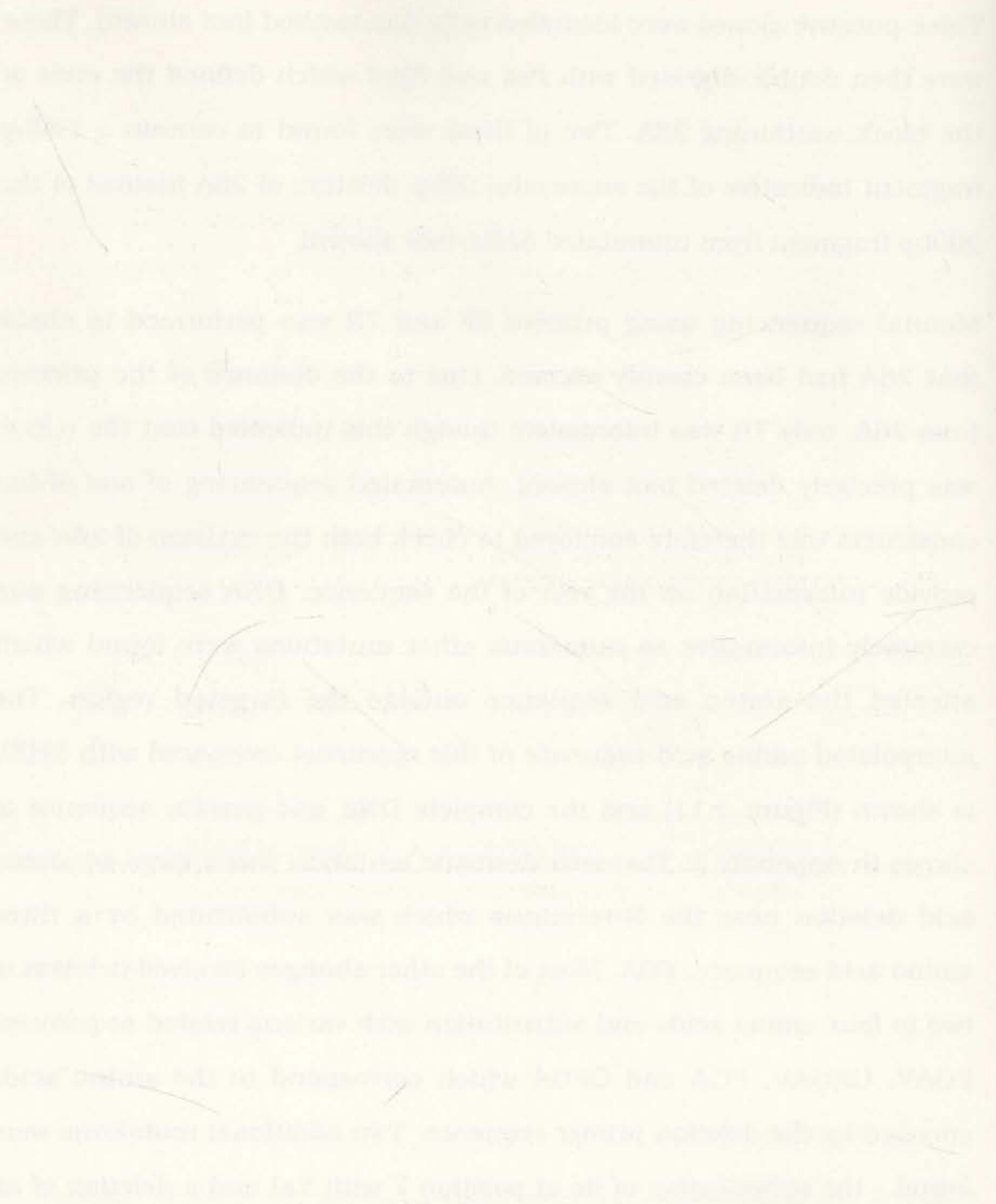


Figure 3.11 Comparison of SHEL and SHELΔmod protein sequence. SHELΔmod amino acid sequence (bottom) is compared with the SHEL amino acid sequence (top). The deletion of 26A from residue 557 to 589 was the desired deletion. A large deletion is present at the N-terminus from residue 22 to 65 and smaller mutations around residues 128, 248, 315 and 340. An Ala is deleted at residue 604 and Ile at residue 7 has been changed to Val.

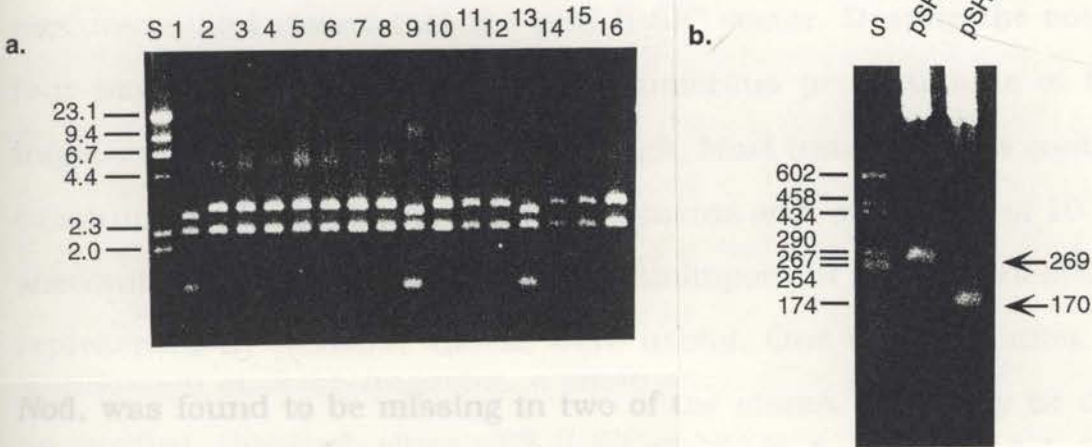
3.3.6.2 Restriction Enzyme Modification of pSHELF and pSHELF Δ 26A

Since 26A was cleanly excised and DNA sequencing showed a correct sequence in the region immediately surrounding the deleted region, it was decided to excise the correct mutated sequence and place it into the corresponding region of pSHELF, to form the correct pSHELF Δ 26A containing *SHEL* with 26A deleted but with otherwise unaltered coding sequence. Appropriate restriction enzyme sites were identified - *Bss*HII which cut 3' to 26A inside the deleted Ala (and once more elsewhere in *SHEL*) and *Spe*I which cut uniquely 5' to 26A. This 338bp fragment contained the desired 26A deletion and no other mutations. The same restriction digests were performed on pSHELF where the 437bp *Bss*HII-*Spe*I fragment was discarded and the other two, a 946bp *Bss*HII-*Spe*I and a 5424bp *Bss*HII fragment were purified. The three fragments were then ligated together to reform *SHEL* with 26A deleted (Figure 3.3). The ligation was complicated by recircularisation of the largest fragment containing sticky *Bss*HII ends and the possibility of inversion of the other two fragments. CIP treatment of the 5424bp *Bss*HII fragment, which contained the entire pET-3d sequence, was effective in reducing self-ligation by 50% (not shown). Using *Bgl*II to screen for correct constructs, 1 out of 42 clones was identified as containing inverted inserts, 1 was an unidentified construct and 3 were the desired constructs (Figure 3.12a). One of the constructs was further digested with *Kpn*I and *Pst*I, which flank exon 26A, and the fragment size was compared to pSHELF (Figure 3.12b). The fragment size correlated closely with that expected from the correct deletion of 26A. Plasmid DNA purified by cesium chloride centrifugation (Section 2.5) this construct was made and the insert was DNA sequenced in its entirety by automated sequencing and found to be the correct pSHELF Δ 26A sequence (Appendix 3).

3.4 DISCUSSION

3.4.1 Construction of SHEL

The full-length tropoelastin gene, SHEL, encoding the distinct isoform SHEL, was successfully constructed and cloned into various expression vectors. The full-length gene was constructed by ligating



Construct	Expected Size (bp)	Observed Size (bp)
pSHELFA26A	2660, 2319, 1495	2600, 2300, 1500
recircularised 'vector'	2871, 2319	2900, 2300

Figure 3.12 Screening for pSHELFA26A. **a.** Potential pSHELFA26A clones were screened with *Bgl*I. Lanes 1, 9 and 13 are candidate pSHELFA26A clones while all the others are 'vector' fragments consisting of recircularised 5424bp *Bss*HI fragment. λ /*Hind*III size markers are shown in kb. **b.** A candidate pSHELFA26A was digested with *Pst*I/*Kpn*I, alongside pSHELFA26A control, to release the block containing exon 26A. The fragment generated from pSHELFA26A was measured as precisely 99bp smaller than the fragment from pSHELFA26A. pBS II SK⁺/*Hae*III size markers (S) are shown in bp.

that unfavourable codon bias should not be a hindrance to high-level expression of SHEL. To our knowledge, SHEL appears to be the largest synthetically produced gene to date (Wagner et al., 1988; Genbank).

3.4 DISCUSSION *SHEL* Into Expression Vectors

3.4.1 Construction of *SHEL*

The full-length tropoelastin gene, *SHEL*, encoding the distinct isoform *SHEL*, was successfully constructed and cloned into a series of expression vectors. The full-length gene was constructed by ligation of three smaller precursors and cloned into the pBS II SK⁺ vector. Despite the complex four-way ligation and possibility of numerous permutations of insert fragments, the ligation efficiency was high. Most transformants contained constructs with the correct order of fragments with only 2 out of 10 being aberrant. Orientation in the vector was unimportant so both orientations, represented by pSHELA and B, were useful. One of the ligation sites, *NotI*, was found to be missing in two of the clones. This may be due to mutation(s) in the 8bp recognition site which exclusively GC-containing. Extensive restriction enzyme digestions confirmed two correct clones, one containing *SHEL* in each possible orientation, with all restriction sites used in the construction of *SHEL* intact and each of the eight individual blocks amenable to individual excision. The DNA sequence of the synthetic gene differs significantly from the natural gene. These differences encode high-use codons in *E. coli* tailoring the gene for high level expression in recombinant *E. coli* systems. The codon adaptation index is an approximate indication of the suitability of a sequence for high-level expression (Sharp and Li, 1987). The natural tropoelastin gene has an index of 0.174 while *SHEL* has an index of 0.754 (Martin *et al.*, 1995). Highly expressed *E. coli* genes typically have an index of >0.45 (Sharp and Li, 1987) indicating that unfavourable codon bias should not be a hindrance to high-level expression of *SHEL*. To our knowledge, *SHEL* appears to be the largest synthetically produced gene to date (Gröger *et al.*, 1988; Genbank).

3.4.2 Cloning of *SHEL* into Expression Vectors

SHEL was cloned into a range of expression vectors to determine the system best suited to recombinant tropoelastin expression. pSHEL C contains *SHEL* inserted into pGEX-2T as a *Bam*HI fragment. *SHEL* is inserted downstream of the gene for GST and this construct was designed for production of *SHEL* as a fusion with GST. Previous work (Indik *et al.*, 1990) suggested unfused recombinant tropoelastin would be unstable in *E. coli* so it was considered important to have a fusion expression system for *SHEL*. pSHEL C cloning was complicated by contamination with pBS II SK⁺. Due to the close size of *SHEL* (2.2kb) and pBS II SK⁺ (2.9kb) when large amounts of DNA were loaded onto the preparatory gel used for purification of *SHEL* fragment, a small amount of pBS II SK⁺ DNA was co-purified. However, since pBS II SK⁺-containing XL1-Blue will appear blue on plates with IPTG/X-Gal it was relatively easy to assess the degree of contamination and the low levels found (10%) did not present any major problems. A correct clone containing forward-oriented *SHEL* and confirmed by extensive restriction enzyme digestion.

Cloning of *SHEL* as an *Nco*I-*Bam*HI fragment into pTrc99A presented no significant problems. The *Nco*I site contains the initiation codon ATG to allow *SHEL* to be expressed as an unfused polypeptide. Since the two cloning ends were incompatible only one possible orientation was possible, greatly facilitating cloning and screening. Again, extensive restriction enzyme digestion confirmed the correct pSHEL D construct.

The cloning of *SHEL* into the pND211 expression vector resulted in numerous problems. This ligation was more difficult since pND211 contains an *Nco*I cloning site which was incompatible with the *Bam*HI end of *SHEL*. There are two *Bam*HI sites within pND211. However, they flank the *Nco*I site and are therefore not able to be used for cloning if the *Nco*I site

is to be utilised for direct expression (N. Dixon, personal communication). End-filling was therefore necessary after the initial *NcoI* ligation to fill the two remaining incompatible ends and allow a blunt-end ligation to take place. Since this is a multi-step process a low efficiency of ligation was expected. From control ligations it was apparent that end-filling and blunt-end ligation greatly reduced the overall number of transformants indicating that the ligation reaction was very inefficient, despite excess ligase added. Two putative clones were found but the size of the smaller of the two fragments (expected to be 2988bp) produced after *PstI* screening was different in the two clones. Since it was difficult to tell by agarose electrophoresis which, if either, of these was correct, further digestions were necessary. The first, c16, was found to have further incorrectly sized fragments with other restriction enzymes also. The pattern found was consistent with a truncation at the 3' end of *SHEL* reducing the overall size by approximately 200bp, as determined by agarose gel electrophoresis. This clone also appeared to have lost both *NcoI* recognition sites.

The second putative clone, c17, appeared correct as judged by restriction enzyme digestion but again did not cut with *NcoI*. End-filling and blunt end ligation was expected to reform an *NcoI* site at the 3' end while the 5' *NcoI* should have reformed by simple ligation. However, it is possible that inappropriate end-filling at the 5' end may have occurred which would remove one base eliminating the *NcoI* site. Similarly, partial end-filling at the other site may still allow ligation to occur but eliminate the *NcoI* recognition site. Preliminary expression work suggested that the start ATG codon which is part of the *NcoI* recognition site, was intact and able to direct expression (Section 4.3.3). The actual nature of the junctions can be determined by DNA sequencing but this was not pursued since two other unfused *SHEL* constructs were available. Thus pSHELE was kept in reserve for use if needed **only**.

Cloning of *SHEL* into pET-3d as an *NcoI*-*Bam*HI fragment, again to direct expression as the native sequence, was a straightforward exercise. This was also a simple directed ligation with only one orientation possible resulting in over 80% of colonies containing the desired construct. DNA sequencing of both junctions confirmed the integrity of the construct, named pSHELF.

3.4.3 Construction of *SHEL*Δ26A Isoform

The construction of the *SHEL*Δ26A isoform encoding tropoelastin with exon 26A deleted, was not as straightforward as anticipated. The mutagenesis reaction was performed using a commercial kit with a primer designed to eliminate 26A from pSHELF. At the same time, a unique restriction site, *PmlI*, was removed. Ordinarily, with this two primer method a second primer is used to create a selectable mutation elsewhere in the plasmid by mutating a unique restriction. This allows linearisation of any unmutated plasmids by the selected restriction enzyme thus greatly increasing the proportion of circular mutated plasmids for transformation. Since the mutagenic primer in this work destroyed an unique *PmlI* restriction site, a second primer was unnecessary in this case. Thus digesting the mutation reaction with *PmlI* would enrich for those plasmids which would consequently contain the desired deletion also.

Two clones were found to be missing 26A. However, the one chosen for sequence analysis was unexpectedly found to be extensively mutated in regions outside the target sequence. The majority of the mutations resulted in the substitution of amino acids with GFGAV-related peptides. This is the peptide sequence encoded by the 5' end of the mutagenic primer suggesting that inappropriate primer binding was the cause of the unwanted

mutations. The other two mutations were an Ile(7)Val substitution encoded by a single base change and the deletion of an Ala caused by the precise deletion of an Ala codon.

Given that additional mutations arose due to incorrect priming during mutagenesis, it was envisaged that further attempts might yield similar results. Each clone found would need to be thoroughly sequenced to ensure no mutations and this would be a costly and time-consuming exercise if the mutation frequency was high as suggested by the present results. DNA sequencing confirmed that in the construct examined 26A was cleanly excised and that the immediate surrounding sequences were intact. Therefore, it was considered faster and more convenient to use carefully selected restriction enzyme sites to remove this correct region containing the desired mutation from pSHELF Δ mod and to insert it into the corresponding region of pSHELF, resulting in the formation of *SHELA26A*. Fortuitously, an enzyme site, *Bss*HIII, was located in the very short space between the 3' end of the 26A region and the Ala deletion which cut only in one other site in pSHELF. All other enzyme sites in this region were multiple cutters and could not be used. There was a large stretch of unmutated DNA 5' to 26A allowing a greater choice of sites in this region. *Spe*I was chosen as it cut uniquely in pSHELF and when used in conjunction with *Bss*HIII gave fragments of convenient size.

Using these two enzymes it was straightforward to remove the *Spe*I-*Bss*HIII fragment containing the 26A deletion from pSHELF Δ mod and religate it into pSHELF. Since the ligation involved three fragments, the largest of which could recircularise to form a viable plasmid, it was very important to dephosphorylate this 'vector' fragment. Although the ligation was not highly efficient, a number of correct clones were isolated resulting in the formation of a plasmid containing the sequence for a second isoform of

human tropoelastin, *SHELΔ26A*. This isoform was only cloned in pET-3d as this construct had been determined as the most favourable to expression with *SHEL* (Chapter 4).

CHAPTER 4

3.5 CONCLUSION

Two synthetic genes for two different isoforms of human tropoelastin were cloned, *SHEL* and *SHELΔ26A*, with and without sequences corresponding to exon 26A respectively. *SHEL* was constructed from precursor plasmids as pSHELA and pSHELB. In addition, *SHEL* was cloned into a collection of expression vectors for expression as both a fusion with GST (pSHEL C) and as the native polypeptide (pSHELD, pSHELE and pSHEL F). The *SHELΔ26A* isoform of human tropoelastin was formed by mutagenesis of pSHEL F which resulted in the formation of an aberrant form of *SHEL*, *SHELΔmod*. Subsequent restriction enzyme manipulation and ligation formed the correct *SHELΔ26A*.

CHAPTER 4

**OPTIMISATION OF EXPRESSION OF
GST-SHEL AND SHEL ISOFORMS**

4.1 INTRODUCTION

Previous attempts at expression of unfused recombinant tropoelastin by other workers has resulted in a rapidly degraded product (Indik *et al.*, 1990). Intact tropoelastin isoforms have, however, been produced as fusion proteins albeit in an insoluble form (Indik *et al.*, 1990). Even when expressed as a protein fusion, a portion of bovine tropoelastin still exhibited some degradation (Grosso *et al.*, 1991). Polypeptides which are unstable and rapidly degraded when expressed directly are often rendered stable as fusion proteins (Das, 1990; Goeddel, 1990; Uhlén and Moks, 1990; Marston, 1986) as demonstrated with human tropoelastin (Indik *et al.*, 1990). However, it is still desirable to express SHEL as an unfused protein if possible since this would eliminate the need for subsequent removal of a fusion partner. Given the previous observations, both fusion and direct expression systems were constructed for SHEL (Chapter 3).

Fusions with GST have been routinely used in our laboratory with a variety of proteins resulting in excellent overexpression levels (Riley *et al.*, 1994; S. Bannan and A.S. Weiss, unpublished). Fusions with GST have been reported to increase the solubility of proteins (Smith and Johnston, 1988) making this potentially a good system for SHEL production since previous expression of tropoelastin as a fusion with influenza NS1 protein was found to result in the production of insoluble protein (Indik *et al.*, 1990). The construct pSHEL C under the control of the IPTG-inducible *tac* promoter will allow expression of SHEL as a fusion with GST. SHEL was also cloned into three different systems for unfused expression containing different strong promoters; pSHEL D is under the control of the *trc* promoter and pSHEL F is under the control of the T7 promoter, both of which are IPTG-inducible. pSHEL E is controlled by two tandem λ promoters and is heat inducible. The survey of a variety of different expression systems,

both fusion and direct, should enable the optimal system for overexpression to be chosen resulting in maximum protein yield.

Many recombinant proteins produced in *E. coli* are in the form of insoluble inclusion bodies regardless of whether they are produced as fusions or directly expressed (Marston, 1986; Schein, 1989). It is not known why inclusion bodies form but factors such as lower growth temperature, lower IPTG levels and shorter induction times, can help prevent them (Schein, 1989). Other factors thought to hinder solubility include large stretches of hydrophobic amino acids and a high Pro content in the expressed protein (Schein, 1989) both of which are characteristic of tropoelastin.

The overall level of expression of recombinant genes in *E. coli* can be influenced by an ensemble of factors. Temperature is important and 37°C is usually chosen for growth and expression of most systems but in some cases a lower temperature is used, especially for heat-inducible vectors or to enhance solubility of the recombinant protein (Schein and Noteborn, 1988). The host strain used for expression can be a factor influencing expression levels as well as the type of media used, whether rich or minimal (Ausubel *et al.*, 1990). Stability of the plasmid is vital and inadequate antibiotic levels or unstable plasmids resulting from toxic genes can cause the culture to be overgrown by bacteria not containing the desired plasmid and thus greatly reducing overall expression levels and protein yield, a problem particularly noted with the pET expression system (Studier *et al.*, 1990). The length of time of induction is also important particularly if the protein is produced in a soluble form and is unstable and easily degraded. Poor expression may also result from unfavourable codon bias in the gene of choice (Section 3.1) but since SHEL has been codon-optimised this variable has been removed.

This chapter describes the assessment of each clone, pSHEL C to pSHEL F,

for protein production. Various parameters were altered during growth and induction to find the optimal expression conditions for expression of SHEL both directly and as a fusion protein. Optimised conditions for expression of SHEL from pSHELF were used successfully for SHEL Δ 26A and also the mutant form SHEL Δ mod.

4.2 MATERIALS AND METHODS

4.2.1 *E. coli* Strains

E. coli strains used were from existing laboratory stocks. XL1-Blue, DH5 α and BL21(DE3) are described in Chapter 2.2.

NM522: *supE thi* Δ (*hsdMS-mcrB*) 5 Δ (*lac-proAB*) F'[*proAB*⁺ *lacF* *lacZ* Δ M15]

TG1: *supE hsd* Δ 5 *thi* Δ (*lac-proAB*) F'[*traD*36 *proAB*⁺ *lacF* *lacZ* Δ M15]

4.2.2 Bacterial Growth Media

Stability of pSHELF plasmids was checked by plating cultures just before LB and 2TY are described in Chapter 2.2. Terrific broth (TB) was made according to Sambrook *et al.* (1989). M9LB was 1.0% tryptone, 0.5% NaCl, 0.4% glucose with M9 salts added as described in Studier *et al.* (1990). All media were used with 50 μ g/ml ampicillin.

4.2.3 Small-Scale Expression

A number of variables were altered during experiments to optimise expression. The specific conditions are described within each experiment. In general, optimisation and growth of pSHEL Δ C, pSHEL Δ D, pSHELF,

pSHELF Δ mod and pSHELF Δ 26A was carried out in 5-10ml cultures of media containing 50 μ g/ml ampicillin. Media was inoculated with a single colony of *E. coli* bearing the desired plasmid and grown overnight at the specified temperature with shaking at 280rpm. Cultures were diluted 1/20 into fresh media containing 50 μ g/ml ampicillin and growth monitored spectrophotometrically by absorbance at 600nm (A_{600}). Cultures were induced with the specified amount of IPTG when they reached an A_{600} of approximately 0.8 and growth continued for the times specified with regular readings of A_{600} taken without dilution. One ml samples were taken before and at various times after induction, spun down and resuspended in 200 μ l 1x SDS-PAGE loading buffer for analysis by 8% SDS-PAGE (Section 2.7). Small-scale cultures of pSHELE were grown as above except cultures were initially grown at 30°C and induced by raising the temperature to 42°C.

4.2.4 Plasmid Stability Test

Stability of pSHELF plasmids was checked by plating cultures just before induction, i.e. when the culture reached A_{600} of approximately 0.8. LB plates with no additives or containing 1mM IPTG, 50 μ g/ml ampicillin or both IPTG and ampicillin were used (Studier *et al.*, 1990). The culture was plated at dilutions from 10^5 to 2×10^6 using LB as diluent. Plates were incubated at 37°C overnight and colonies counted.

4.3 RESULTS

4.3.1 Optimisation of pSHEL C Expression

Expression of GST-SHEL from pSHEL C resulted in an overexpressed protein of approximately 88 ± 2 kDa on SDS-PAGE in accordance with the expected 89.9 kDa. To optimise expression conditions, a subset of variables were altered and expression assessed by SDS-PAGE. These variables included IPTG levels, temperature and host strain. For each experiment cells were examined under phase-contrast microscopy (Section 2.3) and in no case was any evidence of inclusion bodies seen.

IPTG at 0.1, 0.5 and 1 mM was used to induce *E. coli* XL1-Blue containing pSHEL C at 30 and 37°C for three hours. Slower growth after IPTG addition indicated expression occurred with all IPTG levels and at both temperatures (Figure 4.1) with no substantial differences seen. Gel analysis indicated that overexpression had occurred to a similar extent in each case (not shown) but expression was generally very poor and inconsistent between repetitions of experiments making further analysis inconclusive. *E. coli* XL1-Blue strain is not usually used as an expression host so experiments were undertaken to determine if other hosts were more effective.

pSHEL C was used to transform into DH5 α , NM522 and TG1 *E. coli* strains by electroporation (Section 2.4). Cultures, grown in 2TY media and induced with 1 mM IPTG, were monitored by spectrophotometry and SDS-PAGE. Gel analysis over several experiments indicated overexpression occurred in all strains with DH5 α clearly the best strain, consistently and selectively producing the most overexpressed protein with XL1-Blue the poorest (Figure 4.2). GST-SHEL expression in DH5 α was estimated at 30% total cell protein by scanning densitometry (Chapter 2.10).

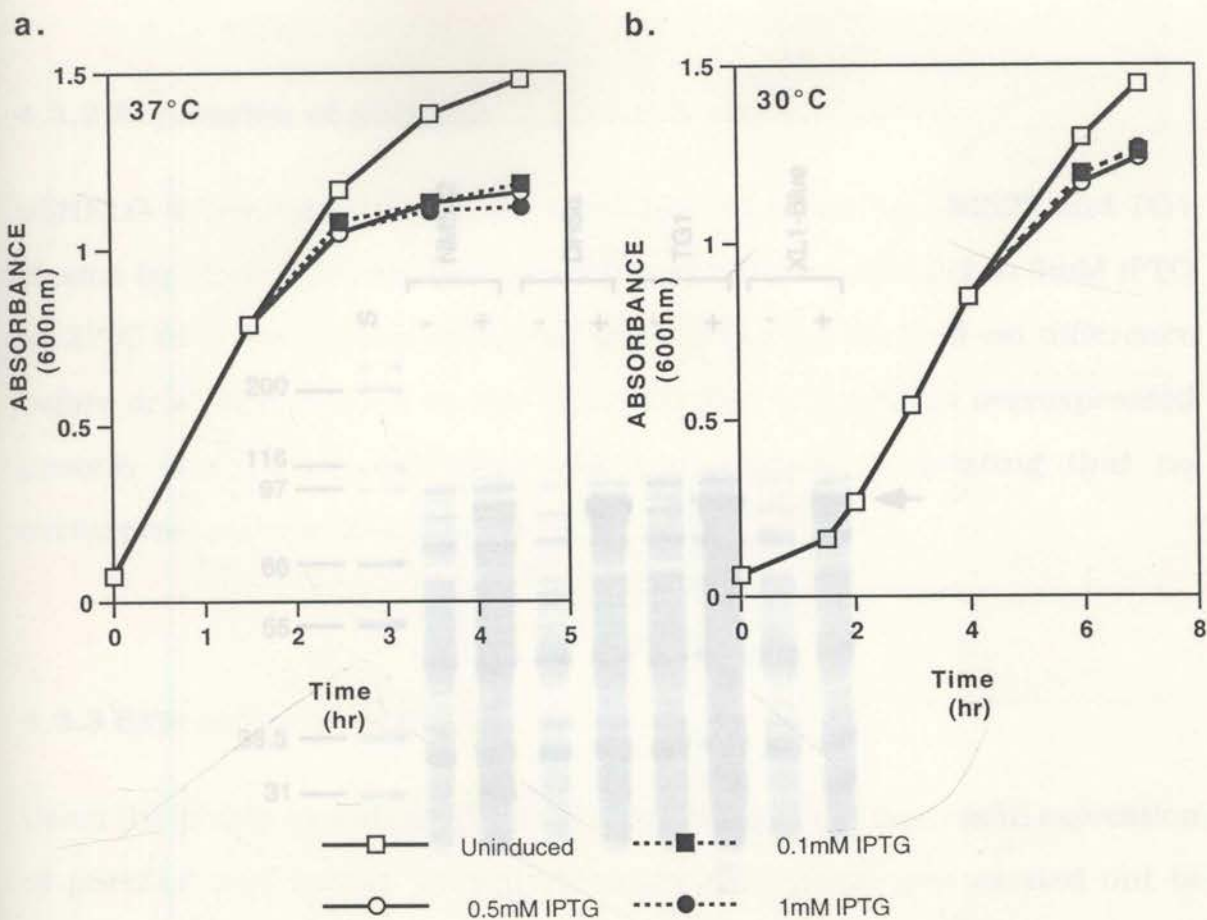


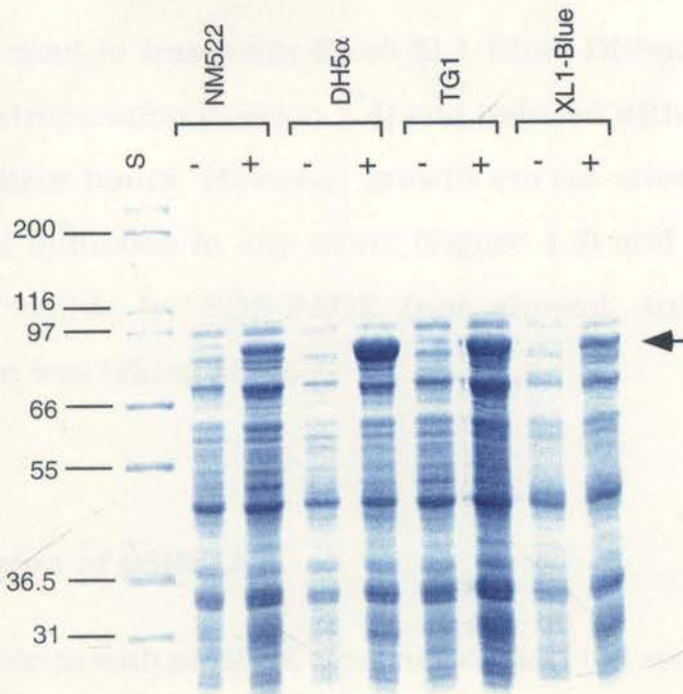
Figure 4.2 pSHEL expression in various *E. coli* strains. Uninduced cultures (-) and cultures induced with 1mM IPTG (+) for three hours for each of the strains indicated were analysed by 8% SDS-PAGE. GST-SHEL (arrow, 88kDa) is expressed in all strains but at

Figure 4.1 Growth curves for pSHEL in XL1-Blue. Growth curves of uninduced cultures and cultures induced with 0.1, 0.5 and 1mM IPTG at 30 and 37°C are shown. Cultures were induced at an absorbance of approximately 0.8. In all cases, IPTG addition slowed growth noticeably with a similar effect seen at both 30 and 37°C.

Routine GST-SHEL expression from pSHEL in all other experiments was therefore carried out in DH5 α at 37°C with 0.1mM IPTG induction.

4.3.2 Expression of pSHEL

pSHEL was expressed in *E. coli* strains NM522 and TG1 at 37°C for three hours before or after induction with 0.1 to 5mM IPTG. No difference in protein was observed between uninduced and induced cultures. Overexpression of pSHEL was observed in DH5 α and XL1-Blue. The intensity of the band was higher in DH5 α than in XL1-Blue, indicating that no



4.3.3 Exp

Given the pSHEL expression in DH5 α and XL1-Blue, a preliminary experiment was carried out to ascertain whether pSHEL could be useful but no optimisation was performed. Expression of pSHEL in DH5 α appeared to be taking place as judged by SDS-PAGE but the overexpressed band was not very intense when compared with the other *E. coli* proteins (Figure 4.4). No growth curves were produced since the induced and uninduced cultures were

Figure 4.2 pSHEL expression in various *E. coli* strains. Uninduced cultures (-) and cultures induced with 1mM IPTG (+) for three hours for each of the strains indicated were analysed by 8% SDS-PAGE. GST-SHEL (arrow, 88kDa) is expressed in all strains but at different levels with no expression seen in uninduced cultures. Highest levels of expression are seen in DH5 α while expression is poorest in XL1-Blue. Size markers (S) are shown in kDa.

Routine GST-SHEL expression from pSHEL C in all other experiments was therefore carried out in DH5 α at 37°C with 0.1mM IPTG induction.

4.3.2 Expression of pSHELD

pSHELD was used to transform *E. coli* XL1-Blue, DH5 α , NM522 and TG1 strains by electroporation (Section 2.4) and induced with 0.1 to 5mM IPTG at 37°C for three hours. However, growth curves showed no difference before or after induction in any strain (Figure 4.3) and no overexpressed protein was visible by SDS-PAGE (not shown), indicating that no overexpression was taking place.

4.3.3 Expression of pSHELE

Given the problems with pSHELE construction and the successful expression of pSHELF (see below), only preliminary expression was carried out to ascertain whether pSHELE could be useful but no optimisation was performed. Expression of pSHELE in DH5 α appeared to be taking place as judged by SDS-PAGE but the overexpressed band was not very intense when compared with the other *E. coli* proteins (Figure 4.4). No growth curves were produced since the induced and uninduced cultures were grown at different temperatures and were therefore not directly comparable.

Figure 4.3 Growth curves for pSHELD in various *E. coli* strains. pSHELD in XL1-Blue, NM522, TG1 and DH5 α was induced with 1mM IPTG. No difference in growth curves in the presence (filled circles) and absence (open circles) of IPTG is noted for any strain.

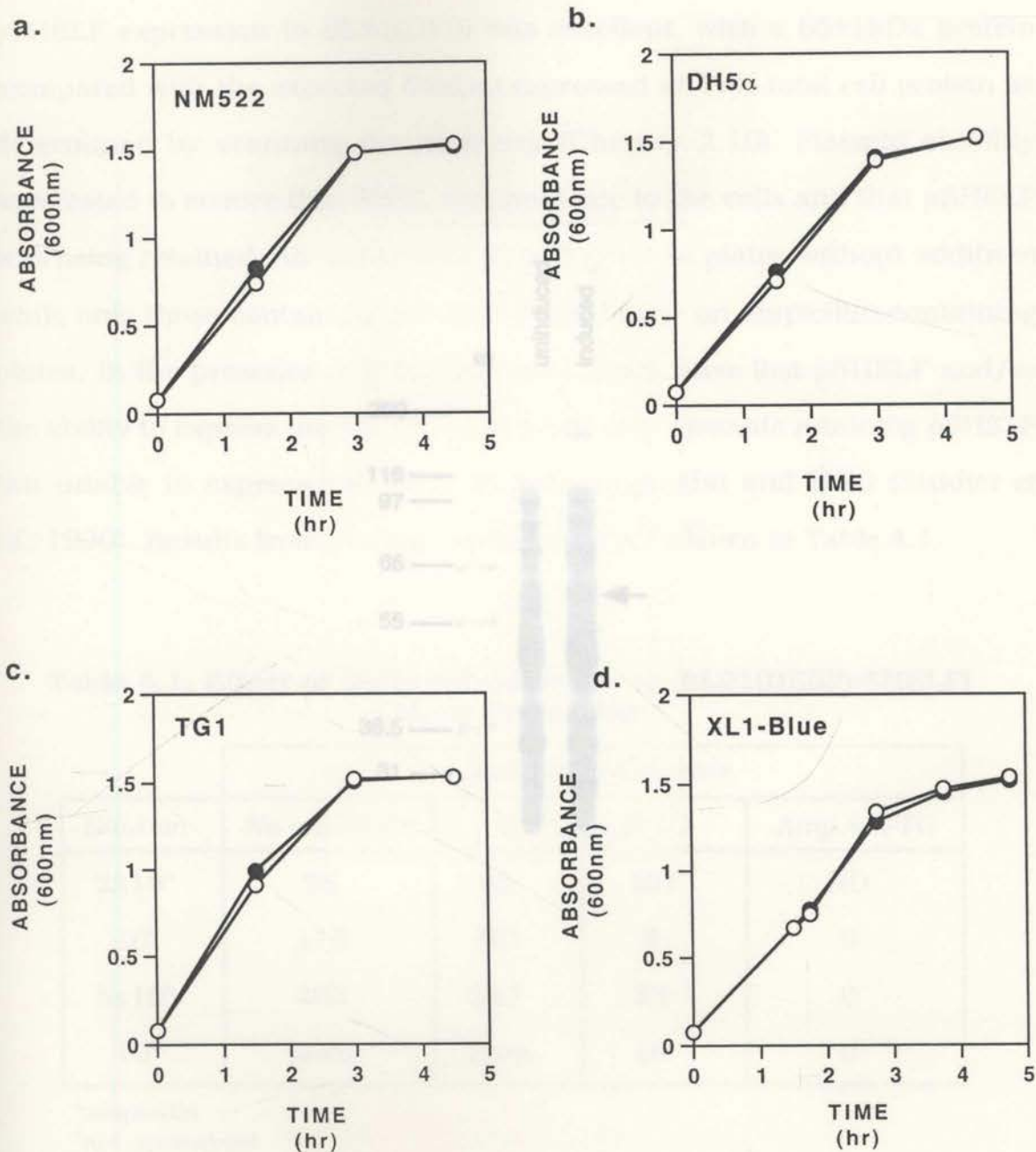



Figure 4.4 Expression of pSHELE in DH5 α . A putative pSHELE clone was induced by growth at 42°C for two hours and analysed by 8% SDS-PAGE alongside an uninduced culture grown at 30°C. An overexpressed band at approximately the correct size (arrow) is present in the induced sample. Size markers (kDa) are shown in kDa.

Figure 4.3 Growth curves for pSHELD in various *E. coli* strains. pSHELD in XL1-Blue, NM522, TG1 and DH5 α was induced with 1mM IPTG. No difference in growth curves in the presence (filled circles) and absence (open circles) of IPTG is noted for any strain.

4.3.4. Optimisation of pSHELF Expression

pSHELF expression in BL21(DE3) was excellent, with a 65 ± 1 kDa protein (compared with the expected 64 kDa) expressed at 17% total cell protein as determined by scanning densitometry (Chapter 2.10). Plasmid stability was tested to ensure that SHELF was not toxic to the cells and that pSHELF was being retained. All viable cells should grow on plates without additives while only those containing pSHELF grow on ampicillin-containing plates. In the presence of IPTG, only those which have lost pSHELF and/or the ability to express proteinase K will grow on ampicillin and IPTG (Studier et al., 1990). Results from

Table 4.1. Effect of



BL21(DE3)[pSHELF]

Dilution	Colonies			
	No add	Amp	IPTG	Amp.+ IPTG
2×10^8	96	85	ND ¹	ND
10^8	175	ND	3	0
5×10^7	493	517	23	0
10^7	lawn	lawn	46	0

¹ampicillin
not determined

Figure 4.4 Expression of pSHELE in DH5 α . A putative pSHELE clone was induced by growth at 42°C for two hours and analysed by 8% SDS-PAGE alongside an uninduced culture grown at 30°C. An overexpressed band at approximately the correct size (arrow) is present in the induced sample. Size markers (S) are shown in kDa.

different rich media were tested (Figure 4.5). M9LB did not work as well as the other media; LB, 2TY and TB, which were all similarly effective. 2TY appeared to be marginally better as judged by SDS-PAGE and was therefore routinely used.

4.3.4. Optimisation of pSHELF Expression

pSHELF expression in BL21(DE3) was excellent, with a 65 ± 1 kDa protein (compared with the expected 64 kDa) expressed at 17% total cell protein as determined by scanning densitometry (Chapter 2.10). Plasmid stability was tested to ensure that SHEL was not toxic to the cells and that pSHELF was being retained. All viable cells should grow on plates without additives while only those containing pSHELF should grow on ampicillin-containing plates. In the presence of IPTG only cells which have lost pSHELF and/or the ability to express protein will grow while only mutants retaining pSHELF but unable to express will grow on both ampicillin and IPTG (Studier *et al.*, 1990). Results from plating experiments are shown in Table 4.1.

Table 4.1. Effect of Different Additives on BL21(DE3)[pSHELF] Colony Formation

Dilution	Number of Colonies			
	No additives	Amp.*	IPTG	Amp.+ IPTG
2×10^6	96	85	ND [†]	ND
10^6	175	ND	3	0
5×10^5	493	517	23	0
10^5	lawn	lawn	46	0

*ampicillin

[†]not determined

A number of variables were altered to optimise expression. A selection of different rich media were tested (Figure 4.5). M9LB did not work as well as the other media; LB, 2TY and TB, which were all similarly effective. 2TY appeared to be marginally better as judged by SDS-PAGE and was therefore routinely used.

IPTG concentration was varied to determine the lowest concentration capable of induction, since a relatively high concentration of 0.4mM IPTG is recommended for pET vectors (Studier *et al.*, 1990). IPTG from 0.001 to 0.6mM was used. Low levels, although capable of induction also resulted in high background expression of *E. coli* proteins (Figure 4.5). 0.04mM IPTG appeared to be the lowest concentration capable of producing good overexpression with little background. With higher IPTG amounts, however, there was a decrease in overexpression. Therefore no advantage was gained with higher IPTG amounts and 0.04mM was routinely used.

The optimum time for induction after various induction times appeared optimal with increased SHEL present. Two hours after various induction times appeared optimal for overexpression. Over many months it was consistently observed that induction was extremely poor with almost no SHEL present by SDS-PAGE. This always coincided with extremely slow growth of cultures with over three hours required before A_{600} reached 0.8 instead of the usual one and a half hours. SDS-PAGE of overnight cultures showed that expression of SHEL was taking place constitutively with no IPTG required (Figure 4.5). Re-transformation of pSHEL into fresh *E. coli* cells did not have any effect. Constitutive expression was repressed by including 2% glucose in overnight cultures, followed by dilution into fresh media without glucose for induction

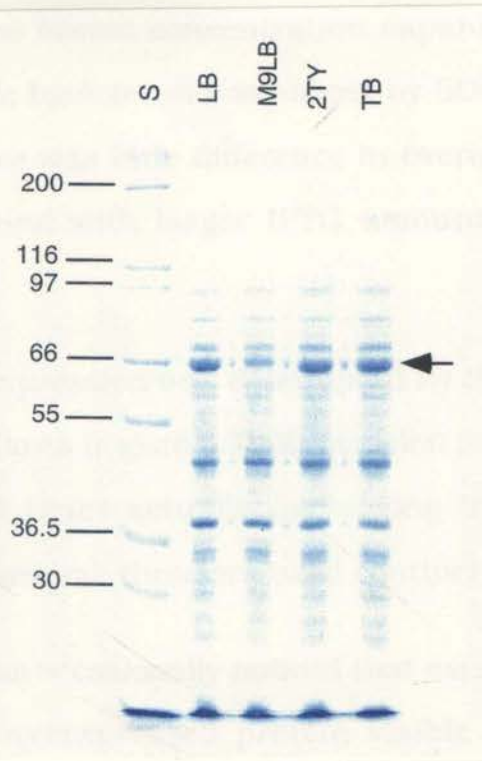


Figure 4.5 Expression of pSHEL in various media. pSHEL was induced with 1mM IPTG for three hours in LB, 2TY, M9LB or TB and analysed by 8% SDS-PAGE alongside uninduced samples. Expression of SHEL (arrow) can be seen in all samples at a high level except in M9LB where expression is poor. Expression in the other media is comparable in this case. Size markers (S) are shown in kDa.

IPTG concentration was varied to determine the lowest concentration capable of induction, since a relatively high concentration of 0.4mM IPTG is recommended for pET vectors (Studier *et al.*, 1990). IPTG from 0.001 to 0.6mM was used. Low levels, although capable of induction also resulted in high background expression of *E. coli* proteins (Figure 4.6). 0.04mM IPTG appeared to be the lowest concentration capable of producing good overexpression with little background as judged by SDS-PAGE. With higher amounts, however, there was little difference in overexpression. Therefore no advantage was gained with larger IPTG amounts and 0.04mM was routinely used.

The optimum time for expression was determined by SDS-PAGE of samples after various induction times (Figure 4.7). Expression for two hours appeared optimal with increased times actually decreasing the overall amount of SHEL present. Two hours was therefore used routinely for overexpression.

Over many months it was occasionally noticed that expression was extremely poor with almost no overexpressed protein visible by SDS-PAGE. This always coincided with extremely slow growth of cultures with over three hours required before A_{600} reached 0.8 instead of the usual one and a half hours. SDS-PAGE of overnight cultures showed that expression of SHEL was taking place constitutively with no IPTG required (Figure 4.8). Re-transformation of pSHELF into fresh *E. coli* cells did not have any effect. Constitutive expression was repressed by including 2% glucose in overnight cultures, followed by dilution into fresh media without glucose for induction by IPTG (Figure 4.8) which resulted in consistent high overexpression levels. Less than 0.04mM results in a high background of *E. coli* proteins. Little difference in overexpression levels or background can be seen above this level.

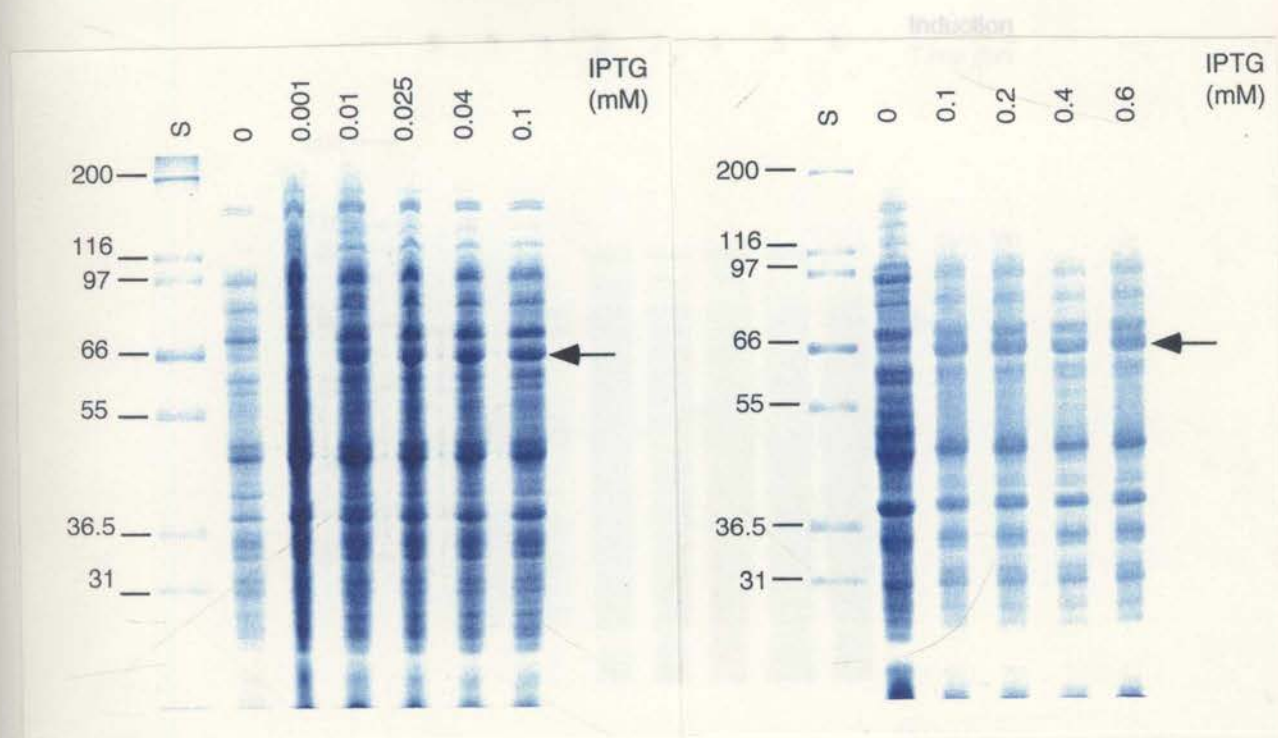


Figure 4.6 Effect of IPTG concentration on pSHELF expression. IPTG from 0.001 to 0.6mM was used to induce pSHELF expression for two hours and samples analysed by 8% SDS-PAGE alongside an uninduced sample. Overexpressed SHEL is marked with an arrow. 0.001mM did not have any effect although induction is seen with all other IPTG levels used. Less than 0.04mM results in a high background of *E. coli* proteins. Little difference in overexpression levels or background can be seen above this level.

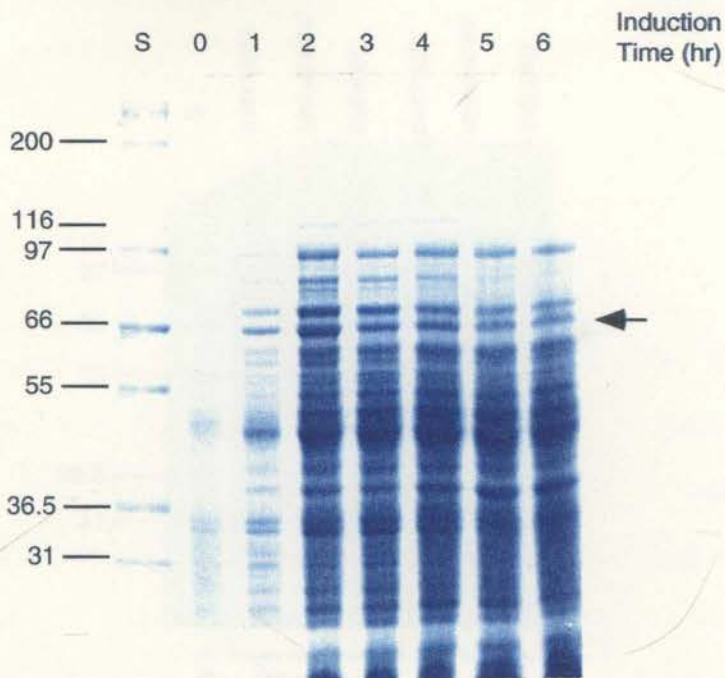


Figure 4.7 Time course of pSHEL expression in 2TY. pSHEL was grown in 2TY media and induced with 0.04mM IPTG and expression assessed by 8% SDS-PAGE after induction times of one to six hours, alongside an uninduced sample. The position of SHEL is marked with an arrow. Overexpression appears to reach a maximum at two hours with the amount of SHEL decreasing over longer induction times. In the presence of glucose constitutive expression is repressed with no SHEL visible in overnight or uninduced cultures. Size markers (S) are shown in kDa.

Routine expression of pSHELF was carried out by growing cells in 2TY containing 2% glucose and 50µg/ml ampicillin overnight, followed by dilution into fresh 2TY and ampicillin without glucose, before induction with 0.04mM IPTG for two hours at 37°C after the culture reached A_{600} of 0.8. Expression levels of approximately 17% total cell protein were obtained. With these conditions no inclusion bodies were observed by phase contrast microscopy (Section 2.3).

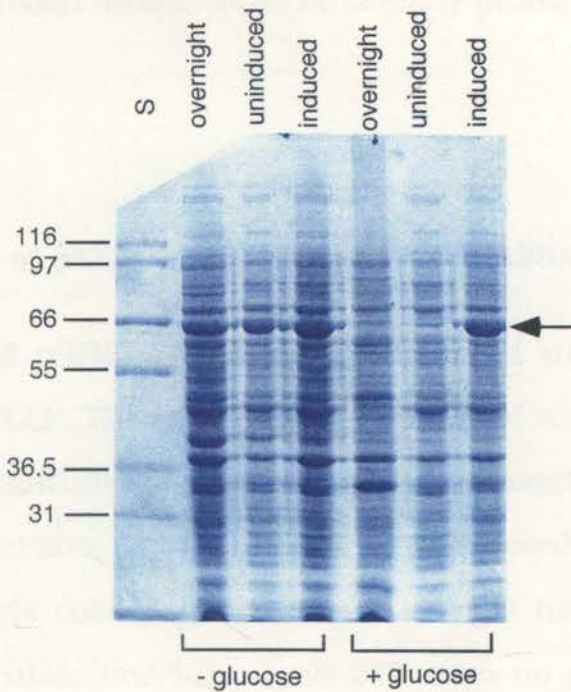


Figure 4.8 Constitutive expression of pSHELF in BL21(DE3). pSHELF was grown in 2TY overnight in the presence (+ glucose) or absence (- glucose) of 2% glucose and induced with 0.04mM IPTG for two hours after reaching an A_{600} of 0.8. In the absence of glucose cultures took two to three times longer to reach this level. Samples of overnight, uninduced and induced cultures were analysed by 8% SDS-PAGE and are shown. The position of SHEL is marked with an arrow. In the absence of glucose, SHEL is constitutively expressed in overnight cultures and is clearly present in the uninduced sample. In the presence of glucose constitutive expression is repressed with no SHEL visible in overnight or uninduced cultures. Size markers (S) are shown in kDa.

Routine expression of pSHELF was carried out by growing cells in 2TY containing 2% glucose and 50 μ g/ml ampicillin overnight, followed by dilution into fresh 2TY and ampicillin without glucose, before induction with 0.04mM IPTG for two hours at 37°C after the culture reached A_{600} of 0.8. Expression levels of approximately 17% total cell protein were obtained. With these conditions no inclusion bodies could be seen by phase contrast microscopy (Section 2.3).

4.3.5 Expression of pSHELF Δ mod and pSHELF Δ 26A

pSHELF Δ mod and pSHELF Δ 26A were expressed under the conditions optimised for pSHELF. The only difference observed was that pSHELF Δ mod was expressed constitutively and was therefore allowed to express overnight without IPTG induction. This was achieved by inoculating a 10ml culture of 2TY with a single colony, grown for six to eight hours at 37°C. One ml was used to inoculate one litre fresh 2TY with no glucose present and grown overnight before harvesting cells. Expression levels of both isoforms of tropoelastin and also SHELF Δ mod were approximately the same when grown under the same conditions (Figure 4.9). SHELF Δ 26A was expressed as a 60.0kDa protein and SHELF Δ mod as a 56.8kDa protein. No inclusion bodies could be seen under phase contrast microscopy (Section 2.3) in either case.

Figure 4.9 Comparative expression of SHELF, SHELF Δ 26A and SHELF Δ mod. Cultures containing pSHELF, pSHELF Δ 26A and pSHELF Δ mod were grown under identical conditions in the presence of glucose in overnight cultures and induced with 0.04mM IPTG for two hours. Uninduced (-) and induced (+) cultures were analysed by 8% SDS-PAGE. The level of overexpression is comparable for all three forms. The positions of SHELF (63.5), SHELF Δ 26A (60.0) and SHELF Δ mod (56.8) are marked with an arrow. Size markers and the size of each overexpressed protein is shown in kDa.

4.4. DISCUSSION

4.4.1 Growth Curves

Expression of

taken while

determining

SDS-PAGE

cell's resour

necessary to

could not be

4.4.2 Expre

Expression of

a marked d

strains. The

expression

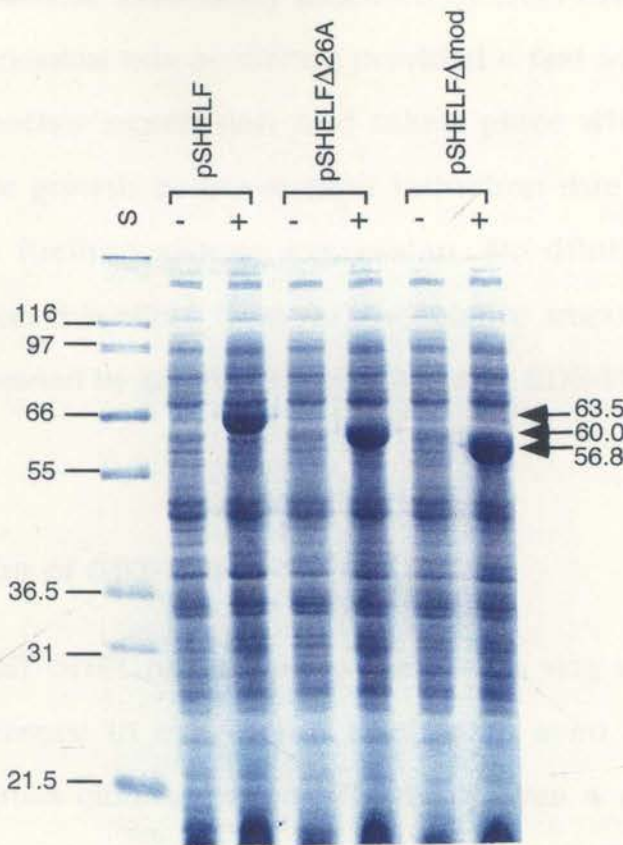


Figure 4.9 Comparative expression of SHEL, SHEL Δ 26A and SHEL Δ mod. Cultures containing pSHEL, pSHEL Δ 26A and pSHEL Δ mod were grown under identical conditions in the presence of glucose in overnight cultures and induced with 0.04mM IPTG for two hours. Uninduced (-) and induced (+) cultures were analysed by 8% SDS-PAGE. The level of overexpression is comparable for all three forms. The positions of SHEL (63.5), SHEL Δ 26A (60.0) and SHEL Δ mod (56.8) are marked with an arrow. Size markers and the size of each overexpressed protein is shown in kDa.

frequently insoluble (Frangioni and Neel, 1993). This is in contrast to the recombinant fusion proteins of human tropoelastin produced from cDNA which was produced in an insoluble form (Indik *et al.*, 1990; Bedell-Hogan *et al.*, 1993). Since there was no evidence of inclusion body formation the

Growth curves

simple means of

without the need for

diversion of the

of culture was

of overexpression

E was necessary.

successful. However,

different *E. coli*

significantly poorer

used. While the

three other strains were good expression hosts, DH5 α was more consistent

and was therefore used as the standard host strain. No difference in the

amount of expression was seen with altered IPTG levels or temperature.

No inclusion bodies could be seen under any of the conditions used indicating

that GST-SHEL was produced in a soluble form even at 37°C. Solubility

4.4. DISCUSSION

4.4.1 Growth Curves

Expression conditions were easily assessed by SDS-PAGE. Growth curves taken while expression was occurring provided a fast and simple means of determining whether expression had taken place without the need for SDS-PAGE since growth is slower after induction due to diversion of the cell's resources fuelling protein expression. No dilution of culture was necessary to detect this effect. However, the relative amount of overexpression could not be assessed by growth curves alone and SDS-PAGE was necessary.

4.4.2 Expression of GST-SHEL

Expression of GST-SHEL fusion from pSHEL C was very successful. However, a marked difference in expression levels was seen in different *E. coli* strains. The initial cloning strain, XL1-Blue, was a significantly poorer expression host compared with the other three strains used. While the three other strains were good expression hosts, DH5 α was more consistent and was therefore used as the standard host strain. No difference in the amount of expression was seen with altered IPTG levels or temperature. No inclusion bodies could be seen under any of the conditions used indicating that GST-SHEL was produced in a soluble form even at 37°C. Solubility was confirmed after cell lysis (See Section 5.3.1.1), in agreement with other reports of high solubility of GST-fusion proteins (Smith and Johnston, 1988) although some other reports have found that GST fusions are frequently insoluble (Frangioni and Neel, 1993). This is in contrast to the recombinant fusion proteins of human tropoelastin produced from cDNA which was produced in an insoluble form (Indik *et al.*, 1990; Bedell-Hogan *et al.*, 1993). Since there was no evidence of inclusion body formation the

faster growth conditions of 37°C were used. [1990] were unable to obtain

successful expression of their cDNA clones in an unfused system, citing extreme degradation as the problem. The system used here, however,

4.4.3 Expression of pSHELD and pSHELE

elastin isoforms removing the need for any additional purification away from a fusion partner. Although No expression of SHEL from pSHELD was seen in DH5 α . No evidence of not conclusive since different host strains and vectors were used, the any overexpression could be detected by either SDS-PAGE or by a change excellent levels of overexpression indicate that codon manipulation was a in growth rates compared with uninduced cultures. Amman *et al.* (1988) useful procedure in this case. Media pSHELF-containing BL21(DE3) cells recommend a high level of IPTG for induction of the *trc* promoter but 1 to on media containing different additives showed that pSHELF was relatively 5mM IPTG, considerably higher than that used for the other vectors, failed stable and that SHEL was not highly toxic to the cells. Almost the same to produce any overexpression. Other experiments in our laboratory using number of cells were seen on plates containing ampicillin as on plates different genes also failed to show any overexpression in pTrc-based with no additives suggesting almost all cells retained the plasmid. Since constructs (A. Stortchevoi, personal communication). the presence of IPTG will induce protein production, growth slows

A protein band from induced DH5 α containing the pSHELE construct could be detected at approximately the expected size by SDS-PAGE and was not present in uninduced cells. However, the band was not very intense, nor did the intensity increase greatly with time. This may be the correct SHEL product indicating that the ATG start codon was intact despite the loss of the *NcoI* site (Section 3.3.4). However, no growth curves could be produced due to different growth temperatures of induced and uninduced cultures. Since this system of overexpression is not widely used there are little other data to compare with these results. Because the data are inconclusive and expression appeared low especially in the light of subsequent pSHELF expression, pSHELE was not used for further experiments. with no detectable differences.

Levels of expression were high even with IPTG levels ten times lower than the recommended 0.4mM (Studler *et al.*, 1990). However, the most critical

4.4.4 Expression of pSHELF, pSHELF Δ 26A and pSHELF Δ mod

parameter for good expression levels was the length of the induction period:

Direct expression of tropoelastin isoforms was possible and highly successful

using the pET vector system. Indik *et al.* (1990) were unable to obtain successful expression of their cDNA clones in an unfused system, citing extreme degradation as the problem. The system used here, however, allows excellent direct expression of tropoelastin isoforms removing the need for any additional purification away from a fusion partner. Although not conclusive since different host strains and vectors were used, the excellent levels of overexpression indicate that codon manipulation was a useful procedure in this case. Plating pSHELF-containing BL21(DE3) cells on media containing different additives showed that pSHELF was relatively stable and that SHELF was not highly toxic to the cells. Almost the same number of cells were seen on plates containing ampicillin as on plates with no additives suggesting almost all cells retained the plasmid. Since the presence of IPTG will induce protein production, growth slows dramatically and colonies will not form on plates. Between 2-4% grew on IPTG alone indicating that 2-4% of cells had probably lost the plasmid. This is similar to the 2% level typical of pET plasmids (Studier *et al.*, 1990). No colonies grew on both IPTG and ampicillin plates indicating that no mutants exist which retain plasmid but have lost expression ability. The conditions used for growth and overexpression are therefore conducive to high-level expression as the plasmid is being maintained by a high proportion of cells. A toxic product would result in the loss of pSHELF and therefore a lower proportion of colonies on ampicillin plates and an increase in number on IPTG plates (Studier *et al.*, 1990). Optimal conditions determined for pSHELF expression were successfully transferred to pSHELF Δ 26A with no detectable differences.

Levels of expression were high even with IPTG levels ten times lower than the recommended 0.4mM (Studier *et al.*, 1990). However, the most critical parameter for good expression levels was the length of the induction period: more than two hours reduced expression levels, perhaps due to proteolytic

degradation. As for GST-SHEL, no inclusion bodies were seen, indicating the SHEL and SHEL Δ 26A products were produced predominantly as soluble polypeptides.

The major problem with pET constructs was constitutive expression. This was not seen at the beginning of the work but became apparent some time later and tended to be unpredictable. The T7 promoter in pET vectors is tightly regulated but the expression of T7 RNA polymerase from the *lacUV5* promoter is known to occur at a basal level without IPTG induction (Studier *et al.*, 1990). Since the products in this case were apparently not toxic, allowing expression of SHEL and SHEL Δ 26A from constitutively expressed cultures overnight was an attractive option for high yields of protein. However, this approach was often unsuccessful. Much of the problem could be attributed to high levels of proteolytic degradation with extended overexpression times resulting in poor yields of full-length protein. A second major problem was unreliable constitutive expression. However, pSHEL Δ mod was expressed very successfully in this way and constitutive expression in this system was highly reproducible. The cause of this unreliable constitutive expression is unknown and may possibly be due to subtle differences in composition with media stocks e.g. trace presence of lactose, increased protease resistance of the protein or mutations to DNA sequence in the bacterial genome. Since constitutive expression was troublesome for SHEL and SHEL Δ 26A it was necessary to repress it. A number of possibilities existed for this. A different pET vector could be tried but this was not desirable since expression in the present system was extremely good. The second option outlined by Studier *et al.* (1990) concerned the role of T7 lysozyme as a natural inhibitor of T7 RNA polymerase. T7 lysozyme is produced by bacteria containing pLysS and pLysE plasmids which carry the gene for T7 lysozyme and are chloramphenicol resistant. This would require maintaining pSHEL Δ and

pSHEL Δ 26A in the presence of pLysS or pLysE and reassessing expression. This option has the disadvantage of needing chloramphenicol as well as ampicillin in cultures. A slight lag time in expression may be expected with pLysS and an overall reduction in expression levels with pLysE (Studier *et al.*, 1990). Rather than take this option, a simpler method was tried using glucose in overnight cultures. Glucose acts to inhibit the *lacUV5* promoter by catabolite repression and this procedure has been recommended for other constitutively expressing systems (GST Gene Fusion Manual, Amrad Pharmacia Biotech). This was successful in inhibiting constitutive expression allowing high levels of overexpression after induction.

4.5 CONCLUSION

By constructing and analysing various expression systems, two constructs were identified which resulted in substantial overexpression. SHEL was successfully expressed in a soluble form at a high level as a fusion with GST and directly, using pSHEL Δ C and pSHEL Δ F which expressed at a level of 30% and 17% total cell protein respectively. This is the first instance of successful direct expression of any recombinant tropoelastin. Expression conditions for both the direct and fusion systems were optimised by trialling different hosts, media and induction times. Conditions for direct expression of SHEL were successfully transferred to the second isoform SHEL Δ 26A and the mutant form SHEL Δ mod.

CHAPTER 5

**PURIFICATION OF GST-SHEL AND
SHEL ISOFORMS**

5.1 INTRODUCTION

Previous recombinant work with tropoelastin has yielded relatively modest amounts of purified protein between 2-10mg per litre of culture (Grosso *et al.*, 1991; Indik *et al.*, 1990). Low yields may have been the result of low levels of expression possibly caused by rare codons in the natural gene. In contrast, codon-optimised SHEL and SHEL Δ 26A show very high expression with both GST fusion and direct expression systems (Chapter 4), potentially allowing a greatly increased yield.

Fusion expression systems are usually designed to facilitate purification by exploiting a property of the fusion partner to allow specific purification using affinity chromatography. With the GST fusion system, the GST portion binds specifically to glutathione agarose allowing purification of GST fusion proteins away from other proteins (Smith and Johnston, 1988). The fusion protein can then be eluted from the agarose by competition with free reduced glutathione. A disadvantage of fusion systems, however, is that the fusion partner has to be removed to provide the native polypeptide for subsequent studies which therefore adds an extra step to the purification protocol. The GST portion of GST fusions is designed to be readily removed by specific cleavage with proteases, in this case thrombin, which cuts between GST and the recombinant protein leaving the desired protein with an additional Gly-Ser dipeptide sequence at the N-terminus (Smith and Johnston, 1988). The purification is essentially a single step and conducive to maintaining protein structure, eliminating the need for other treatments such as cyanogen bromide or further chromatographic steps but is only feasible for soluble fusion proteins.

For directly expressed SHEL a novel system for purification had to be designed. As unfused tropoelastin has been shown to be very unstable (Indik *et al.*, 1990) and tissue-derived tropoelastin is rapidly degraded

(Rucker, 1982; Foster *et al.*, 1975; Narayanan and Page, 1974; Sandberg *et al.*, 1971), the main criteria for purification is to minimise the number of steps involved, to use relatively fast techniques to minimise degradation and to avoid overly harsh techniques such as cyanogen bromide.

Several different protocols exist for purifying tropoelastin from tissues. These include salt-induced coacervation (Smith *et al.*, 1972) and alcohol solubilisation (Sandberg *et al.*, 1971) which is based on the unusually high solubility of tropoelastin in short-chain alcohols first noted by Partridge (1967). Other techniques which have been successfully used include ion-exchange, gel filtration (Rucker, 1982) and reverse-phase high performance liquid chromatography (RP-HPLC) (Indik *et al.*, 1990, Soskel *et al.*, 1987).

A common contaminant in recombinant protein preparations is endotoxin (Marston, 1986). These pyrogenic compounds are derived from the lipopolysaccharide layer from the outer membrane of the bacterial cell. In addition to being toxic if the protein is used in living systems, the hydrophobicity of endotoxins allows them to interact with other hydrophobic proteins such as tropoelastin affecting its properties. The minimisation of endotoxin is therefore a priority in SHEL purification (McPherson *et al.*, 1996).

This chapter describes the purification of GST-SHEL and problems encountered during this procedure which restricted its further use. The development of a fast, simple and highly effective purification procedure for unfused SHEL is described and the subsequent purification of SHEL Δ 26A and SHEL Δ mod, including the removal of degradation products. A simple means of reducing endotoxin is also described. The final protein products are confirmed as correct by a variety of protein analysis techniques.

Glutathione agarose beads (Sigma Chemical Company, USA) were swollen

5.2 MATERIALS AND METHODS

5.2.1 Materials

Lysis buffer consisted of 50mM Tris-HCl pH 8.0, 100mM NaCl, 1mM EDTA and was sterilised by autoclaving before use. Lysozyme, DNaseI and phenylmethylsulfonyl fluoride (PMSF) were from Boehringer Mannheim, Germany. Stock PMSF solutions were made by dissolving the solid at 100mM in isopropanol. All other chemicals used were of analytical reagent grade.

5.2.2 Lysis of pSHEL C Cultures

Lysis and purification was carried out on cultures grown under optimal conditions as determined in Chapter 4. The final optimal lysis conditions are described here with variations tested as described in Section 5.3. Cells were harvested by centrifugation at 10 000g and resuspended in 10 volumes lysis buffer. 1mg/ml lysozyme, freshly dissolved in lysis buffer, was added and cells incubated at 4°C for 30min. 0.5mM PMSF and 1% Triton-X 100 was added for a further 30min at 4°C followed by 10mM MgCl₂ and 10µg/ml DNaseI for 20min. 5ml aliquots of the cell solution were sonicated for 10s at a time followed by 30s intervals on ice until lysis was complete as judged by phase contrast microscopy (Section 2.3). Typically five or six cycles were necessary. The supernatant was separated from the insoluble pellet by centrifugation at 12 000g for 10min.

5.2.3 Glutathione Agarose Binding

Glutathione agarose beads (Sigma Chemical Company, USA) were swollen

in 10 volumes phosphate-buffered saline (PBS) pH 7.4 (Sambrook *et al.*, 1989) for one hour at 4°C. Beads were spun at 500g, liquid removed and beads washed twice in PBS, then resuspended in an equal volume PBS to give a 50% slurry. 10µl cell lysate supernatant was mixed with 10-40µl bead slurry and incubated five minutes at room temperature with mixing. The beads were washed three times with one ml PBS by vortexing and centrifuging briefly to collect beads. Beads were resuspended in 20µl MQW, SDS-PAGE loading buffer added (Section 2.7) and boiled before being run on SDS-PAGE.

Large scale binding was performed using a glutathione agarose column made by filling a 20ml syringe, containing a teflon frit at the end, with pre-swollen beads. A piece of tubing was attached to the column to allow flow control. 6ml lysate was loaded onto the column at 1ml/min, flow-through collected and reloaded twice. The column was washed with five column volumes PBS containing 1% Triton-X 100. The protein was eluted with five column volumes 50mM Tris-HCl pH 8.0 containing 5mM reduced glutathione and 3ml fractions were collected.

5.2.4 Thrombin Cleavage

Cleavage of GST-SHEL bound to glutathione agarose was performed by washing and resuspending beads in 1x thrombin cleavage buffer (50mM Tris-HCl, pH 8.0, 150mM NaCl, 2.5mM CaCl₂) and adding human thrombin (Sigma) from 0.1 to 1% (w/w) thrombin:fusion protein at 25°C for one hour (Smith and Johnston, 1988). Soluble bacterial lysates used as substrate were incubated similarly with 1x thrombin cleavage buffer, added from a 10x stock.

5.2.5 Lysis of pSHELF Cultures

The sonication protocol tested for SHEL purification was as for GST-SHEL (Section 5.2.2). The usual lysis protocol used for pSHELF cultures was a combined lysozyme/freeze-thaw method. Cells were harvested and resuspended in 10 volumes lysis buffer with 1mg/ml lysozyme and 0.5mM PMSF at 4°C for 30min with occasional mixing. Cells were divided into 5ml aliquots in 10ml polypropylene tubes and frozen in liquid nitrogen, followed by thawing in room temperature water. Freeze-thaw was repeated another one to two times until the cell suspension became highly viscous. $MgCl_2$ and DNaseI were added as in Section 5.2.2 and incubated at room temperature for 15-20min until viscosity was reduced. Lysis was checked by phase contrast microscopy (Section 2.3). PMSF was added again and lysate cleared by centrifugation at 12 000g.

5.2.6 Alcohol Solubilisation

This protocol is based on a modification of that by Sandberg *et al.* (1971). 1.5 volumes cold n-propanol was added to the soluble tropoelastin-containing fraction in five aliquots at 15min intervals at 4°C with stirring. 2.5 volumes cold n-butanol was then similarly added and allowed to stir overnight. The precipitate was removed by centrifugation at 10 000g. Any suspended particulates remaining were removed by filtration through filter paper (Whatman No.41). The solution was removed by rotary evaporation using a vacuum pump and trap cooled with dry ice. Drying was aided by keeping the alcohol solution at between 30 and 37°C. When dry, the residue was washed twice with 10ml chloroform and the washings discarded, taking care not to lose any suspended particles. The flask was air-dried and the residue dissolved in ice-cold sterile 50mM ammonium acetate, pH

5.0. Any undissolved particles were not removed at this stage. The solution was extensively dialysed against 50mM ammonium acetate, pH 5.0, i.e. 10ml solution was dialysed against at least 5L buffer in total with three changes of buffer solution over two days. Particulate matter was removed by centrifugation at 5000g. Soluble SHEL solution was concentrated by lyophilisation.

5.2.7 RP-HPLC

Concentrated SHEL in 50mM ammonium acetate was separated from degradation products by RP-HPLC. Two alternative methods were used. Initially, perfusion chromatography (POROS, PerSeptive Biosystems, USA) using an R2 reverse phase column (4.6 x 100mm) run at 9ml/min along a 30-80% acetonitrile, 0.1% trifluoroacetic acid (TFA) gradient over 7min was used. Alternatively, a Techogel10 C18 column (2.2 x 25cm) was used with a flow rate of 8ml/min. A 30-80% acetonitrile, 0.1% TFA gradient over 55min was used after a 10min initial wash with 30% acetonitrile/0.1% TFA. The column was equilibrated for 10min between runs due to its large volume. A maximum of 30-50mg SHEL was loaded at any one time. For both methods sample detection was at 214 and 280nm simultaneously. Both methods were performed using Pharmacia (Sweden) pumps and detectors. The solution was removed from the collected samples by lyophilisation and purified SHEL weighed to determine yield.

5.2.11 Endotoxin Determination

5.2.8 Purification of SHEL Δ 26A and SHEL Δ mod

The same procedure used for purification of SHEL was used without any modifications for both SHEL Δ 26A and SHEL Δ mod.

5.2.9 Spectrophotometric Determination of Yield

An extinction coefficient of $19\ 320\text{Mcm}^{-1}$ at 280nm was used as determined by the Genetics Computer Group/ Protein Analysis/ Peptidesort program (University of Wisconsin, USA) provided by the Australian National Genomic Information Service and was found to be the same for all three forms.

To determine the concentration of protein solutions, A_{280} of the appropriate protein in ammonium acetate, pH 5.0 or PBS, pH 7.4 was read using a Cary model spectrophotometer. The following relation was used:

$$\frac{A_{280} \times \text{MW}}{19\ 320} = \text{mg/ml}$$

where MW (molecular weight) = 63 500 for SHEL, 60 000 for SHEL Δ 26A and 56 800 for SHEL Δ mod.

5.2.10 Mass Spectrometry

HPLC-purified samples were dried and 100 μ g sent to the Oxford Centre for Molecular Science, Oxford University, U.K., the Department of Pharmacy, University of Sydney or to the Australian Government Analytical Laboratories (Sydney, NSW) for analysis. In each case, analyses were performed by electrospray mass spectrometry according to standard protocols.

5.2.11 Endotoxin Determination

Unpurified samples, samples purified by HPLC or run through an endotoxin removing column (De-toxi Gel, Pierce Chemical Company, USA) were sent to Stanford Consulting Laboratories (Sydney, NSW) for LAL chromogenic endotoxin determination.

5.2.12 Circular Dichroism (CD)

SHEL was dissolved in pure water at 0.8mg/ml. CD was performed in a 0.1mm cuvette at 20 and 50°C using a Jasco J-720 spectropolarimeter from 184 to 240nm. Fifty cycles were obtained from 184 to 200nm and twenty cycles from 200 to 240nm. Data were expressed in mean residue ellipticity ($\text{degcm}^2\text{dmol}^{-1}$). Secondary structure was estimated using the variable selection method and the Varselec program (Manavalan and Johnson, 1987) with 33 reference spectra in the basis set.

5.3 RESULTS

5.3.1 Purification of GST-SHEL

5.3.1.1 Cell Lysis

A number of experiments were performed before adequate lysis conditions were found. Sonication after lysozyme treatment of cells was found to disrupt cells adequately but the GST-SHEL protein was found in the insoluble fraction (not shown). An alternative lysis protocol using 10% Triton-X 100 and lysozyme to lyse cells at 4°C with the addition of DNaseI and MgCl_2 resulted in about 50% soluble protein (not shown). This was promising but the Triton-X 100 concentration was too high for subsequent glutathione agarose binding (Smith and Johnston, 1988). A modified protocol combining these two i.e. lysozyme, 1% Triton-X 100 lysis, addition of MgCl_2 and DNaseI and sonication was effective in lysing cells with >95% solubility of GST-SHEL (Figure 5.1) and this technique was used subsequently.

5.3.1.2 Glutathione Agarose Binding

Analytical scale binding of cell lysates to glutathione agarose beads showed that binding was selective for GST-SHEL (Figure 5.2a). However, binding capacity was far below the expected 8µg fusion protein per ml agarose (Smith and Johnson, 1988). Large scale purification using a column was somewhat better and binding appeared to be extremely non-specific. Purification of smaller sized fragments of GST-SHEL on glutathione agarose was successful but likewise a large amount of GST was eluted.

5.3.1.3 Thrombin Cleavage

Analytical scale thrombin cleavage of GST-SHEL on glutathione agarose beads. A wide range of thrombin concentrations (0.01 to 1% (w/w) thrombin) were used from 0.1 to 1% (w/w) thrombin. GST-SHEL (26kDa) was evident on SDS-PAGE gels of supernatant and pellet. GST was clearly present in the supernatant in numerous experiments. To determine whether thrombin was degrading SHEL, the entire cell lysate was subject to cleavage with increasing concentrations of thrombin. 0.01U thrombin was the lower limit for cleavage but 0.05U and greater are more effective (Figure 5.3). GST was clearly present. However, with 0.01U thrombin a band at approximately 64kDa could be discerned which may represent SHEL although this was not

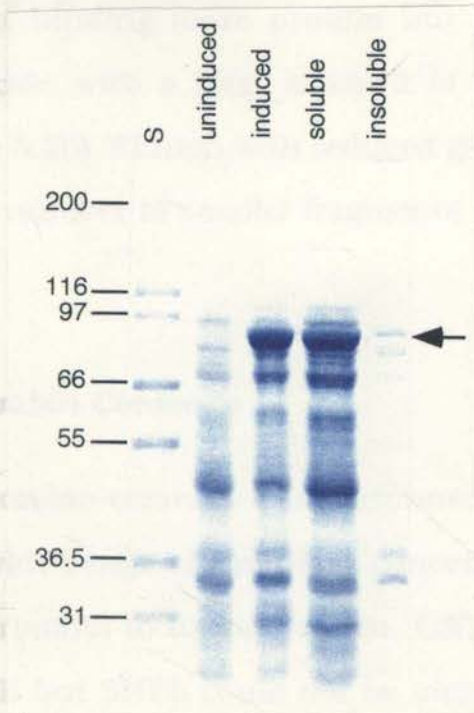


Figure 5.1 Lysis of DH5α expressing GST-SHEL. Uninduced and induced cultures of DH5α containing pSHEL were analysed by 8% SDS-PAGE. The total cell culture was lysed by sonication and the lysate cleared by centrifugation. Equivalent volumes of soluble supernatant and insoluble pellet are shown. Greater than 95% of GST-SHEL (arrow, estimated visually) is found in a soluble form in the supernatant. Size markers are shown in kDa.

that SHEL was indeed being cleaved by thrombin. Therefore, due to the problems with agarose binding and thrombin cleavage it was decided to concentrate instead on purification of unfused SHEL from pSHEL.

5.3.1.2 *Glutathione Agarose Binding*

Analytical scale binding of cell lysates to glutathione agarose beads showed that binding was selective for GST-SHEL (Figure 5.2a). However, binding capacity was far below the expected 8mg fusion protein per ml agarose (Smith and Johnson, 1988). Large scale purification using a column was somewhat better at binding more protein but binding appeared to be extremely non-specific with a large amount of smaller sized fragments binding also (Figure 5.2b). Elution with reduced glutathione was successful but likewise a large number of smaller fragments were eluted.

5.3.1.3 *Thrombin Cleavage*

Analytical scale thrombin cleavage was performed on GST-SHEL bound to agarose beads. A wide range of thrombin concentrations were used from 0.1 to 1% (w/w) thrombin to fusion protein. GST (26kDa) was evident on beads by SDS-PAGE but SHEL could not be identified in the supernatant in numerous experiments. To determine whether thrombin was degrading SHEL, the entire cell lysate was subject to cleavage with increasing concentrations of thrombin. 0.01U thrombin was the lower limit for cleavage but 0.05U and greater are more effective (Figure 5.3). GST was clearly present. However, with 0.01U thrombin a band at approximately 64kDa could be discerned which may represent SHEL although this was not nearly as intense as the GST band. With higher thrombin concentrations this band disappeared and smaller fragments at 45, 34 and 22kDa were noted indicating that SHEL was indeed being cleaved by thrombin. Therefore, due to the problems with agarose binding and thrombin cleavage it was decided to concentrate instead on purification of unfused SHEL from pSHELF.

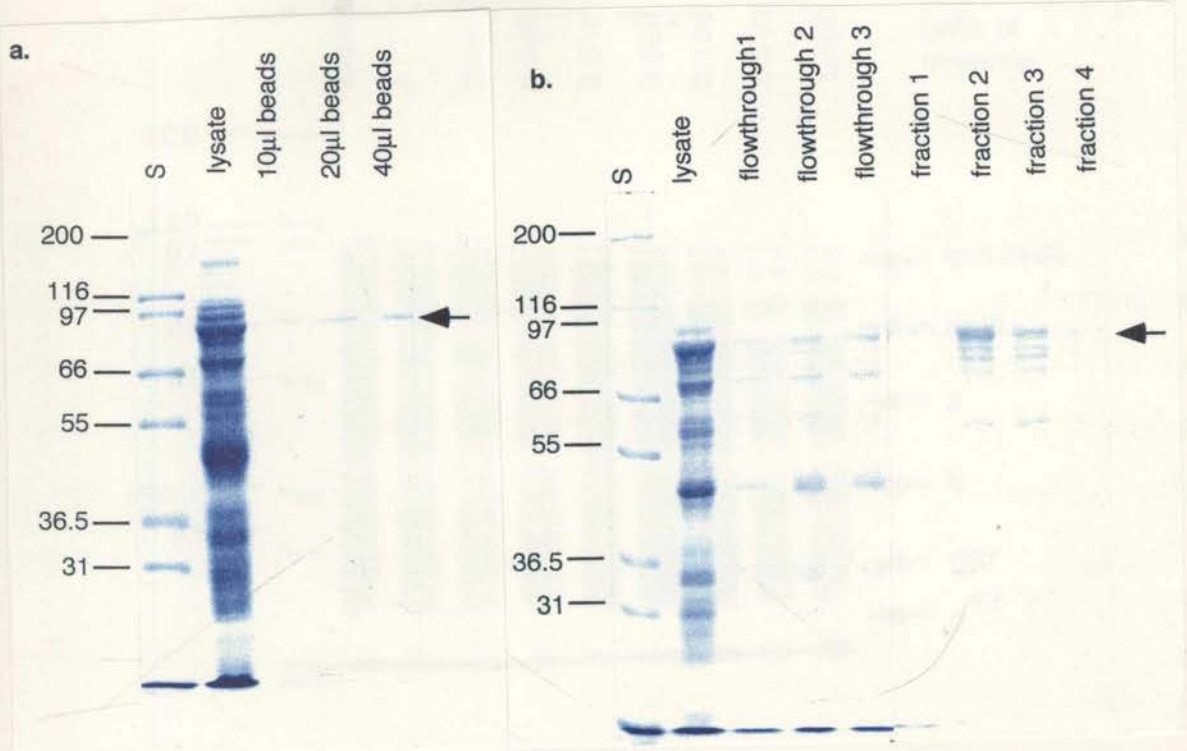
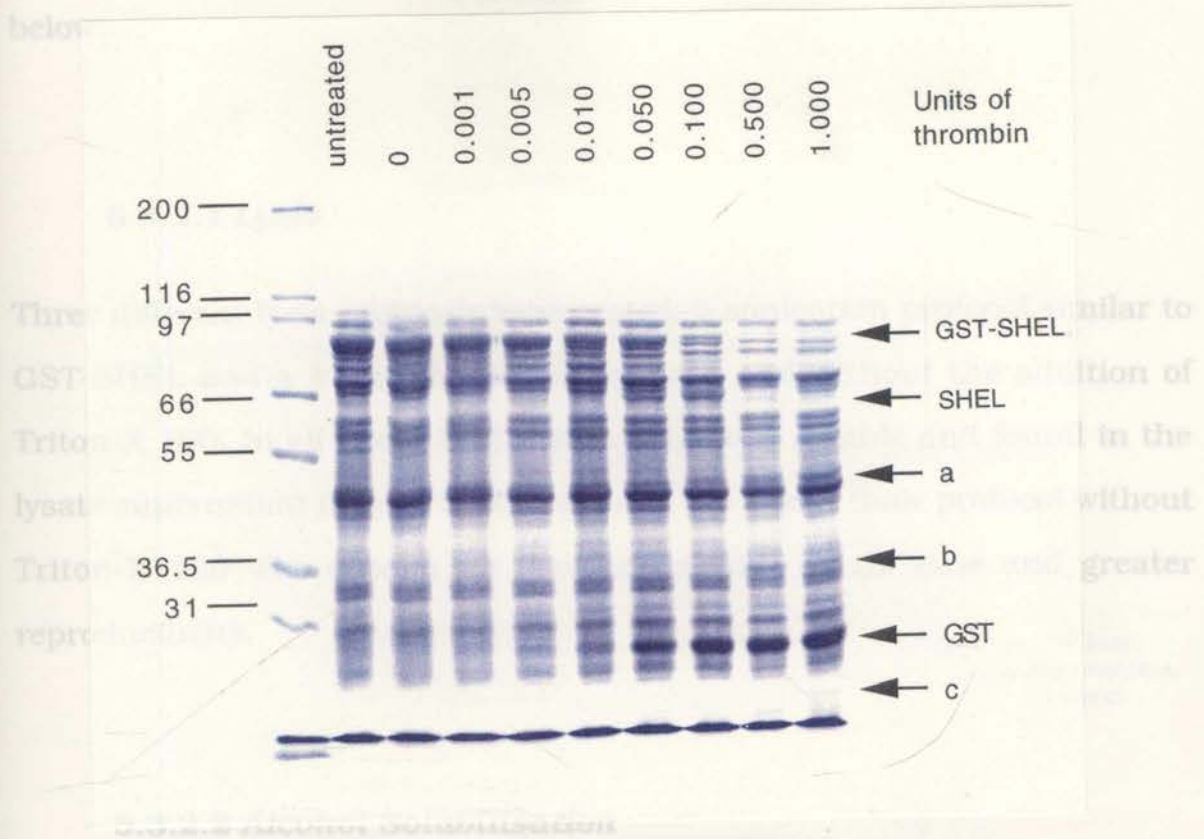


Figure 5.2 Binding of GST-SHEL to glutathione agarose. **a.** Analytical scale binding of soluble cell lysate to glutathione agarose beads. 10µl lysate was bound to 10, 20 and 40µl beads and each analysed by 8% SDS-PAGE. Binding appears selective for GST-SHEL (arrow) but binding capacity is low even with the largest amount of beads used, compared with the amount of GST-SHEL in the lysate. **b.** Column binding of GST-SHEL (arrow) to glutathione agarose. 4µl total soluble lysate is shown with equivalent volumes of flowthrough from each of the three passages through the column. GST-SHEL is not present in the flowthrough indicating it has bound to the column. 20µl samples of the first four fractions eluted from the column are shown. Subsequent fractions (not shown) did not contain any protein. GST-SHEL is successfully eluted from the column but numerous smaller fragments are also present in the elution.

5.3.2 Purification of SHEL

The overall purification scheme designed for SHEL is shown as a flow chart in Figure 5.4. The development of each step is described in detail below.



A modification of the alcohol solubilisation procedure used with tissue-extracted tropoelastin (Sandberg et al., 1971) was used to purify recombinant SHEL in essentially a single step. This simple procedure was highly selective, with SHEL the only protein solubilised by propanol/butanol as judged by

Figure 5.3 Thrombin cleavage of soluble cell lysate containing GST-SHEL. Increasing amounts of thrombin (indicated in units) were added to soluble cell lysate and analysed by 8% SDS-PAGE. GST can be clearly seen at approximately 26kDa with thrombin concentrations above 0.01U while GST-SHEL decreases. SHEL, at approximately 64kDa, can be discerned at intermediate thrombin concentrations of 0.05 and 0.1U. Increasing thrombin further results in removal of the SHEL band and the appearance of three smaller bands (a,b,c) at approximately 45, 34 and 22kDa.

residue inside the flask consisting of purified SHEL and some lipid (Figure 5.6). A wash with chloroform removed the lipids as judged by the clouding of the chloroform solution.

5.3.2 Purification of SHEL

The overall purification scheme designed for SHEL is shown as a flow chart in Figure 5.4. The development of each step is described in detail below.

5.3.2.1 Lysis

Three different lysis protocols were tested: a sonication protocol similar to GST-SHEL and a freeze-thaw protocol with and without the addition of Triton-X 100. In all cases SHEL was completely soluble and found in the lysate supernatant (Figure 5.5a). Of these, the freeze-thaw protocol without Triton-X 100 was chosen for routine use due to its ease and greater reproducibility.

5.3.2.2 Alcohol Solubilisation

A modification of the alcohol solubilisation procedure used with tissue-extracted tropoelastin (Sandberg *et al.*, 1971) was used to purify recombinant SHEL in essentially a single step. This simple procedure was highly selective, with SHEL the only protein solubilised by propanol/butanol as judged by SDS-PAGE. All *E. coli* proteins were precipitated by the alcohols and easily removed by centrifugation and filtration (Figure 5.5b). Unfortunately, some SHEL was also precipitated indicating that the procedure was not completely effective. The alcohol solution was removed by rotary evaporation leaving a residue inside the flask consisting of purified SHEL and some lipid (Figure 5.6). A wash with chloroform removed the lipids as judged by the clouding of the chloroform solution.

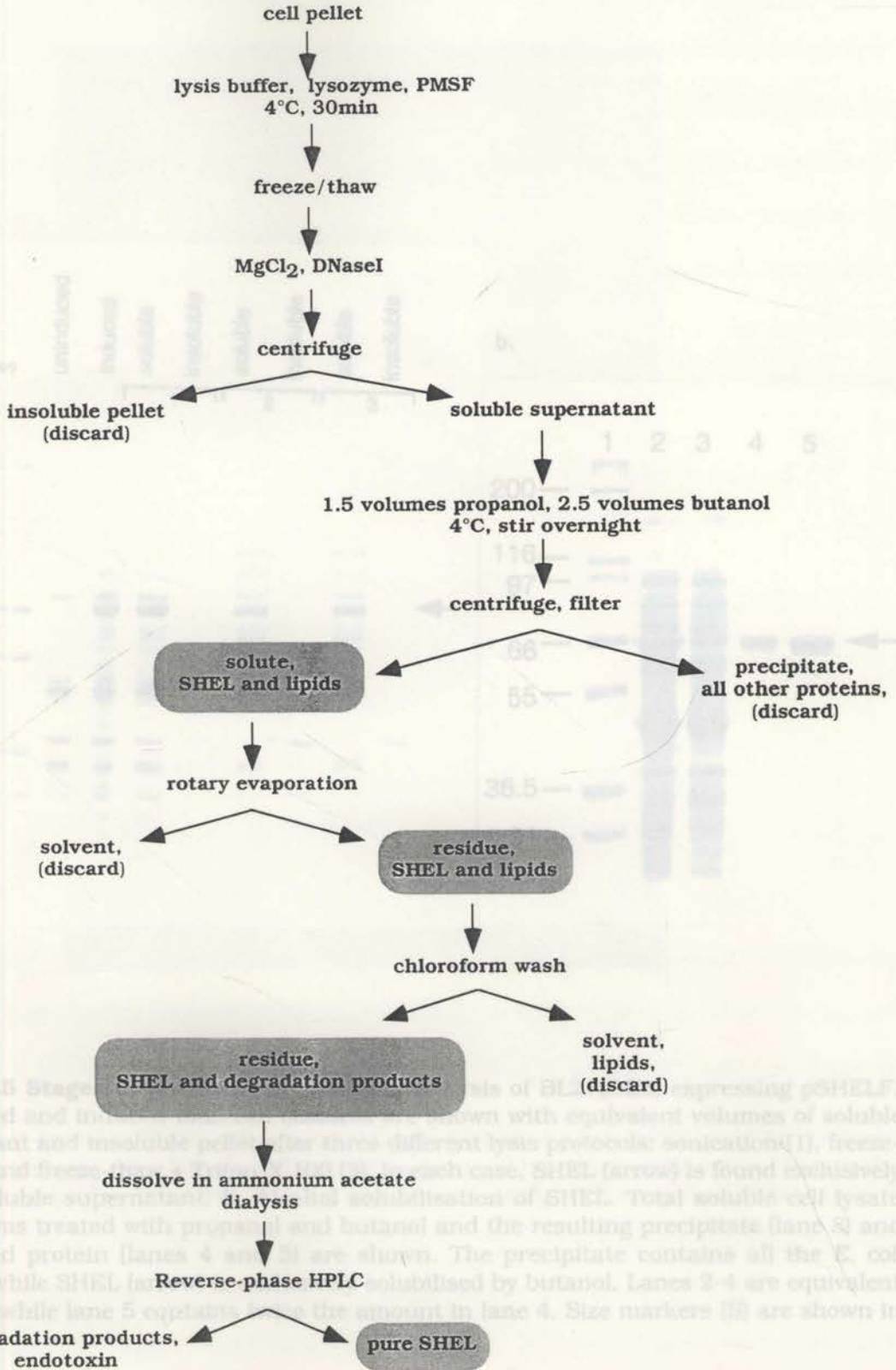


Figure 5.4 Overview of the purification protocol for SHEL

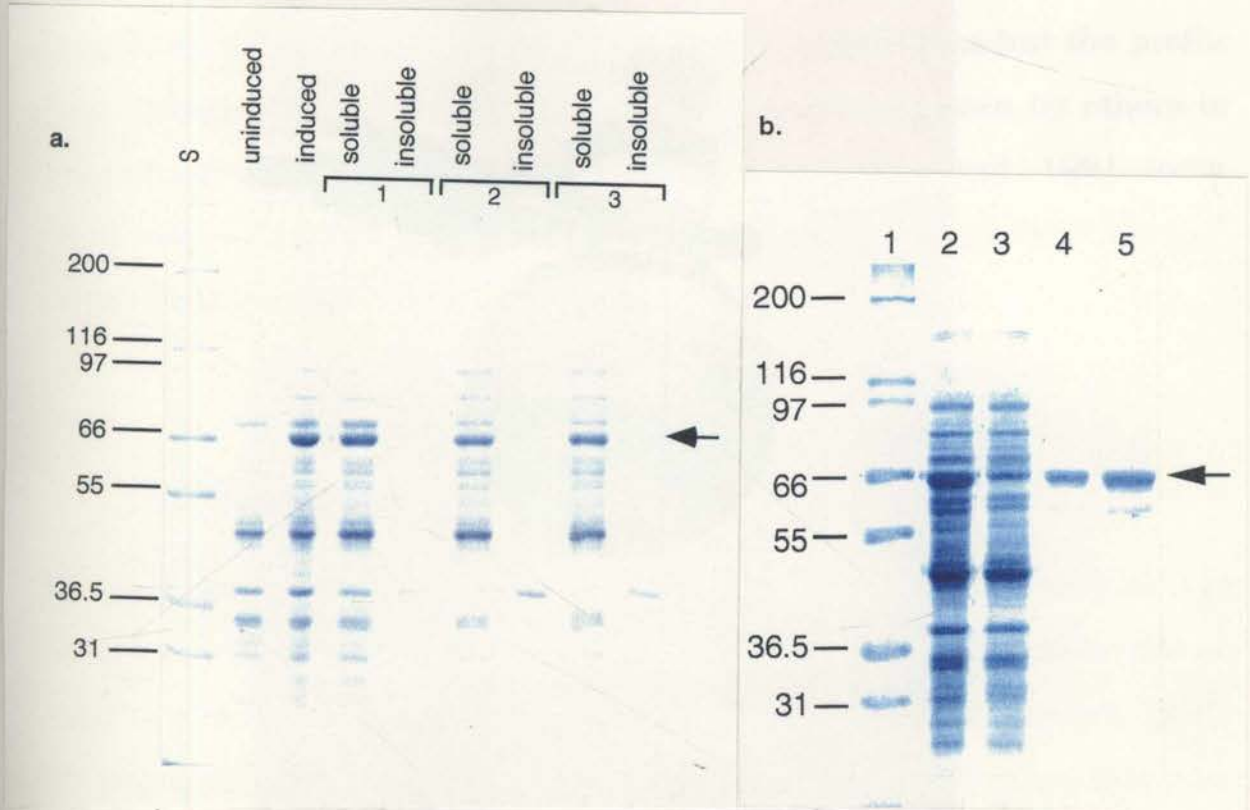


Figure 5.5 Stages of purification of SHEL. **a.** Lysis of BL21(DE3) expressing pSHEL. Uninduced and induced total cell cultures are shown with equivalent volumes of soluble supernatant and insoluble pellet after three different lysis protocols; sonication (1), freeze-thaw (2) and freeze-thaw + Triton-X 100 (3). In each case, SHEL (arrow) is found exclusively in the soluble supernatant. **b.** Alcohol solubilisation of SHEL. Total soluble cell lysate (lane 2) was treated with propanol and butanol and the resulting precipitate (lane 3) and solubilised protein (lanes 4 and 5) are shown. The precipitate contains all the *E. coli* proteins while SHEL (arrow) is exclusively solubilised by butanol. Lanes 2-4 are equivalent amounts while lane 5 contains twice the amount in lane 4. Size markers (S) are shown in kDa.

The residue inside the flask was dissolved in ammonium acetate buffer with some difficulty but was greatly enhanced by cooling on ice and resulted in a clear solution.

remove the y

freeze-drying

some degra

degradation,

was always

recombinant

et al., 1990;

et al., 1985;

et al., 1985;

5.3.2.

In most inst

interfere with

able to remo

Experiments

using FPLC

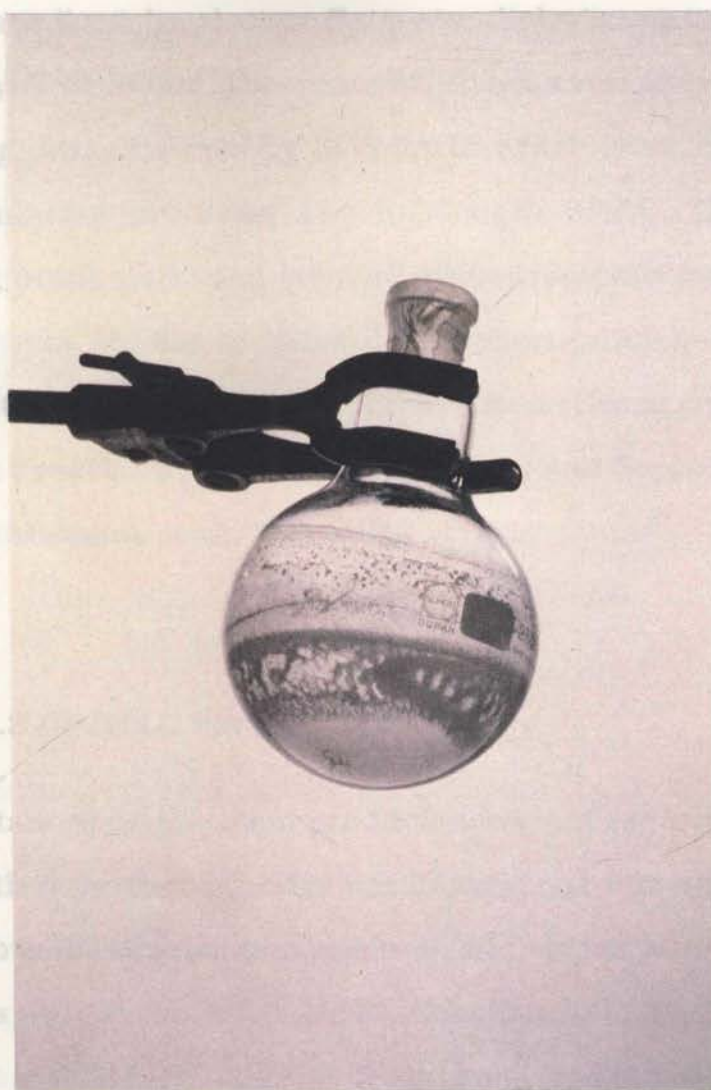


Figure 5.6 Purified SHEL after removal of alcohol. A flask containing an extensive residue remaining after the alcohol mixture is removed by rotary evaporation. The residue consists largely of purified SHEL as the only protein, along with some lipid contamination.

column was used. This did not result in any separation of degradation

products (not shown) but removed endotoxins efficiently (see below). This

column had the advantage of fast separation (<7min) due to the high flow

rate used and therefore had a high throughput. However, there was a high

waste of solvent and the column capacity was low (approximately 1mg)

resulting in multiple runs to purify an average 1L preparation of SHEL.

The residue inside the flask was dissolved in ammonium acetate buffer with some difficulty but was greatly enhanced by cooling on ice and resulted in a yellowish solution. Extensive dialysis appeared to completely remove the yellow colour. The dilute SHEL solution, after concentration by freeze-drying, was analysed by SDS-PAGE which revealed the presence of some degradation products and full-length SHEL. The proportion of degradation products varied greatly between preparations but the profile was always very similar to those degradation profiles seen by others in recombinant systems and tissue preparations (Grosso *et al.*, 1991; Indik *et al.*, 1990; Franzblau *et al.*, 1989; Davidson and Sephel, 1987; Chipman *et al.*, 1985; Mecham *et al.*, 1976). A yield of approximately 30-40mg from 1L culture was routinely obtained using these methods.

5.3.2.3 RP-HPLC Purification

5.3.3 Purification of SHEL26A

In most instances degradation products were not removed as they did not interfere with in further experiments. However, it was still important to be able to remove the degradation products and obtain pure full-length SHEL. Experiments with Superose 12 size fractionation and Mono S cation exchange using FPLC and SMART systems (both from Pharmacia Biotech, Sweden) were unsuccessful in removing degradation products and resulted in losses of SHEL apparently due to non-specific binding to the columns (not shown). Reverse-phase HPLC however, was very successful in removing degradation products. Initially, a POROS Perfusion Chromatography reverse phase column was used. This did not result in any separation of degradation products (not shown) but removed endotoxins efficiently (see below). This column had the advantage of fast separation (<7min) due to the high flow rate used and therefore had a high throughput. However, there was a high waste of solvent and the column capacity was low (approximately 1mg) resulting in multiple runs to purify an average 1L preparation of SHEL.

Therefore, a reverse-phase C18 column was used instead. This much larger preparative scale column had a higher capacity (approximately 100mg) allowing fewer runs to be made compensating for the much longer run time. Conventional reverse-phase chromatography also separated degradation products extremely well as seen by multiple peaks on the elution profile (Figure 5.7a). Samples from the various peaks analysed by SDS-PAGE revealed complete removal of degradation products was achieved with full-length SHEL eluting in the final peak (Figure 5.7b). Removal of solvent by centrifugal evaporation and/or freeze-drying completed the purification protocol. Dried SHEL was weighed to determine yield and stored dry until needed. A final yield of approximately 30-40mg from 1L culture was routinely obtained using these methods.

5.3.3 Purification of SHEL Δ 26A

The purification protocol used for SHEL (outlined in Figure 5.4) was likewise used for SHEL Δ 26A with no modifications or difficulties. Figure 5.8 shows various stages of purification for SHEL Δ 26A. The final yield of protein obtained was similar to SHEL with approximately 30-40mg purified from 1L culture volume. Degradation products were again present.

Figure 5.7 Reverse-phase HPLC purification of SHEL. a. Typical HPLC elution profile of SHEL, as monitored by absorbance at 214nm, passed through a C18 RP-HPLC column. The numbered peaks correspond to fractions collected. b. 8% SDS-PAGE analysis of the numbered fractions collected in Figure 5.7a. Equivalent volumes from each fraction are shown. Full-length SHEL eluted largely in the final peak (arrow) with earlier peaks containing variously degraded products. Size markers (S) are shown in kDa.

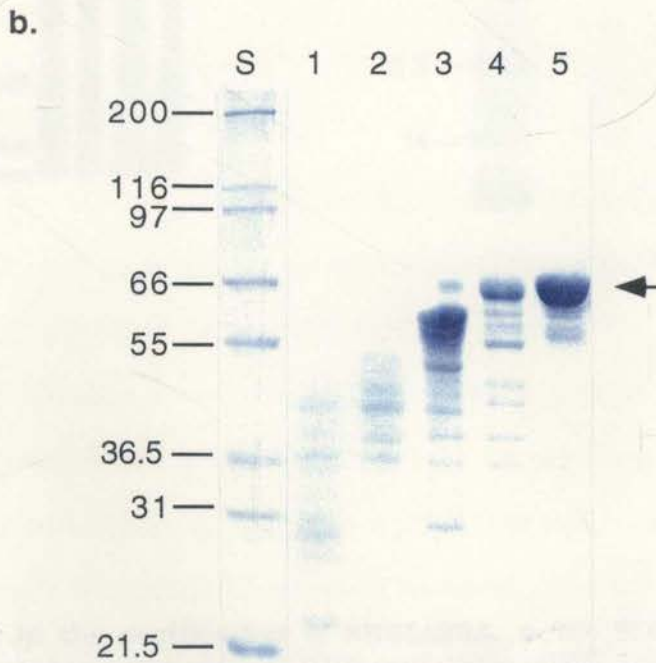
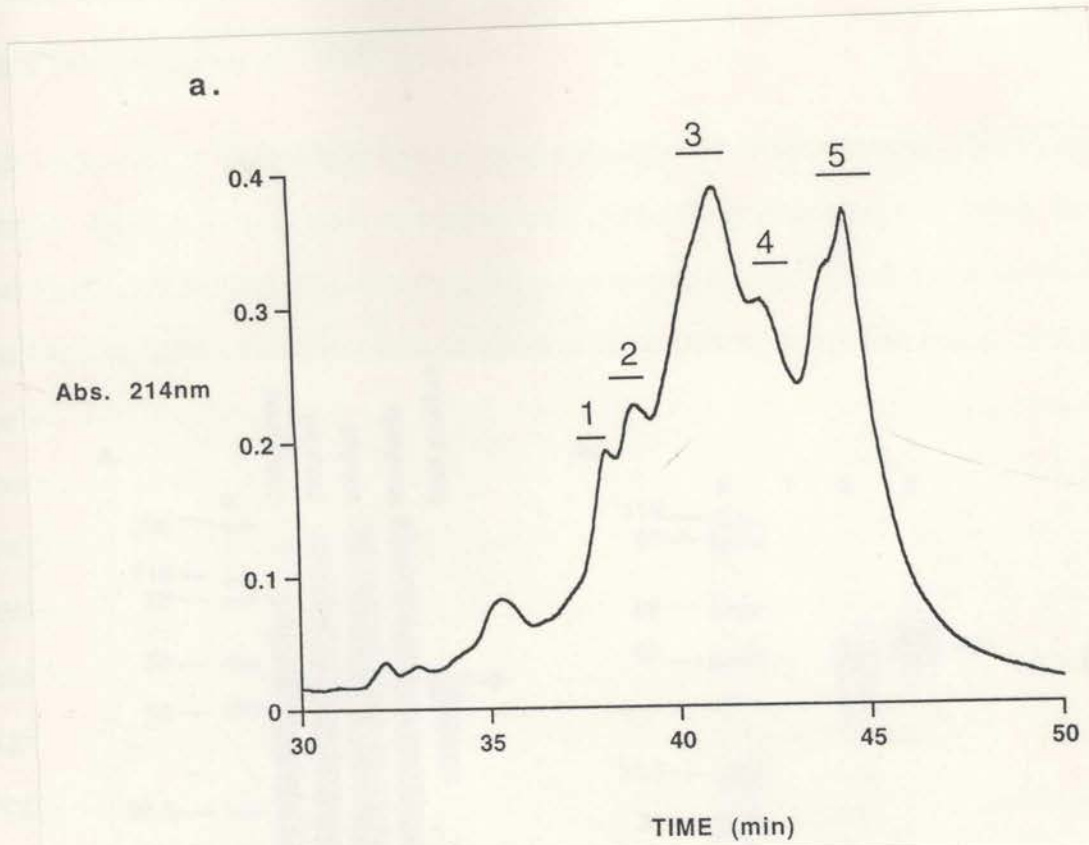


Figure 5.7 Reverse-phase HPLC purification of SHEL. a. Typical HPLC elution profile of SHEL, as monitored by absorbance at 214nm, passed through a C18 RP-HPLC column. The numbered peaks correspond to fractions collected. b. 8% SDS-PAGE analysis of the numbered fractions collected in Figure 5.7a. Equivalent volumes from each fraction are shown. Full-length SHEL eluted largely in the final peak (arrow) with earlier peaks containing variously degraded products. Size markers (S) are shown in kDa.

5.3.4 Purification of SHEL Δ mod

Although not a naturally occurring isoform of tropoelastin, SHEL Δ mod proved useful in various experiments including comparison with SHEL and SHEL Δ 26A (see Chapter 7). Furthermore, it was used as a source to produce smaller tropoelastin domains (see Chapter 6) for other work in the laboratory.

The stages in the purification of SHEL Δ 26A were also carried out. This was done by first expressing SHEL Δ 26A in BL21(DE3) cells. The cells were then induced with IPTG and the culture supernatant was collected. The soluble and insoluble fractions were separated by centrifugation. The soluble fraction was dialysed into a buffer containing 0.5 M NaCl and 0.1 M Tris-HCl, pH 7.5. The insoluble fraction was resuspended in the same buffer. The soluble and insoluble fractions were then subjected to HPLC purification. The HPLC-purified fractions were then analysed by SDS-PAGE. The results are shown in Figure 5.8.

Figure 5.8 shows the stages in the purification of SHEL Δ 26A. Panel (a) shows an 8% SDS-PAGE analysis of uninduced and induced samples of BL21(DE3) containing pSHEL Δ 26A, with equivalent volumes of soluble and insoluble lysate and the final purified product after alcohol solubilisation (arrow). Degradation products are evident. Panel (b) shows an 8% SDS-PAGE of HPLC-purified fractions. Fraction 3 contains largely full-length SHEL Δ 26A (arrow). Size markers (S) are shown in kDa.

To determine whether the degradation products were due to endogenous proteases from *E. coli* or whether they resulted from early termination of expression, HPLC-purified full-length SHEL, SHEL Δ 26A and SHEL Δ mod were mixed with soluble *E. coli* BL21(DE3) lysate, made in the same way as cultures expressing SHEL (Section 5.3.2.1). Lysate was made from cells lacking pET plasmid. 48hr incubation at 37°C resulted in a reduction in the total full-length tropoelastin present in each case compared with zero

Figure 5.8 Stages in the purification of SHEL Δ 26A. **a.** 8% SDS-PAGE analysis of uninduced and induced samples of BL21(DE3) containing pSHEL Δ 26A, with equivalent volumes of soluble and insoluble lysate and the final purified product after alcohol solubilisation (arrow). Degradation products are evident. **b.** 8% SDS-PAGE of HPLC-purified fractions. Fraction 3 contains largely full-length SHEL Δ 26A (arrow). Size markers (S) are shown in kDa.

5.3.4 Purification of SHEL Δ mod

Although not a naturally occurring isoform of tropoelastin, SHEL Δ mod proved useful in various experiments including comparison with SHEL and SHEL Δ 26A (see Chapter 7). Furthermore, it was used as a source to produce smaller tropoelastin domains (see Chapter 6) for other work in the laboratory. Therefore, purification of SHEL Δ mod was also carried out. The same procedure as for SHEL was used as outlined in Figure 5.4 with the only modification being the use of overnight expression as described in Section 4.3.5. Selected stages in the purification are shown in Figure 5.9. Due to the overnight expression the final yield obtained was extremely high with approximately 200mg obtained from 1L culture volume. Degradation products were also evident with this form of tropoelastin also.

5.3.5 Source of Degradation Activity

To ascertain whether the degradation products were the result of endogenous proteases from *E. coli* or whether they resulted from early termination of expression, HPLC-purified full-length SHEL, SHEL Δ 26A and SHEL Δ mod were mixed with soluble *E. coli* BL21(DE3) lysate, made in the same way as cultures expressing SHEL (Section 5.3.2.1). Lysate was made from cells lacking pET plasmid. 48hr incubation at 37°C resulted in a reduction in the total full-length tropoelastin present in each case compared with zero time controls. This demonstrated that proteases present in the *E. coli* lysate were capable of degrading tropoelastin prior to purification (Figure 5.10). Degradation products are evident.

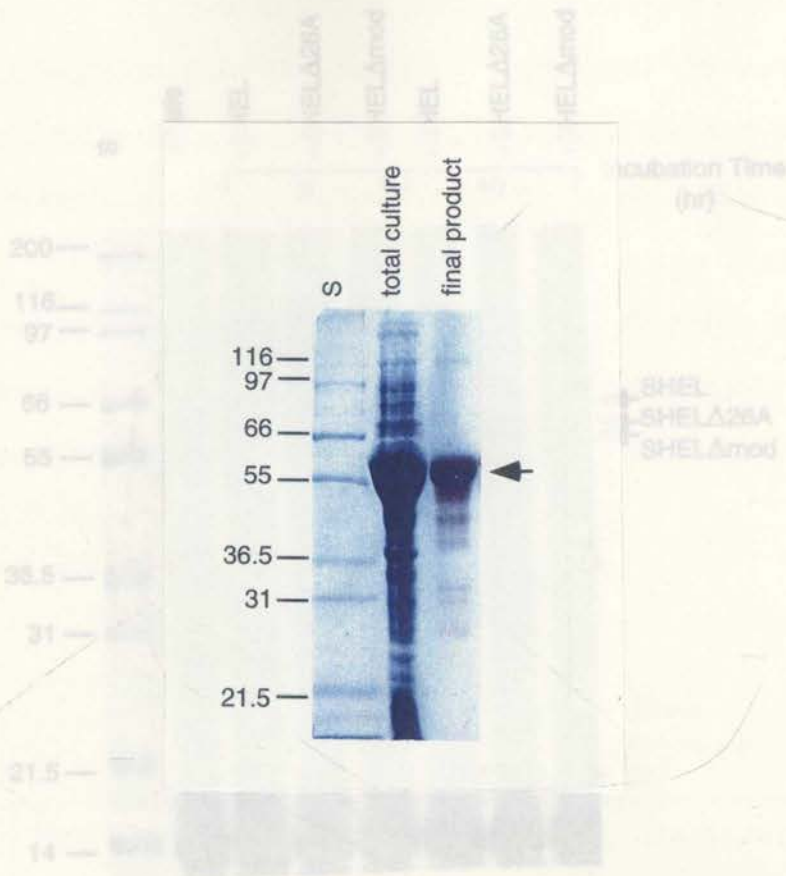


Figure 5.10 Degradation of SHEL, SHEL Δ 26A and SHEL Δ mod by *E. coli* lysate. BL21(DE3) *E. coli* lysate was mixed with equivalent amounts of SHEL, SHEL Δ 26A and SHEL Δ mod. The degradation products were analyzed by SDS-PAGE. The most readily degraded. Size markers (S) are shown in kDa.

Figure 5.9 Stages of purification of SHEL Δ mod. 8% SDS-PAGE analysis of total BL21(DE3) culture containing pSHEL Δ mod and final SHEL Δ mod product after alcohol solubilisation (arrow). Degradation products are evident.

5.3.6 Characterisation of Purified Proteins

5.3.6.1 N-terminal Protein Sequencing

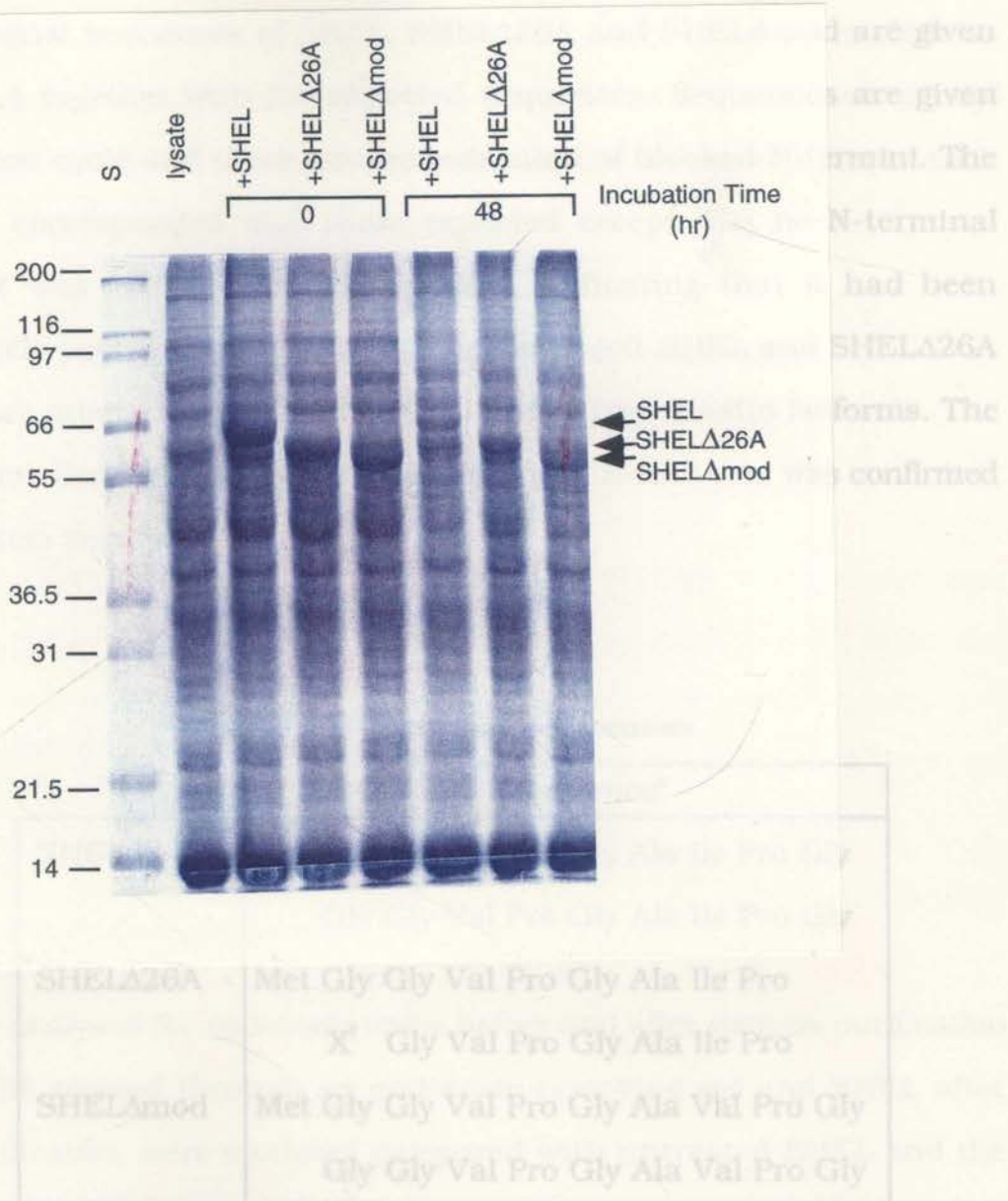


Figure 5.10 Degradation of SHEL, SHELΔ26A and SHELΔmod by *E. coli* lysate. BL21(DE3) *E. coli* lysate was mixed with equivalent amounts of SHEL, SHELΔ26A and SHELΔmod. The position of each tropoelastin is marked with an arrow. After 48hr incubation the amount of each tropoelastin is greatly reduced compared with a zero time control. Of the three forms, SHEL appears to be the most readily degraded. Size markers (S) are shown in kDa.

5.3.6.2 Mass Spectrometry

Mass spectrometry analysis of both SHEL and SHELΔ26A was performed

5.3.6 Characterisation of Purified Proteins

5.3.6.1 N-terminal Protein Sequencing

The N-terminal sequences of SHEL, SHEL Δ 26A and SHEL Δ mod are given in Table 5.1 together with the expected sequences. Sequences are given from the first cycle and there was no indication of blocked N-termini. The sequences corresponded with those expected except that no N-terminal formyl-Met was identified in any protein, indicating that it had been quantitatively post-translationally removed in *E. coli*. SHEL and SHEL Δ 26A are therefore precisely equivalent to the natural tropoelastin isoforms. The Ile to Val mutation identified by DNA sequencing in SHEL Δ mod was confirmed by the protein sequence.

SHEL	63 489	63 495
SHEL Δ 26A	60 017	60 028
SHEL Δ mod	58 839	56 844

Table 5.1 N-terminal Sequences

	Sequence*
SHEL	Met Gly Gly Val Pro Gly Ala Ile Pro Gly Gly Gly Val Pro Gly Ala Ile Pro Gly
SHEL Δ 26A	Met Gly Gly Val Pro Gly Ala Ile Pro X [†] Gly Val Pro Gly Ala Ile Pro
SHEL Δ mod	Met Gly Gly Val Pro Gly Ala Val Pro Gly Gly Gly Val Pro Gly Ala Val Pro Gly

*The expected sequence is shown on top and determined sequence below.

[†]An X represents a residue unable to be identified unambiguously.

5.3.6.2 Mass Spectrometry

Mass spectrometry analysis of both SHEL and SHEL Δ 26A was performed

to confirm that no changes had occurred in the amino acid sequence. Mass spectrometry of SHEL Δ mod was likewise used to confirm the sequence found by DNA sequencing. Table 5.2 lists the expected molecular mass alongside that measured by mass spectrometry. In all cases molecular mass closely corresponded with the theoretical mass without the N-formyl Met confirming that the proteins were missing the N-terminal Met in each case.

Table 5.2 Mass Spectrometry Measurements

	Theoretical Mass (Da)*	Measured Mass (Da)
SHEL	63 489	63 495
SHEL Δ 26A	60 017	60 026
SHEL Δ mod	56 839	56 844

*theoretical mass without N-formyl Met

5.3.6.3 Endotoxin Levels

SHEL was analysed for endotoxin levels before and after various purification steps. SHEL passed through an endotoxin-removing gel and SHEL after HPLC purification were analysed compared with untreated SHEL and the results shown in Table 5.3. Endotoxin levels were initially very high but were significantly reduced with gel and HPLC purification, with HPLC being a more effective means of endotoxin removal. Levels as low as 14EU/g have been obtained after HPLC purification. Thus, HPLC-purified SHEL used in subsequent experiments was largely endotoxin free compared with untreated SHEL.

Table 5.3 Endotoxin Levels in Selected Preparations of SHEL

Method of Purification	Endotoxin Level (EU/g)	
	Crude	Pure
RP-HPLC	>430	<53
De-toxi Gel	185 000	770

5.3.6.4 Circular Dichroism

SHEL in water at 20°C exhibited a CD spectrum with a minimum near 200nm (Figure 5.11) and a second minimum near 220nm. At 50°C the spectrum was very similar but the minimum at 200nm was slightly less negative. The secondary structure calculated was 3±1% α -helix, 37±3% antiparallel β -sheet, 4±1% parallel β -sheet, 21±1% β -turn and 33±2% other, including random coil. These indicate a substantial contribution of β -sheet and β -turn to the structure of human tropoelastin.

Figure 5.11 Circular dichroism spectrum of SHEL. SHEL was dissolved in water at 0.84mg/ml and spectra obtained at 20 and 50°C. A minimum is seen near 200nm and a second minimum near 220nm for both temperatures. The magnitude of the peak at 200nm is slightly less negative at 50°C than at 20°C.

5.4 DISCUSSION

5.4.1 GST-SHEL Purification

Initial lysis conditions suggested that GST-SHEL was insoluble. However, no inclusion bodies were seen under phase contrast microscopy suggesting

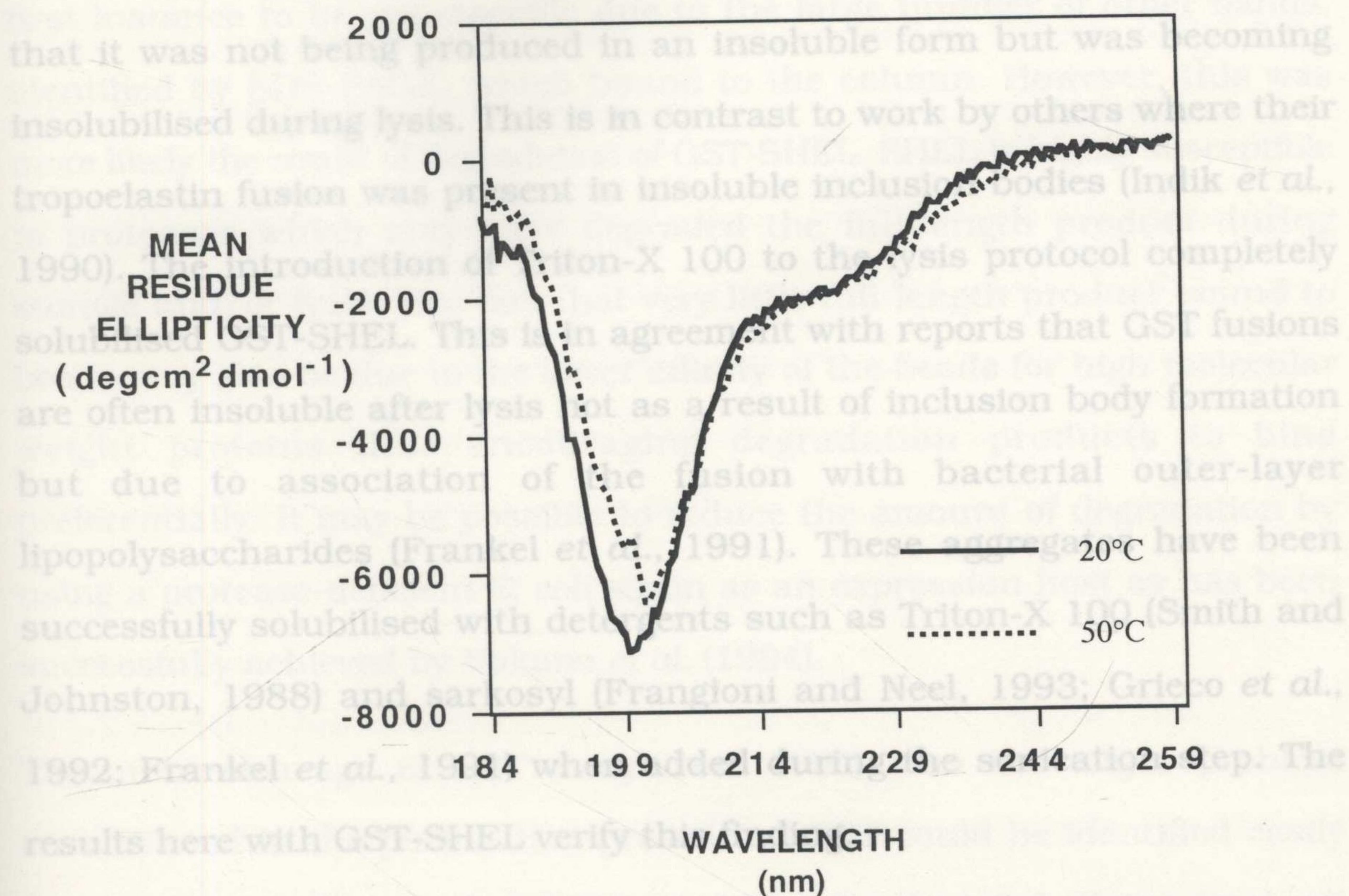


Figure 5.11 Circular dichroism spectrum of SHEL. SHEL was dissolved in water at 0.84mg/ml and spectra obtained at 20 and 50°C. A minimum is seen near 200nm and a second minimum near 220nm for both temperatures. The magnitude of the peak at 200nm is slightly less negative at 50°C than at 20°C.

5.4 DISCUSSION

5.4.1 GST-SHEL Purification

Initial lysis conditions suggested that GST-SHEL was insoluble. However, no inclusion bodies were seen under phase contrast microscopy suggesting that it was not being produced in an insoluble form but was becoming insolubilised during lysis. This is in contrast to work by others where their tropoelastin fusion was present in insoluble inclusion bodies (Indik *et al.*, 1990). The introduction of Triton-X 100 to the lysis protocol completely solubilised GST-SHEL. This is in agreement with reports that GST fusions are often insoluble after lysis not as a result of inclusion body formation but due to association of the fusion with bacterial outer-layer lipopolysaccharides (Frankel *et al.*, 1991). These aggregates have been successfully solubilised with detergents such as Triton-X 100 (Smith and Johnston, 1988) and sarkosyl (Frangioni and Neel, 1993; Grieco *et al.*, 1992; Frankel *et al.*, 1991) when added during the sonication step. The results here with GST-SHEL verify this finding.

Binding of GST-SHEL to glutathione agarose was successful but binding capacity appeared very low. Theoretically, 1ml swollen glutathione agarose beads should be capable of binding 8mg fusion protein (Smith and Johnston, 1988). However, another report demonstrated that binding capacity actually decreases with increasing fusion protein size (Frangioni and Neel, 1993) probably as a result of steric hindrance. Glutathione agarose was shown to bind 8-12 times less of an 83kDa fusion protein than a 26kDa fusion protein with as little as 0.5 to 1 μ g of an 83kDa protein binding to 10 μ l 50% bead slurry (Frangioni and Neel, 1993). This is in a similar range to the binding capacity seen by the 90kDa GST-SHEL in this work. It was also suggested that different brands of beads may have markedly different binding capacities; the brand used in the experiments here (Sigma) having

a twofold lesser capacity than Pharmacia brand beads (Frangioni and Neel, 1993). Both these factors perhaps contributed to the low binding capacity seen with GST-SHEL.

Large scale binding of GST-SHEL to an agarose column appeared in the first instance to be non-specific due to the large number of other bands, identified by SDS-PAGE, which bound to the column. However, this was more likely the result of degradation of GST-SHEL. SHEL is highly susceptible to proteases which may have degraded the full-length product during storage and/or lysis. The fact that very little full-length product bound to beads may also be due to the lower affinity of the beads for high molecular weight proteins thus encouraging degradation products to bind preferentially. It may be possible to reduce the amount of degradation by using a protease-deficient *E. coli* strain as an expression host as has been successfully achieved by Nakano *et al.* (1994).

5.4.2 Purification of SHEL

Thrombin cleavage of GST away from SHEL was the major problem encountered in the purification procedure. GST could be identified easily after thrombin cleavage but SHEL could not be detected. Using total cell lysates as substrate it was clearly seen that SHEL was undergoing preferential cleavage by thrombin into smaller fragments while no change in other bacterial proteins could be discerned. With lower thrombin concentrations full-length SHEL could be identified. The recognition site of thrombin is given as Leu-Val-Pro-Arg-Gly-Ser with cleavage after Arg (Smith and Johnston, 1988). However, thrombin has been shown to be able to recognize other sites preferentially at P4-P3-Pro-Arg/Lys-P1'-P2', where P3 and P4 are hydrophobic amino acids and P1' and P2' are nonacidic amino acids (Chang, 1985). A second major recognition site is P2-Arg/Lys-P1' where P2 or P1' are Gly (Chang, 1985). SHEL has a large number of Arg and Lys residues some of which are similar but not identical to these

typical thrombin recognition sites, yet SHEL is clearly thrombin sensitive. Strictly controlled proteolysis conditions can result in specific cleavage at the fusion junction as demonstrated in this work but the extent and ease of SHEL degradation may make this very much a 'hit or miss' procedure. Since the only Met is a synthetically engineered one precisely at the GST-SHEL junction, cyanogen bromide could be used to release SHEL from GST if desired (Indik *et al.*, 1990).

Therefore, despite excellent overexpression, problems with both glutathione agarose binding and thrombin cleavage precluded use of pSHEL_C as a major source of SHEL. It was decided instead to concentrate on tropoelastin isoform production from the unfused system, pSHEL_F, which has been shown in Chapter 4 to overexpress well.

5.4.2 Purification of SHEL

The purification of directly-expressed SHEL was very successful. The protocol developed for SHEL was subsequently used for SHEL Δ 26A and SHEL Δ mod. The procedure involves an essentially single step which purifies SHEL from all other contaminating proteins. Each of the three forms of SHEL were produced as soluble proteins with no sign of inclusion bodies. The solubility of SHEL in *E. coli* lysates greatly simplified its purification which was easily achieved using a modification of a widely-used protocol for purification of tropoelastin from tissues (Sandberg *et al.*, 1971) based on the unusually high solubility of tropoelastin in short chain alcohols (Partridge, 1967) allowing its selective solubilisation into a propanol/butanol mixture. Although not all of SHEL was solubilised, the technique was successful in precipitating all other contaminating proteins producing a single-step purification that is fast, inexpensive and simple. This is in

contrast with the much harsher, hazardous procedure of cyanogen bromide digestion used previously (Grosso *et al.*, 1991; Indik *et al.* 1990) and undoubtedly simplified the overall purification procedure. More time consuming and less specific combinations of methods such as ammonium sulfate salting out, gel filtration and ion-exchange chromatography traditionally used in protein purifications were therefore avoided. GST-SHEL, in contrast, was not soluble in butanol (not shown) indicating that the GST portion had significantly altered the solubility properties. This method is probably therefore unable to be used successfully with tropoelastin fusion proteins and demonstrates the value of producing unfused recombinant tropoelastin.

SHEL often showed degradation which varied in amount in different preparations. This degradation was not unexpected as tropoelastin seems to have a high susceptibility to proteases. The source of the degradation was shown to come from endogenous *E. coli* proteases. Since the extent of degradation varied with different preparations it is unlikely that degradation products are the result of premature termination of expression although this possibility as a contribution could not be excluded. Furthermore, the degradation profile seen with recombinant SHEL and SHEL Δ 26A is remarkably similar to degradation profiles seen by others in tropoelastin purified from isolated tissues and tissue culture (Hayashi *et al.*, 1995; Franzblau *et al.*, 1989; Rucker, 1982; Mecham and Foster, 1977) indicating that tropoelastin may have regions of extreme susceptibility to proteolysis (see Chapter 6.). Degradation products could be easily removed by reverse phase-HPLC. Both ion-exchange and size fractionation, which are milder purification techniques, were ineffective. Losses onto these columns were noted, an effect previously seen by others also (Rucker, 1982), possibly due to the hydrophobicity of tropoelastin and coacervation in high salt buffers. RP-HPLC was able to purify the smaller fragments on the basis of

their lower hydrophobicity with the degradation products eluting first and full-length SHEL last.

The yields of SHEL and SHEL Δ 26A were high with 30-40mg obtained from one litre of culture. This compares extremely favourably with the 4mg/L obtained using cDNA clones (Indik *et al.*, 1990). The potential for even higher yields is shown by 200mg/L obtained for SHEL Δ mod. 30-40mg/L is a conservative yield based on high reproducibility and quality of final product. With extended induction times and better control of proteolysis, a higher yield could almost certainly be obtained. Some protein is also lost in the alcohol purification step, which, if recovered would increase yield further. A high-cell density fermentation procedure which may allow even greater yields is currently under investigation in the laboratory (A.S. Weiss, personal communication).

5.4.3 Confirmation of Proteins

The purified protein products were subjected to various analyses to confirm their integrity. N-terminal sequencing confirmed the integrity of the amino termini of the two isoforms in addition to clearly detecting a residue change at position 7 in SHEL Δ mod. This method also indicated that no formyl Met was present in any of the proteins. Mass spectrometry confirmed the correct composition with the size calculated correlating precisely with removal of a Met. Formyl Met can often be removed by *E. coli* aminopeptidases. This is a particularly efficient process if the next amino acid contains a short side-chain, such as the Gly in tropoelastin(s), which gives cleavage efficiencies approaching 100% (Meinzel *et al.*, 1993) resulting in this case in SHEL and SHEL Δ 26A products equivalent to the natural primary sequence(s). In contrast, successful purification of GST-SHEL by thrombin

cleavage would result in the presence of two additional amino terminal residues, Gly-Ser, in addition to the Met. Endotoxin levels were greatly decreased after RP-HPLC purification. This is important for further studies with tropoelastin as the hydrophobic endotoxins can interact with hydrophobic domains of tropoelastin and may therefore interfere with physical characterisation (see Chapter 7). Furthermore, a low endotoxin level is a critical requirement for any future *in vivo* studies in animals.

5.4.4 Circular Dichroism

The CD spectrum of the SHEL isoform of human tropoelastin in water at 20°C was similar to the CD spectra published for bovine tropoelastin (Debelle and Alix, 1995), α -elastin (Tamburro *et al.*, 1977), polypeptides of elastin (Urry, 1982) and κ -elastin (Debelle *et al.*, 1995). A negative peak at 200nm is usually indicative of random protein conformation (Johnson, 1990). However, as pointed out by Debelle and Alix (1995) an all- β class of protein, containing β -sheet in a mainly distorted form or in short irregular strands (β -II proteins; Wu *et al.*, 1992), has a similar spectrum (Manavalan and Johnson, 1983; Wu *et al.*, 1992). This is indeed precisely what was determined by secondary structure fitting of the SHEL spectrum, with 41±4% β -sheet identified and 21±1% β -turn, although 33±2% was undefined and likely to be random coil. α -helix was found to be quite low with only 3% identified and likely to be attributed to the cross-linking domains. A similar spectrum was seen at 50°C but with a slightly increased minimum value, similar to that seen by Urry (1982) and Tamburro *et al.* (1977) for elastin polypeptides and α -elastin. No coacervation occurred at this temperature since no NaCl was present. These results demonstrate that the recombinant form of tropoelastin, SHEL, has the same overall secondary structure components as naturally-derived tropoelastin and soluble elastins

and that physical studies can be interpreted as being relevant to the natural situation. The recombinant tropoelastin SHEL, and presumably also SHEL Δ 26A, is therefore a viable alternative to naturally-derived tropoelastin for structural and other associated physical studies. Further physical characterisation, based on these results, is currently being carried out on both isoforms and derivatives of SHEL and SHEL Δ 26A using CD (S. Jensen and A.S. Weiss, unpublished).

5.5 CONCLUSION

Recombinant human tropoelastin isoforms have been successfully produced and purified to produce material suitable for many further applications. The purification procedure for GST-SHEL presented some difficulties but the procedure for directly-expressed tropoelastin isoforms involving butanol solubilisation is simple, fast and efficient, providing a substantially improved method for the purification of recombinant tropoelastin. Degradation products are minimised and easily removed resulting in a high-quality final product. The final yields obtained are a significant improvement on current methods used for tropoelastin production with 50mg easily obtained from one litre of bacterial culture. The purified products appear correct by a number of criteria and have the added advantage of removal of the bacterially-derived N-formyl Met. For the first time, large quantities of selected human tropoelastin isoforms can be readily obtained for study.

CHAPTER 6

**PROTEOLYTIC SUSCEPTIBILITY OF
TROPOELASTIN ISOFORMS TO HUMAN
SERUM AND INDIVIDUAL PROTEASES**

in inadequate or faulty elastin fibre repair at the site of injury (Section 1.3.2).

6.1 INTRODUCTION

Serine protease inhibitors can reduce the degradation of tropoelastin caused by serum (Romero *et al.*, 1986). Tropoelastin is highly susceptible to proteolytic degradation (Christner *et al.*, 1978). This is evident in the substantial amounts of degraded product kallikrein was a candidate serum protease responsible for degradation, isolated from natural sources which can be substantially reduced by adding other experiments proposed that plasmin was the protease involved inhibitors, particularly of serine proteases (Franzblau *et al.*, 1989; Rich and Foster, 1984; Rucker, 1982; Sandberg and Wolt, 1982). In the purification of SHEL and SHEL Δ 26A from *E. coli*, degradation products with sizes similar to those seen in other studies during both purification and storage have been noted (Chapter 5; Franzblau *et al.*, 1989; Sandberg and Wolt, 1982). Since the tropoelastins were purified from different sources, it may be that certain regions of tropoelastin are more susceptible to protease action.

Experiments have shown that mammalian serum contains proteases which are capable of degrading tropoelastin (Romero *et al.*, 1986). Thus, any newly-synthesized unprotected tropoelastin exposed to blood, such as in the blood vessel wall, would be rapidly degraded. It has been proposed that EBP-bound tropoelastin is protected from proteolytic degradation and that this protection can be modelled using S-GAL, a peptide based on the elastin binding domain of EBP (Hinek and Rabinovitch, 1994). Proteolytic degradation of tropoelastin *in vivo* may have important consequences for normal elastogenesis and tissue repair processes. For example, soluble elastin and tropoelastin peptides have been demonstrated to be chemotactic (Wachi *et al.*, 1995; Bisaccia *et al.*, 1994; Grosso and Scott, 1993a,b). Furthermore, soluble elastin peptides may be involved in the autoregulation of tropoelastin production at the mRNA level (McGowan *et al.*, 1996; Foster and Curtiss, 1990; Foster *et al.*, 1990) and this process may be modulated by proteases (McGowan *et al.*, 1996). However, proteolysis could also result

in inadequate or faulty elastin fibre repair at the site of injury (Section 1.3.2).

6.2.1 Reagents

Serine protease inhibitors can reduce the degradation of tropoelastin caused by serum (Romero *et al.*, 1986). This same study suggested that plasma kallikrein was a candidate serum protease responsible for degradation. Other experiments proposed that plasmin was the protease involved (McGowan *et al.*, 1996). In earlier experiments, porcine thrombin was shown to be able to digest heterogeneous porcine tropoelastin *in vitro* (Torres *et al.*, 1977). In Chapter 5, human thrombin was clearly demonstrated to cleave recombinant GST-SHEL in a specific and reproducible manner.

6.2.2 Serum Proteolysis of SHEL

Thus, the protease involved in the serum-induced degradation of tropoelastin remains speculative.

In this chapter, the proteolytic susceptibility of SHEL and SHEL Δ 26A to human serum and individual proteases was examined. Serum was confirmed to have tropoelastin degrading ability, with the protease identified as a serine protease with trypsin or plasmin-like specificity. SHEL and SHEL Δ 26A were shown to be susceptible to a number of serine proteases and the regions of susceptibility identified by precise mapping. Potential inhibitors were evaluated and the process of coacervation is demonstrated to substantially protect tropoelastin from degradation.

PAGE

Serum-digested peptides to be used for sequencing were purified by the addition of 1.5 volumes *n*-propanol followed by 2.5 volumes *n*-butanol and stirred overnight. The organic solvents were removed by rotary evaporation and peptides resuspended in 50mM sodium phosphate buffer, pH 7.8.

6.2 MATERIALS AND METHODS

6.2.1 Reagents

Thrombin (0.01-1U), human SHEL and SHEL Δ 26A were obtained as described in Chapters 4 and 5. Human plasma kallikrein (3×10^{-4} - 3×10^{-5} U), human plasmin (7×10^{-4} - 1×10^{-5} U), bovine Hirudin, PMSF, human thrombin, human plasma kallikrein, human plasmin and human leukocyte elastase (HLE) were obtained from Sigma. Bovine trypsin (1.5×10^{-4} - 4×10^{-5} U) and human leukocyte elastase (1.6×10^{-4} - 3.2×10^{-5} U) were added to 10 μ g SHEL or SHEL Δ 26A in 50mM sodium phosphate buffer, pH 7.8 in a total volume of 20 μ l. All reactions were performed at 37°C for one hour. The degradation profile was analysed by 8, 10 or 12% SDS-PAGE. The degradation products were analysed by HPLC as described in Section 2.9.

6.2.2 Serum Proteolysis of SHEL

Human serum was obtained from fresh intravenous blood, centrifuged at 2000g to remove red blood cells and then allowed to clot before serum was removed. Aliquots (20 μ l) were stored at -20°C and thawed when needed. 15 μ g tropoelastin in 50mM sodium phosphate buffer, pH 7.8 was incubated with 0.5 μ l serum in a 20 μ l reaction for between 1 and 18hr at 37°C. Similar experiments were conducted with or without prior addition of inhibitors. Inhibitors were added at the following concentrations; 0.5 or 1U hirudin, 0.5 or 5mM Pefabloc SC, 1 or 5mM PMSF, 25mM EDTA, 50 or 250 μ M Pefabloc PK. All inhibitors were dissolved in water except PMSF which was dissolved in isopropanol. Reactions were analysed by 8% SDS-PAGE. Serum-digested peptides to be used for sequencing were purified by the addition of 1.5 volumes n-propanol, followed by 2.5 volumes n-butanol and stirred overnight. The organic solvents were removed by rotary evaporation and peptides resuspended in 50mM sodium phosphate buffer, pH 7.8.

human leukocyte elastase, 1.6×10^{-5} U, serum 1 μ l) was added (as determined in Section 6.2.3) for 10-80min. Various dilutions of serum from 1/2 to

6.2.3 Proteolytic Assays

A range of enzyme concentrations was originally used to determine the optimal amount for subsequent experiments. Thrombin (0.01-1U), human plasma kallikrein (3×10^{-4} - 3×10^{-3} U), human plasmin (7×10^{-5} - 4×10^{-7} U), bovine trypsin (5×10^{-4} - 4×10^{-3} U) and human leukocyte elastase (1.6×10^{-4} - 3.2×10^{-3} U) were added to 10 μ g SHEL or SHEL Δ 26A in 50mM sodium phosphate buffer, pH 7.8 in a total volume of 20 μ l. All reactions were performed at 37°C for one hour. The degradation profile was analysed by 8, 10 or 12% SDS-PAGE.

6.2.4 N-terminal Sequencing

Gels were poured, run and blotted as described in Section 2.8. N-terminal sequencing is described in Section 2.9.

6.2.5 Peptide Preparation and Use

S-GAL, N-VVGSPSAQDEASPLS -C, is a peptide representing the elastin binding domain of EBP (Hinek and Rabinovitch, 1994). It was synthesised by Chiron Mimotopes (Australia) and purified by RP-HPLC as described in Section 5.2.7, except that a 0-100% acetonitrile 0.1% TFA gradient was used. A large molar excess of S-GAL in MQW (10 to 200-fold) was added to 15 μ g SHEL in 50mM sodium phosphate pH 7.8, made up to a total volume of 40 μ l and pre-incubated at 37°C for one hour, as suggested by Hinek and Rabinovitch (1994) before the selected protease (kallikrein, 6 - 15×10^4 U; thrombin, 0.1-0.2U; trypsin, 2×10^3 U; plasmin, 1.5 - 3.7×10^5 U; human leukocyte elastase, 1.6×10^3 U, serum 1 μ l) was added (as determined in Section 6.2.3) for 10-80min. Various dilutions of serum from 1/2 to

1/50 in 50mM sodium phosphate pH 7.8 were used and both SHEL and SHEL Δ 26A were used for each experiment.

6.3.1 Degradation of SHEL By Serum

A peptide representing a region of SHEL cleaved by a selection of serine proteases: N- AAKAQLRAAAGLGA -C (serine protease site peptide, SPS-peptide; See Results) was synthesised by Chiron Mimotopes (Australia) to test whether its presence could protect SHEL from degradation by acting as a competitor. Experiments were conducted in parallel with S-GAL using identical procedures (see above). Both SHEL and SHEL Δ 26A were used. Each reaction was analysed by 10% SDS-PAGE. Gels were scanned by densitometry and the volume of full-length SHEL calculated as described in Section 2.10.

6.2.6 Proteolysis During Coacervation

10mg/ml SHEL in 50mM sodium phosphate, pH 7.8 and 150mM NaCl was allowed to coacervate at 37°C until cloudy before adding human plasma kallikrein (6×10^4 U), thrombin (1U), plasmin (1.5×10^5 U), trypsin (2×10^3 U), HLE (1.6×10^3 U) and serum (0.75 μ l) for one hour. Control reactions were performed at 16°C for three hours. Extent of proteolysis was monitored by SDS-PAGE.

6.3 RESULTS

6.3.1 Degradation of SHEL By Serum

Human tropoelastin was degraded by human serum into discrete bands, resistant to further degradation. The same degradation profile was seen by SDS-PAGE with overnight incubation as with incubations left for one hour (Figure 6.1a). Figure 6.1b clearly shows the peptide fragments after purification from serum using butanol. The sizes of the major bands are approximately 50, 45, 35, 28, 27, 25, 22 and 18kDa, visually similar to that obtained by Romero *et al.* (1986) using porcine tropoelastin. The pattern of peptides produced was reproducible over many separate experiments. Similar results were obtained with SHEL Δ 26A (Figure 6.1b) but the 22 and 18kDa bands were absent and replaced by a 15kDa band.



6.3.2 Effect of Protease Inhibitors on Serum Degradation

Figure 6.2 shows the amount of full-length SHEL after incubation with serum in the presence and absence of various protease inhibitors. Wide-spectrum serine protease inhibitors were found to inhibit degradation since both Pefabloc SC and PMSF protected tropoelastin from cleavage (Figure 6.2). In contrast, EDTA, which is an inhibitor of metalloproteases, appeared to promote digestion. Protease inhibitors specific for the serine proteases thrombin and kallikrein were also tested. Hirudin, a highly specific inhibitor of thrombin, did not appear to significantly inhibit degradation whereas Pefabloc PK, specific for kallikrein, inhibited proteolysis (Figure 6.2).

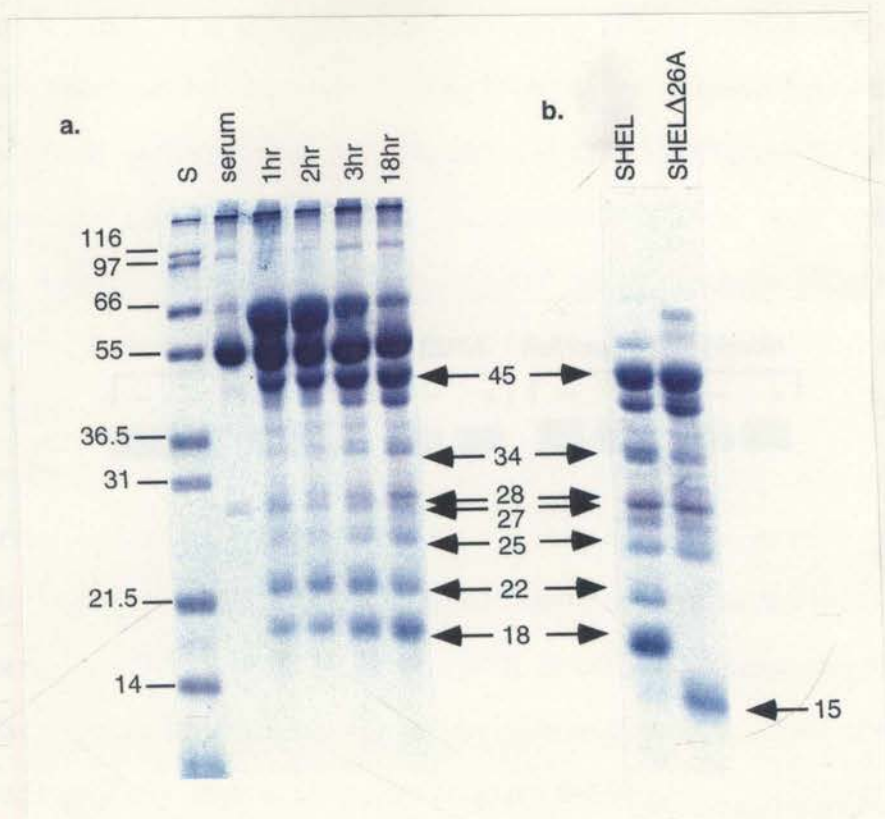
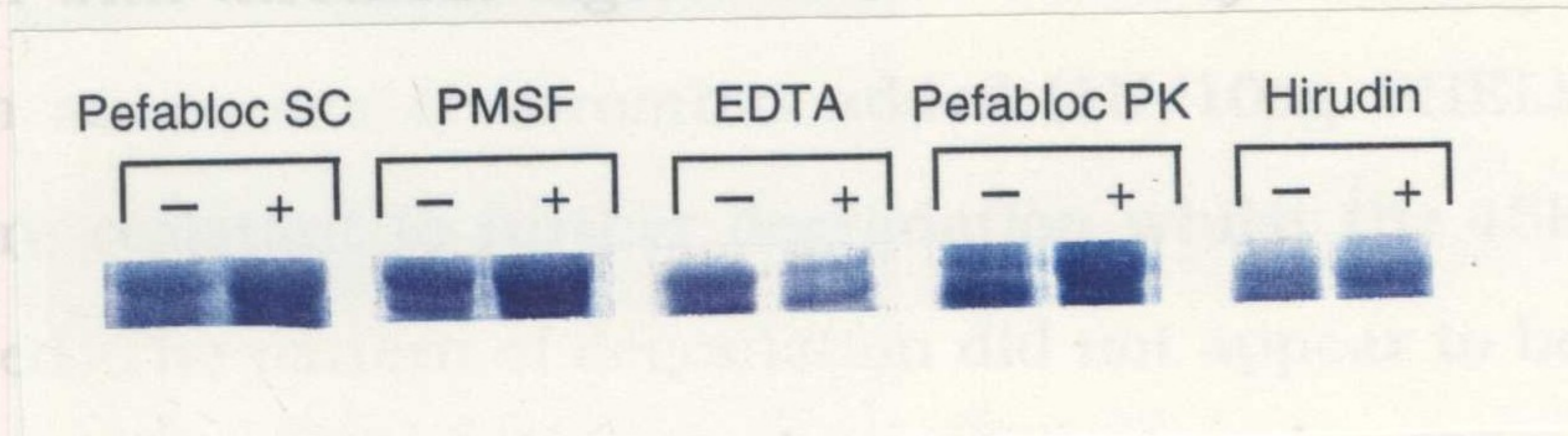


Figure 6.1 Degradation of SHEL with serum. **a.** After addition of serum to SHEL for 1, 2, 3 or 18hr, SHEL is fragmented into a number of distinct bands as seen by 10% SDS-PAGE. Products from overnight digestion are very similar to products present after one hour of digestion. **b.** SHEL and SHEL Δ 26A peptide fragments produced by serum digestion and purified by butanol solubilisation were analysed by 10% SDS-PAGE. A band at 15kDa appears with SHEL Δ 26A (arrow) in place of the 22 and 18kDa bands. Approximate sizes of fragments produced are shown in kDa. Size markers (S) are shown in kDa.

6.3.3 Degradation of SHEL with Specific Proteases

6.3.3.1 Human Thrombin

In Chapter 5, it was shown that thrombin was able to cleave GST-SHEL extensively and in a reproducible manner. When increasing amounts of thrombin were added to pure SHEL, four major fragments were identified by SDS-PAGE estimated at 45, 34, 22 and 13kDa (Figure 6.3a) in addition to faint minor bands. The sizes of the major products were very similar to those seen with thrombin digests of GST-SHEL lysates (Section 5.3.1.3).



Even with the smaller bands were the same as for serum-produced peptides. When hirudin was added to reactions, degradation was inhibited (not shown), unlike the results seen with serum. The pattern of degradation seen with SHELΔ26A was slightly different, with the 22kDa fragment reduced in size to about 15kDa, consistent with this fragment not containing 26A (Figure 6.3b).

Figure 6.2 Effect of protease inhibitors on serum degradation of SHEL. The presence (+) or absence (-) of various protease inhibitors on the amount of full-length SHEL was analysed by 8% SDS-PAGE. Full-length SHEL is increased in the presence of Pefabloc SC (0.5mM), Pefabloc PK (50μM) and PMSF (5mM) compared with serum alone, while there is no noticeable effect in the presence of hirudin (1U). In contrast, the presence of EDTA results in a decrease in the amount of full-length SHEL.

6.3.3 Degradation of SHEL with Specific Proteases

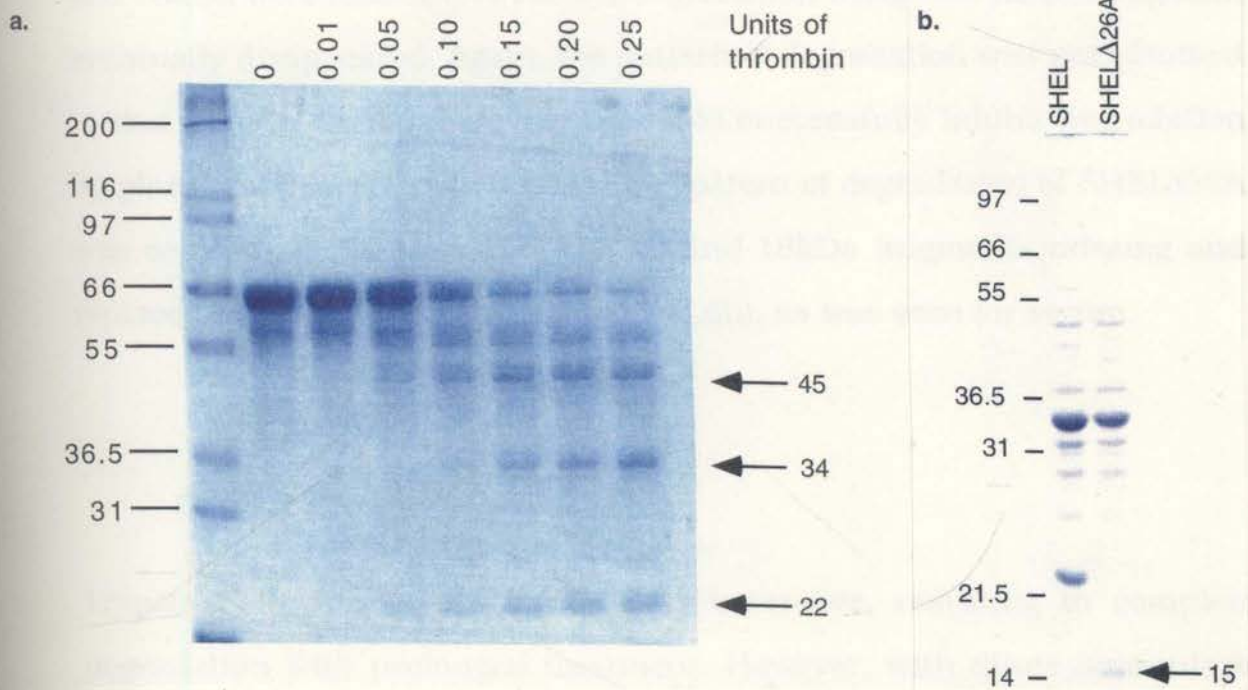
6.3.3.1 Human Thrombin

In Chapter 5, it was shown that thrombin was able to cleave GST-SHEL extensively and in a reproducible manner. When increasing amounts of thrombin were added to pure SHEL, four major fragments were identified by SDS-PAGE estimated at 45, 34, 22 and 13kDa (Figure 6.3a) in addition to faint minor bands. The sizes of the major products were very similar to those seen with thrombin digests of GST-SHEL lysates (Section 5.3.1.3). Even with an excess of thrombin added (1U/10 μ g SHEL) the smaller bands were resistant to further degradation whilst the 45kDa fragment disappeared. The pattern of degradation did not appear to be the same as for serum-produced peptides. When hirudin was added to reactions, degradation was inhibited (not shown), unlike the results seen with serum. The pattern of degradation seen with SHEL Δ 26A was slightly different, with the 22kDa fragment reduced in size to about 15kDa, consistent with this fragment not containing 26A (Figure 6.3b).

Figure 6.3 Effect of thrombin on SHEL and SHEL Δ 26A. a. Increasing amounts of thrombin were added to SHEL and analysed by 8% SDS-PAGE. Three major degradation products are seen estimated at 45, 34 and 22kDa, as well as a 13kDa fragment not seen in this gel. b. Effect of thrombin (1U) on degradation of SHEL Δ 26A compared with SHEL, analysed by 8% SDS-PAGE. A band at 15kDa (arrow) appears in place of the 22kDa band. Fragment sizes are estimated in kDa. Size markers (S) are shown in kDa.

6.3.3.2 Human Plasma Kallikrein

Like thrombin, increasing amounts of human plasma kallikrein added to SHEL resulted in specific and reproducible degradation. Three major fragments were identified by SDS-PAGE (Figure 6.4a) estimated to be 45, 22 and 18kDa, in addition to faint minor bands. The major bands at 45



enzyme (4×10^{-3} U) major bands could be identified at approximately 50, 45, 40, 38, 34, 31, 22 and 16kDa, giving an overall pattern similar to serum products (Figure 6.5a). Indeed, at low enzyme concentrations the trypsin digest profile looked virtually identical to the serum digest profile. However,

Figure 6.3 Effect of thrombin on SHEL and SHEL Δ 26A. **a.** Increasing amounts of thrombin were added to SHEL and analysed by 8% SDS-PAGE. Three major degradation products are seen estimated at 45, 34 and 22kDa, as well as a 13kDa fragment not seen in this gel. **b.** Effect of thrombin (1U) on degradation of SHEL Δ 26A compared with SHEL, analysed by 8% SDS-PAGE. A band at 15kDa (arrow) appears in place of the 22kDa band. Fragment sizes are estimated in kDa. Size markers (S) are shown in kDa.

the 22 and 18kDa fragments were replaced by a single fragment at 15kDa.

6.3.3.2 Human Plasma Kallikrein

Like thrombin, increasing amounts of human plasma kallikrein added to SHEL resulted in specific and reproducible degradation. Three major fragments were identified by SDS-PAGE (Figure 6.4a) estimated to be 45, 22 and 18kDa, in addition to faint minor bands. The major bands at 45 and 18kDa were resistant to further degradation whilst the 22kDa fragment eventually disappeared. Again, the pattern of degradation was not identical to that seen by serum. Pefabloc PK could successfully inhibit degradation by plasma kallikrein (not shown). The pattern of degradation of SHEL Δ 26A was somewhat different, with the 22 and 18kDa fragments missing and replaced by a 15kDa fragment (Figure 6.4b), as was seen for serum.

6.3.3.3 Bovine Trypsin

Trypsin digestion of SHEL was very extensive, resulting in complete degradation with prolonged treatment. However, with dilute amounts of enzyme (4×10^{-3} U) major bands could be identified at approximately 50, 45, 40, 38, 34, 31, 22 and 18kDa, giving an overall pattern similar to serum products (Figure 6.5a). Indeed, at low enzyme concentrations the trypsin digest profile looked virtually identical to the serum digest profile. However, trypsin digestion was not easily reproducible due to the vigorous action of trypsin on SHEL. Similar results were obtained using SHEL Δ 26A (Figure 6.5b) except that the sizes of the smaller fragments below 34kDa were all reduced in size by approximately 4kDa and as for kallikrein and serum, the 22 and 18kDa fragments were replaced by a single fragment at 15kDa.

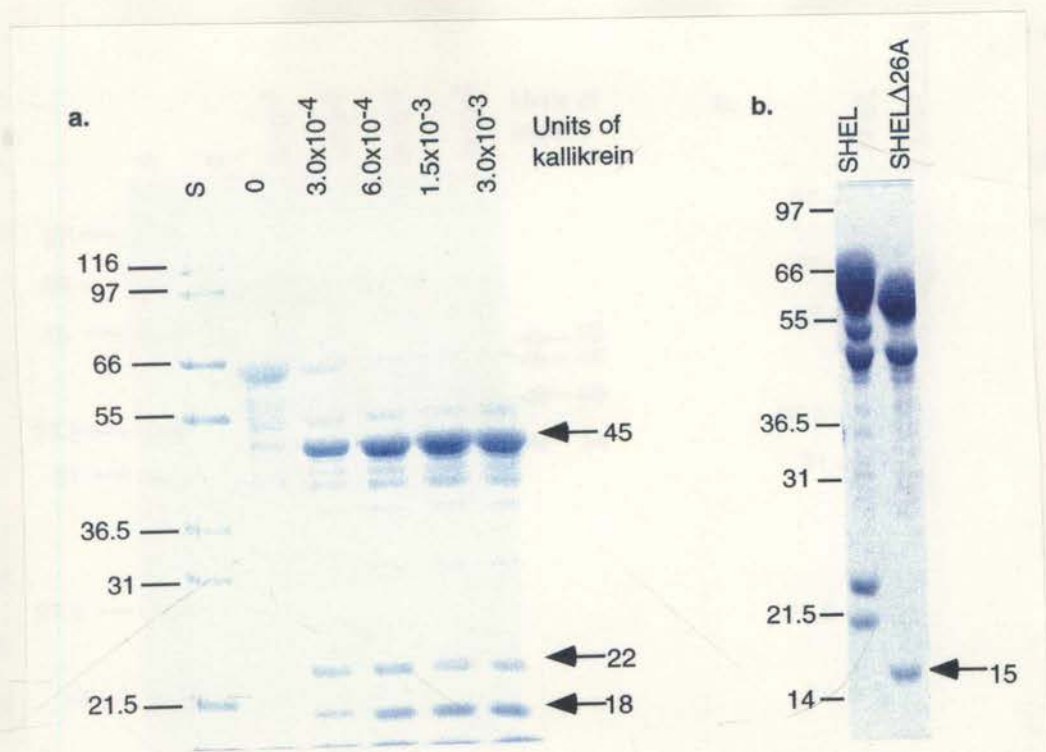


Figure 6.4 Effect of kallikrein on SHEL and SHEL Δ 26A. **a.** Increasing concentrations of kallikrein were added to SHEL and analysed by 8% SDS-PAGE. Three major fragments are seen at 45, 22 and 18kDa. The 22kDa fragment disappears with higher concentrations or longer incubations with kallikrein. **b.** Effect of kallikrein (6×10^{-4} U) on degradation of SHEL Δ 26A compared with SHEL, analysed by 8% SDS-PAGE. Only two fragments are seen with SHEL Δ 26A at 45 and 15kDa (arrow). Fragment sizes and size markers (S) are shown in kDa.

6.3.3.4 Human Plasmin

Using plasmin at low concentrations also gave a profile very similar to both serum and trypsin (Figure 6.6a), while at high concentration extensive degradation occurred. Major bands could be isolated using low concentration

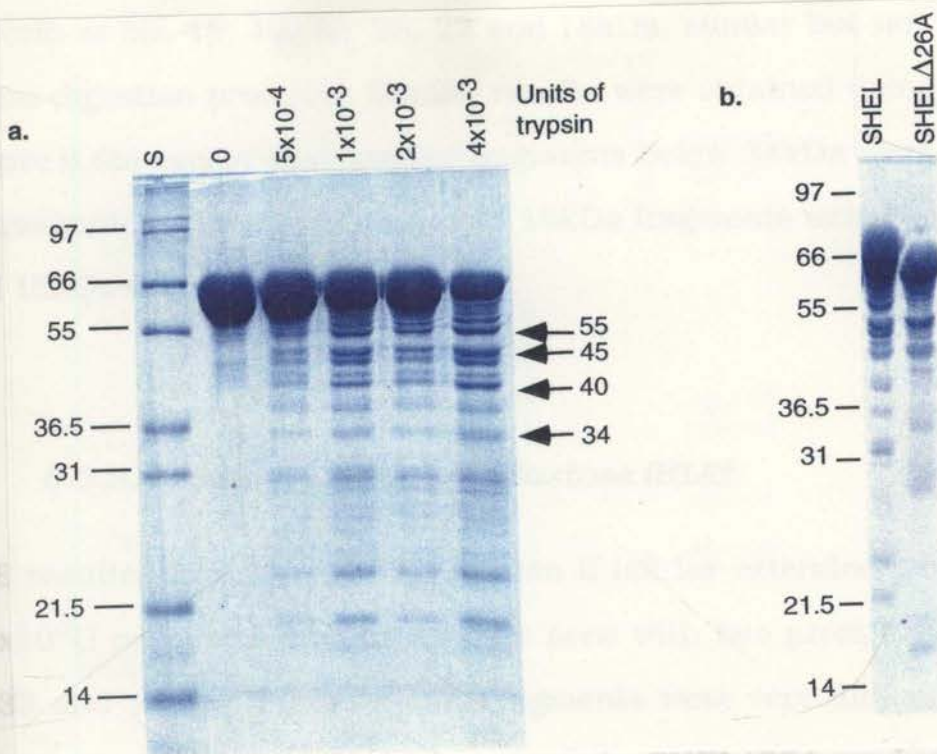


Figure 6.5 Effect of bovine trypsin on SHEL and SHELΔ26A. **a.** Increasing concentrations of bovine trypsin were added to SHEL and analysed by 10% SDS-PAGE. Dilute amounts of trypsin produce prominent bands at 50, 45, 40, 34, 31-25, 22 and 18kDa, similar to serum-produced peptides. Higher concentrations completely degrade SHEL (not shown). **b.** Effect of bovine trypsin (2×10^{-3} U) on SHELΔ26A compared with SHEL, analysed by 10% SDS-PAGE. The overall pattern of fragments is the same as for SHEL but the size of the smaller fragments are all approximately 4kDa less. Fragment sizes and size markers (S) are shown in kDa.

peptides corresponded either to the N-terminus of SHEL or to cleavage sites C-terminally adjacent to a Lys or Arg. Sequences of peptides are shown in Table 6.1 and the positions of the cleavage sites is indicated diagrammatically in Figure 6.8.

6.3.3.4 Human Plasmin

Using plasmin at low concentrations also gave a profile very similar to both serum and trypsin (Figure 6.6a), while at high concentration extensive degradation occurred. Major bands could be isolated using low concentration plasmin at 55, 45, 40, 34, 28, 22 and 18kDa, similar but not identical to serum-digestion products. Similar results were obtained using SHEL Δ 26A (Figure 6.6b) except that smaller fragments below 34kDa were reduced by approximately 4kDa and the 22 and 18kDa fragments were replaced by 17 and 15kDa fragments.

6.3.3.5 Human Leukocyte Elastase (HLE)

HLE resulted in extensive degradation if left for extended periods. Using 1.6×10^2 U numerous fragments were seen with two prominent fragments at 32 and 18kDa (Figure 6.7a). Fragments were very difficult to isolate, however, and overdigestion occurred easily. SHEL Δ 26A produced a similar profile but with all fragments appearing 4kDa smaller (Figure 6.7b).

6.3.4 Mapping of Protease-Susceptible Sites

The thrombin, kallikrein, plasmin, trypsin and serum-produced peptides indicated in Figures 6.1 to 6.7 by an arrow, were N-terminally sequenced and assigned to regions of SHEL. Peptides corresponded either to the N-terminus of SHEL or to cleavage sites C-terminally adjacent to a Lys or Arg. Sequences of peptides are shown in Table 6.1 and the positions of the cleavage sites is indicated diagrammatically in Figure 6.8.

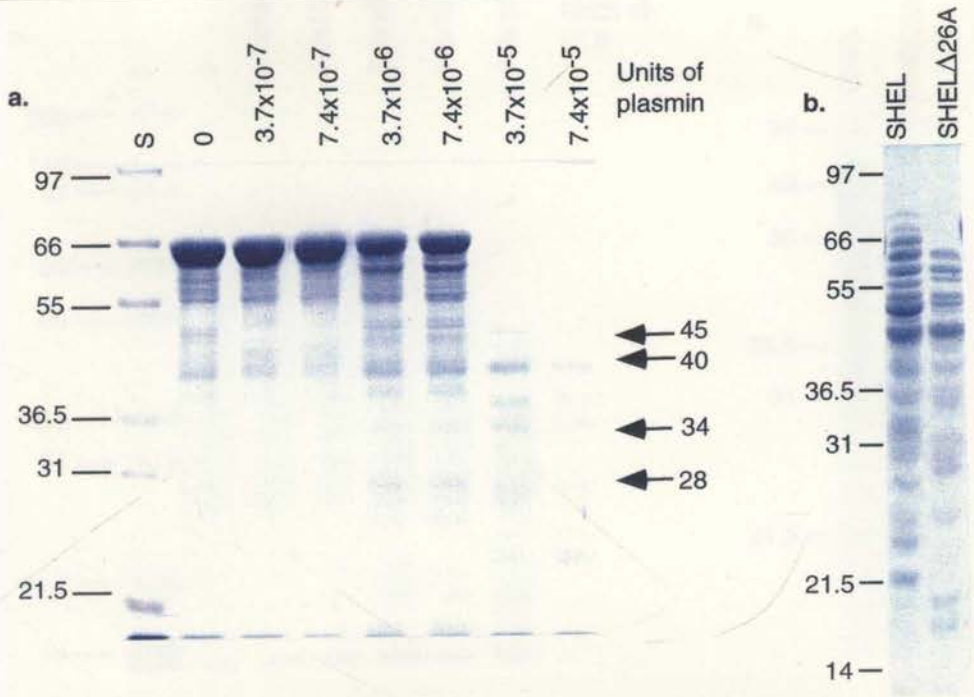


Figure 6.6 Effect of plasmin on SHEL and SHEL Δ 26A. **a.** Increasing concentrations of plasmin were added to SHEL and analysed by 10% SDS-PAGE. Dilute amounts of plasmin produce prominent bands at 50, 45, 40, 34, 28, 22 and 18kDa similar to serum-produced peptides. Higher concentrations of plasmin or longer incubations completely degrade SHEL (not shown). **b.** Effect of plasmin (7.4×10^{-5} U) on SHEL Δ 26A compared with SHEL, analysed by 10% SDS-PAGE. The overall pattern is similar to SHEL but the smaller fragments are approximately 4kDa smaller. Fragment sizes and size markers (S) are shown in kDa.

Table 6.1 . N-terminal Sequences of Protease-Produced Tropoelastin Peptides

	Size (kDa)*	Sequence [†]	Position
thrombin	45	GGVPGAIPG	
	34	K /APGVGGAF	152/153
	22 (19)	R /AAAGLG	515/516
kallikrein	45	GGVPGAIPG	
	22 (19)	R /AAAGLG	515/516
	18 (15)	R /SLSPELREGD	564/565
trypsin	55	GGVPGAIPG	
	45	GGVPGAIPG	
	40	GGVPGAIPG	
	34	GGVPGAIPG	
plasmin	55	GGVPGAIP	
	45	K /AAKAGAGL + GGVPGAIP	78/79
	40	K /AAKAGAGL + K /AGAGLGGV	78/79 + 81/82
	34	K /AAKAGAGL + K /AGAGLGGV	78/79 + 81/82
	28	K /AAKAGAGL + K /AGAGLGGV	78/79 + 81/82
serum	50	GGVPGAIPGGVP	
	45	GGVPGAIPGG	
	34	GGVPGAIPGGVP	
	28 (25)	GGVPGAIPG + K /AAQFGLVPGV(?) [‡]	441/442
	27	GGVPGAIPGGVPGGFYPG	
	25 (20)	GGVPGAIPG + K /SAAKVAKAQ(?)	503/504
	22 (19)	R /AAAGLG	515/516
	18 (15)	R /SLSPELRE	564/565
	13	GGVPGAIP	

*Size of fragments are calculated from SDS-PAGE and are approximate. Sizes in brackets are the sizes determined from the position of the cleavage determined by N-terminal sequencing.

[†]A slash (/) indicates an internal cleavage site adjacent to an R or K residue (bold). N-terminal sequence of residues to the right of these sites was obtained allowing the precise location of the cleavage site to be allocated and the exact size of the fragment to be calculated.

[‡]A question mark (?) indicates that this designation is tentative. The peptide is likely to be present at a very low level and as a mixture with other peptides.

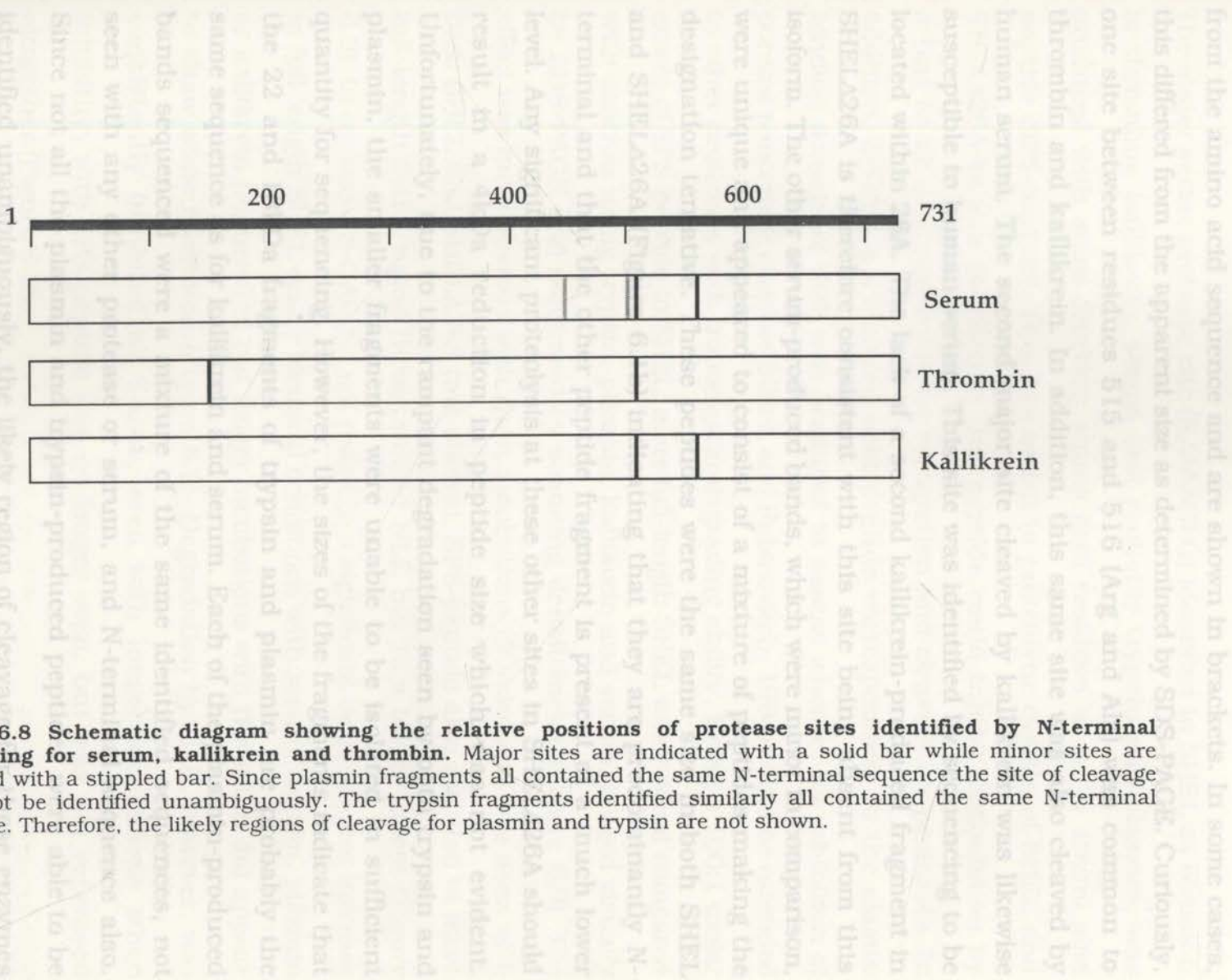


Figure 6.8 Schematic diagram showing the relative positions of protease sites identified by N-terminal sequencing for serum, kallikrein and thrombin. Major sites are indicated with a solid bar while minor sites are indicated with a stippled bar. Since plasmin fragments all contained the same N-terminal sequence the site of cleavage could not be identified unambiguously. The trypsin fragments identified similarly all contained the same N-terminal sequence. Therefore, the likely regions of cleavage for plasmin and trypsin are not shown.

The actual sizes, in kDa, of the fragments shown in Table 6.1 were determined from the amino acid sequence and are shown in brackets. In some cases, this differed from the apparent size as determined by SDS-PAGE. Curiously, one site between residues 515 and 516 (Arg and Ala) was common to thrombin and kallikrein. In addition, this same site was also cleaved by human serum. The second major site cleaved by kallikrein was likewise susceptible to human serum. This site was identified by sequencing to be located within 26A. The lack of a second kallikrein-produced fragment in SHELΔ26A is therefore consistent with this site being absent from this isoform. The other serum-produced bands, which were minor in comparison, were unique and appeared to consist of a mixture of peptides making the designation tentative. These peptides were the same size in both SHEL and SHELΔ26A (Figure 6.1b) indicating that they are predominantly N-terminal and that the other peptide fragment is present at a much lower level. Any significant proteolysis at these other sites in SHELΔ26A should result in a 4kDa reduction in peptide size which was not evident. Unfortunately, due to the rampant degradation seen by both trypsin and plasmin, the smaller fragments were unable to be isolated in sufficient quantity for sequencing. However, the sizes of the fragments indicate that the 22 and 18kDa fragments of trypsin and plasmin are probably the same sequence as for kallikrein and serum. Each of the plasmin-produced bands sequenced were a mixture of the same identified sequences, not seen with any other protease or serum, and N-terminal sequence also. Since not all the plasmin and trypsin-produced peptides were able to be identified unambiguously, the likely region of cleavage for these enzymes is not shown in Figure 6.8.

6.3.5 Effect of S-GAL and SPS- Peptide on Degradation

The major serine protease site (R/AAAGLG) identified in SHEL as common to thrombin, kallikrein, serum and probably trypsin and plasmin, was produced with some flanking amino acid residues as a 14 amino acid peptide (SPS-peptide). This was added to proteolytic digests of SHEL and SHEL Δ 26A to assess whether this peptide could inhibit degradation by acting as an alternative site for recognition and cleavage by proteases. In addition, S-GAL, a 15 amino acid peptide corresponding to the elastin binding domain of EBP was produced to assess whether its inhibition of porcine pancreatic elastase (Hinek and Rabinovitch, 1994) could be extended to other proteases with tropoelastin-degrading ability. Using a 100:1 molar excess of SPS-peptide to SHEL, more full-length SHEL was evident compared with controls using trypsin, plasmin, kallikrein and serum, judged visually by SDS-PAGE and confirmed by scanning densitometry (Figure 6.9). The effect was most obvious with short incubations (20min) and was seen with both SHEL and SHEL Δ 26A (not shown). SPS-peptide also resulted in more full-length SHEL using thrombin and HLE but to a lesser extent (Figure 6.9). In contrast, S-GAL did not result in a significant or consistent increase in full-length SHEL under identical conditions with serum, trypsin, plasmin or kallikrein (Figure 6.9) but longer incubations with thrombin did appear to show some inhibition (Figure 6.9). Degradation by HLE, however, was consistently inhibited by S-GAL, even with longer incubations when inhibition with SPS-peptide was no longer seen, but was not repressed altogether (Figure 6.9).

Effect of S-GAL and the SPS-peptide on degradation of SHEL. Addition of SPS-peptide or S-GAL to SHEL reactions containing proteases was examined by 10% SDS-PAGE. The conditions used are serum, 1/2 dilution 30min; trypsin 10min; plasmin 1.5×10^{-6} U 20min; kallikrein 15×10^{-6} U 40min; thrombin 0.1U 20min; HLE 70min. Thrombin and kallikrein were used with a 300:1 peptide:SHEL ratio while the others were used with a 100:1 ratio. Gels were scanned by densitometry and the relative amount of each full-length SHEL band is shown in a histogram. In each case, the presence of SPS-peptide resulted in more full-length SHEL remaining than in control reactions, while the presence of S-GAL also resulted in more full-length SHEL in the presence of thrombin and HLE only.

6.3.6 Effect of Coacervation on Degradation of SHEL

SHEL, when in the coacervated state at 37°C was significantly protected from degradation by trypsin, plasmin and kallikrein (Figure 6.10a) but not by plasmin or thrombin (not shown). The effect of HLE on SHEL (not shown) was not due to the presence of high concentrations of SHEL in the reaction mixture as control reactions (not shown) were performed at a lower temperature not conducive to coacervation and did not show any difference in degradation in the presence or absence of SHEL (Figure 6.10b).

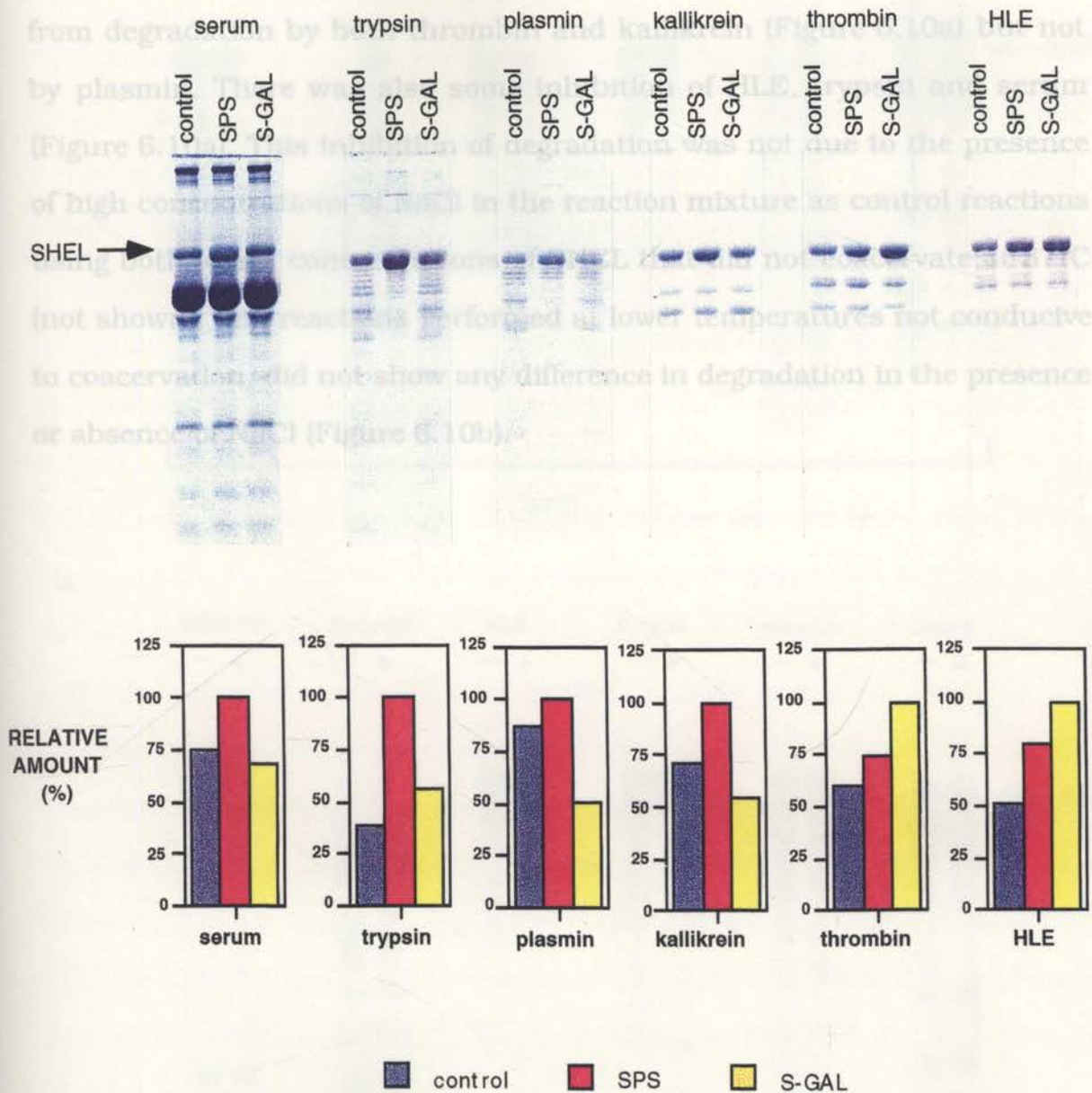


Figure 6.9 Typical effect of S-GAL and the SPS-peptide on degradation of SHEL. Addition of SPS-peptide or S-GAL to SHEL reactions containing proteases was examined by 10% SDS-PAGE. The conditions used are serum, 1/2 dilution 20min; trypsin 20min; plasmin 1.5×10^{-5} U 20min; kallikrein 15×10^{-4} U 40min; thrombin 0.1U 20min; HLE 70min. Thrombin and kallikrein were used with a 200:1 peptide:SHEL ratio while the others were used with a 100:1 ratio. Gels were scanned by densitometry and the relative amount of each full-length SHEL band is shown in a histogram. In each case, the presence of SPS-peptide resulted in more full-length SHEL remaining than in control reactions, while the presence of S-GAL also resulted in more full-length SHEL in the presence of thrombin and HLE only.

6.3.6 Effect of Coacervation on Degradation of SHEL

SHEL, when in the coacervated state at 37°C was significantly protected from degradation by both thrombin and kallikrein (Figure 6.10a) but not by plasmin. There was also some inhibition of HLE, trypsin and serum (Figure 6.10a). This inhibition of degradation was not due to the presence of high concentrations of NaCl in the reaction mixture as control reactions using both lesser concentrations of SHEL that did not coacervate at 37°C (not shown), and reactions performed at lower temperatures not conducive to coacervation, did not show any difference in degradation in the presence or absence of NaCl (Figure 6.10b).

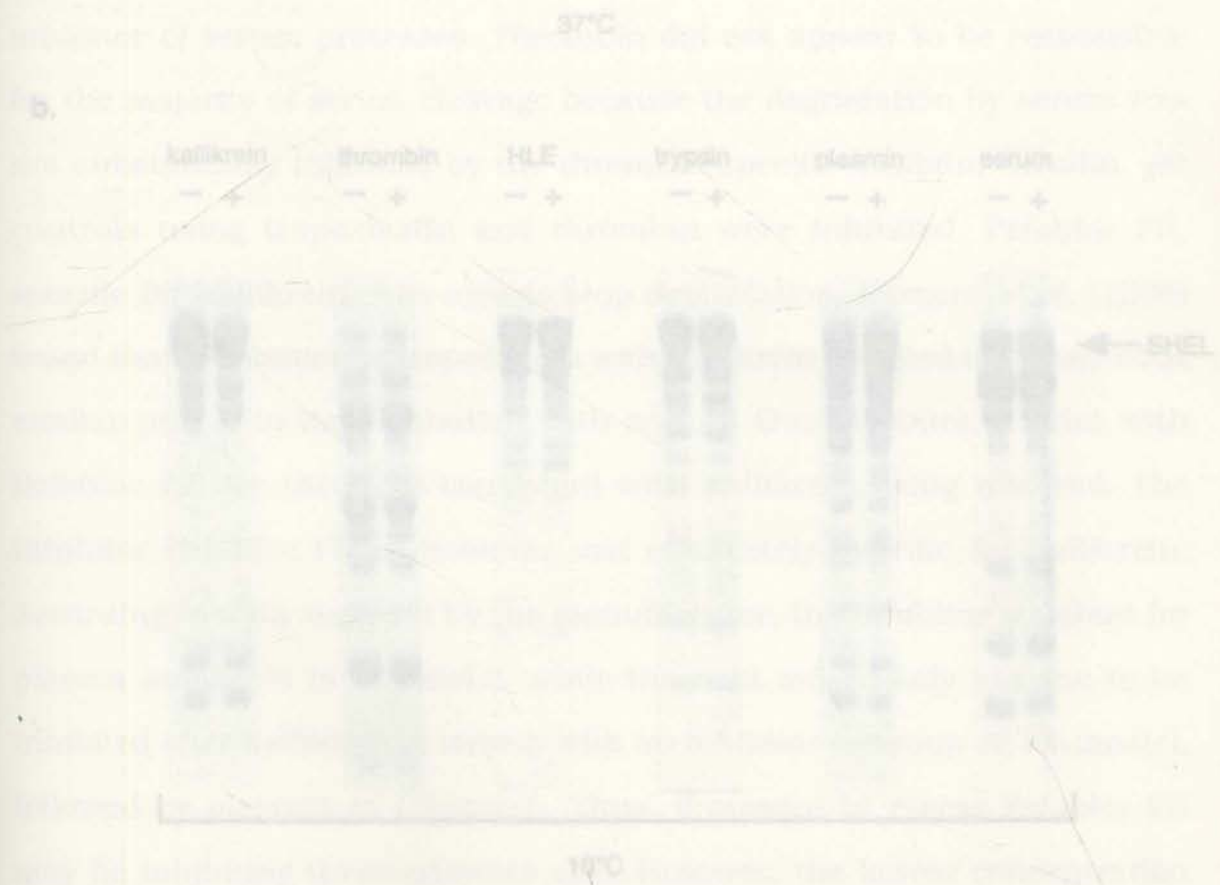


Figure 6.10 Effect of coacervation on the degradation of SHEL by proteases. a. SHEL degradation in the presence of NaCl conducive to coacervation of SHEL at 37°C (+) was compared to SHEL which did not coacervate at 37°C (-). b. Control reactions in the presence (+) and absence (-) of NaCl were performed at 18°C. Significant protection from kallikrein and thrombin proteolysis is seen when SHEL is coacervated. Protection is also seen from serum, trypsin and HLE while some is seen with plasmin. At 18°C all of the proteases degraded SHEL to a similar extent in both the presence and absence of NaCl.

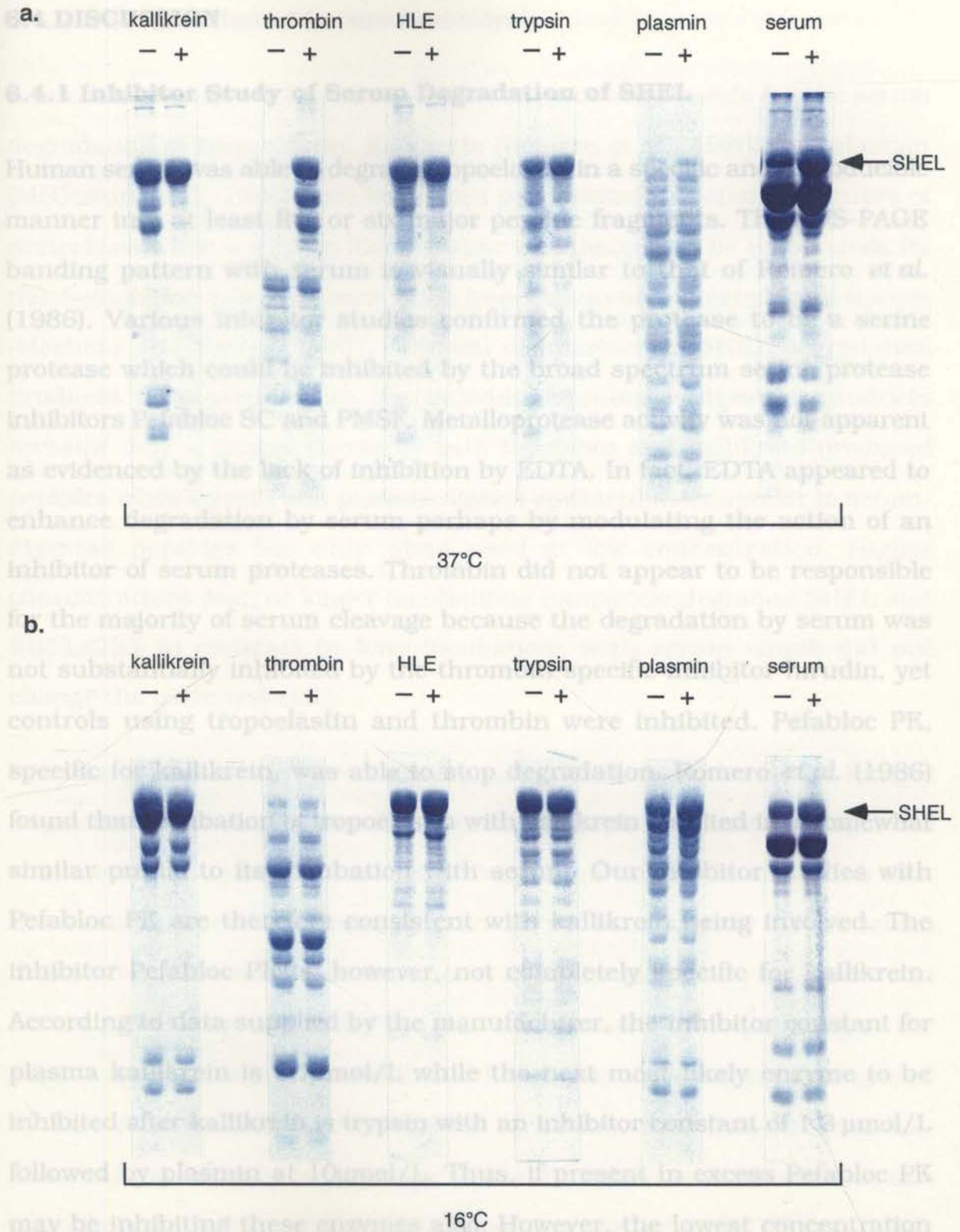


Figure 6.10 Effect of coacervation on the degradation of SHEL by proteases. a. SHEL degradation in the presence of NaCl conducive to coacervation of SHEL at 37°C (+) was compared to SHEL which did not coacervate at 37°C (-). **b.** Control reactions in the presence (+) and absence (-) of NaCl were performed at 16°C. Significant protection from kallikrein and thrombin proteolysis is seen when SHEL is coacervated. Protection is also seen from serum, trypsin and HLE while none is seen with plasmin. At 16°C all of the proteases degraded SHEL to a similar extent in both the presence and absence of NaCl.

6.4 DISCUSSION

6.4.1 Inhibitor Study of Serum Degradation of SHEL

Human serum was able to degrade tropoelastin in a specific and reproducible manner into at least five or six major peptide fragments. The SDS-PAGE banding pattern with serum is visually similar to that of Romero *et al.* (1986). Various inhibitor studies confirmed the protease to be a serine protease which could be inhibited by the broad spectrum serine protease inhibitors Pefabloc SC and PMSF. Metalloprotease activity was not apparent as evidenced by the lack of inhibition by EDTA. In fact, EDTA appeared to enhance degradation by serum perhaps by modulating the action of an inhibitor of serum proteases. Thrombin did not appear to be responsible for the majority of serum cleavage because the degradation by serum was not substantially inhibited by the thrombin-specific inhibitor hirudin, yet controls using tropoelastin and thrombin were inhibited. Pefabloc PK, specific for kallikrein, was able to stop degradation. Romero *et al.* (1986) found that incubation of tropoelastin with kallikrein resulted in a somewhat similar profile to its incubation with serum. Our inhibitor studies with Pefabloc PK are therefore consistent with kallikrein being involved. The inhibitor Pefabloc PK is, however, not completely specific for kallikrein. According to data supplied by the manufacturer, the inhibitor constant for plasma kallikrein is $0.7\mu\text{mol/L}$ while the next most likely enzyme to be inhibited after kallikrein is trypsin with an inhibitor constant of $1.3\mu\text{mol/L}$ followed by plasmin at $10\mu\text{mol/L}$. Thus, if present in excess Pefabloc PK may be inhibiting these enzymes also. However, the lowest concentration at which complete inhibition was seen ($50\mu\text{M}$) was the manufacturer's recommended amount for inhibition of kallikrein in plasma samples.

Similarly, the profile of SHEL seen after kallikrein digestion only showed limited similarity to the serum produced profile i.e. the presence of a 45kDa fragment and two fragments around 20kDa . Sequencing of the peptides showed that both the sites recognised by kallikrein were recognised

6.4.2 Identification of Serum Proteolysis

A number of enzymes have been proposed to be responsible for the serum degradation of tropoelastin. Kallikrein (Romero *et al.*, 1986) and plasmin (McGowan *et al.*, 1996) have both been put forward as potential sources of proteolysis while a trypsin-like protease was thought to be responsible for the degradation products seen when tropoelastin was isolated from tissues (Mecham and Foster, 1977). A visual comparison of SHEL degradation products from serum with the individual protease digestion products revealed only a limited similarity with thrombin and kallikrein-produced peptides while trypsin and plasmin digests appeared more similar to serum-digested peptides but only when used at low concentration. Higher concentrations and/or longer incubations completely degraded SHEL and SHELΔ26A in contrast to long incubations with serum which did not change the pattern greatly.

Increasing amounts of thrombin degraded SHEL easily but only 3 major fragments were noted, unlike serum-produced peptides where 5-6 fragments were noted. Coupled with the observation from the inhibitor studies that the thrombin-specific inhibitor hirudin did not substantially reduce serum degradation, thrombin does not appear to be the major enzyme involved in serum proteolysis of SHEL. This was corroborated by sequencing of the peptide products which showed that although one of the two sites recognised by thrombin was likewise recognised by serum, the other site was not. This may have been a consequence of low thrombin concentration but this is unlikely since both sites are recognised to a similar extent (Figure 6.3).

Similarly, the profile of SHEL seen after kallikrein digestion only showed limited similarity to the serum produced profile i.e. the presence of a 45kDa fragment and two fragments around 20kDa. Sequencing of the peptides showed that both the sites recognised by kallikrein were recognised

by serum. The other serum-produced fragments, however, were not seen as major products of kallikrein digestion although some other fragments were present at a very low level (Figure 6.4). Long incubations with kallikrein (overnight) failed to increase the intensity of other fragments nor increase the resemblance to serum digestion products (not shown), indicating that kallikrein was unlikely to be responsible for the additional serum-produced fragments. The sequencing data, effect of a kallikrein specific protease inhibitor and visual appearance of the digestion products by SDS-PAGE are all consistent with the involvement of kallikrein in serum digestion. However, the presence of other serum peptide fragments not seen as major products of kallikrein digestion indicates that kallikrein alone is not responsible for the pattern seen in serum digests.

In contrast to thrombin and kallikrein, plasmin and trypsin resulted in extensive degradation which could completely degrade SHEL if incubated for extended periods. The degradation profile seen with plasmin was quite unlike that seen by McGowan *et al.* (1996) where only 68 and 45kDa bands were seen, suggesting that the degradation had not proceeded very far in that case. Each of these digestion profiles were more similar to serum products than either thrombin or kallikrein. By visual inspection trypsin and plasmin appeared almost identical to serum digests and each other but only at low concentration.

There was some difficulty in the sequencing of plasmin and trypsin peptides. The plasmin-produced peptides that were sequenced were found to consist of a mixture of at least two overlapping sequences at 78/79 and 81/82 (K/AAK and K/AGA) which were the same in all of the peptide fragments sequenced. In addition, sequence from the N-terminus of SHEL was also present, which made these peptides very difficult to identify unambiguously. The presence of the same peptides throughout each fragment may be an

artifact resulting from this sequence co-migrating through the entire gel with other peptides and so contaminating each subsequent peptide (J. McGovern, Biomolecular Resource Facility, Australian National University, personal communication). This may have been compounded by the low levels of peptide obtained for each fragment due to the rampant degradation by plasmin.

Similarly, low levels and poor resolution made it impossible to obtain sequence for the smaller trypsin peptides. However, clear sequence data were obtained for the larger fragments which all corresponded to N-terminal sequences as was the case for the same peptides from serum. This, coupled with the observation that Pefabloc PK could also inhibit trypsin in controlled reactions (not shown) and the visual similarity of peptide fragments is consistent with trypsin-like enzyme involvement with serum proteolysis but the lack of sequence data for the more informative smaller fragments means that the identification is not definitive. Similarly, the visual similarity is also consistent with plasmin involvement but this was not able to be confirmed by sequencing. Since serum proteolysis was more defined and limited than either plasmin or trypsin alone, this indicates that the presence of trypsin-like activity is probably much lower in serum and/or is more easily destroyed.

HLE digestion profile was also extensive but was different to both serum, trypsin and plasmin. HLE is a serine elastase and cleaves predominantly at Val residues (Keil, 1992). The difference between elastase digests of SHEL and SHEL Δ 26A was more notable as most fragments, including the largest ones, were smaller in SHEL Δ 26A, indicating that digestion was occurring preferentially from the N-terminal end which does not appear to be the case for the other enzymes or serum. HLE involvement in serum proteolysis is therefore unlikely.

In summary, by N-terminal sequencing, visual inspection of the degradation profiles and the effect of the inhibitors the results are consistent with kallikrein involvement in addition to at least one other enzyme probably present at a lower level. Plasmin or another trypsin-like enzyme or combination of enzymes are the most likely to be involved in the serum digestion of SHEL. Detectable thrombin and HLE activity in serum are unlikely.

6.4.3 Mapping of Protease Sensitive Sites

The pattern of degradation of purified tropoelastin seen by others is remarkably similar to the sizes of peptides generated by our proteolysis experiments. The sizes seen by Mecham and Foster (1977) by their trypsin-like protease associated with tropoelastin, 57, 45, 36, 24.5 and 13-14kDa, are very similar to the number and sizes of peptides generated by serum and the individual serine proteases on both SHEL and SHEL Δ 26A indicating that cleavage may be occurring in the same or similar places. A similar profile was seen with tropoelastin from human fibroblast cell culture (Davidson and Sephel, 1987). Sequencing confirmed that one site between residues 515 and 516 was common to thrombin, kallikrein and serum and from the SDS-PAGE pattern, probably also plasmin and trypsin. All the peptides sequenced confirmed that cleavage occurred after a Lys or Arg as expected for many serine proteases (Keil, 1992). However, tropoelastin contains a large number of Lys and Arg (35 and 10 respectively) yet only a small number of these residues were actually recognised and cleaved. The fact that these same sites may be recognized by different serine proteases may be due to their accessibility and/or the surrounding amino acids.

6.4.4 Protection from Degradation

Preferred recognition sites for kallikrein and thrombin are strongly influenced by the surrounding amino acids. The binding site of EBP has been used previously to model this interaction

(Mecham *et al.*, 1989). A peptide, 3-GAL, which represents the elastin binding site of EBP has been used previously to model this interaction

by the adjacent amino acid residues (Chang, 1985; Keil, 1992) but it would not have been possible *a priori* to predict where preferential cleavage occurs in human tropoelastin. For example, kallikrein cleaves preferentially at Arg residues preceded by a bulky residue (Keil, 1992). Both sites identified by N-terminal sequencing fall into this category, with Leu-Arg at 515 and Arg-Arg at 564. However, another Arg preceded by a Leu at 571 does not appear to be recognised. The highly specific and limited proteolysis of SHEL and SHEL Δ 26A by kallikrein has allowed kallikrein treatment to be used to produce isolated C-terminal portions of tropoelastin for further study (S. Jensen and A.S. Weiss, unpublished). The thrombin sites identified, however, do not fit the preferred sites for thrombin. Thrombin recognises predominantly P2-Lys/Arg-P1' where either P2 or P1' are Gly, or P4-P3-Pro-Arg/Lys-P1'-P2', where P4 and P3 are hydrophobic and P1' and P2' are non-acidic residues (Chang, 1985) with Arg greatly favoured over Lys (Keil, 1992). Neither SHEL nor SHEL Δ 26A contain these exact sites although the site at 152 (Lys-Pro-Lys-Ala-Pro) is similar to the latter recognition site of P3-Pro-Lys-P1'-P2'. Which sites are recognised and cleaved may therefore be under the influence of tropoelastin secondary structure. Trypsin cleaves predominantly at Arg and Lys with a preference for Arg, while plasmin preferentially cleaves at Lys (Keil, 1992). Since there are more Lys than Arg in tropoelastin, it would be expected that these proteases would cleave more extensively as is shown to be the case.

6.4.4 Protection from Degradation

Experiments have demonstrated that EBP can protect tropoelastin from degradation by binding primarily to the VGVAPG sequence of tropoelastin (Mecham *et al.*, 1989). A peptide, S-GAL, which represents the elastin binding site of EBP has been used previously to model this interaction

(Hinek and Rabinovitch, 1994). It has been noted that S-GAL and EBP have some homology with the N-terminal sequence of proteases such as kallikrein, HLE and plasmin and are therefore proposed to bind to the same sequence in tropoelastin, thus acting as competitive inhibitors of the proteases (Hinek and Rabinovitch, 1994; Hinek *et al.*, 1993). Hinek and Rabinovitch (1994) showed that S-GAL could significantly inhibit degradation of elastin by porcine pancreatic elastase and inferred that HLE and other serine proteases could be similarly inhibited from degrading tropoelastin. In this work, the use of S-GAL did not show any significant or consistent inhibition of proteolysis of SHEL or SHEL Δ 26A by serum, trypsin, plasmin or kallikrein although some inhibition could be seen with thrombin. However, significant and reproducible inhibition was seen with HLE but complete inhibition of degradation could not be achieved, even with the large excess of S-GAL used. The S-GAL used was HPLC-purified to remove any truncated products and it may be possible that the peptide was damaged or irreversibly denatured by this process. However, samples of S-GAL which were not HPLC purified gave similar results (not shown). There is no direct evidence that SPS-peptide is actually cleaved by any protease. However, the presence of a similar amount of a different peptide (S-GAL) did not exert the same effect. Thus, the effect of SPS-peptide is probably not simply due to the non-specific presence of a peptide in the reaction. SPS-peptide is therefore likely to be interacting directly with the proteases for tropoelastin to exert its effect. However, protection from degradation was in no way complete and degradation could still occur to a significant extent. In addition, a large peptide to protein ratio (200 or 100:1) was necessary to detect any effect which could best be noted by short incubations. Thus, although not highly efficient as an inhibitor, could allow the degradation to persist longer in the presence of proteases, including human serum. Future work could determine the effect of non-cleavable analogues of SPS-peptide or similar peptides to

N-terminal sequencing data revealed one site in SHEL which was commonly recognised by thrombin, kallikrein, serum and probably trypsin and plasmin (Section 6.3.4). This site and its flanking amino acids was synthesised and this SPS-peptide added to proteolytic digests of SHEL and SHEL Δ 26A. This peptide was not expected to bind to tropoelastin but simply act as a competitor by being recognised by the protease thus slowing degradation of SHEL and SHEL Δ 26A. There was reproducible evidence of protection from degradation of SHEL and SHEL Δ 26A by the presence of SPS-peptide. The amount of full-length protein was greater in the presence of SPS-peptide than in the presence of S-GAL or control digestions and was similar for both isoforms. This was most notable in the presence of low enzyme concentrations or shorter incubations and was most obvious with trypsin, plasmin, kallikrein and serum although protection from the other proteases was noted although at a reduced level. This indicates that each of the proteases and serum could recognise this peptide to some extent and therefore this is a potential inhibitor of proteolysis of tropoelastin.

There is no direct evidence that SPS-peptide is actually cleaved by any protease. However, the presence of a similar amount of a different peptide (S-GAL) did not exert the same effect. Thus, the effect of SPS-peptide is probably not simply due to the non-specific presence of a peptide in the reaction. SPS-peptide is therefore likely to be interacting directly with the proteases (or tropoelastin) to exert its effect. However, protection from degradation was in no way complete and degradation could still occur to a significant extent. In addition, a large peptide to protein ratio (200 or 100:1) was necessary to detect any effect which could best be noted by short incubations. Thus, SPS-peptide, although not highly efficient as an inhibitor, could allow full-length tropoelastin to persist longer in the presence of proteases, including human serum. Future work could determine the effect of non-cleavable analogues of SPS-peptide or similar peptides to

provide more effective proteolytic protection for SHEL and SHEL Δ 26A. In summary, the inhibition of degradation of SHEL and SHEL Δ 26A by S-GAL was only noted significantly with HLE but more extensive protection could not be shown. However, a reproducible inhibition was seen in the presence of SPS-peptide with each protease and serum, and was most notable with trypsin, kallikrein and serum. This peptide provides an alternative site for interaction with proteases and results in the persistence of full-length tropoelastin for longer periods although does not protect it completely from degradation.

6.4.5 Proteolysis of Coacervated Tropoelastin

Coacervation of SHEL and SHEL Δ 26A at 37°C resulted in significant protection from proteolysis by kallikrein and thrombin and to a lesser extent by HLE, trypsin and serum. No protection was seen from attack by plasmin. The presence of 150mM NaCl did not appear to cause the inhibition since the same reactions performed under conditions not conducive to coacervation (16°C) were digested to a similar extent in the presence or absence of NaCl. Although it is possible that a simple change in conformation at 37°C could result in altered proteolytic susceptibility, this is unlikely since coacervated and non-coacervated SHEL, both at 37°C, were digested at different rates. The inhibition of proteolysis is therefore probably due to steric restriction in the coacervate. Of the enzymes tested, the activity of kallikrein was most significantly inhibited by coacervation. From the N-terminal sequencing results, kallikrein predominantly recognises only two sites in SHEL, both of which are in close proximity, and only one in SHEL Δ 26A. The coacervation of tropoelastin appears to mask these sites making them less accessible to kallikrein. With thrombin, the inhibition

was not as complete as with kallikrein. Thrombin recognises predominantly two sites in SHEL also but these are more distant from each other. The process of coacervation may mask these sites but if either site is slightly more accessible proteolysis would result and consequently allow easier access to the second site. The other proteases (HLE, trypsin, plasmin) and also serum, recognise and cleave at many more sites within SHEL making efficient masking of all sites by coacervation unlikely and resulting in some sites remaining available for recognition and proteolysis to occur. Thus, these proteases are not as significantly inhibited by coacervation. These results indicate that in the extracellular matrix, coacervation of tropoelastin may serve an additional role to those already proposed (Section 1.2.7) by providing, to a certain extent, protection from proteolysis including that caused by human serum. These results could be extended to the nascent elastic fibre where newly laid tropoelastin in the coacervate form would be largely protected from extracellular proteases before cross-linking makes this protection essentially permanent.

6.4.6 Possible Consequences of Serum Degradation of Tropoelastin

It is clear from these results and those of others that serum contains factors capable of degrading tropoelastin. A number of serine proteases present in human blood have been shown here to be able to degrade tropoelastin specifically and reproducibly. Thus, tropoelastin when secreted by cells into the extracellular matrix is vulnerable to extensive degradation prior to being insolubilised by lysyl oxidase and cross-linked. This is especially significant in blood vessels where damaged vessels may contain a number of these proteases during normal blood coagulation. Any tropoelastin secreted at this time and not protected, for example by EBP or by coacervation, would be fragmented. These results suggest that coacervation

may indeed provide some protection from digestion, as seen with the inhibition of degradation of coacervated SHEL (Section 6.3.6; Figure 6.10). However, protection is by no means complete. It has previously been suggested that tropoelastin may be under negative feedback autoregulation and upon accumulation in the extracellular matrix may inhibit the production of elastin mRNA (Foster and Curtiss, 1990). Elastin peptides produced by proteases such as elastase have been shown to produce negative feedback inhibition when added to undamaged fibroblast cultures while stimulating tropoelastin production in protease-damaged cultures (Foster *et al.*, 1990). It has been suggested that serine protease mediated proteolysis of tropoelastin may be an important modulator of tropoelastin production and that plasmin may be involved in this process (McGowan *et al.*, 1996). Our results are consistent with this proposal although the specific enzyme(s) proposed differ slightly.

It is interesting to note that most of the cleavages identified in serum occur in the C-terminal half of the tropoelastin molecule and that most of the larger fragments were from the N-terminus (Figure 6.8; Table 6.1). Thus, the action of proteases in serum on tropoelastin serves to degrade the C-terminal portion leaving a large N-terminal segment. These shortened molecules may not be incorporated into newly synthesised or growing elastic fibres due to the absence of the highly conserved C-terminus which is shown to be responsible for binding with microfibrillar proteins (Brown-Augsburger *et al.*, 1996; 1994). This is analogous to the case in supravalvular aortic stenosis, where an elastin gene truncation results in tropoelastin molecules missing the C-terminus with the result of severe aortic disease (Ewart *et al.*, 1994). Similarly, in fetal lamb ductus arteriosus a truncated tropoelastin missing the C-terminus is not incorporated into the elastic fibre (Hinek and Rabinovitch, 1993). The action of serum on human tropoelastin therefore results in tropoelastin molecules which may not be

insolubilised and may persist in the extracellular matrix. Any fibres cross-linked may be aberrant due to improper alignment, resulting in a loss of elastic properties and strength. The persistence of soluble peptides may serve to inhibit further tropoelastin production by negative feedback inhibition (Foster and Curtiss, 1990). At the same time peptides are chemotactic, as demonstrated by several studies (Bisaccia *et al.*, 1994; Grosso and Scott, 1993b), and may serve to recruit tissue-repairing cells to the site of injury, accelerating repair of the wound.

6.5 CONCLUSION

Human serum was shown to be capable of degrading SHEL and SHEL Δ 26A into a number of discrete fragments. This activity was confirmed to be from a serine protease and the regions of susceptibility to serum were precisely mapped by N-terminal sequencing. A number of other serine proteases were shown to be capable of degrading SHEL and SHEL Δ 26A. From the pattern of degradation, use of selective inhibitors and N-terminal sequencing the protease responsible for serum degradation was consistent with a trypsin-like protease but kallikrein is also a likely contributor. Significant or consistent inhibition of proteolysis did not take place using S-GAL, except with thrombin and HLE, but reproducible inhibition was provided by SPS-peptide. However, the process of coacervation was shown to provide the most significant protection against proteolysis, including by serum, and was most notable for proteases which cleaved a limited number of sites.

CHAPTER 7

**FACTORS INFLUENCING THE
COACERVATION CHARACTERISTICS OF
HUMAN TROPOELASTIN ISOFORMS**

7.1 INTRODUCTION

As described previously (Section 1.2.7), tropoelastin has a propensity for intermolecular interaction, or coacervation, through an inverse temperature transition. Of particular relevance to elastic fibre formation, tropoelastin is completely soluble in aqueous solutions but on raising the temperature towards the physiological range the solution becomes cloudy as the tropoelastin molecules aggregate via interactions between the hydrophobic domains including the oligopeptide repetitive sequences, GVGVP, GGVP and GVGVP. Coacervation is proposed as a vital early step in elastic fibre formation, by concentrating the tropoelastin molecules and possibly aligning them into correct register for subsequent cross-linking (Urry, 1978). In addition, it was shown in the previous chapter that coacervation may protect tropoelastin from proteolysis in the extracellular matrix prior to cross-linking. Ultrastructurally, coacervates are seen as fibrous structures similar in size to mature elastin fibres (Section 1.2.7) and it is therefore thought that coacervation is a crucial step in elastogenesis. It has been shown experimentally that coacervation of tropoelastin is a prerequisite for cross-linking by lysyl oxidase *in vitro* (Narayanan *et al.*, 1978). It has also been suggested that tropoelastin may be inhibited from premature coacervation inside the cell by binding to a companion protein such as EBP and it has been proposed that EBP may function as a molecular chaperone for tropoelastin (Hinek and Rabinovitch, 1994).

Coacervation can be monitored by following turbidity formation using a spectrophotometer. The temperature of onset of coacervation is highly dependent on a range of factors including peptide concentration, NaCl concentration and pH, as revealed by this method (Urry, 1982). A vast amount of coacervation data has been obtained by using polypeptide models of the repetitive tetra-, penta- and hexapeptide regions of tropoelastin

which demonstrate the effect of amino acid differences on this process (Urry, 1988; 1984). Since coacervation of polypeptide models of tropoelastin has been shown to result in fibre formation (Section 1.2.7) the heterogeneous polypeptide population is regarded as a good model for elastic fibre morphogenesis. However, it is restricted as a model for tropoelastin coacervation. Coacervation studies have also been performed using α -elastin (Miyakawa *et al.*, 1995; Urry, 1982; Urry and Long, 1977) but α -elastin is highly heterogeneous and partially cross-linked, making the exact nature of the molecules difficult to define. Tropoelastin is more physiologically relevant to fibre formation as it is the coacervation of tropoelastin which is the starting point for elastic fibre formation. However, only a single coacervation curve has been generated using a mixture of chick aortic tropoelastin splice forms (Urry, 1978) in contrast to the large number of studies using simpler polyoligopeptide models. The effect of pH on chick and bovine tropoelastin coacervation has been demonstrated using a subjective visual method (Sykes and Partridge, 1974; Whiting *et al.*, 1974). No studies into the coacervation behaviour of human tropoelastin have been performed, nor have any individual intact isoforms been compared. Thus, despite the importance of coacervation to fibrillogenesis, very little is known about this process using physiological forms of tropoelastin under physiologically relevant conditions.

Tropoelastin purified from animal tissues is heterogeneous because different splice forms commonly exist within these tissues. Using the synthetic genes *SHEL* and *SHEL Δ 26A*, defined isoforms of human tropoelastin can be produced in abundance to provide adequate amounts of tropoelastin for detailed coacervation experiments. Furthermore, the exact sequences of these tropoelastins are known thus removing complications arising from interpretations of data in terms of amino acid sequence and relative contributions of splice variants.

The chapter describes for the first time detailed coacervation behaviour of human tropoelastin and a defined single form of intact tropoelastin, SHEL. The effects of peptide, NaCl concentration and pH are examined and their relative contributions to coacervation compared. The coacervation characteristics of a second isoform, SHEL Δ 26A and SHEL Δ mod are also assessed. The effect of an EBP model, S-GAL, is demonstrated in addition to the effect of lipid impurities on coacervation. Optimal coacervation is demonstrated to occur at 37°C, 150mM NaCl and pH 7 to 8. A model is proposed for tropoelastin assembly under the precise conditions found in the extracellular matrix.

7.2 MATERIALS AND METHODS

7.2.1 Coacervation

Coacervation was assayed by monitoring turbidity through light scattering at 300nm using a Cary 3 spectrophotometer and software (Kinetic Application version 3.02). The cuvette holder was connected to a recirculating water bath to control the temperature. Light scattering by each solution was assayed for 10min at specific temperatures between 4 and 70°C. To study the effect of tropoelastin concentration, SHEL was dissolved in phosphate buffered saline (PBS, 10mM sodium phosphate pH 7.4, 150mM NaCl) at concentrations of 1 to 40mg/ml. Following each time course the solution was placed on ice to return to baseline. Independent checks were periodically made using fresh preparations. The maximum change in turbidity at each temperature was recorded and expressed as a percentage of maximum turbidity for each concentration to generate a series of coacervation curves as described by Urry (1982). To study the effect of NaCl concentration SHEL was dissolved at 20mg/ml in 10mM phosphate buffer at pH 7.4.

Coacervation curves were generated by adding NaCl prior to each time course at increments from 0 to 200mM. To study the effect of pH, 20mg/ml SHEL was dialysed against PBS containing 150mM NaCl over the pH range 5.4 to 8.4 in each instance prior to coacervation. Coacervation of SHEL Δ mod was performed similarly.

Some variations were required for coacervation studies of SHEL Δ 26A, due to problems with lipid contamination (See Section 7.3.8). Coacervation experiments with SHEL Δ 26A were generally carried out at lower protein concentrations since preparations above 20mg/ml were not able to be obtained free from lipid. Protein was initially dissolved in PBS and preliminary coacervation carried out to ascertain the extent of lipid contamination. The samples were then centrifuged at an appropriate temperature, as explained in Section 7.3.8, before the supernatant protein concentration was determined by spectrophotometry (Chapter 5.2.9) and coacervation experiments performed. To determine the effect of NaCl concentration the sample was treated in the same way before being dialysed against 50mM ammonium acetate, pH 5.0, dried and redissolved in 10mM sodium phosphate, pH 7.4.

7.2.2 S-GAL preparation and use

S-GAL preparation is described in Section 6.2.5. S-GAL was added to various concentrations of SHEL in PBS from 1-20mg/ml at approximately 2:1 molar ratio (i.e. 50 μ g S-GAL per mg SHEL) to ensure an excess of S-GAL. The solution was incubated at 37°C for one hour before coacervation curves were produced (Section 7.2.1) starting at 37°C. Control coacervation curves were produced on identically-treated SHEL samples in the absence of S-GAL.

7.2.3 Preparation of Lipid and Use in Coacervation

A lipid preparation was obtained during the purification protocol of SHEL/SHELΔ26A (See Figure 5.4). The chloroform wash of dried SHEL obtained after butanol/propanol removal (Section 5.3.2.2) was placed into a clean flask and the chloroform removed by rotary evaporation. The lipid residue was washed extensively with 50mM ammonium acetate, pH 5.0 or PBS until the aqueous solution became cloudy. A portion of the cloudy suspension was dried and subjected to gas chromatography analysis, performed by Mr Zia Ahmad (Human Nutrition Unit, Department of Biochemistry, University of Sydney) to identify fatty acids. The remainder of the cloudy suspension was centrifuged at 4°C at 12 000rpm in a microfuge for 10min and the supernatant retained. 15 and 30μl aliquots of the soluble lipid phase was added to 5mg/ml SHEL in PBS and coacervation performed (Section 7.2.1).

The coacervation curve for 40mg/ml SHEL (Figure 7.1b) was derived from Figure 7.1a by expressing the maximum change in light scattering at each temperature as a percentage of the overall maximum. Coacervation occurred over a narrow range of temperatures (< 5°C) for this concentration and commenced just below human body temperature. Coacervation was essentially complete at 37°C. Time courses were obtained for other concentrations in a similar way and a comparison of the coacervation curves is shown in Figure 7.2. As the concentration of SHEL was increased, curves were shifted to lower coacervation temperatures and became sharper. As concentration was further increased, the curves clustered around the physiologically relevant temperature of 37°C. Indeed, there was little difference over the range 20 to 40mg/ml indicating less concentration dependence at high concentrations.

7.3 RESULTS

7.3.1 Effect of Tropoelastin Concentration on Coacervation of SHEL

Time courses for light scattering by 40mg/ml SHEL at six temperatures are shown in Figure 7.1a. This concentration was the maximum used in these experiments and no significant change in turbidity was noted below 31°C. However, at 35°C coacervation was readily observed as evidenced by increased turbidity and this was essentially complete within 10min. At 37°C this was reduced to 2.5min and had reached a maximum since no substantial increases in absorbance were seen at higher temperatures. Higher temperatures displayed more rapid coacervation but maximum turbidity was no higher than that seen at 37°C. Time courses for lower concentrations were similarly rapid but with higher temperatures necessary for coacervation (not shown). Following each time course, the solution was placed on ice for 15min to return to baseline, although the solution became clear in less than 30s. In controlled studies, no hysteresis was observed.

The coacervation curve for 40mg/ml SHEL (Figure 7.1b) was derived from Figure 7.1a by expressing the maximum change in light scattering at each temperature as a percentage of the overall maximum. Coacervation occurred over a narrow range of temperatures (< 5°C) for this concentration and commenced just below human body temperature. Coacervation was essentially complete at 37°C. Time courses were obtained for other concentrations in a similar way and a comparison of the coacervation curves is shown in Figure 7.2. As the concentration of SHEL was increased, curves were shifted to lower coacervation temperatures and became sharper. As concentration was further increased, the curves clustered around the physiologically relevant temperature of 37°C. Indeed, there was little difference over the range 20 to 40mg/ml indicating less concentration dependence at high concentrations.

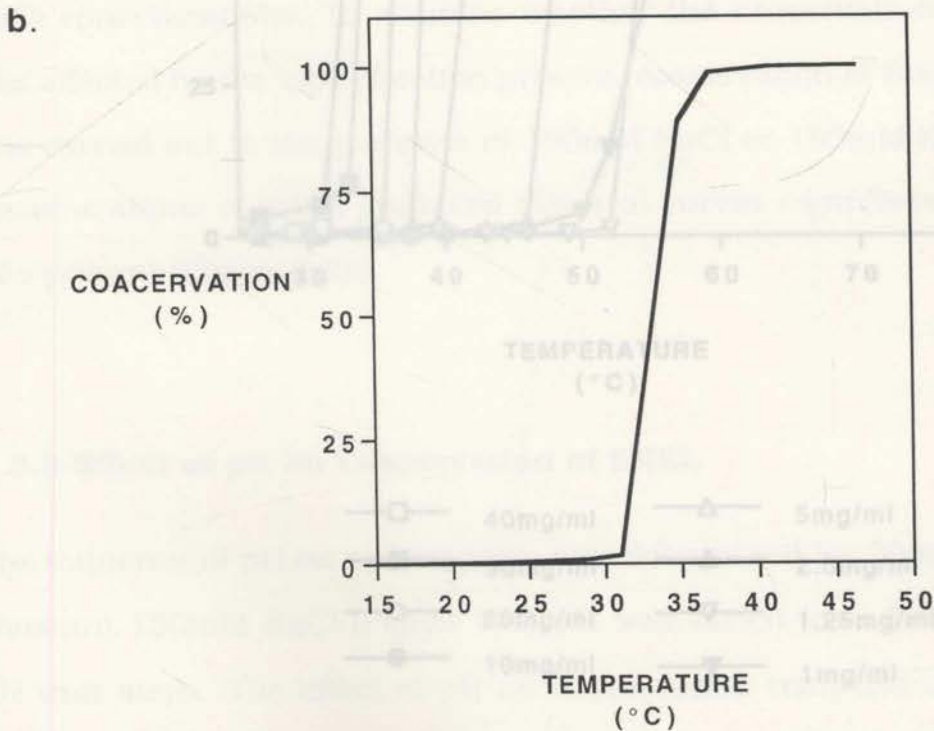
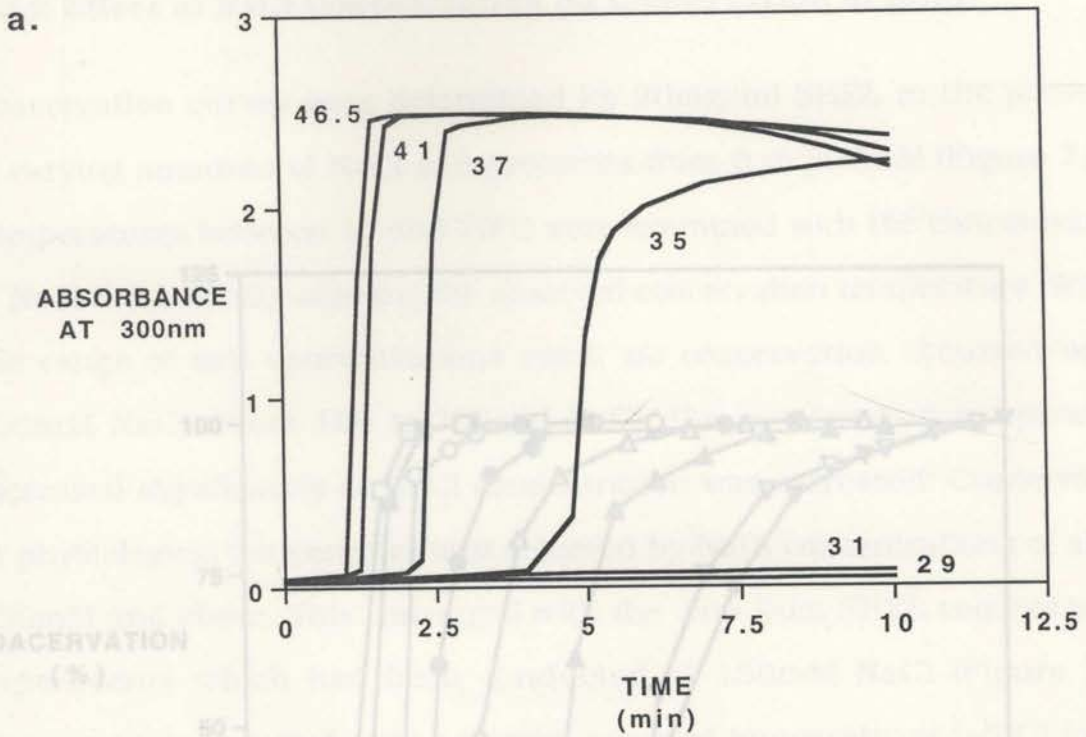
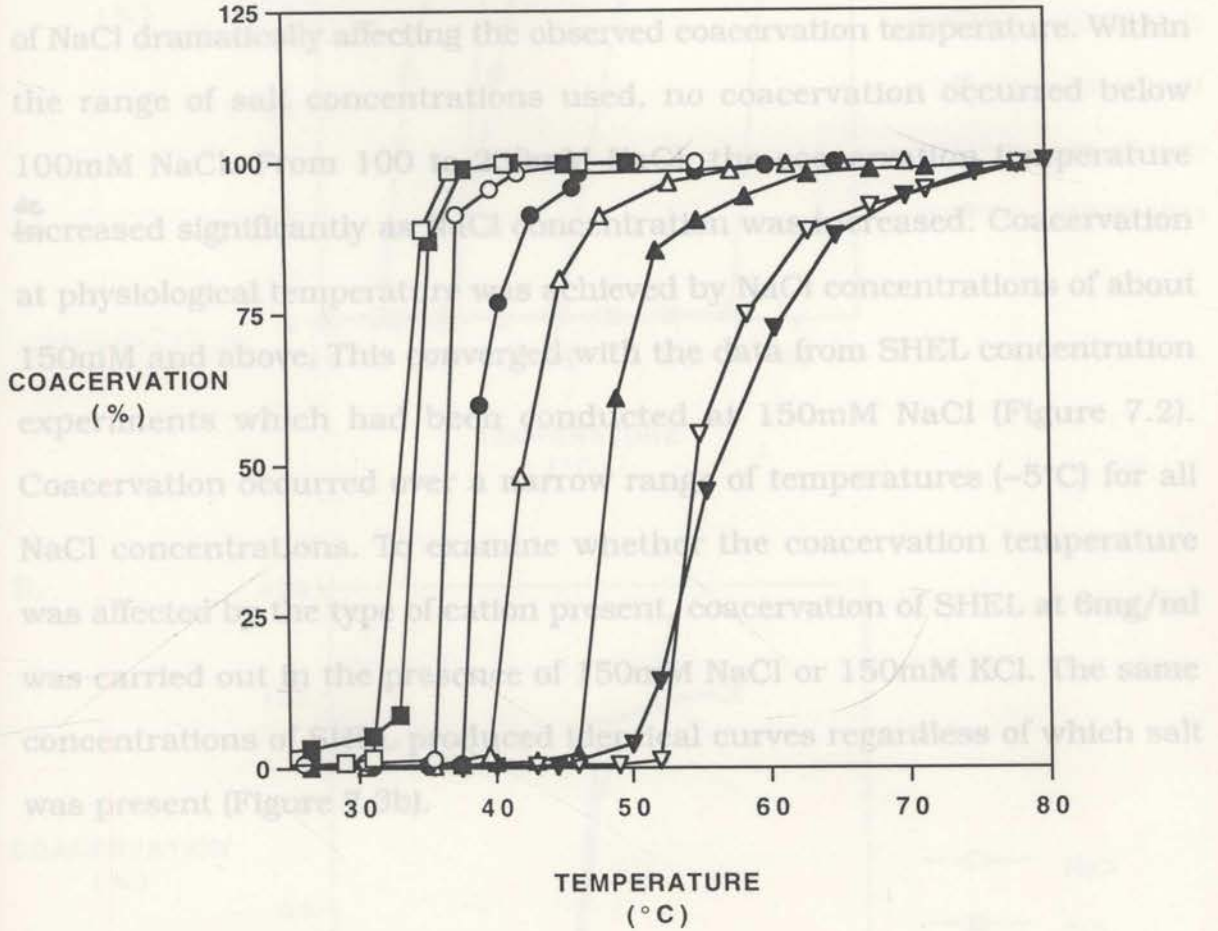


Figure 7.1 Coacervation of 40mg/ml SHEL. a. Selected time courses of turbidity formation by 40mg/ml SHEL in PBS. The temperature of each run is indicated in °C. Time courses below 29°C were unremarkable and are not shown. b. Coacervation curve of 40mg/ml SHEL in PBS derived from Figure 7.1a, describing maximal turbidity at each temperature expressed as a percentage of the peak value. Maximum coacervation has been achieved by 37°C.

7.3.2 Effect of NaCl Concentration on Coacervation of SHEL

Coacervation curves were determined for 20mg/ml SHEL in the presence of varying amounts of NaCl at increments from 0 to 200mM (Figure 7.3a). Temperatures between 10 and 70°C were examined with the concentration of NaCl dramatically affecting the observed coacervation temperature. Within the range of salt concentrations used, no coacervation occurred below 100mM NaCl.



7.3.3 Effect of pH on Coacervation of SHEL

The influence of pH on coacervation was determined for 20mg/ml SHEL at constant 150mM NaCl. The effect of pH on coacervation temperature was not as dramatic nor as obvious as the concentration of either SHEL or NaCl. Increasing the pH showed a trend towards lowering the coacervation

Figure 7.2 Effect of SHEL concentration on coacervation. Coacervation curves for various concentrations of SHEL in PBS were derived from time courses as in Figure 7.1a.

7.3.2 Effect of NaCl Concentration on Coacervation of SHEL

Coacervation curves were determined for 20mg/ml SHEL in the presence of varying amounts of NaCl at increments from 0 to 200mM (Figure 7.3a). Temperatures between 10 and 70°C were examined with the concentration of NaCl dramatically affecting the observed coacervation temperature. Within the range of salt concentrations used, no coacervation occurred below 100mM NaCl. From 100 to 200mM NaCl, the coacervation temperature increased significantly as NaCl concentration was increased. Coacervation at physiological temperature was achieved by NaCl concentrations of about 150mM and above. This converged with the data from SHEL concentration experiments which had been conducted at 150mM NaCl (Figure 7.2). Coacervation occurred over a narrow range of temperatures (~5°C) for all NaCl concentrations. To examine whether the coacervation temperature was affected by the type of cation present, coacervation of SHEL at 6mg/ml was carried out in the presence of 150mM NaCl or 150mM KCl. The same concentrations of SHEL produced identical curves regardless of which salt was present (Figure 7.3b).

7.3.3 Effect of pH on Coacervation of SHEL

The influence of pH on coacervation was determined for 20mg/ml SHEL at constant 150mM NaCl (Figure 7.4). pH was varied from 5.4 to 8.4 in 0.5 pH unit steps. The effect of pH on coacervation temperature was not as dramatic nor as obvious as the concentration of either SHEL or NaCl. Increasing the pH showed a trend towards lowering the coacervation temperature. The effect was more subtle with a change of pH from 5.4 to 8.4, corresponding to a 1000-fold change in $[H^+]$ yet only lowering the midpoint from 42 to 36°C.

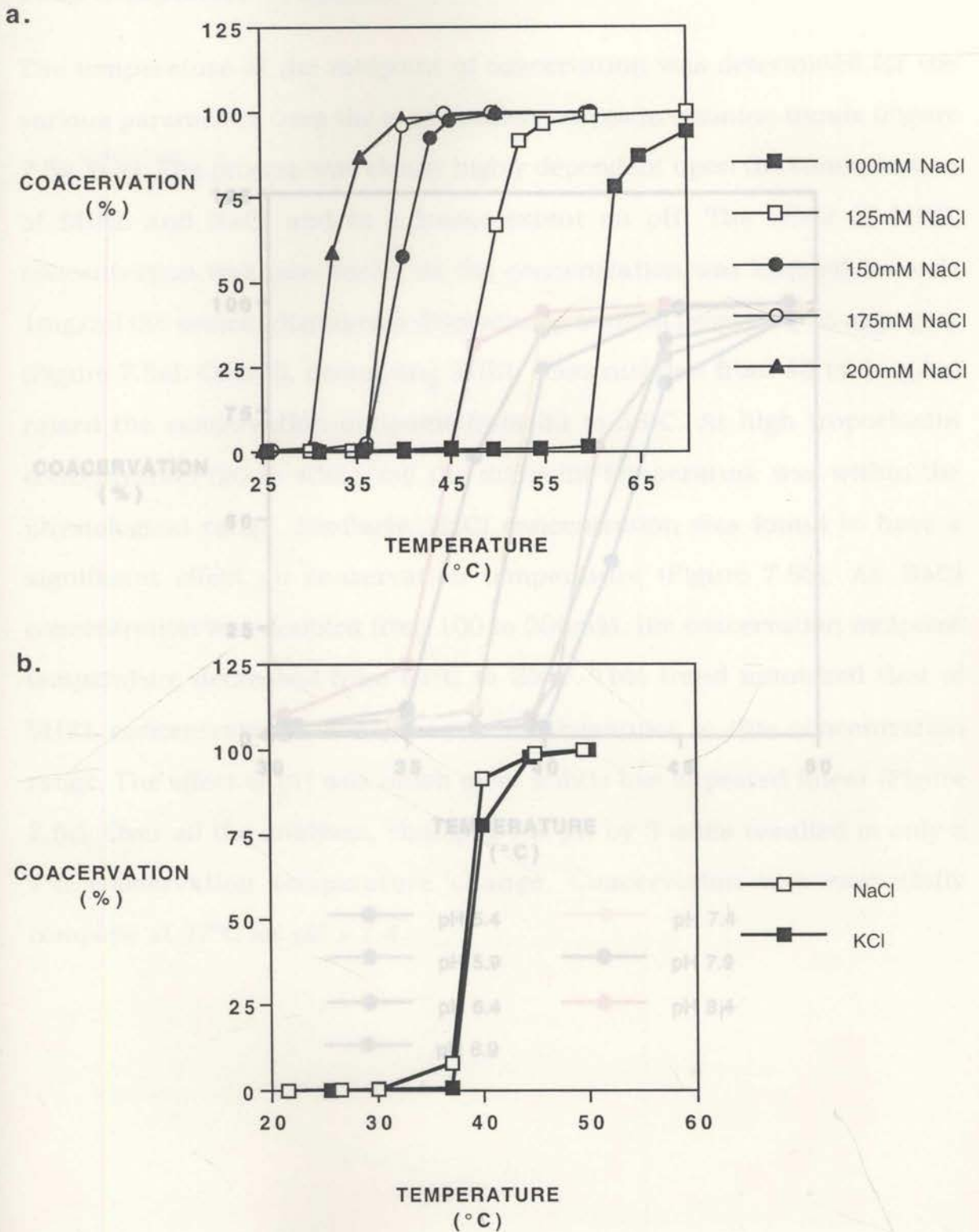


Figure 7.3 Effect of salts on coacervation of SHEL. **a.** Coacervation curves for SHEL (20mg/ml) at pH 7.4 with increasing concentrations of NaCl. No coacervation was seen below 100mM NaCl. **b.** Comparison between coacervation curves for 6mg/ml SHEL in the presence of 150mM NaCl or KCl. There is no noticeable difference in the presence of either salt.

7.3.4 Comparison of Effects

The temperature of the midpoint of coacervation was determined for the various parameters from the coacervation curves to examine trends (Figure 7.5a, b, c). The process was clearly highly dependent upon the concentration of SHEL and NaCl, and to a lesser extent on pH. The effect of SHEL concentration was non-linear; as the concentration was lowered towards 1mg/ml the process displayed a dramatic increase in temperature to aggregate (Figure 7.5a). Overall, decreasing SHEL concentration from 40 to 1mg/ml raised the coacervation midpoint from 33 to 37°C. At high tropoelastin (20 to 40mg/ml) the midpoint temperature was within the physiological range. Similarly, NaCl concentration was found to have a significant effect on coacervation temperature (Figure 7.5b). As NaCl concentration was doubled from 100 to 200mM, the coacervation midpoint temperature decreased from 31°C to 32°C. This trend mimicked that of SHEL concentration in this concentration range. The effect of pH was much more subtle but appeared linear (Figure 7.5c). Over all the analyses, changing pH by 3 units resulted in only a 7°C coacervation temperature change. Coacervation was essentially complete at 37°C for pH > 7.4.

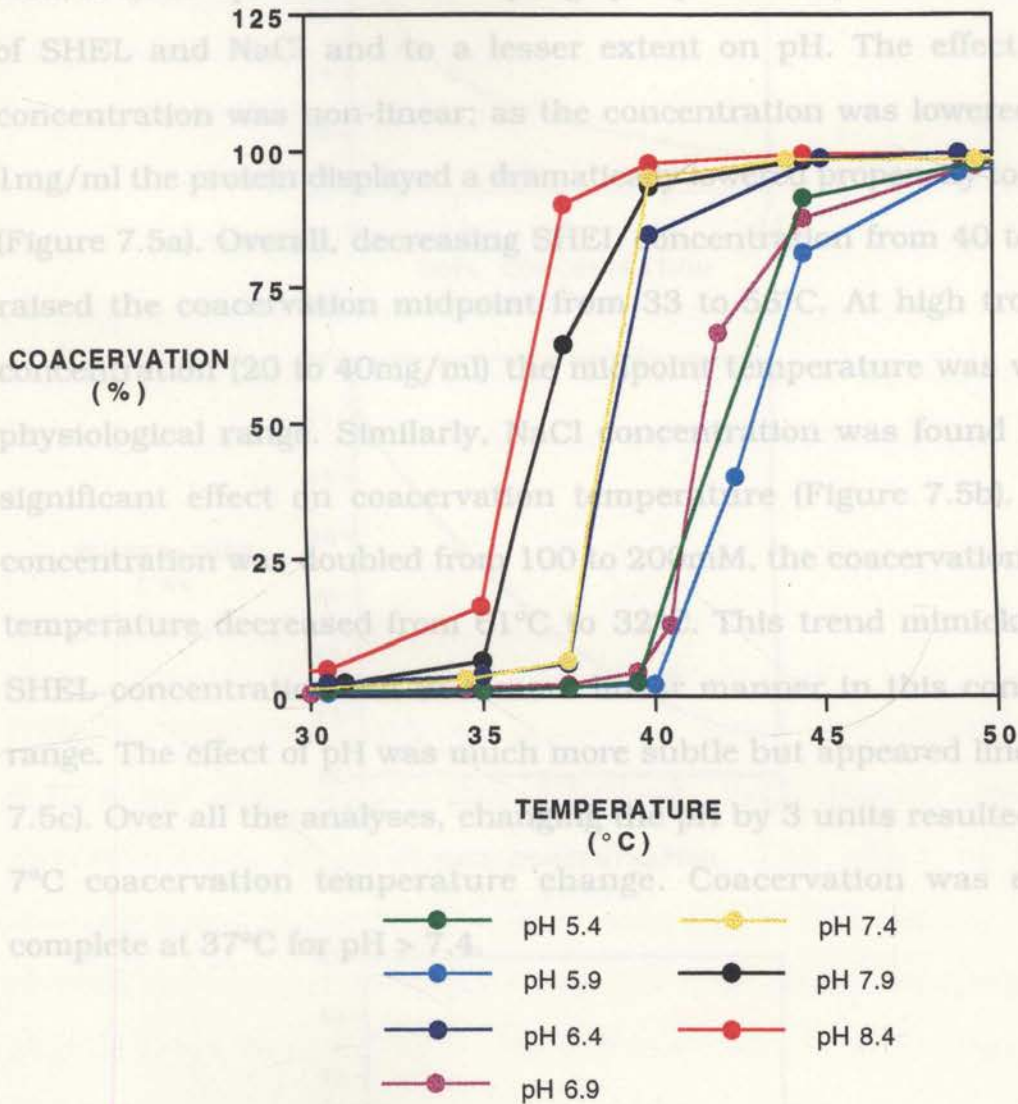


Figure 7.4 Effect of pH on coacervation of SHEL. Coacervation curves for SHEL (20mg/ml) in 150mM NaCl at various pH values.

7.3.4 Comparison of Effects

The temperature of the midpoint of coacervation was determined for the various parameters from the coacervation curves to examine trends (Figure 7.5a, b, c). The process was clearly highly dependent upon the concentration of SHEL and NaCl and to a lesser extent on pH. The effect of SHEL concentration was non-linear; as the concentration was lowered towards 1mg/ml the protein displayed a dramatically lowered propensity to aggregate (Figure 7.5a). Overall, decreasing SHEL concentration from 40 to 1mg/ml raised the coacervation midpoint from 33 to 56°C. At high tropoelastin concentration (20 to 40mg/ml) the midpoint temperature was within the physiological range. Similarly, NaCl concentration was found to have a significant effect on coacervation temperature (Figure 7.5b). As NaCl concentration was doubled from 100 to 200mM, the coacervation midpoint temperature decreased from 61°C to 32°C. This trend mimicked that of SHEL concentration but in a more linear manner in this concentration range. The effect of pH was much more subtle but appeared linear (Figure 7.5c). Over all the analyses, changing the pH by 3 units resulted in only a 7°C coacervation temperature change. Coacervation was essentially complete at 37°C for pH > 7.4.

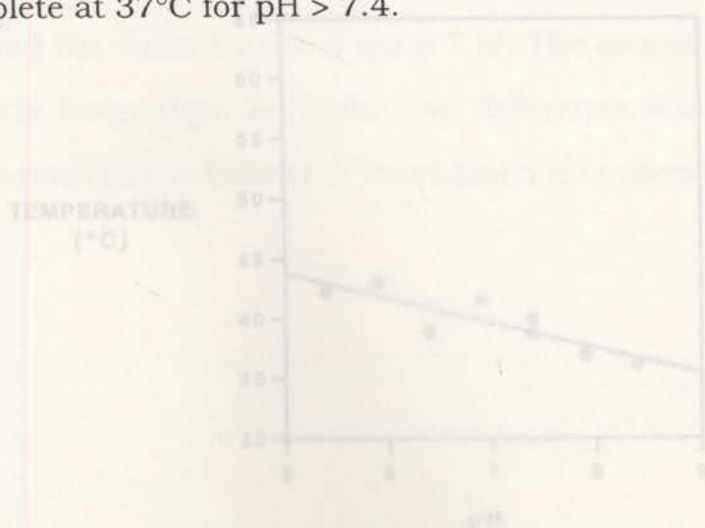
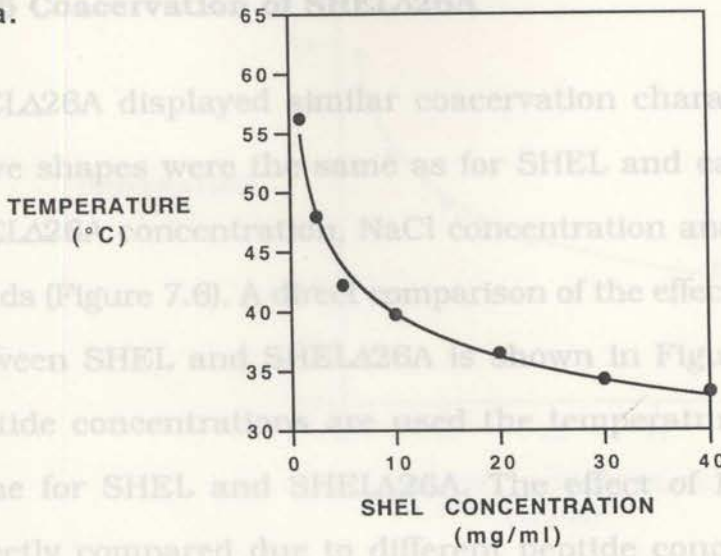


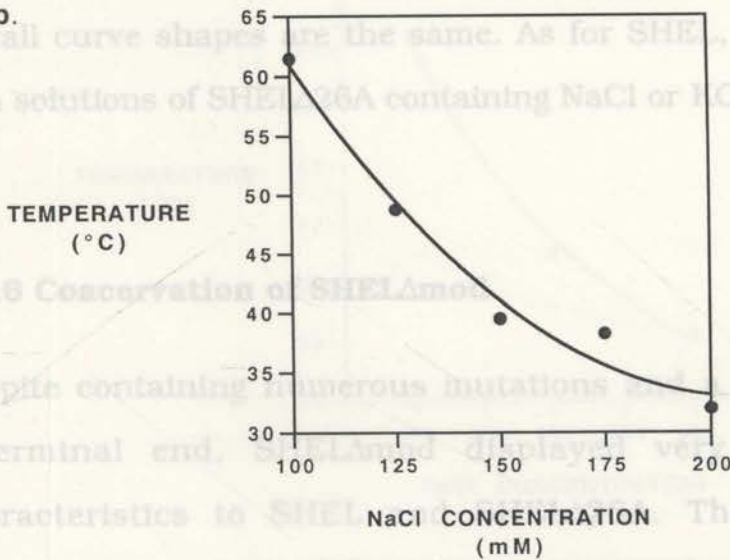
Figure 7.5 Comparison of different parameters on coacervation of SHEL. Temperature of the midpoint of coacervation is plotted against a. SHEL concentration, b. NaCl concentration and c. pH. Plots are provided to illustrate the trends.

7.3.5 Coacervation of SHELΔ26A

a.



b.



c.

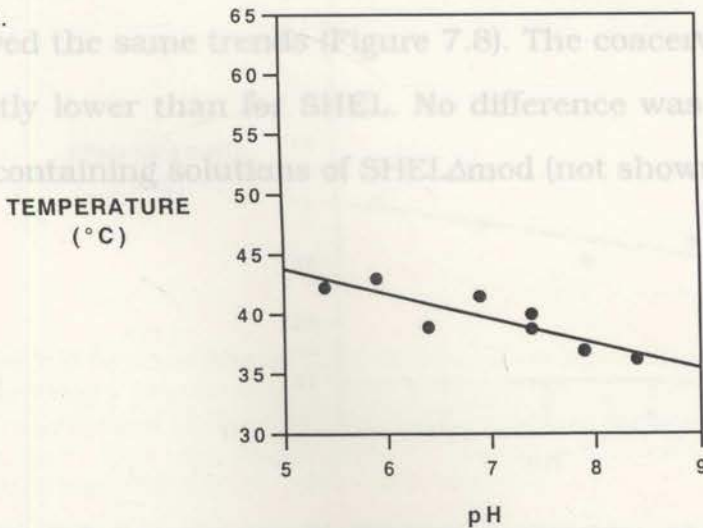


Figure 7.5 Comparison of different parameters on coacervation of SHEL. Temperature at the midpoint of coacervation is plotted against a. SHEL concentration, b. NaCl concentration and c. pH. Plots are presented to illustrate the trends.

7.3.5 Coacervation of SHELΔ26A

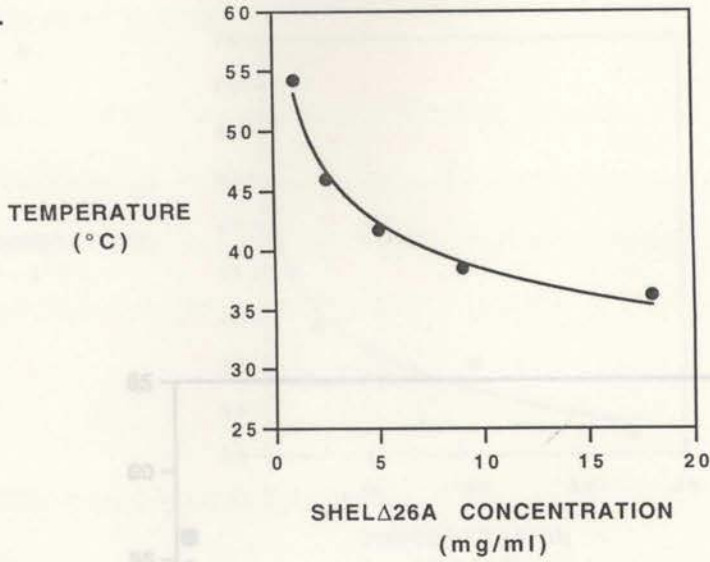
SHELΔ26A displayed similar coacervation characteristics to SHEL. The curve shapes were the same as for SHEL and each of the parameters of SHELΔ26A concentration, NaCl concentration and pH exhibited the same trends (Figure 7.6). A direct comparison of the effect of peptide concentration between SHEL and SHELΔ26A is shown in Figure 7.7. Where the same peptide concentrations are used the temperature of coacervation is the same for SHEL and SHELΔ26A. The effect of NaCl and pH cannot be directly compared due to different peptide concentrations used but the overall curve shapes are the same. As for SHEL, no difference was seen with solutions of SHELΔ26A containing NaCl or KCl (not shown).

7.3.6 Coacervation of SHELΔmod

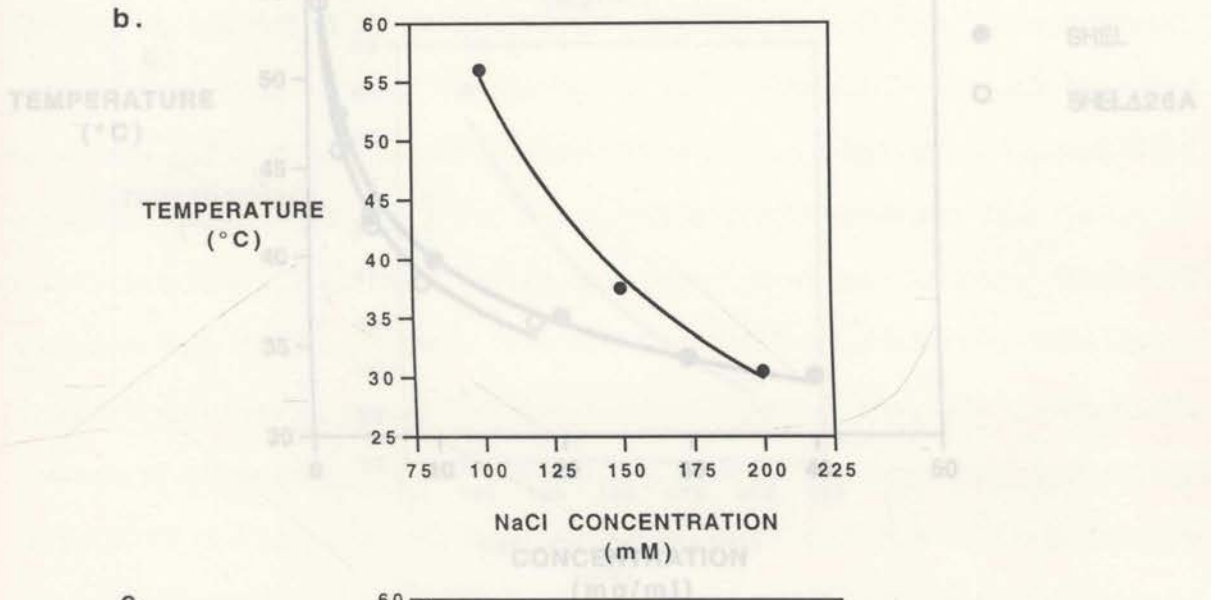
Despite containing numerous mutations and a large deletion near the N-terminal end, SHELΔmod displayed very similar coacervation characteristics to SHEL and SHELΔ26A. The effect of increasing concentrations of the protein, increasing NaCl concentration and pH all showed the same trends (Figure 7.8). The coacervation temperatures were slightly lower than for SHEL. No difference was seen between NaCl and KCl containing solutions of SHELΔmod (not shown).

Figure 7.8 Comparison of different parameters on coacervation of SHELΔ26A. Temperature at the onset of coacervation is plotted against a. SHELΔ26A concentration, b. NaCl concentration and c. pH. The concentration of SHELΔ26A in b. is 8ug/ml and c. is 12ug/ml. This is done to illustrate the trends.

a.



b.



c.

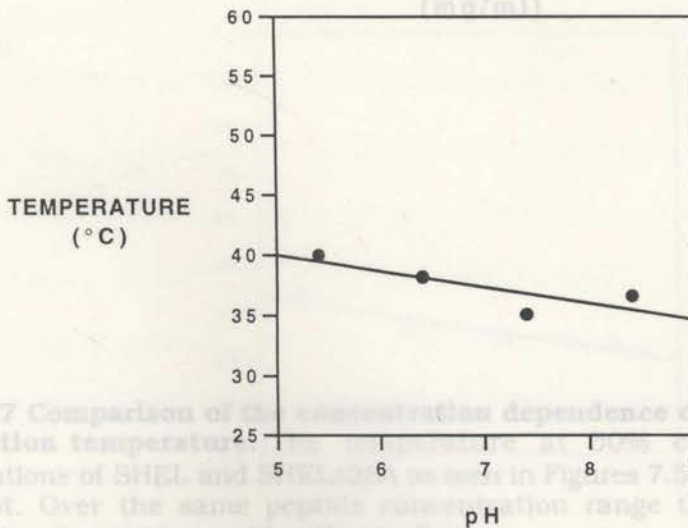


Figure 7.7 Comparison of the concentration dependence of SHEL and SHELΔ26A on coacervation temperature. The concentration dependence of SHEL and SHELΔ26A on coacervation for different concentrations of SHEL and SHELΔ26A as shown in Figures 7.5b and 7.6a are shown on the same plot. Over the same peptide concentration range there is little difference in coacervation temperature with either buffer.

Figure 7.6 Comparison of different parameters on coacervation of SHELΔ26A. Temperature at the midpoint of coacervation is plotted against **a.** SHELΔ26A concentration, **b.** NaCl concentration and **c.** pH. The concentration of SHELΔ26A in **b.** is 8mg/ml and **c.** is 12mg/ml. Plots are drawn to illustrate the trends.

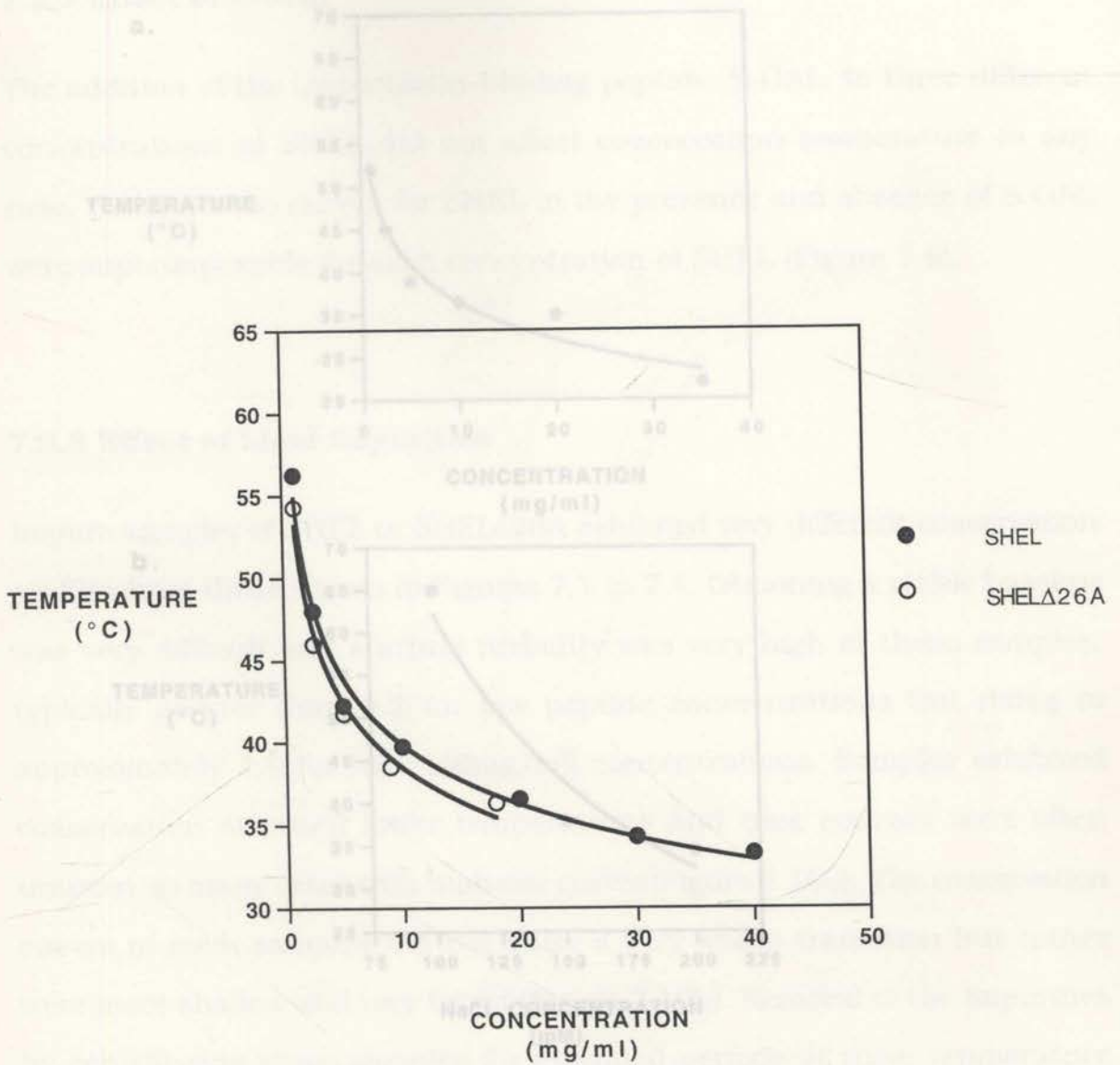


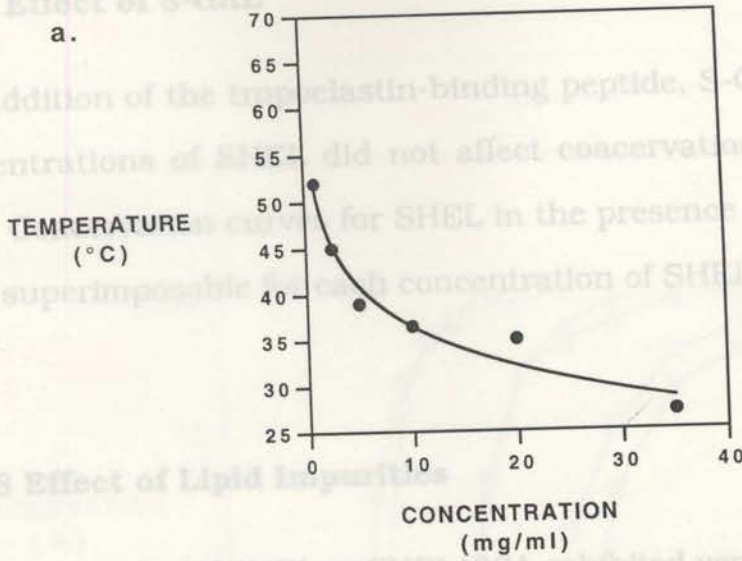
Figure 7.7 Comparison of the concentration dependence of SHEL and SHEL Δ 26A on coacervation temperature. The temperature at 50% coacervation for different concentrations of SHEL and SHEL Δ 26A as seen in Figures 7.5a and 7.6a are shown on the same plot. Over the same peptide concentration range there is little difference in coacervation temperature with either isoform.

Figure 7.8 Comparison of different parameters on coacervation of SHEL Δ mod. Temperature at the midpoint of coacervation is plotted against a. SHEL Δ mod concentration, b. NaCl concentration and c. pH. The concentration of SHEL Δ mod in b. and c. is 20mg/ml. Plots are presented to illustrate the trends.

7.3.7 Effect of S-GAL

The addition of the tropoelastin-binding peptide, S-GAL, to three different concentrations of SHEL did not affect coacervation temperature in any case. The coacervation curves for SHEL in the presence and absence of S-GAL were superimposable at each concentration of SHEL (Figure 7.9).

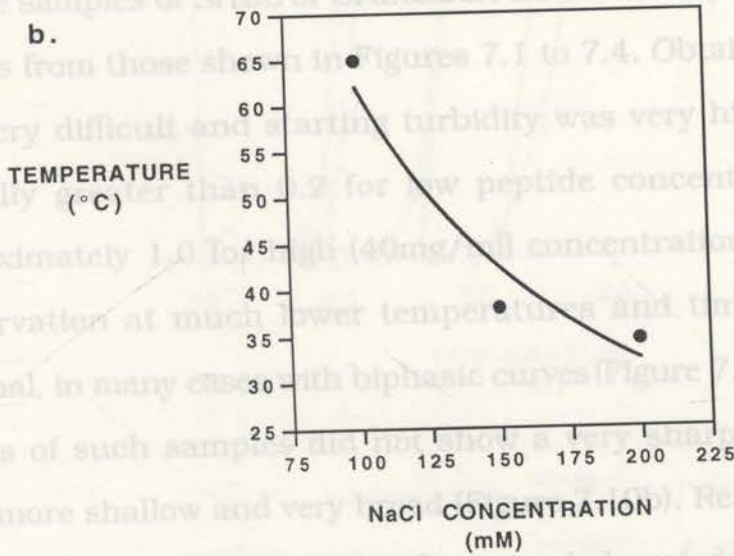
a.



7.3.8 Effect of Lipid Impurities

Impure samples of SHEL or SHELΔ26A exhibited very different coacervation profiles from those shown in Figures 7.1 to 7.4. Obtaining a stable baseline was very difficult and starting turbidity was very high in these samples, typically higher than 1.0 for low peptide concentrations but rising to approximately 1.0 for high (40mg/ml) concentrations. Samples exhibited coacervation at much lower temperatures and time courses were often unusual, in many cases with biphasic curves (Figure 7.10a). The coacervation curves of such samples were much shallower than those of pure samples, transition but rather were more shallow and very low (0.1 to 0.2). Removal of the impurities by centrifuging these samples for extended periods at room temperature resulted in the formation of a coacervate which was separated from the supernatant. Equivalent tropoelastin concentrations from either the supernatant or the coacervate pellet exhibited quite different coacervation profiles (Figure 7.10b). The coacervation curve from the supernatant fraction had a sharp transition and time courses were smooth as in Figure 7.1a, while the pellet fraction resembled the total contaminated sample both in the time courses and in the subsequent coacervation curves.

b.



c.

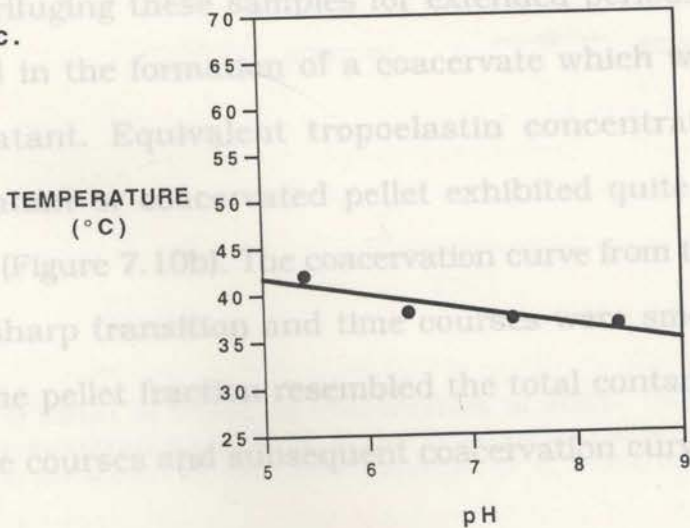


Figure 7.8 Comparison of different parameters on coacervation of SHELΔmod. Temperature at the midpoint of coacervation is plotted against **a.** SHELΔmod concentration, **b.** NaCl concentration and **c.** pH. The concentration of SHELΔmod in **b.** and **c.** is 20mg/ml. Plots are presented to illustrate the trends.

7.3.7 Effect of S-GAL

The addition of the tropoelastin-binding peptide, S-GAL, to three different concentrations of SHEL did not affect coacervation temperature in any case. Coacervation curves for SHEL in the presence and absence of S-GAL were superimposable for each concentration of SHEL (Figure 7.9).

7.3.8 Effect of Lipid Impurities

Impure samples of SHEL or SHEL Δ 26A exhibited very different coacervation profiles from those shown in Figures 7.1 to 7.4. Obtaining a stable baseline was very difficult and starting turbidity was very high in these samples, typically greater than 0.2 for low peptide concentrations but rising to approximately 1.0 for high (40mg/ml) concentrations. Samples exhibited coacervation at much lower temperatures and time courses were often unusual, in many cases with biphasic curves (Figure 7.10a). The coacervation curves of such samples did not show a very sharp transition but rather were more shallow and very broad (Figure 7.10b). Removal of the impurities by centrifuging these samples for extended periods at room temperature resulted in the formation of a coacervate which was separated from the supernatant. Equivalent tropoelastin concentrations from either the supernatant or coacervated pellet exhibited quite different coacervation profiles (Figure 7.10b). The coacervation curve from the supernatant fraction had a sharp transition and time courses were smooth as in Figure 7.1a, while the pellet fraction resembled the total contaminated sample both in the time courses and subsequent coacervation curves.

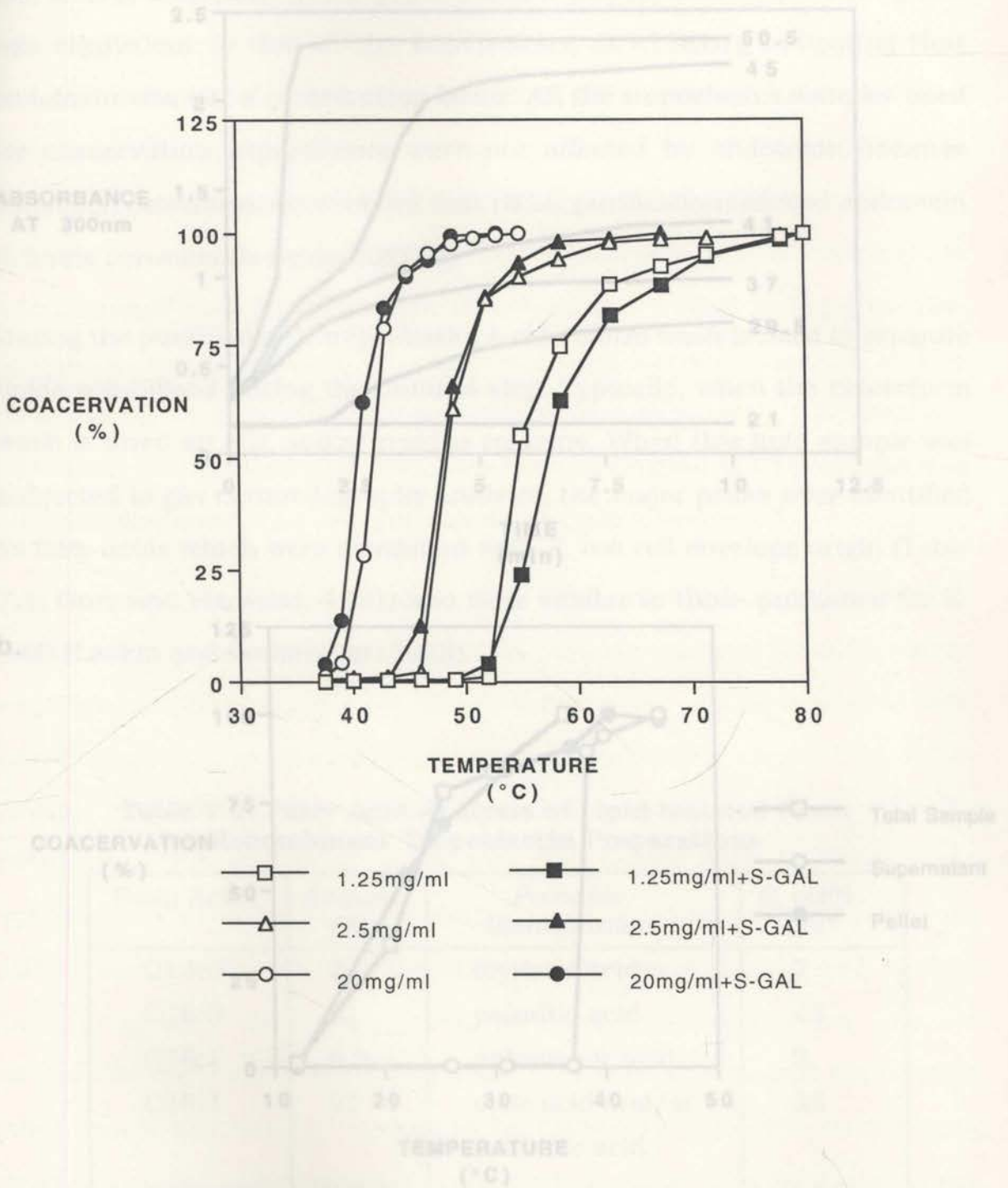


Figure 7.10. Effect of impurities on coacervation. a. Representative time courses for

Figure 7.9 Effect of S-GAL on coacervation of SHEL. Coacervation curves for three different concentrations of SHEL in the presence and absence of S-GAL, added at a 2:1 molar ratio are shown. In each case, the presence of S-GAL has not altered the curves.

curve for a sample of impure SHEL (1.25mg/ml) is shown along with those for the supernatant (8mg/ml) and coacervated pellet from the same sample that had been adjusted to 7.5mg/ml. The curve shape of the coacervated pellet resembles the curve shape of the total impure sample while the curve from the supernatant sample resembles the coacervation curves of pure SHEL samples as seen in Figures 7.2, 7.3 and 7.4. The same results were seen with SHEL.

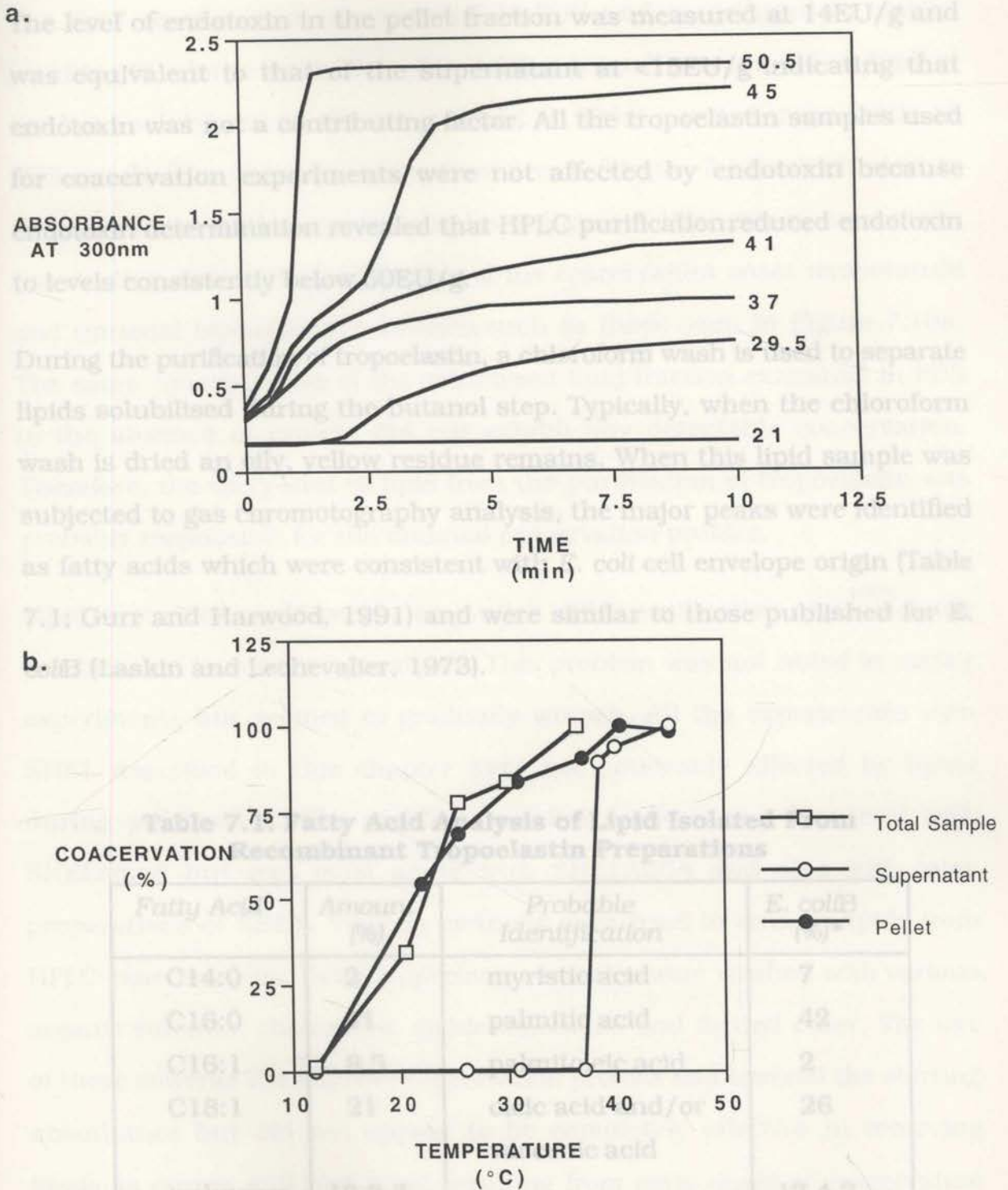


Figure 7.10. Effect of impurities on coacervation. **a.** Representative time courses for lipid-contaminated SHEL Δ 26A at 6mg/ml. The temperature of each time course is indicated in °C. Curves are biphasic in shape, unlike time courses seen in Figure 7.1a. The same time courses were seen for contaminated samples of SHEL. **b.** The coacervation curve for a sample of impure SHEL Δ 26A at 14mg/ml is shown with those for the supernatant (8mg/ml) and coacervated pellet from the same sample that had been adjusted to 7.5mg/ml. The curve shape of the coacervated pellet resembles the curve shape of the total impure sample while the curve from the supernatant sample resembles the coacervation curves of pure SHEL samples as seen in Figures 7.2, 7.3 and 7.4. The same results were seen with SHEL.

The level of endotoxin in the pellet fraction was measured at 14EU/g and was equivalent to that of the supernatant at <15EU/g indicating that endotoxin was not a contributing factor. All the tropoelastin samples used for coacervation experiments were not affected by endotoxin because endotoxin determination revealed that HPLC purification reduced endotoxin to levels consistently below 50EU/g.

During the purification of tropoelastin, a chloroform wash is used to separate lipids solubilised during the butanol step. Typically, when the chloroform wash is dried an oily, yellow residue remains. When this lipid sample was subjected to gas chromatography analysis, the major peaks were identified as fatty acids which were consistent with *E. coli* cell envelope origin (Table 7.1; Gurr and Harwood, 1991) and were similar to those published for *E. coli*B (Laskin and Lechevalier, 1973).

Table 7.1. Fatty Acid Analysis of Lipid Isolated From Recombinant Tropoelastin Preparations

Fatty Acid	Amount (%)	Probable Identification	<i>E. coli</i> B (%)*
C14:0	2	myristic acid	7
C16:0	41	palmitic acid	42
C16:1	8.5	palmitoleic acid	2
C18:1	21	oleic acid and/or vaccenic acid	26
unknown peaks	12,3,3		12,4,2

* Laskin and Lechevalier (1973)

The lipid residue was resuspended in PBS and centrifuged to clarify, resulting in a large insoluble pellet. Adding a small amount (15 or 30 μ l) of the lipid solubilised in the supernatant to 500 μ l purified tropoelastin in PBS resulted in altered coacervation curves (Figure 7.11) which start to resemble those of the impure samples in Figure 7.10b with an increase in the starting absorbance, alteration of the coacervation onset temperature and unusual biphasic time courses such as those seen in Figure 7.10a. The same concentration of the solubilised lipid fraction examined in PBS in the absence of protein did not exhibit any detectable coacervation. Therefore, the carry-over of lipid from the purification of tropoelastin was probably responsible for the unusual coacervation profiles.

Lipid impurities could persist even after HPLC purification and ^{were} ~~was~~ quite troublesome in some preparations. This problem was not noted in earlier experiments but seemed to gradually worsen. All the experiments with SHEL described in this chapter were not noticeably affected by lipids during purification. The problem was first noticed at a low level with SHEL Δ mod but was most acute with SHEL Δ 26A and also with later preparations of SHEL. Various methods were tried to remove lipids from HPLC-pure samples. Dried tropoelastin samples were washed with various organic solvents; chloroform, dichloromethane and diethyl ether. The use of these solvents did improve coacervation profiles and lowered the starting absorbance but did not appear to be completely effective in removing lipids as curves still had a tail resulting from early onset of coacervation (not shown). The addition of lipase and phospholipase A₂ to both the cell lysate and purified protein samples was effective to a similar extent but again did not appear to remove lipids completely (not shown). The only totally effective way to remove the lipid contaminants was centrifugation at the appropriate temperature to remove the components resulting in the lower portion of the time course curves (Figure 7.10a).

7.4 DISCUSSION

7.4.1 Coacervation

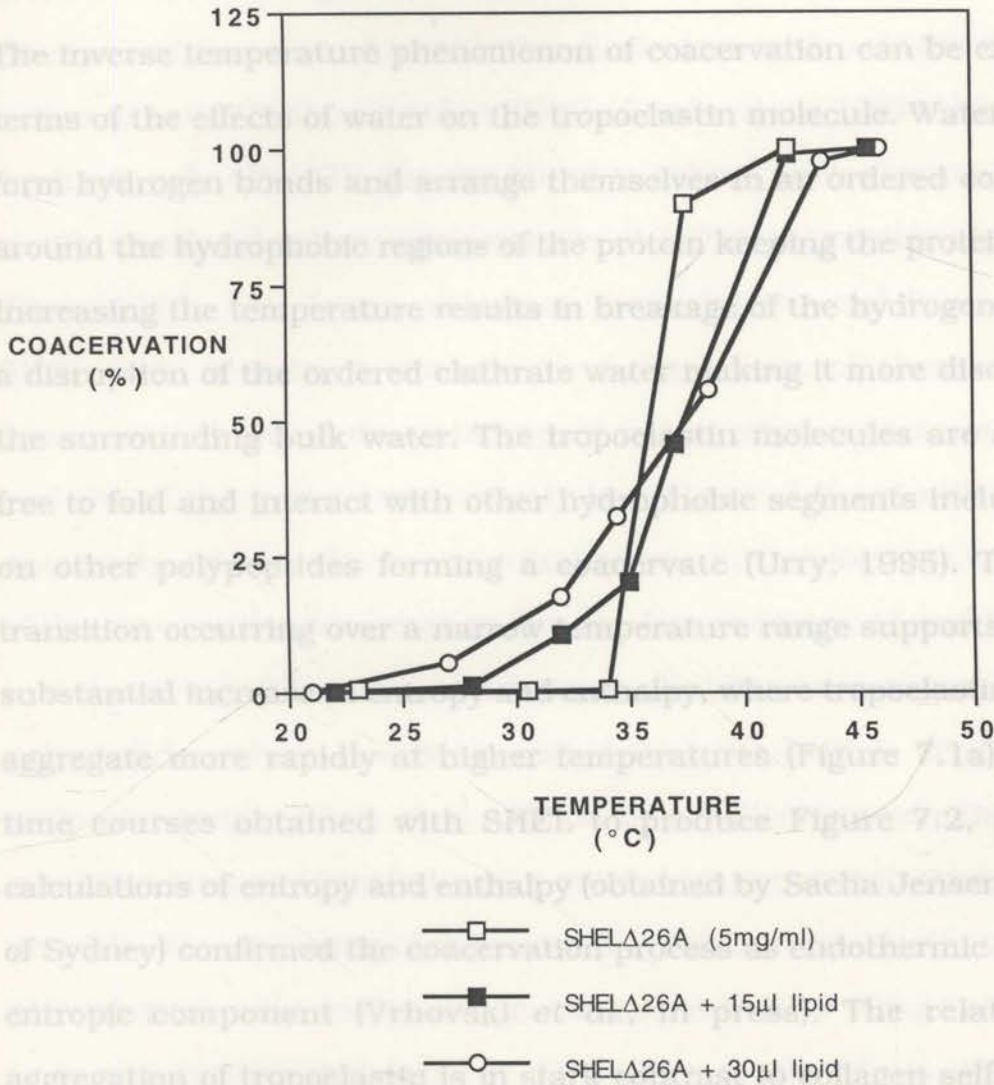


Figure 7.11 Effect of lipid addition on coacervation of SHELΔ26A. The coacervation curve for purified SHELΔ26A at 5mg/ml is shown. After addition of 15 and 30μl lipid extract the coacervation curves are no longer sharp and begin to resemble those contaminated samples seen in Figure 7.10b. After addition of lipid, the time courses (not shown) were identical in shape to those of Figure 7.10a.

7.4.2 Purification Affecting SHEL Coacervation

displays coacervation ability. SHEL concentration, NaCl concentration and pH were all found to affect the temperature at which coacervation initiated. The effect of SHEL concentration on coacervation is clearly non-linear. Increasing the concentration of tropoelastin resulted in a shift of coacervation

7.4 DISCUSSION

7.4.1 Coacervation

The inverse temperature phenomenon of coacervation can be explained in terms of the effects of water on the tropoelastin molecule. Water molecules form hydrogen bonds and arrange themselves in an ordered configuration around the hydrophobic regions of the protein keeping the protein unfolded. Increasing the temperature results in breakage of the hydrogen bonds and a disruption of the ordered clathrate water making it more disordered like the surrounding bulk water. The tropoelastin molecules are accordingly free to fold and interact with other hydrophobic segments including those on other polypeptides forming a coacervate (Urry, 1995). The sudden transition occurring over a narrow temperature range supports a model of substantial increase in entropy and enthalpy, where tropoelastin molecules aggregate more rapidly at higher temperatures (Figure 7.1a). Using the time courses obtained with SHEL to produce Figure 7.2, preliminary calculations of entropy and enthalpy (obtained by Sacha Jensen, University of Sydney) confirmed the coacervation process as endothermic with a large entropic component (Vrhovski *et al.*, in press). The relatively rapid aggregation of tropoelastin is in stark contrast to collagen self-association which may typically take several hours (Kadler *et al.*, 1987).

7.4.2 Parameters Affecting SHEL Coacervation

It is clear that the well defined isoform of human tropoelastin, SHEL, displays coacervation ability. SHEL concentration, NaCl concentration and pH were all found to affect the temperature at which coacervation initiated. The effect of SHEL concentration on coacervation is clearly non-linear. Increasing the concentration of tropoelastin resulted in a shift of coacervation

towards lower temperatures and a sharpening of the curve, with a reduction in the temperature range over which coacervation was essentially complete (Figure 7.2). This suggests co-operativity in the intermolecular aggregation process and is comparable with the effects seen with α -elastin and tandem arrays of poly-VPGG and poly-VPGVG (Kondo *et al.*, 1987; Urry, 1978). In contrast, poly-APGVGV was not found to exhibit such sharpening but was simply translated to lower temperatures at higher polypeptide concentrations (Urry, 1978). The forms of human tropoelastin used here, SHEL and SHEL Δ 26A, contain a consecutive array of six of these hexapeptide sequences, the most dramatic repeat in the sequences accounting for 5 and 6% of the protein respectively (see Figure 3.6) yet still showed co-operativity. As tropoelastin concentration was further increased, the lowering of the coacervation temperature became less pronounced and this resulted in a clustering of the curves. This same effect has been seen with synthetic polypeptides where it was suggested that the limit is dependent upon molecular weight (Urry *et al.*, 1985). In practice tropoelastin is near its solubility limit at 40mg/ml and a much higher concentration may not be possible. The clustering of the curves for human tropoelastin occurs in the physiological range so that at concentrations of 20 to 40mg/ml tropoelastin is in the coacervated form at 37°C. The coacervate is, therefore, the physiologically relevant form of the naked protein. *In vivo*, tropoelastin is known to be hydroxylated at proline residues to a variable degree and this hydroxylation is capable of affecting the coacervation temperature of polypeptides of elastin (Urry *et al.*, 1979). Despite recombinant tropoelastins lacking hydroxylation, the curves seen here are very similar to the curve produced from chick tropoelastin (Urry, 1978) which presumably would be hydroxylated. There was no difference in curves in the presence of either salt similar to results seen with polypentapeptides (Kondo *et al.*, 1987) and NaCl concentration was found to significantly alter the coacervation temperature of SHEL. The effect has been proposed to be due to NaCl

decreasing the effective concentration of water by binding it in hydration shells, thereby conversely increasing effective protein concentration (Urry, 1978). No coacervation was seen in the temperature range examined if NaCl was below 100mM. This was in marked contrast to the effect seen with synthetic polypeptides and α -elastin, and even chick aortic tropoelastin, where coacervation could still occur in distilled water (Urry, 1978). For SHEL, increasing NaCl concentration from 100mM to 200mM facilitated coacervation and significantly lowered the temperature of this effect. Coacervation curves were not appreciably sharper with increasing NaCl (Figure 7.3a). Others (Miyakawa *et al.*, 1995; Urry and Long, 1977) have noted that the effect of NaCl on polypeptides mimicked the effect of increasing tropoelastin concentration such that if increasing tropoelastin concentration caused coacervation curves to become translated to lower temperatures and to steepen, then NaCl did the same. Such an effect was not detected with SHEL, with each curve appearing similarly sharp. The dependence upon NaCl addition was not the same as for tropoelastin concentration and appeared to approach linearity in the region 100-200mM NaCl in comparison with the more logarithmic effect of SHEL concentration (Figure 7.5a,b). Differential scanning calorimetry studies performed with synthetic polypeptides clearly showed a linear relationship between NaCl concentration and transition temperature of coacervation (Luan *et al.*, 1991) and our results are consistent with this. Significantly, extracellular Na^+ concentration is approximately 150mM (Tietz, 1982) and this amount of NaCl was needed to bring about coacervation of SHEL in the physiological temperature range of 30-40°C with an effective maximum at 37°C (Figures 7.3a, 7.5b). KCl appears to affect coacervation in the same way as NaCl since there was no difference in curves in the presence of either salt similar to results seen with polypentapeptides (Kondo *et al.*, 1987) and α -elastin (Kaibara *et al.*, 1992).

The effect of pH on coacervation was more subtle, yet covered a 1000-fold range of $[H^+]$. There was an approximately linear effect on coacervation temperature which is consistent with the linear pH effect seen at high ionic strength using chick and bovine tropoelastins (Sykes and Partridge, 1974; Whiting *et al.*, 1974). With higher pH, a lower temperature of coacervation was seen (Figure 7.5c) but this was not as significant as either NaCl or tropoelastin concentration. The effect is probably due to the pH of the buffer approaching the isoelectric point of SHEL (11.2) and therefore affecting the charges on populations of specific residues. Coacervation is expected to be maximal at the isoelectric point as was seen with α -elastin (Kaibara *et al.*, 1992), chick (Sykes and Partridge, 1974) and bovine (Whiting *et al.*, 1974) tropoelastins. Extracellular pH is approximately 7.4 (Tietz, 1982) while intracellularly it is more variable but is generally lower. For example, pH inside fibroblasts is 6.6 (Ritter *et al.*, 1992) and in muscle cells is 6.9 (Tietz, 1982). Thus, the normal pH fluctuations seen *in vivo* are probably not enough to greatly affect coacervation of tropoelastin, although it may be expected that coacervation may be slightly more favoured extracellularly.

7.4.3 Comparison of Coacervation of SHEL, SHEL Δ 26A and SHEL Δ mod

The two human tropoelastin isoforms used, SHEL and SHEL Δ 26A, differ by a 33 amino acid sequence containing the most hydrophilic repeat sequence in human tropoelastin, 26A. However, the two isoforms show identical coacervation properties and coacervate at the same temperature at equivalent peptide concentrations. Therefore the presence of this 26A region does not affect the coacervation ability of tropoelastin despite altering the hydrophobicity of the protein. Bedell-Hogan *et al.* (1993) found that the isoform without 26A is a poorer substrate for lysyl oxidase and is not

as readily cross-linked. The results shown here indicate that this difference is not caused by a difference in the ability of the isoforms to coacervate. Any difference in the physiological function of these isoforms or their ability to be cross-linked into fibres may be due to changes in secondary structure or some other undetermined function of 26A, e.g. binding of molecules such as sugars, proteoglycans or microfibrillar proteins.

It is significant that SHEL Δ mod also displayed very similar coacervation characteristics to both SHEL and SHEL Δ 26A. This protein is missing, in addition to 26A, a substantial hydrophobic segment from the N-terminus yet coacervates with the same overall characteristics as SHEL and SHEL Δ 26A. This indicates that the deleted segment, which although is hydrophobic, is not vital to coacervation. The remaining portion contains enough hydrophobic repeat regions to maintain coacervation. Thus, even relatively major mutations in tropoelastin do not necessarily abolish coacervation. This raises the prospect that related mutant molecules, if present in the extracellular matrix may still be able to coacervate and possibly be incorporated into fibres. However, if these molecules have reduced elastic properties, the overall effectiveness of the elastic fibre may be consequently altered.

7.4.4 Effect of S-GAL on Coacervation

KCl in place of NaCl did not noticeably affect SHEL coacervation. This is similar to results seen with α -elastin (Kaibara *et al.*, 1992) and the polypentapeptide of elastin (Kondo *et al.*, 1987) where little difference in coacervation temperature was seen by using K⁺ or Na⁺ as the cation. This indicates that intracellularly, where KCl is high and NaCl is low, tropoelastin is in an environment conducive to coacervation. Presumably, however,

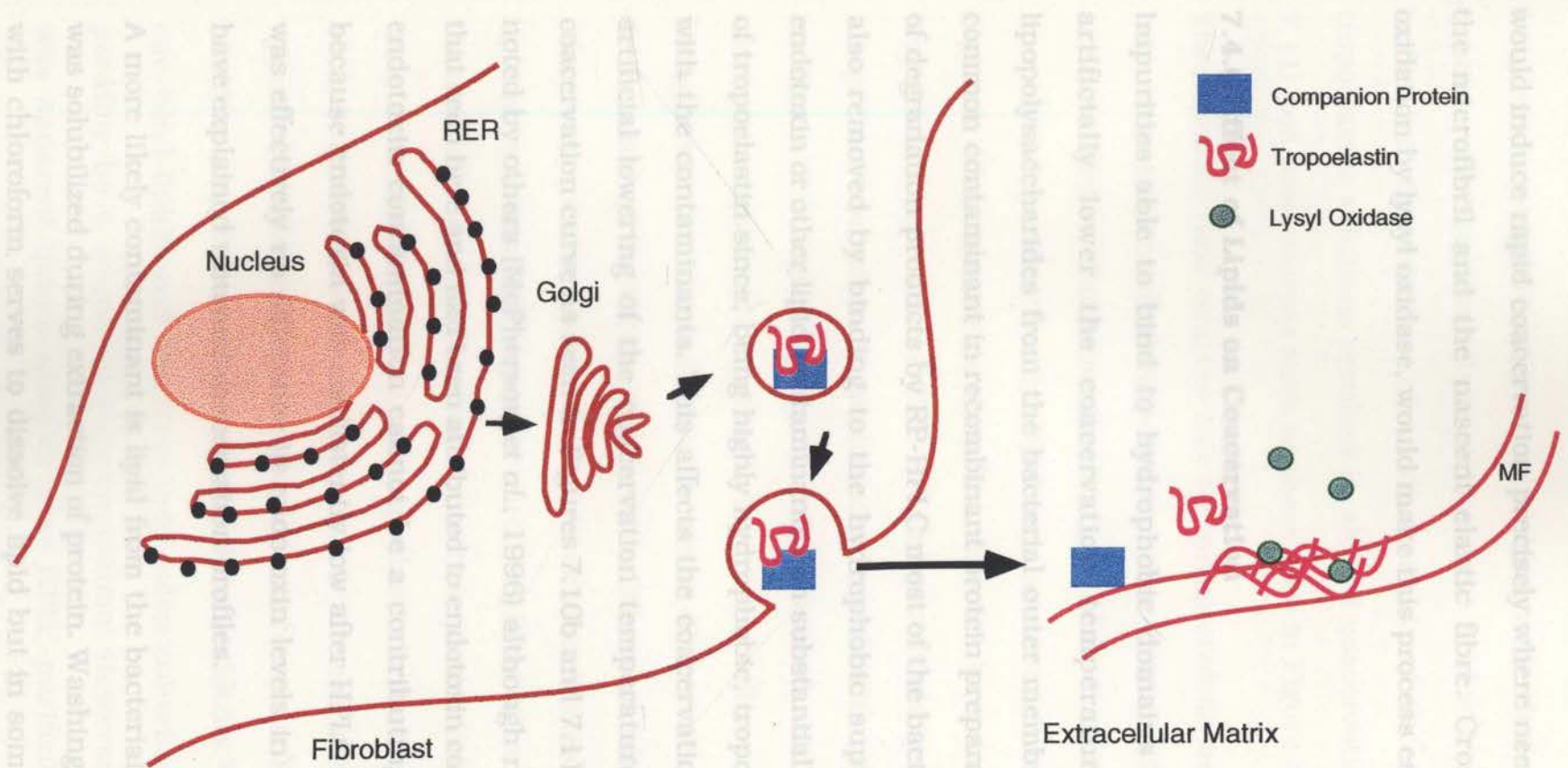
tropoelastin does not coacervate intracellularly since this would inhibit secretion and subsequently elastic fibre formation in the extracellular matrix.

From the results obtained in this chapter, a model for tropoelastin assembly can be proposed (Figure 7.12) which is based on and extends the model It has previously been suggested that intracellular binding of tropoelastin to a companion protein such as EBP will protect tropoelastin from proteases and inhibit its coacervation (Hinek and Rabinovitch, 1994). Other tropoelastin binding proteins have also been recently identified which may perform a similar role (Davis and Mecham, 1996b). To model EBP, S-GAL has been used previously to demonstrate that coacervation of κ -elastin will be inhibited in its presence (Hinek *et al.*, 1992b). However, the use of S-GAL with SHEL, following the technique of Hinek *et al.* (1992) did not have any effect on coacervation. There are differences between this experiment with SHEL and that of Hinek *et al.* (1992). This study used tropoelastin instead of κ -elastin and a much lower NaCl concentration was used, 150mM compared with 1.5M in the experiments described by Hinek *et al.* (1992). These may have contributed to the different result seen. However, it is possible that S-GAL binding to SHEL does not impair coacervation noticeably since there are many other possible hydrophobic regions for interaction. Alternatively, S-GAL may not have bound adequately to SHEL or was easily displaced. More definitive results may perhaps be obtained by using EBP instead of S-GAL. In addition, other proteins proposed to bind tropoelastin intracellularly, such as microfibrillar proteins, could be studied this same way.

on of tropoelastin would be high. In addition, the concentration of previously cross-linked elastin in the nascent elastic fibre is very high, providing further hydrophobic domains for tropoelastin to interact with and therefore effectively increasing the total concentration to levels where coacervation would be rapidly promoted. Thus, when tropoelastin is released the high effective concentration in the appropriate NaCl, pH and temperature environment found in the extracellular matrix

7.4.5 A Model for Tropoelastin Assembly *In Vivo*

From the results obtained in this chapter, a model for tropoelastin assembly can be proposed (Figure 7.12) which is based on and extends the model proposed by Hinek (1995). If tropoelastin does bind a companion protein, such as EBP, intracellularly (Hinek, 1995) the effective concentration of free tropoelastin will be greatly reduced. Intracellularly, tropoelastin may be produced at high levels but binds to the companion protein and therefore never accumulates to a high enough effective concentration to cause intracellular coacervation at body temperature where it would be detrimental to the cell. Davis and Mecham (1996b) have suggested that two newly identified tropoelastin companion proteins may act as molecular chaperones for tropoelastin in the RER to assist in proper folding. EBP is the only companion protein studied in detail to date and it has been shown that the EBP-tropoelastin complex is exported to the extracellular matrix where the tropoelastin component is separated from EBP and released directly onto the microfibrillar surface where it free to interact with other components (Hinek, 1995; Section 1.2.6; Figure 1.2). When all the variables are superimposed, coacervation of greater than 10mg/ml tropoelastin (SHEL or SHELΔ26A) at pH 7-8 and 150mM NaCl is essentially complete at 37°C, conditions which are found in the extracellular matrix. No information is available on the actual tropoelastin concentration in the extracellular matrix but upon delivery to the surface of the microfibril and/or nascent elastic fibre the local concentration of tropoelastin would be high. In addition, the concentration of previously cross-linked elastin in the nascent elastic fibre is very high, providing further hydrophobic domains for tropoelastin to interact with and therefore effectively increasing the total concentration to levels where coacervation would be rapidly promoted. Thus, when tropoelastin is released the high effective concentration in the appropriate NaCl, pH and temperature environment found in the extracellular matrix



- Companion Protein
- Tropoelastin
- Lysyl Oxidase

Figure 7.12. Proposed model for tropoelastin assembly. This model is based on that proposed by Hinek (1995). Tropoelastin made inside the cell (e.g. fibroblast) is rapidly bound to a companion protein (Hinek, 1995) resulting in a relatively low effective concentration of free polypeptide. Coacervation is therefore inhibited. The tropoelastin/companion protein complex is exported through the cell's rough endoplasmic reticulum (RER) and Golgi secretion system to the extracellular matrix (Hinek, 1995). At the microfibril (MF) and/or growing elastic fibre surface, tropoelastin is released from the companion protein resulting in a high local concentration of free tropoelastin. This, coupled with the appropriate salt concentration, pH and temperature of the extracellular matrix induces rapid coacervate formation. Lysyl oxidase, which is present in the extracellular matrix can now initiate cross-linking, permanently fixing the tropoelastin molecules into the nascent elastic fibre.

would induce rapid coacervation precisely where needed at the surface of the microfibril and the nascent elastic fibre. Cross-linking, following oxidation by lysyl oxidase, would make this process essentially irreversible.

tropoelastin solutions resulted in altered coacervation properties (Figure 7.11) and time courses such as those seen in Figure 7.10a.

7.4.6 Effect of Lipids on Coacervation

The biphasic time courses can be interpreted as an association of lipid

Impurities able to bind to hydrophobic domains on tropoelastin can artificially lower the coacervation temperature. Endotoxins are lipopolysaccharides from the bacterial outer membrane layer and are a common contaminant in recombinant protein preparations. In the removal of degradation products by RP-HPLC most of the bacterial endotoxins were also removed by binding to the hydrophobic support. A high level of endotoxin or other lipid contaminants can substantially affect the properties of tropoelastin since, being highly hydrophobic, tropoelastin can aggregate with the contaminants. This affects the coacervation curves causing an artificial lowering of the coacervation temperature and a 'tail' on the coacervation curve as seen in Figures 7.10b and 7.11. This effect has been noted by others (McPherson *et al.*, 1996) although not as dramatically as that seen here and had been attributed to endotoxin contamination. However, endotoxin contamination cannot be a contributing factor in this work because endotoxin was consistently low after HPLC purification and there was effectively no difference in endotoxin levels in samples which would have explained unusual coacervation profiles.

A more likely contaminant is lipid from the bacterial cell membrane which possibly be a source of re-aggregation. However, lipid contamination was solubilized during extraction of protein. Washing the dry SHEL residue was apparent before samples were HPLC-purified and the use of new HPLC columns did not alleviate the problem. In the experiments outlined here, endotoxin and other lipids have effectively removed by a combination of chloroform washes, followed by coacervation where necessary, resulting

fatty acid composition was consistent with that expected for *E. coli* membranes. Only a small proportion of the lipid was solubilised in aqueous buffer but the addition of small amounts of the lipid extract to pure tropoelastin solutions resulted in altered coacervation properties (Figure 7.11) and time courses such as those seen in Figure 7.10a.

The biphasic time courses can be interpreted as an association of lipid with tropoelastin which appears to occur more readily than tropoelastin self-association. This forms the first part of the time course which plateaus at a level dependent on the lipid concentration. The second phase of the biphasic time course is therefore due to the unaffected tropoelastin-tropoelastin interaction. This second phase always occurs at the same temperature which is dependent on tropoelastin concentration as shown in Figure 7.2. Centrifuging the contaminated sample at a temperature conducive to the lipid-tropoelastin interaction will remove the lipid impurities along with the tropoelastin to which it is bound, an effect clearly demonstrated in Figure 7.10b. The failure of alternative methods to adequately remove the lipid contaminants indicates that the tropoelastin-lipid interaction is a very tight one. This illustrates the care that must be taken to ensure removal of all impurities, particularly endotoxin and lipids from recombinant samples of tropoelastin before embarking on physical studies. However, what is not apparent is the reason why lipid contamination appeared to worsen over time. No obvious change in the protocol or solutions could be pinpointed as the source of these problems. C18 RP-HPLC columns can bind lipids and therefore lipid-laden columns if not cleaned could possibly be a source of recontamination. However, lipid contamination was apparent before samples were HPLC-purified and the use of new HPLC columns did not alleviate the problem. In the experiments outlined here, endotoxin and other lipids were effectively removed by a combination of chloroform washes, followed by centrifugation where necessary, resulting

in highly purified protein.

Elastin has long been known to be able to bind fatty acids and lipids (Norde *et al.*, 1985; Tokita *et al.*, 1977; Claire *et al.*, 1976), a feature which has been proposed to be an important contributor in the development of atherosclerosis. It is clear from these results that tropoelastin is also capable of binding fatty acids and lipids and that this can affect its coacervation properties. It has been proposed that lipid binding to elastin chains would disrupt fibre formation because chains would not be able to associate properly. The binding of lipids to extended chains would prevent the chain from returning to its relaxed state and thereby remove some of its elasticity (Urry, 1978). This has been demonstrated experimentally by stress-strain measurements which indicate that elastin-fatty acid complexes are less elastic (Norde *et al.*, 1985; Kagan *et al.*, 1977). Interestingly, when lipids are present in SHEL solutions the coacervation process starts to become irreversible. Even with extended treatment on ice the turbidity does not return to its starting level (Figure 7.10a). Studies have also demonstrated that longer chain fatty acids, especially C16 and C18, have the highest binding affinity for elastin and produce the greatest effect on elasticity (Norde *et al.*, 1985; Kagan *et al.*, 1977). These fatty acids are shown in Table 7.1 to be the most abundant *E. coli* fatty acids binding to SHEL. In addition, the binding of fatty acids to elastin has been demonstrated to inhibit lysyl oxidase mediated cross-linking, with oleate (C18) showing the greatest inhibitory effect (Kagan *et al.*, 1981). The results shown here indicate that the presence of excess lipids in the environment of the forming elastic fibre may affect normal coacervation and cross-linking and the subsequent function of the elastic fibre.

7.5 CONCLUSION

These results are fully consistent with an essential role played by coacervation in elastic fibre assembly during the major stages of elastin formation. Coacervation is finely tuned to occur under extracellular physiological conditions of temperature, NaCl concentration and pH. Coacervation is strongly influenced by peptide and NaCl concentration and to a lesser extent pH. The same trends were seen for the second tropoelastin isoform, SHEL Δ 26A, with little difference in coacervation temperature. SHEL Δ mod was also able to coacervate and exhibited the same trends as the two isoforms of tropoelastin. S-GAL, a model of EBP, did not appear to inhibit coacervation of SHEL. Contaminating lipids from *E. coli* were shown to alter coacervation curves dramatically.

CHAPTER 8

GENERAL DISCUSSION

8.1 RECOMBINANT TROPOELASTIN PRODUCTION

Until recently, tropoelastin research relied exclusively on the availability of tropoelastin from animal sources. This was a time-consuming process involving the raising of animals under strict dietary conditions which limited the amount of tropoelastin obtained (Rich and Foster, 1982; Rucker, 1982). Human tropoelastin became available for the first time through the use of recombinant DNA technology (Indik *et al.*, 1990). This allowed the production of a single isoform of tropoelastin and potentially increased the total amounts available. However, recombinant tropoelastins have so far only been available in limited quantities (Grosso *et al.*, 1991; Indik *et al.*, 1990) and thus the potential of recombinant systems for tropoelastin production has not been fully exploited. It was a major aim of this work to construct and optimise a recombinant system for the production of distinct isoforms of human tropoelastin which would produce a high yield of protein and therefore provide an easily accessible source of tropoelastin for future work.

This aim was successfully achieved and two human tropoelastin isoforms, SHEL and SHEL Δ 26A, were produced in addition to an aberrant form SHEL Δ mod. SHEL and SHEL Δ 26A are produced at high levels with 50mg routinely obtained from one litre of culture. This is 5-10 fold higher than other published recombinant tropoelastin systems (Grosso *et al.*, 1991; Indik *et al.*, 1990) and emphasises the value of a systematic approach to high-level protein production. The polypeptide sequence of tropoelastin is repetitive and its natural gene demonstrates a particular codon bias which, together with its overall size, may make it less than ideal for recombinant production in *E. coli*. To preclude this as a possible source of overexpression problems, the entire gene precursors for SHEL were synthesised with an *E. coli* preferred codon bias and other convenient DNA modifications to

assist cloning (Martin *et al.*, 1995). Following the assembly of full-length *SHEL*, four different expression vectors with very different properties including one fusion system, were chosen for cloning of *SHEL* since it was not possible to know *a priori* which system would be most appropriate. Each one was assessed for overexpression. Fine-tuning of expression by altering conditions of growth, induction and purification were successful in improving the amount of *SHEL* produced and this approach allowed the optimal two systems for *SHEL* production to be chosen. Following problems with GST-*SHEL* purification the final system of choice for *SHEL* production, and consequently *SHEL* Δ 26A, consisted of expression of unfused *SHEL* from pSHELF and this is the first published account of successful unfused tropoelastin expression (Martin *et al.*, 1995).

The purification protocol for *SHEL* and *SHEL* Δ 26A was based on a protocol for tropoelastin extraction from tissues and is essentially a single-step procedure involving alcohol solubilisation. This work provides a simple and highly effective method for purification of soluble unfused tropoelastin from recombinant systems, eliminating the need for techniques such as CNBr cleavage. Although some degradation products were usually present, this was not unexpected due to tropoelastin's protease susceptibility and these were completely removed by RP-HPLC allowing the recovery of full-length protein. An added advantage was that endotoxin was greatly reduced by RP-HPLC, a critical requirement for future *in vivo* animal studies. One problem encountered during the purification was the carry-over of lipids from the *E. coli* extract into tropoelastin preparations. This demonstrated that tropoelastin, like elastin, can effectively bind lipids and that this binding is strong enough to allow co-purification to occur. This previously unaddressed problem has the potential to affect tropoelastin from all sources, tissue and recombinant, and could interfere considerably with further tropoelastin studies. The only effective way found to remove lipids was

through centrifugation at the appropriate temperature where both lipids and affected tropoelastin were coacervated and thereby removed. Using expression conditions and purification protocol defined by this work, further work in this laboratory has successfully focused on high-cell density fermentation to scale up production of both SHEL and SHEL Δ 26A with the potential for the production of gram quantities.

Each of the two human tropoelastin isoforms was confirmed by N-terminal sequencing and mass spectrometry as being the desired protein sequence. Despite numerous mutations, SHEL Δ mod proved to be useful in coacervation studies and provided a large stock for C-terminal domains obtained by proteolytic cleavage. As an added advantage, the N-formyl methionine was removed by *E. coli* resulting in the two tropoelastin isoforms having precisely the same sequence as the naturally-derived isoforms and removing any possible complications arising from the presence of an extraneous amino acid. SHEL was further analysed by CD and, rather than being completely random, the spectrum was found to be consistent with that of all- β proteins within the resolution provided. The spectrum was identical to previously obtained spectra for other elastin-related molecules and the data are therefore consistent with SHEL having the same types of secondary structure as these molecules. This work has led to more detailed structural characterisation of SHEL, SHEL Δ 26A and smaller domains of each currently under way in this laboratory using CD (S. Jensen and A.S. Weiss, unpublished).

8.2 PROTEOLYTIC SUSCEPTIBILITY

SHEL and SHEL Δ 26A each exhibited degradation products when purified as a consequence of endogenous *E. coli* proteases. Thrombin readily degraded

GST-SHEL during purification. Numerous reports of degraded tropoelastin from many different sources are known (Franzblau *et al.*, 1989; Rich and Foster, 1984; Rucker, 1982; Sandberg and Wolt, 1982). Interestingly, the patterns of degradation products are often similar, indicating tropoelastin may have regions of increased proteolytic susceptibility.

This work confirmed previous reports of serine protease tropoelastin-degrading activity in human serum (Romero *et al.*, 1986) and extended these results by precisely mapping the specific sites of cleavage. Significantly, this work showed that all of the larger fragments were from the N-terminus and were missing the highly conserved C-terminal region which is important for interaction with microfibrils. Unprotected tropoelastin exposed to serum can therefore result in degradation of tropoelastin which can remove the C-terminus. If these molecules are cross-linked they may not be properly incorporated into fibres or may result in decreased elastic function. The enzyme responsible for serum degradation was not identified unequivocally but was found to be trypsin-like. Complete mapping of thrombin and plasma kallikrein cleavage sites of SHEL was also achieved which showed that thrombin activity in serum was not primarily responsible for tropoelastin degradation but that kallikrein activity was likely. One highly susceptible cleavage site was identified as common to most of the enzymes studied and serum. This region was supplied exogenously as a peptide to proteolytic digests and was shown to slow degradation of full-length SHEL and SHELΔ26A by serum and, variably, by all the proteases tested. This peptide is therefore a likely inhibitor of serine-protease mediated tropoelastin degradation and can be used as a starting point for developing more efficient, non-cleavable inhibitors. In contrast, it was demonstrated that S-GAL, a peptide representing the elastin binding site of EBP, did not result in widespread inhibition of proteolysis. Only HLE was significantly inhibited and thrombin also showed some inhibition. Serum and the other

serine proteases studied did not show any reproducible inhibition. The process of coacervation, on the other hand, was demonstrated to provide significant protection from proteolysis by serum and all enzymes, except plasmin. The protection was almost total for kallikrein but was reduced for proteases which cleaved SHEL and SHEL Δ 26A in many more places. This work therefore demonstrated that coacervation can provide the additional role of proteolytic protection for tropoelastin from exposure to proteases found in serum and the extracellular matrix.

8.3 COACERVATION

Both human tropoelastin isoforms and the aberrant SHEL Δ mod exhibited coacervation. Coacervation has long been thought to be vital to elastic fibre formation (Urry, 1978). The work described here is consistent with this hypothesis. The temperature of coacervation of both SHEL and SHEL Δ 26A was strongly influenced by protein concentration, NaCl concentration and to a lesser degree pH. It was shown that for both isoforms, optimal temperature, NaCl concentration and pH for complete coacervation at high protein concentrations (>10mg/ml) converge at conditions mimicking those found in the extracellular matrix, indicating that the coacervate is the favoured form of unprotected tropoelastin in the extracellular matrix. This raises many questions on the effect of other matrix molecules, such as MAGP-1, fibrillin and proteoglycans on tropoelastin coacervation. The coacervation assay is a powerful tool to study such interactions and how they influence tropoelastin self-assembly. In addition, the role of extra- and intracellular companion proteins such as EBP, BiP and p74, thought to assist proper folding of tropoelastin and therefore prevent inappropriate coacervation, could be studied using this method.

For the first time, the coacervation characteristics of two distinct isoforms of tropoelastin were studied. The role of 26A in human tropoelastin is unknown. This domain does not exist in any other species studied and one study found that the isoform missing 26A was a poorer substrate for lysyl oxidase (Bedell-Hogan *et al.*, 1993). In this work it was found that there were no differences in the coacervation characteristics of SHEL and SHEL Δ 26A, indicating that the 26A hydrophilic domain does not alter the coacervation temperature of tropoelastin. Any functional differences in the two isoforms are therefore not related to coacervation of the unmodified proteins. However, other as yet unidentified molecules may bind specifically to 26A and may subsequently alter its coacervation characteristics. Candidate molecules thought to bind to 26A could conceivably be studied by coacervation with SHEL Δ 26A acting as a control. The mutant tropoelastin, SHEL Δ mod, exhibited very similar coacervation characteristics to both SHEL and SHEL Δ 26A. This is significant as it indicates that similar mutant tropoelastin molecules may likewise coacervate and may therefore be incorporated into elastic fibres where they have the potential to affect the elastic properties of the fibre.

Lipids and fatty acids are known to interact with cross-linked elastin where they can significantly affect the fibre integrity and are a marker of atherosclerosis (Claire *et al.*, 1976). This study found that tropoelastin could also strongly interact with lipids and fatty acids. This interaction was significant as it dramatically altered the coacervation properties of both tropoelastin isoforms. Lipids and fatty acids were also demonstrated to be difficult to remove from tropoelastin. The lipid contaminants, although of *E. coli* origin, associated with tropoelastin at a temperature lower than that for tropoelastin-tropoelastin coacervation. This work demonstrated that lipids and fatty acids have the potential to disrupt normal coacervation and may result in inappropriate coacervation of tropoelastin *in vivo* if

present during elastogenesis and may result in alteration of the properties of the mature elastic fibre. This work also demonstrated the importance of effective removal of impurities such as lipids from tropoelastin preparations before embarking on studies with tropoelastin. The results here show that coacervation is an easy and effective technique to recognize whether tropoelastin preparations are contaminated with lipids and other hydrophobic molecules and coacervation could therefore be used routinely by researchers to assess tropoelastin purity.

8.4 CONCLUSION

This work has provided a significant advance in the study of human tropoelastin and elastic fibres by the development of a high-level recombinant expression system for two distinct isoforms of human tropoelastin. These tropoelastin isoforms are now readily available in large quantities providing the opportunity for new advances in physical and biological aspects of the elastic fibre. Using these recombinant tropoelastins, some interactions of tropoelastin with proteases, including human serum, were studied resulting in highly susceptible protease recognition sites being mapped potentially allowing new protease inhibitors and protease-resistant tropoelastins to be produced. A significant advance in the understanding of tropoelastin intermolecular interactions was made by a study and comparison of the coacervation characteristics of individual tropoelastin isoforms and the affect of lipids on this interaction. Significantly, coacervation was shown to be tuned to the conditions of the extracellular matrix regardless of the presence of the 26A domain and was also capable of protecting tropoelastin from degradation.



REFERENCES

- Aaron, B.B. and Gosline, J.M. (1980) Optical properties of single elastin fibres indicate random protein conformation *Nature* **287**: 865-867
- Alting-Mees, M.A. and Short, J.M. (1989) pBluescript II: gene mapping vectors *Nuc. Acids Res.* **17**: 9494
- Amman, E., Ochs, B. and Abel, K. (1988) Tightly regulated *tac* promoters useful for the expression of unfused and fused proteins in *Escherichia coli* *Gene* **69**: 301-315
- Ausubel, F.M., Brent, R., Kingston, R.E., Moore, D.D., Seidman, J.G., Smith, J.A. and Struhl, K. (1987) *Current Protocols in Molecular Biology*, Greene Publishing Associates and Wiley Interscience, USA
- Bailey, A.J. and Etherington, D.J. (1980) Metabolism of collagen and elastin. In: *Comprehensive Biochemistry* Vol. 19B Part 1, M. Florkin ed., Elsevier Scientific, Amsterdam, pp 299-459
- Barone, L.M., Faris, B., Chipman, S.D., Toselli, P., Oakes, B.W. and Franzblau, C. (1985) Alteration of the extracellular matrix of the smooth muscle cells by ascorbate treatment *Biochim. Biophys. Acta.* **840**: 245-254
- Barrineau, L.L., Rich, C.B., Przybyla, A. and Foster, J.A. (1981) Differential expression of aortic and lung elastin genes during chick embryogenesis *Dev. Biol.* **87**: 46-51
- Bashir, M.M., Abrams, W.R., Rosenbloom, J., Kucich, U., Bacarra, M., Han, M-D., Brown-Augsberger, P., Mecham, R. and Rosenbloom, J. (1994) Microfibril-associated glycoprotein: characterization of the bovine gene and of the recombinantly expressed protein *Biochem.* **33**: 593-600
- Bashir, M.M., Indik, Z., Yeh, H., Ornstein-Goldstein, N., Rosenbloom, J.C., Abrams, W., Fazio, M., Uitto, J. and Rosenbloom, J. (1989) Characterization of the complete human elastin gene *J. Biol. Chem.* **264**: 8887-8891
- Baule, V.J. and Foster, J.A. (1988) Multiple chick tropoelastin mRNAs *Biochem. Biophys. Res. Comm.* **154**: 1054-1060
- Bedell-Hogan, D., Trackman, P., Abrams, W., Rosenbloom, J. and Kagan, H. (1993) Oxidation, cross-linking, and insolubilization of recombinant tropoelastin by purified lysyl oxidase *J. Biol. Chem.* **268**: 10345-10350

- Belknap, J.K., Grieshaber, N.A., Schwartz, P.E., Orton, E.C., Reidy, M.A. and Majack, R.A. (1996) Tropoelastin gene expression in individual vascular smooth muscle cells. Relationship to DNA synthesis during vascular development and after arterial injury *Circ. Res.* **78**: 388-394
- Bennetzen, J.L. and Hall, B.D. (1982) Codon selection in yeast *J. Biol. Chem.* **257**: 3026-3031
- Bisaccia, F., Castiglione Morelli, M.A., DeBiasi, M., Traniello, S., Spisani, S. and Tamburro, A.M. (1994) Migration of monocytes in the presence of elastolytic fragments of elastin and in synthetic derivatives *Int. J. Peptide Prot. Res.* **44**: 332-341
- Boyd, C.C., Christiano, A.M., Pierce, R.A., Stolle, C.A. and Deak, S.B. (1991) Mammalian tropoelastin: multiple domains of the protein define an evolutionarily divergent amino acid sequence *Matrix* **11**: 235-241
- Braverman, I.M. and Fonferko, E. (1982) Studies in cutaneous aging: I. The elastic fiber network *J. Invest. Dermat.* **78**: 434-443
- Bressan, G.M. and Prockop, D.J. (1977) Synthesis of elastin in aortas from chick embryos. Conversion of newly secreted elastin to cross-linked elastin without apparent proteolysis of the molecule *Biochem.* **16**: 1406-1412
- Bressan, G., Argos, P. and Stanley, K.K. (1987) Repeating structure of chick tropoelastin revealed by complementary DNA cloning *Biochem.* **26**: 1497-1503
- Bressan, G.M., Pasquali-Ronchetti, I., Fornieri, F., Mattioli, F., Castellani, I. and Volpin, D. (1986) Relevance of aggregation properties of tropoelastin to the assembly and structure of elastic fibers *J. Ultrastruct. Mol. Struct. Res.* **94**: 209-216
- Bressan, G. M., Castellani, I., Giro, M.G., Volpin, D., Fornieri, C. and Pasquali-Ronchetti, I. (1983) Banded fibers in tropoelastin coacervates at physiological temperatures *J. Ultrastruct. Res.* **82**: 335-340
- Brown, P., Mecham, L., Tisdale, C. and Mecham, R.P. (1992) The cysteine residues in the carboxy terminal domain of tropoelastin form an intrachain disulfide bond that stabilizes a loop structure and positively charged pocket *Biochem. Biophys. Res. Comm.* **186**: 549-555

- Brown-Augsburger, P., Broekelmann, T., Rosenbloom, J. and Mecham, R.P. (1996) Functional domains on elastin and microfibril-associated glycoprotein involved in elastic fibre assembly *Biochem. J.* **318**: 149-155
- Brown-Augsberger, P., Tisdale, C., Broekelmann, T., Sloan, C. and Mecham, R.P. (1995) Identification of an elastin cross-linking domain that joins three peptide chains *J. Biol. Chem.* **270**: 17778-17783
- Curran, M.E., Atkinson, D.L., Ewart, A.K., Morris, C.A., Leppert, M.F. and Keating, M.T. (1994) Microfibril-associated glycoprotein binds to the carboxy-terminal domain of tropoelastin and is a substrate for transglutaminase *J. Biol. Chem.* **269**: 28443-28449
- and Rosenbloom, J. (1981) Immunoelectron microscope studies on cells synthesizing elastin *Connect. Tissue Res.* **8**: 185-188
- Burnett, W., Yoon, K., Finnigan-Bunick, A. and Rosenbloom, J. (1982) Control of elastin synthesis *J. Invest. Dermat.* **79** (Suppl. 1): 138S-145S
- Castiglione Morelli, M.A., DeBiasi, M., DeStradis, A. and Tamburro, A.M. (1993) An aggregating elastin-like pentapeptide *J. Biomolec. Struct. Dynamics* **11**: 181-190
- Claire, M., Jacotot, B. and Robert, L. (1976) Characterization of lipids associated with macromolecules of the intercellular matrix of human aorta *Connect. Tissue Res.* **4**: 61-71
- Cleary, E.G. (1987) The microfibrillar component of the elastic fibers. In *Connective Tissue Disease. Molecular Pathology of the Extracellular Matrix* J. Uitto and A.J. Perejda eds, Marcel Dekker, New York, USA, pp 55-81
- Chang, J-Y. (1985) Thrombin specificity: requirement for apolar amino acids adjacent to the thrombin cleavage site of polypeptide substrate *Eur. J. Biochem.* **151**: 217-224
- Chipman, S.D., Faris, B., Barone, L.M., Pratt, C.A. and Franzblau, C. (1985) Processing of soluble elastin in cultured neonatal rat smooth muscle cells *J. Biol. Chem.* **260**: 12780-12785
- Christner, P., Weinbaum, G., Sloan, B. and Rosenbloom, J. (1978) Degradation of tropoelastin by proteases *Anal. Biochem.* **88**: 682-688

- Cicilia, G., May, M., Ornstein-Goldstein, N., Indik, Z., Morrow, S., Yeh, H.S., Rosenbloom, J., Boyd, C., Rosenbloom, J. and Yoon, K. (1985) Structure of the 3' portion of the bovine elastin gene *Biochem.* **24**: 3075-3085
- Cox, B.A., Starcher, B.C. and Urry, D.W. (1974) Coacervation of tropoelastin results in fiber formation *J. Biol. Chem.* **249**: 997-998
- Curran, M.E., Atkinson, D.L., Ewart, A.K., Morris, C.A., Leppert, M.F. and Keating, M.T. (1993) The elastin gene is disrupted by a translocation associated with supravalvular aortic stenosis *Cell* **73**: 159-168
- Damiano, V., Tsang, A., Kucich, U., Weinbaum, G. and Rosenbloom, J. (1981) Immuno electron microscope studies on cells synthesizing elastin *Connect. Tissue Res.* **8**: 185-188
- Das, A. (1990) Overproduction of proteins in *Escherichia coli*: vectors, hosts, and strategies *Meth. Enzym.* **182**: 93-112
- Davidson, J.M. and Sphel, G.C. (1987) Regulation of elastin synthesis in organ and cell culture *Meth. Enzym.* **144**: 214-232
- Davidson, J.M., LuValle, P.A., Zoia, O., Quagliano Jr, D. and Giro, M.G. (1997) Ascorbate differentially regulates elastin and collagen biosynthesis in vascular smooth muscle cells and skin fibroblasts by pretranslational mechanisms *J. Biol. Chem.* **272**: 345-352
- Davidson, J.M., Smith, K., Shibahara, S., Tolstoshev, P. and Crystal, R.G. (1982) Regulation of elastin synthesis in developing sheep nuchal ligament by elastin mRNA levels *J. Biol. Chem.* **257**: 747-754
- Davis, E.C. and Mecham, R.P. (1996a) Selective degradation of accumulated secretory proteins in the endoplasmic reticulum. A possible clearance pathway for abnormal tropoelastin *J. Biol. Chem.* **271**: 3787-3794
- Davis, E.C. and Mecham, R.P. (1996b) Chemical cross-linking identifies BiP and a potential molecular chaperone associated with tropoelastin in the ER (abstract) *Mol. Biol. Cell* **7S**: 70a
- DeBelle, L. and Alix, A.J.P. (1995) Optical spectroscopic determination of bovine tropoelastin molecular model *J. Mol. Struct.* **348**: 321-324

- Debelle, L., Alix, A.J.P., Jacob, M., Huvenne, J., Berjot, M., Sombret, B. and Legrand, P. (1995) Bovine elastin and κ -elastin secondary structure determination by optical spectroscopies *J. Biol. Chem.* **270**: 26099-26103
- Debelle, L., Wei, S.M., Jacob, M.P., Hornebeck, W. and Alix, J.P. (1992) Predictions of the secondary structure and antigenicity of human and bovine tropoelastins *Eur. J. Biophys.* **21**: 321-329
- Dietz, H.C. and Pyeritz, R.E. (1995) Mutations in the human gene for fibrillin-1 (FBN1) in the Marfan syndrome and related disorders *Hum. Mol. Gen.* **4**: 1799-1809
- Dorrington, K.L. and McCrum, N.G. (1977) Elastin as a rubber *Biopolymers* **16**: 1201-1222
- Dorrington, K.L., Grut, W. and McCrum, N.G. (1975) Mechanical state of elastin *Nature* **255**: 476-478
- Dubick, M.A., Rucker, R.B., Cross, C.E. and Lost, J.A. (1981) Elastin metabolism in rodent lung *Biochim. Biophys. Acta.* **672**: 303-306
- Elvin, C.M., Thompson, P.R., Argall, M.E., Hendry, P., Stamford, N.P., Lilley, P.E. and Dixon, N.E. (1990) Modified bacteriophage lambda promoter vectors for overproduction of protein in *Escherichia coli* *Gene* **87**: 123-126
- Ewart, A.K., Jin, W., Atkinson, D., Morris, C.A. and Keating, M.T. (1994) Supravalvular aortic stenosis associated with a deletion disrupting the elastin gene *J. Clin. Invest.* **93**: 1071-1077
- Ewart, A.K., Morris, C.A., Atkinson, D., Jin, W., Sternes, K., Spallone, P., Stock, A.D., Leppert, M. and Keating, M.T. (1993) Hemizygoty at the elastin locus in a developmental disorder, Williams syndrome *Nature Gen.* **5**: 11-16
- Faris, B., Ferrera, R., Toselli, P., Nambu, J., Gonnerman, W.A. and Franzblau, C. (1984) Effect of varying amounts of ascorbate on collagen, elastin and lysyl oxidase synthesis in aortic smooth muscle cell cultures *Biochim. Biophys. Acta* **797**: 71-75
- Fazio, M.J., Mattei, M., Passage, E., Chu, M., Black, D., Soloman, E., Davidson, J.M. and Uitto, J. (1991) Human elastin gene: new evidence for localization to the long arm of chromosome 7 *Am. J. Hum. Gen.* **48**: 696-703

- Fazio, M.J., Kahari, V., Bashir, M.M., Saitta, B., Rosenbloom, J. and Uitto, J. (1990) Regulation of elastin gene expression: evidence for functional promoter activity in the 5'-flanking region of the human gene *J. Invest. Dermat.* **94**: 191-196
- Franzblau, C., Pratt, C.A., Parks, B., Calanina, N.M., Offner, G.D., Magyretel, P.J. and Fazio, M.J., Olsen, D.R., Kauh, E.A., Baldwin, C.D., Indik, Z., Ornstein-Goldstein, N., Yeh, H., Rosenbloom, J. and Uitto, J. (1988a) Cloning of full-length elastin cDNAs from a human skin fibroblast recombinant cDNA library: further elucidation of alternative splicing utilizing exon-specific oligonucleotides *J. Invest. Dermat.* **91**: 458-464
- Fazio, M.J., Olsen, D.R., Kuivaniemi, H., Chu, M-L., Davidson, J.M. and Uitto, J. (1988b) Isolation and characterization of human elastin cDNAs, and age-associated variation in elastin gene expression in cultured skin fibroblasts *Lab. Invest.* **58**: 270-277
- Fornieri, C., Quaglino, D., Lungarella, G., Cavarra, E., Tiozzo, R., Giro, M.G., Canciani, M., Davidson, J.M. and Pasquali-Ronchetti, I. (1994) Elastin production and degradation in cutis laxa acquisita *J. Invest. Dermat.* **103**: 583-588
- Foster, J.A. and Curtiss, S.W. (1990) The regulation of lung elastin synthesis *Am. J. Physiol.* **259**: L13-L23
- Foster, J.A., Rich, C.B. and Miller, M.F. (1990) Pulmonary fibroblasts: an *in vitro* model of emphysema. Regulation of elastin gene expression *J. Biol. Chem.* **265**: 15544-15549
- Foster, J.A., Bruenger, E., Rubin, L., Imberman, M., Kagan, H., Mecham, R. and Franzblau, C. (1976) Circular dichroism studies of an elastin cross-linked peptide *Biopolymers* **15**: 833-841
- Foster, J.A., Shapiro, R., Vaynow, P., Crombie, G. and Faris, B. (1975) Isolation of soluble elastin from lathyrctic chicks. Comparison to tropoelastin from copper deficient pigs *Biochem.* **14**: 5343-5347
- Foster, J.A., Rubin, L., Kagan, H. M., Franzblau, C., Bruenger, E. and Sandberg, L.B. (1974) Isolation and characterization of cross-linked peptides from elastin *J. Biol. Chem.* **249**: 6191-6196
- Frangioni, J.V. and Neel, B.J. (1993) Solubilization and purification of enzymatically active glutathione S-transferase (pGEX) fusion proteins *Anal. Biochem.* **210**: 179-187

- Frankel, S., Sohn, R. and Leinwand, L. (1991) The use of sarkosyl in generating soluble protein after bacterial expression *Proc. Natl Acad. Sci. USA* **88**: 1192-1196
- Franzblau, C., Pratt, C.A., Faris, B., Calannino, N.M., Offner, G.D., Mogayzel, P.J. and Troxler, R.F. (1989) Role of tropoelastin fragmentation in elastogenesis in rat smooth muscle cells *J. Biol. Chem.* **264**: 15115-15119
- Gibson, M.A., Hatzinikolas, G., Kumaratilake, J.S., Sandberg, L.B., Nicholl, J.K., Sutherland, G.R. and Cleary, E.G. (1996) Further characterization of proteins associated with elastic fiber microfibrils including the molecular cloning of MAGP-2 (MP25) *J. Biol. Chem.* **271**: 1096-1103
- Gibson, M.A., Sandberg, L.B., Grosso, L.E. and Cleary, E.G. (1991) Complementary DNA cloning establishes microfibril-associated glycoprotein (MAGP) to be a discrete component of the elastin-associated microfibrils *J. Biol. Chem.* **266**: 7596-7601
- Gibson, M.A., Kumaratilake, J.S., and Cleary, E.G. (1989) The protein components of the 12-nanometer microfibrils of elastic and nonelastic tissues *J. Biol. Chem.* **264**: 4590-4598
- Giro, M.G., Duvic, M., Smith, L.T., Kennedy, R., Rapini, R., Arnett, F.C. and Davidson, J.M. (1992) Buschke-Ollendorff syndrome associated with elevated elastin production by affected skin fibroblasts in culture *J. Invest. Dermat.* **99**: 129-137
- Goeddel, D. (1990) Systems for heterologous gene expression *Meth. Enzym.* **185**: 3-7
- Gosline, J.M. (1980) The elastic properties of rubber-like proteins and highly extensible tissues *Symp. Soc. Expt. Biol.* **34**: 331-357
- Gosline, J.M. (1978a) Hydrophobic interaction and a model for the elasticity of elastin *Biopolymers* **17**: 677-695
- Gosline, J.M. (1978b) The temperature-dependent swelling of elastin *Biopolymers* **17**: 697-707
- Gosline, J.M. (1976) The physical properties of elastic tissues *Int. Rev. Connect. Tissue Res.* **7**: 211-249
- Gosline, J.M. and French, C.J. (1979) Dynamic mechanical properties of elastin *Biopolymers* **18**: 2091-2103

- Gotte, L. (1977) Recent observations on the structure and composition of elastin *Adv. Expt. Med. Biol.* **79**: 105-116
- Gray, W.R., Sandberg, L.B. and Foster, J.A. (1973) Molecular model for elastin structure and function *Nature* **246**: 461-466
- Greico, F., Hay, J.M. and Hull, R. (1992) An improved procedure for the purification of protein fused with glutathione S-transferase *Bio/Techniques* **13**: 856-857
- Gröger, G., Ramalho-Ortigao, F., Steil, H. and Seliger, H. (1988) A comprehensive list of chemically synthesized genes *Nuc. Acids Res.* **16**: 7763-7774
- Grosso, L.E. and Mecham, R.P. (1988) In vitro processing of tropoelastin: investigation of a possible transport function associated with the carboxy-terminal domain *Biochem. Biophys. Res. Comm.* **153**: 545-551
- Grosso, L.E. and Scott, M. (1993a) Peptide sequences selected by BA4, a tropoelastin-specific monoclonal antibody, are ligands for the 57-kilodalton bovine elastin receptor *Biochem. J.* **32**: 13369-13374
- Grosso, L.E. and Scott, M. (1993b) PGAIPG, a repeated hexapeptide of bovine and human tropoelastin, is chemotactic for neutrophils and Lewis lung carcinoma cells *Arch. Biochem. Biophys.* **305**: 401-404
- Grosso, L.E., Parks, W.C., Wu, L. and Mecham, R.P. (1991) Fibroblast adhesion to recombinant tropoelastin expressed as a protein-A fusion protein *Biochem. J.* **273**: 517-522
- Gurr, M.I. and Harwood, J.L. (1991) *Lipid Biochemistry- an Introduction* (4th edn), Chapman and Hall, London
- Hall, D. (1976) *The Ageing of Connective Tissue* Academic Press, London
- Hayashi, A., Wachi, H. and Tajima, S. (1995) Presence of elastin-related 45kDa fragment in culture medium: specific cleavage product of tropoelastin in vascular smooth muscle cell culture *Biochim. Biophys. Acta.* **1244**: 325-330
- Heim, R.A., Pierce, R.A., Deak, S.B., Riley, D.J., Boyd, C.D. and Stolle, C.A. (1991) Alternative splicing of rat tropoelastin mRNA is tissue-specific and developmentally regulated *Matrix* **11**: 359-366

- Henderson, M., Polewski, R., Fanning, T.C. and Gibson, M.A. (1996) Microfibril-associated glycoprotein-1 (MAGP-1) is specifically located on the beads of the beaded-filament structure for fibrillin-containing microfibrils as visualised by the rotary shadowing technique *J. Histochem. Cytochem.* **44**: 1389-1397
- Indik, Z., Abrams, W.R., Kucich, U., Gibson, C.W., Mecham, R.P. and Rosenbloom, J. Hinek, A. (1995) The 67 kDa spliced variant of β -galactosidase serves as a reusable protective chaperone for tropoelastin In: *The Molecular Biology and Pathology of Elastic Tissues*. Wiley, Chichester (CIBA Foundation Symposium 192) pp 185-196
- Indik, Z., Yeh, H., Orinstein-Goldstein, N., Kucich, U., Abrams, W., Rosenbloom, J.C. and Hinek, A. and Rabinovitch, M. (1994) 67-kD elastin binding protein is a protective "companion" of extracellular insoluble elastin and intracellular tropoelastin *J. Cell Biol.* **126**: 563-574
- Indik, Z., Yeh, H., Orinstein-Goldstein, N., Sheppard, P., Anderson, N., Rosenbloom, J.C., Hinek, A. and Rabinovitch, M. (1993) The ductus arteriosus migratory smooth muscle cell phenotype processes tropoelastin to a 52 kDa product associated with impaired assembly of elastic laminae *J. Biol. Chem.* **268**: 1405-1413
- Hinek, A., Keeley, F.W. and Callahan, J. (1995) Recycling of the 67-kDa elastin binding protein in arterial monocytes is imperative for secretion of tropoelastin *Expt. Cell Res.* **220**: 312-324
- Hinek, A., Rabinovitch, M., Keeley, F., Okamura-Oho, Y. and Callahan, J. (1993) The 67-kD elastin/laminin-binding protein is related to an enzymatically inactive, alternatively spliced form of β -galactosidase *J. Clin. Invest.* **91**: 1198-1205
- Hinek, A., Callahan, J., Keeley, F. and Rabinovitch, M (1992) The functional significance of the elastin binding sequence in the 67-kD alternatively spliced form of β -Galactosidase (abstract) *Mol. Biol. Cell* **3**: 75a
- Kadler, K.E., Hoytms, Y., and Prockop, D.J. (1987) Assembly of collagen fibrils de novo by Hinek, A., Wrenn, D.S., Mecham, R.P. and Barondes, S.H. (1988) The elastin receptor: a galactoside-binding protein *Science* **239**: 1539-1541
- Hoeve, C.A.J. and Flory, P.J. (1974) The elastic properties of elastin *Biopolymers* **13**: 677-686
- Hsu-Wong, S., Katchman, S.D., Ledo, I., Wu, M., Khillan, J., Bashir, M.M., Rosenbloom, J. and Uitto, J. (1994) Tissue-specific and developmentally regulated expression of human elastin promoter activity in transgenic mice *J. Biol. Chem.* **269**: 18072-18075

- Ikeda, K., Wachi, H., Seyama, Y. and Tajima, S. (1997) Effects of monesin on tropoelastin metabolism in vascular smooth muscle cells: monesin causes intracellular degradation of accumulated tropoelastin *J. Biochem.* **121**: 5-7
- Kagan, H.M., Jordan, P.R., Lerch, R.M., Mukherjee, D.P., Sun, P. and Framblau, C. (1990) Production of recombinant human tropoelastin: characterization and demonstration of immunologic and chemotactic activity *Arch. Biochem. Biophys.* **280**: 80-86
- Kahn, V.M., Owen, D.R., Ruddy, R.W., Carrillo, P., Chen, Y.G. and Utter, J. (1992) Indik, Z., Yeh, H., Ornstein-Goldstein, N., Kucich, U., Abrams, W., Rosenbloom, J.C. and Rosenbloom, J. (1989) Structure of the elastin gene and alternative splicing of elastin mRNA: implications for human disease *Am. J. Med. Gen.* **34**: 81-90
- Kalibera, K., Satal, R., Ohamoto, K., Uemura, Y., Miyakawa, K. and Kondo, M. (1992) Indik, Z., Yeh, H., Ornstein-Goldstein, N., Sheppard, P., Anderson, N., Rosenbloom, J.C., Peltonen, L. and Rosenbloom, J. (1987a) Alternative splicing of human elastin mRNA indicated by sequence analysis of cloned genomic and complementary DNA *Proc. Natl Acad. Sci. USA* **84**: 5680-5684
- Indik, Z., Yoon, K., Morrow, S.D., Cicila, G., Rosenbloom, J., Rosenbloom, J. and Ornstein-Goldstein, N. (1987b) Structure of the 3' region of the human elastin gene: great abundance of Alu repetitive sequences and few coding sequences *Connect. Tiss. Res.* **16**: 197-211
- Johnson Jr, W.C. (1990) Protein secondary structure and circular dichroism: a practical guide *Proteins: Struct. Funct. Gen.* **7**: 205-214
- Johnson, D.J., Robson, P., Hew, Y. and Keeley, F.W. (1995) Decreased elastin synthesis in normal development and in long-term aortic organ and cell cultures is related to rapid and selective destabilization of mRNA for elastin *Circ. Res.* **74**: 1107-1113
- Kadler, K.E., Hojima, Y., and Prockop, D.J. (1987) Assembly of collagen fibrils *de novo* by cleavage of the type I pC-collagen with procollagen C-proteinase *J. Biol. Chem.* **262**: 15696-15701
- Kagan, H.M. and Sullivan, K.A. (1982) Lysyl oxidase: preparation and role in elastin biosynthesis *Meth. Enzym.* **82**: 637-650
- Kagan, H.M., Vaccaro, C.A., Bronson, R.E., Tang, S.S. and Brody, J.S. (1986) Ultrastructural immunolocalization of lysyl oxidase in vascular connective tissue *J. Cell. Biol.* **103**: 1121-1128

- Kagan, H.M., Tseng, L. and Simpson, D.E. (1981) Control of elastin metabolism by elastin ligands. Reciprocal effects on lysyl oxidase activity *J. Biol. Chem.* **256**: 5417-5421
- Kagan, H.M., Jordan, R.E., Lerch, R.M., Mukherjee, D.P., Stone, P. and Franzblau, C. (1977) Factors affecting the proteolytic degradation of elastin *Adv. Expt. Med. Biol.* **79**: 189-205
- Kahn, B., Gauthier, M., Shale, E., Hort, H., Mattel, M.G., Sarfarazi, M., Timpouras, P., Kähäri, V-M., Olsen, D.R., Rhudy, R.W., Carrillo, P., Chen, Y.Q. and Uitto, J. (1992) Transforming growth factor- β up-regulates elastin gene expression in human skin fibroblasts *Lab. Invest.* **66**: 580-588
- Levinson, B., Ottewill, J., Valpey, C., Whitney, S., Yang, S. and Puckman, S. (1993) Are Kaibara, K., Sakai, K., Okamoto, K., Uemura, Y., Miyakawa, K. and Kondo, M. (1992) Elastin coacervate as a protein liquid membrane: effect of pH on transmembrane potential responses *Biopolymers* **32**: 1173-1180
- Levinson, B., Ottewill, J., Valpey, C., Whitney, S., Yang, S. and Puckman, S. (1993) Are Kane, J.F. (1995) Effects of rare codon clusters on high-level expression of heterologous proteins in *Escherichia coli* *Current Opinion Biotech.* **6**: 494-500
- Lillis, M.A. and Cooper, J.M. (1990) The effects of hydration on the dynamic mechanical Kane, J.F., Violand, B.N., Curran, D.F., Staten, N.R., Duffin, K.L. and Bogosian, G. (1992) Novel in-frame two codon translational hop during synthesis of bovine placental lactogen in a recombinant strain of *Escherichia coli* *Nuc. Acids Res.* **20**: 6707-6712
- Carrey, J.C., Keating, M. and Rothman, A.R. (1995) Strong correlation of elastin deletions, Kao, W.W., Bressan, G.M. and Prockop, D.J. (1982) Kinetics of the incorporation of tropoelastin into elastic fibers in embryonic chick aorta *Connect. Tiss. Res.* **10**: 263-274
- Katchman, S.D., Hsu-Wong, S., Ledo, I., Wu, M. and Uitto, J. (1994) Transforming growth factor- β up-regulates human elastin promoter activity in transgenic mice *Biochem. Biophys. Res. Comm.* **203**: 485-490
- Keil, B. (1992) *Specificity of Proteolysis* Springer-Verlag, Berlin and Ballantine, S. (1989) Expression of tetanus toxin fragment C in *E. coli*: high level expression by removing rare Kobayashi, J., Wigle, D., Childs, T., Zhu, L., Keeley, F.W. and Rabinovitch, M. (1994) Serum-induced vascular smooth muscle cell elastolytic activity through tyrosine kinase intracellular signalling *J. Cell. Physiol.* **160**: 121-131
- Keil, B. (1992) *Specificity of Proteolysis* Springer-Verlag, Berlin and Ballantine, S. (1989) Expression of tetanus toxin fragment C in *E. coli*: high level expression by removing rare Kondo, M., Nakashima, Y., Kodama, H. and Okamoto, K. (1987) Study on coacervation of the repeat pentapeptide model of tropoelastin: effect of cations *J. Biochem.* **101**: 89-94
- Manavalan, P., and Johnson Jr, W.C. (1983) Sensitivity of circular dichroism to protein tertiary structure class *Nature* **306**: 831-832

- Laemmli, U.K. (1970) Cleavage of structural proteins during the assembly of the head of bacteriophage T4 *Nature* **227**: 680-685
- Laskin, A.I. and Lechevalier, H.A. (eds) (1973) *CRC Handbook of Microbiology* Vol. II, CRC Press, Cleveland, USA
- Lee, B., Godfrey, M., Vitale, E., Hori, H., Mattei, M.G., Sarfarazi, M., Tspouras, P., Ramirez, F. and Hollister, D.W. (1991) Linkage of Marfan syndrome and a phenotypically related disorder to two different fibrillin genes *Nature* **352**: 330-334
- Levinson, B., Gitschier, J., Vulpe, C., Whitney, S., Yang, S. and Packman, S. (1993) Are X-linked cutis laxa and Menkes disease allelic? *Nature Gen.* **3**: 6
- Li, D., Toland, A.E., Boak, B.B., Atkinson, D.L., Ensing, G.J., Morris, C.A. and Keating, M.T. (1997) Elastin point mutations cause an obstructive vascular disease, supravalvular aortic stenosis *Hum. Mol. Gen.* **6**: 1021-1028
- Lillie, M.A. and Gosline, J.M. (1990) The effects of hydration on the dynamic mechanical properties of elastin *Biopolymers* **29**: 1147-1160
- Lowery, M.C., Morris, C.A., Ewart, A., Brothman, L.J., Zhu, X.L., Leonard, C.O., Carey, J.C., Keating, M. and Brothman, A.R. (1995) Strong correlation of elastin deletions, detected by FISH, with Williams syndrome: evaluation of 235 patients *Am. J. Hum. Gen.* **57**: 49-53
- Luan, C-H., Parker, T.M., Prasad, K.U. and Urry, D.W. (1991) Differential scanning calorimetry studies of NaCl effect on the inverse temperature transition of some elastin-based polytetra-, polypenta-, and polynonapeptides *Biopolymers* **31**: 465-475
- Makoff, M.J., Oxer, M.D., Romanos, M.A., Fairweather, N.F. and Ballantine, S. (1989) Expression of tetanus toxin fragment C in *E. coli*: high level expression by removing rare codons *Nuc. Acids Res.* **17**: 10191-10202
- Manavalan, P., and Johnson Jr, W.C. (1987) Variable selection method improves the prediction of protein secondary structure from circular dichroism spectra *Anal. Biochem.* **167**: 76-85
- Manavalan, P., and Johnson Jr, W.C. (1983) Sensitivity of circular dichroism to protein tertiary structure class *Nature* **305**: 831-832

- Manohar, A. and Anwar, R.A. (1994a) Evidence for a cell-specific negative regulatory element in the first intron of the gene for bovine elastin *Biochem. J.* **300**: 147-152
- Manohar, A. and Anwar, R.A. (1994b) Evidence for the presence of a functional TATA box (ATAAAA) sequence in the gene for bovine elastin *Biochim. Biophys. Acta* **1219**: 233-236
- Marston, A.O. (1986) The purification of eukaryotic polypeptides synthesised in *Escherichia coli* *Biochem. J.* **240**: 1-12
- Martin, S.L., Vrhovski, B. and Weiss, A.S. (1995) Total synthesis and expression in *Escherichia coli* of a gene encoding human tropoelastin *Gene* **154**: 159-166
- Mauviel, A., Chen, Y.Q., Kähäri, V-M., Ledo, I., Wu, M., Rudnicka, L. and Uitto, J. (1993) Human recombinant interleukin-1 β up-regulates elastin gene expression in dermal fibroblasts *J. Biol. Chem.* **268**: 6520-6524
- McGowan, S.E., Lui, R., Harvey, C.S. and Jaekel, E.C. (1996) Serine proteinase inhibitors influence the stability of tropoelastin mRNA in neonatal rat lung fibroblast cultures *Am. J. Physiol.* **270**: L376-L385
- McPherson, D.T., Xu, J. and Urry, D.W. (1996) Product purification by reversible phase transition following *Escherichia coli* expression of genes encoding up to 251 repeats of the elastomeric pentapeptide GVGVP *Prot. Express. Purif.* **7**: 51-57
- Mecham, R.P. (1991) Elastin synthesis and fiber assembly *Annals N.Y. Acad. Sci.* **624**: 137-146
- Mecham, R.P. and Foster, J.A. (1977) Trypsin-like neutral protease associated with soluble elastin *Biochem.* **16**: 3825-3831
- Mecham, R.P. and Heuser, J. (1991) The elastic fiber In: *Cell Biology of the Extracellular Matrix* (2nd edn), E.D. Hay ed., Plenum Press, New York, USA, pp 79-109
- Mecham, R.P. and Heuser, J. (1990) Three-dimensional organization of extracellular matrix in elastic cartilage as viewed by quick freeze, deep etch electron microscopy *Connect. Tissue Res.* **24**: 83-93
- Narayanan, A.S. and Page, R.C. (1974) Molecular weight heterogeneity of tropoelastin resulting from proteolysis during preparation *FEBS Letters* **44**: 59-62

- Mecham, R.P., Broekelmann, T., Davis, E.C., Gibson, M.A. and Brown-Augsberger, P. (1995) Elastic fibre assembly: macromolecular interactions In: *The Molecular Biology and Pathology of Elastic Tissues* Wiley, Chichester (Ciba Foundation Symposium 192) pp 172-184
- Mecham, R.P., Whitehouse, L., Hay, M., Hinek, A. and Sheetz, M.P. (1991) Ligand affinity of the 67 kDa elastin/laminin binding protein is modulated by the protein's lectin domain: visualization of elastin/laminin-receptor complexes with gold-tagged ligands *J. Cell Biol.* **113**: 187-194
- Mecham, R.P., Hinek, A., Entwistle, R., Wrenn, D.S. Griffin, G.L. and Senior, R.M. (1989) Elastin binds to a multifunctional 67-kilodalton peripheral membrane protein *Biochem.* **28**: 3716-3722
- Mecham, R.P., Foster, J.A. and Franzblau, C. (1977) Proteolysis of tropoelastin *Adv. Expt Med. Biol.* **79**: 209-216
- Mecham, R.P., Foster, J.A. and Franzblau, C. (1976) Intrinsic enzyme activity associated with tropoelastin *Biochim. Biophys. Acta* **446**: 245-254
- Megret, C., Lamure, A., Pieraggi, M.T., Lacabanne, C., Guantieri, V. and Tamburro, A.M. (1993) Solid-state studies on synthetic fragments and analogues of elastin *Int. J. Biol. Macromol.* **15**: 305-312
- Meinzel, T., Mechulam, Y. and Blanquet, S. (1993) Methionine as translation start signal: a review of the enzymes of the pathway in *Escherichia coli* *Biochimie* **75**: 1061-1075
- Miyakawa, K., Totoki, M. and Kaibara, K. (1995) Effects of metal cations on coacervation of α -elastin *Biopolymers* **35**: 85-92
- Myers, B., Dubick, M., Last, J.A. and Rucker, R.B. (1983) Elastin synthesis during perinatal lung development in the rat *Biochim. Biophys. Acta* **761**: 17-22
- Nakano, H., Yamazaki, T., Ikeda, M., Masai, H., Miyatake, S. and Saito, T. (1994) Purification of glutathione S-transferase fusion proteins as a non-degraded form by using a protease-negative *E. coli* strain, AD202 *Nuc. Acids Res.* **22**: 543-544
- Narayanan, A.S. and Page, R.C. (1974) Molecular weight heterogeneity of tropoelastin resulting from proteolysis during preparation *FEBS Letters* **44**: 59-62

- Narayanan, A.S., Page, R.C., Kuzan, F. and Cooper, C.G. (1978) Elastin cross-linking in vitro *Biochem. J.* **173**: 857-862
- Narayanan, A.S., Page, R.C. and Kuzan, F. (1977) Studies on the action of lysyl oxidase on soluble elastin *Adv. Expt. Med. Biol.* **79**: 491-508
- Norde, W., Bosgoed, H.M.M. and de Vries, P. (1985) The interaction between alkyl derivatives and elastin *Biophys. Chem.* **21**: 115-126
- Olliver, L., Luvalle, P.A., Davidson, J.M., Rosenbloom, J., Mathew, C.G., Bester, A.J. and Boyd, C.D. (1987) The gene coding for tropoelastin is represented as a single copy sequence in the haploid sheep genome *Collagen Rel. Res.* **7**: 77-89
- Olson, T.M., Michels, V.V., Urban, Z., Csiszar, K., Christiano, A., Driscoll, D.J., Feldt, R.H., Boyd, C.D. and Thibodeau, S.N. (1995) A 30kb deletion within the elastin gene results in familial supravalvular aortic stenosis *Hum. Mol. Gen.* **4**: 1677-1679
- Parks, W.C. and Deak, S.B. (1990) Tropoelastin heterogeneity: implications for protein function and disease *Am. J. Resp. Cell Mol. Biol.* **2**: 399-406
- Parks, W.C., Roby, J.D., Wu, L.C. and Grosso, L.E. (1992) Cellular expression of tropoelastin mRNA splice variants *Matrix* **12**: 156-162
- Parks, S.B., Secrist, H., Wu, L.C. and Mecham, R.P. (1988) Developmental regulation of tropoelastin isoforms *J. Biol. Chem.* **263**: 4416-4423
- Partridge, S.M. (1967) Gel filtration using a column packed with elastin fibres *Nature* **213**: 1123-1125
- Partridge, S.M. and Whiting, A.H. (1977) The coacervate-sol transition observed with α -elastin and its N-formyl o-methyl derivative *Adv. Expt. Med. Biol.* **79**: 715-721
- Partridge, S.M., Elsdon, D.F., Thomas, J., Dorfman, A., Telser, A. and Ho, P. (1964) Biosynthesis of the desmosine and isodesmosine cross-bridges in elastin *Biochem. J.* **93**: 30-33
- Pierce, R.A., Mariani, T.J. and Senior, R.M. (1995) Elastin in lung development and disease In: *The Molecular Biology and Pathology of Elastic Tissues* Wiley, Chichester (Ciba Foundation Symposium 192) pp 199-214

- Pierce, R.A., Kolodziej, M.E. and Parks, W.C. (1992a) 1, 25-dihydroxyvitamin D₃ represses tropoelastin expression by a posttranslational mechanism *J. Biol. Chem.* **267**: 11593-11599
- Pierce, R.A., Alatawi, A., Deak, S.B. and Boyd, C.D. (1992b) Elements of the rat tropoelastin gene associated with alternative splicing *Genomics* **12**: 651-658
- Pierce, R.A., Deak, S.B., Stolle, C.A. and Boyd, C.D. (1990) Heterogeneity of rat tropoelastin mRNA revealed by cDNA cloning *Biochem.* **29**: 9677-9683
- Pollock, J., Baule, V.J., Rich, C.B., Ginsburg, C.D., Curtiss, S.W. and Foster, J.A. (1990) Chick tropoelastin isoforms. From the gene to the extracellular matrix *J. Biol. Chem.* **265**: 3697-3702
- Prescott, B., Renugopalakrishnan, V. and Thomas, G.J. (1987) Raman spectrum and structure of elastin in relation to Type-II β -turns *Biopolymers* **26**: 934-936
- Prosser, I.W. and Mecham, R.P. (1988) Regulation of extracellular matrix accumulation: a short review of elastin biosynthesis In: *Self-assembling Architecture* J.E. Varner ed., Alan. R. Liss Inc., New York, USA, pp 1-23
- Raju, K. and Anwar, R.A. (1987) Primary structures of bovine elastin a, b, and c deduced from the sequences of cDNA clones *J. Biol. Chem.* **262**: 5755-5762
- Rapaka, R.S. and Urry, D.W. (1978) Coacervation of sequential polypeptide models of tropoelastin *Int. J. Peptide Prot. Res.* **11**: 97-108
- Raybould, M.C., Birley, A.J., Moss, C., Hultén, M. and McKeown, C.M.E. (1994) Exclusion of an elastin gene (ELN) mutation as the cause of pseudoxanthoma elasticum (PXE) in one family *Clin. Gen.* **45**: 48-51
- Reiser, K., McCormick, R.J. and Rucker, R.B. (1992) Enzymatic and nonenzymatic cross-linking of collagen and elastin *FASEB J.* **6**: 2439-2449
- Rich, C.B. and Foster, J.A. (1989) Characterization of rat heart tropoelastin *Arch. Biochem. Biophys.* **268**: 551-558
- Rich, C.B. and Foster, J.A. (1984) Isolation of tropoelastin a from lathyrtic chick aortae *Biochem. J.* **217**: 581-584

- Rich, C.B. and Foster, J.A. (1982) Isolation of soluble elastin- lathyrisism *Meth. Enzym.* **82**: 665-673
- Riley, L.G., Junius, F.K., Swanton, M.K., Vesper, N.A., Williams, N.K., King, G.F. and Weiss, A.S. (1994) Cloning, expression and spectroscopic studies of the Jun leucine zipper domain *Eur. J. Biochem.* **219**: 877-886
- Ritter, M., Woll, E., Haussinger, D. and Lang, F. (1992) Effects of bradykinin on cell volume and intracellular pH in NIH 3T3 fibroblasts expressing the ras oncogene *FEBS Letters* **307**: 367-370
- Romero, N., Tinker, D., Hyde, D. and Rucker, R.B. (1986) Role of plasma and serum proteases in the degradation of elastin *Arch. Biochem. Biophys.* **244**: 161-168
- Rosenberg, A.H., Goldman, E., Dunn, J.J., Studier, F.W. and Zubay, G. (1993) Effects of consecutive AGG codons on translation in *Escherichia coli*, demonstrated with a versatile codon test system *J. Bacter.* **175**: 716-722
- Rosenbloom, J. (1984) Biology of disease. Elastin: relation of protein and gene structure to disease *Lab. Invest.* **51**: 605-623
- Rosenbloom, J. and Cywinski, A. (1976a) Biosynthesis and secretion of tropoelastin by chick aorta cells *Biochem. Biophys. Res. Comm.* **69**: 613-620
- Rosenbloom, J. and Cywinski, A. (1976b) Inhibition of proline hydroxylation does not inhibit secretion of tropoelastin by chick aorta cells *FEBS Letters* **65**: 246-250
- Rosenbloom, J., Abrams, W.R. and Mecham, R. (1993) Extracellular matrix 4: the elastic fiber *FASEB J.* **7**: 1208-1218
- Rosenbloom, J., Bashir, M., Yeh, H., Rosenbloom, J., Ornstein-Goldstein, N., Fazio, M., Kahari, V. and Uitto, J. (1991) Regulation of elastin gene expression *Annals N.Y. Acad. Sci.* **624**: 116-136
- Ross, R. and Bornstein, P. (1969) The elastic fiber: I. The separation and partial characterization of its macromolecular components *J. Cell Biol.* **40**: 366-381
- Rucker, R.B. (1982) Isolation of soluble elastin from copper-deficient chick aorta *Meth. Enzym.* **82**: 650-657

- Rucker, R.B. and Dubick, M.A. (1984) Elastin metabolism and chemistry: potential roles in lung development and structure *Environ. Health Perspect.* **55**: 179-191
- Rucker, R.B., Goettlich-Riemann, W., and Tom, K. (1973) Properties of chick tropoelastin *Biochem. Biophys. Acta* **317**: 193-211
- Sage, H. (1982) Structure-function relationships in the evolution of elastin *J. Invest. Dermat.* **79**(Supp 1): 146S-153S
- Sage, H. and Gray, W.R. (1980) Studies on the evolution of elastin-II. Histology *Comp. Biochem. Physiol.* **66B**: 13-22
- Sage, H. and Gray, W.R. (1979) Studies on the evolution of elastin-I. Phylogenetic distribution *Comp. Biochem. Physiol.* **64B**: 313-327
- Sage, H. and Gray, W.R. (1977) Evolution of elastin structure *Adv. Expt. Med. Biol.* **79**: 291-309
- Sakai, L.Y., Keene, D.R. and Engvall, E. (1986) Fibrillin, a new 350-kD glycoprotein, is a component of extracellular microfibrils *J. Cell Biol.* **103**: 2499-2509
- Sambrook, J., Fritsch, E.F. and Maniatis, T. (1989) *Molecular cloning: a laboratory manual* (2nd edn), Cold Spring Harbor Laboratory Press, Cold Spring Harbor, USA
- Sandberg, L.B. and Davidson, J.M. (1984) Elastin and its gene *Peptide Prot. Rev.* **3**: 169-226
- Sandberg, L.B. and Wolt, T.B. (1982) Production and isolation of soluble elastin from copper-deficient swine *Meth. Enzym.* **82**: 657-665
- Sandberg, L.B., Soskel, N.T. and Leslie, J.C. (1981) Elastin structure, biosynthesis, and relation to disease states *N. Engl. J. Med.* **304**: 566-579
- Sandberg, L.B., Bruenger, E. and Cleary, E.G. (1974) Tropoelastin purification: improvements using enzyme inhibitors *Anal. Biochem.* **64**: 249-254
- Sandberg, L.B., Zeikus, R.D. and Coltrain, I.M. (1971) Tropoelastin purification from copper-deficient swine: a simplified method *Biochim. Biophys. Acta* **236**: 542-545

- Saunders, N.A. and Grant, M.E. (1985) The secretion of tropoelastin by chick-embryo artery cells *Biochem. J.* **230**: 217-225
- Saunders, N.A. and Grant, M.E. (1984) Elastin biosynthesis in chick-embryo arteries. Studies on the intracellular site of synthesis of tropoelastin *Biochem. J.* **221**: 393-400
- Schein, C.H. (1989) Production of soluble recombinant proteins in bacteria *Bio/Tech.* **7**: 1141-1149
- Schein, C.H. and Noteborn, M.H.M. (1988) Formation of soluble recombinant proteins in *Escherichia coli* is favored by lower growth temperature *Bio/Tech.* **6**: 291-294
- Schein, J., Carpousis, A. and Rosenbloom, J. (1977) Evidence that tropoelastin exists as a random coil *Adv. Expt. Med. Biol.* **79**: 727-739
- Sephel, G.C., Buckley, A. and Davidson, J.M. (1987) Developmental initiation of elastin gene expression by human fetal skin fibroblasts *J. Invest. Dermat.* **88**: 732-735
- Serafini-Fracassini, A., Field, J.M., Spina, M., Stephens, W.G.S. and Delf, B. (1976) The macromolecular organization of the elastin fibril *J. Mol. Biol.* **100**: 73-84
- Shapiro, S.D. (1994) Elastinolytic metalloproteinases produced by human mononuclear phagocytes. Potential roles in destructive lung disease *Am. J. Resp. Critical Care Med.* **150**: S160-S164
- Sharp, P.M. and Li, W. (1987) The codon adaptation index- a measure of directional synonymous codon usage bias, and its potential applications *Nuc. Acids Res.* **15**: 1281-1295
- Sharp, P.M., Tuohy, T.M. and Mosurski, K.R. (1986) Codon usage in yeast: cluster analysis clearly differentiates highly and lowly expressed genes *Nuc. Acids Res.* **14**: 5125-5143
- Smith, D.B. and Johnson, K.S. (1988) Single-step purification of polypeptides expressed in *Escherichia coli* as fusions with glutathione S-transferase *Gene* **67**: 31-40
- Smith, D.W., Brown, D.M. and Carnes, W.H. (1972) Preparation and properties of salt-soluble elastin *J. Biol. Chem.* **247**: 2427-2432

- Soskel, N.T. and Sandberg, L.B. (1987) Pulmonary emphysema. From animal models to human diseases In: *Connective Tissue Disease. Molecular Pathology of the Extracellular Matrix* J.Uitto and A.J. Perejda eds, Marcel Dekker, New York, USA, pp 423-453
- Tinker, D., Romero-Chapman, N., Reiser, K., Hyde, D. and Rucker, R. (1990) Elastin
- Soskel, N.T., Wolt, T.B. and Sandberg, L.B. (1987) Isolation and characterization of insoluble and soluble elastins *Meth. Enzym.* **144**: 196-214
- Starcher, B.C., Saccoman, G. and Urry, D.W. (1973) Coacervation and ion-binding studies on aortic elastin *Biochim. Biophys. Acta* **310**: 481-486
- Stone, P.J., Morris, S.M., Martin, B.M., McMahon, M.P., Faris, B. and Franzblau, C. (1988) Repair of protease-damaged elastin in neonatal rat aortic smooth muscle cell cultures *J. Clin. Invest.* **82**: 1644-1654
- Torres, A.R., Alvarez, V., Sandberg, L.B. and Gray, W.R. (1977) The isolation and amino
- Stone, P.J., Franzblau, C. and Kagan, H.M. (1982) Proteolysis of insoluble elastin *Meth. Enzym.* **82**: 588-637
- Studier, F.W., Rosenberg, A.H., Dunn, J.J. and Dubendorff, J.W. (1990) Use of T7 RNA polymerase to direct expression of cloned genes *Meth. Enzym.* **185**: 60-89
- Sykes, B. and Partridge, S.M. (1974) Salt-soluble elastin from lathyrctic chicks *Biochem. J.* **141**: 567-572
- Tamburro, A.M., DeStradis, A. and D'Alessio, L. (1995) Fractal aspects of elastin supramolecular structure *J. Biomolec. Struct. Dynamics* **12**: 1161-1172 A.J. Perejda eds, Marcel Dekker, New York, USA, pp 393-422
- Tamburro, A.M., Guantieri, V., Pandolfo, L. and Scopa, A. (1990) Synthetic fragments and analogues of elastin II. Conformational studies *Biopolymers* **29**: 855-870
- Tamburro, A.M., Guantieri, V., Daga-Gordini, D. and Abatangelo, G. (1977) Conformational transitions of α -elastin *Biochim. Biophys. Acta* **492**: 370-376
- Uitto, J., Hoffmann, H. and Prockop, D.J. (1976) Synthesis of elastin and procollagen by
- Tassabehji, M., Metcalfe, K., Fergusson, W.D., Carette, M.J.A., Dore, J.K., Donnai, D., Read, A.P., Pröschel, C., Gutowski, N.J., Mao, X. and Sheer, D. (1996) LIM-kinase deleted in Williams syndrome *Nature Gen.* **13**: 272-273
- Tietz, N.W. (1982) (ed.) *Fundamentals of Clinical Chemistry* (2nd edn.), W.B. Saunders Company, Philadelphia, USA
- Uitto, J., Prockop, D.J. and Ramakrishna, S. (1996) Elastin synthesis and elasticity due to internal chain dynamics *J. Polym. Sci. Part A: Polym. Chem.* **34**: 1-10

- Tinker, D. and Rucker, R.B. (1985) Role of selected nutrients in synthesis, accumulation, and chemical modification of connective tissue proteins *Physiol. Rev.* **65**: 607-657
- Tinker, D., Romero-Chapman, N., Reiser, K., Hyde, D. and Rucker, R. (1990) Elastin metabolism during recovery from impaired crosslink formation *Arch. Biochem. Biophys.* **278**: 326-332
- Tokita, K., Kanno, K. and Ikeda, K. (1977) Elastin sub-fraction as binding site for lipids *Atherosclerosis* **28**: 111-119
- Torchia, D.A. and Peiz, K.A. (1973) Mobility of elastin chains as determined by ¹³C nuclear magnetic resonance *J. Mol. Biol.* **76**: 419-424
- Torres, A.R., Alvarez, V.L., Sandberg, L.B. and Gray, W.R. (1977) The isolation and amino acid sequence of some thrombin produced porcine tropoelastin peptides *Adv. Expt. Med. Biol.* **79**: 267-276
- Uhlén, M. and Moks, T. (1990) Gene fusions for purpose of expression: an introduction *Meth. Enzym.* **185**: 129-143
- Uitto, J. (1979) Biochemistry of the elastic fibers in normal connective tissues and its alterations in diseases *J. Invest. Dermat.* **72**: 1-10
- Uitto, J. and Ryhänen, L.J. (1987) Pathology of the elastic fibers In: *Connective Tissue Disease: Molecular Pathology of the Extracellular Matrix* J. Uitto and A.J. Perejda eds, Marcel Dekker, New York, USA, pp 399-422
- Uitto, J., Fazio, M., Bashir, M. and Rosenbloom, J. (1991) Elastic fibers of the connective tissue In: *Biochemistry, Physiology and Molecular Biology of the Skin* Vol. 1 L.A. Goldsmith ed., Oxford University Press, New York, USA, pp 530-557
- Uitto, J., Hoffmann, H. and Prockop, D.J. (1976) Synthesis of elastin and procollagen by cells from embryonic aorta *Arch. Biochem. Biophys.* **173**: 187-200
- Urry, D.W. (1995) Elastic biomolecular machines *Sci. Am.* **Jan.**: 44-49
- Urry, D.W. (1988) Entropic elastic processes in protein mechanisms I. Elastic structure due to an inverse temperature transition and elasticity due to internal chain dynamics *J. Prot. Chem.* **7**: 1-34

- Urry, D.W. (1984) Protein elasticity based on conformations of sequential polypeptides: the biological elastic fiber *J. Prot. Chem.* **3**: 403-436
- Urry, D.W. (1982) Characterization of soluble peptides of elastin by physical techniques *Meth. Enzym.* **82**: 673-716
- Urry, D.W. (1978) Molecular perspectives of vascular wall structure and disease: the elastic component *Perspectives Biol. Med.* **21**: 265-295
- Urry, D.W. (1974) Arterial mesenchyme and arteriosclerosis. Studies on the conformation and interactions of elastin *Adv. Expt. Med. Biol.* **43**: 211- 243
- Urry, D.W. and Long, M.M. (1977) On the conformation, coacervation and function of polymeric models of elastin *Adv. Expt. Med. Biol.* **79**: 685-714
- Urry, D.W. and Long, M.M. (1976) Conformations of the repeat peptides of elastin in solution: an application of proton and carbon-13 magnetic resonance to the determination of polypeptide secondary structure *CRC Crit. Rev. Biochem.* **4**: 1-45
- Urry, D.W., Show, R.G. and Prasad, K.U. (1985) Polypentapeptide of elastin: temperature dependence and correlation with elastomeric force *Biochem. Biophys. Res. Comm.* **130**: 50-57
- Urry, D.W., Sugano, H., Prasad, K.U., Long, M.M. and Bhatnagar, R.S. (1979) Prolyl hydroxylation of the polypentapeptide model of elastin impairs fiber formation *Biochem. Biophys. Res. Comm.* **90**: 194-198
- Urry, D.W., Long, M.M., Cox, B.A., Ohnishi, T., Mitchell, L.W. and Jacobs, M. (1974a) The synthetic polypentapeptide of elastin coacervates and forms filamentous aggregates *Biochim. Biophys. Acta* **371**: 597-602
- Urry, D.W., Long, M.M., Ohnishi, T. and Jacobs, M. (1974b) Circular dichroism and absorption of the polytetrapeptide of elastin: a polymer model for the β -turn *Biochem. Biophys. Res. Comm.* **61**: 1427-1483
- Urry, D.W., Starcher, B. and Partridge, S.M. (1969) Coacervation of solubilized elastin effects a notable conformational change *Nature* **222**: 795-796
- Volpin, D. and Ciferri, A. (1970) Thermoelasticity of elastin *Nature* **225**: 382

- Volpin, D., Urry, D.W., Cox, B.A. and Gotte, L. (1976) Optical diffraction of tropoelastin and α -elastin coacervates *Biochim. Biophys. Acta* **439**: 253-258
- Vrhovski, B., Jensen, S. and Weiss, A.S. (1997) Coacervation characteristics of recombinant human tropoelastin *Eur. J. Biochem.*(in press)
- Vulpe, C., Levinson, B., Whitney, S., Packman, S. and Gitschier, J. (1993) Isolation of a candidate gene for Menkes disease and evidence that it encodes a copper-transporting ATPase *Nature Gen.* **3**: 7-13
- Wachi, H., Seyama, Y., Yamashita, S., Suganami, H., Uemura, Y., Okamoto, K., Yamada, H. and Tajima, S. (1995) Stimulation of cell proliferation and autoregulation of elastin expression by elastin peptide VPGVG in cultured chick vascular smooth muscle cells *FEBS Letters* **368**: 215-219
- Weis-Fogh, T. and Andersen, S.O. (1970) New molecular model for the long-range elasticity of elastin *Nature* **227**: 718-721
- Werb, Z., Banda, M.J., McKerrow, J.H. and Sandhaus, R.A. (1982) Elastases and elastin degradation *J. Invest. Dermat.* **79**(Supp. 1): 154s-159s
- Whiting, A., Sykes, B.C. and Partidge, S.M. (1974) Isolation of salt-soluble elastin from ligamentum nuchae of copper-deficient calf *Biochem. J.* **141**: 573-575
- Wolfe, B.L., Rich, C.B., Goud, H.D., Terpestra, A.J., Bashir, M., Rosenbloom, J., Sonenshein, G.E. and Foster, J.A. (1993) Insulin-like growth factor-I regulates transcription of the elastin gene *J. Biol. Chem.* **268**: 12418-12426
- Wrenn, D.S., Parks, W.C., Whitehouse, L.A., Crouch, E.C., Kucich, U., Rosenbloom, J. and Mecham, R.P. (1987) Identification of multiple tropoelastins secreted by bovine cells *J. Biol. Chem.* **262**: 2244-2249
- Wu., J., Yang, J.T. and Wu, C-S. C. (1992) β -II conformation of all- β proteins can be distinguished from unordered form by circular dichroism *Anal. Biochem.* **200**: 359-364
- Yeh, H., Anderson, N., Ornstein-Goldstein, N., Bashir, M.M., Rosenbloom, J.C., Abrams, W., Indik, Z., Yoon, K., Parks, W., Mecham, R. and Rosenbloom, J. (1989) Structure of the bovine elastin gene and S1 nuclease analysis of alternative splicing of elastin mRNA in the bovine nuchal ligament *Biochem.* **28**: 2365-2370

- Yeh, H., Ornstein-Goldstein, N., Indik, Z., Sheppard, P., Anderson, N., Rosenbloom, J.C., Cicila, G., Yoon, K. and Rosenbloom, J. (1987) Sequence variation of bovine elastin mRNA due to alternative splicing *Collagen Rel. Res.* **7**: 235-247
- Zhang, M-C., Giro, M.G., Quaglino Jnr, D. and Davidson, J.M. (1995) Transforming growth factor- β reverses a posttranscriptional defect in elastin synthesis in a cutis laxa skin fibroblast strain *J. Clin. Invest.* **95**: 986-994
- Zhang, H., Apfelroth, S.D., Hu, W., Davis, E.C., Sanguinieti, C., Bonadio, J., Mecham, R.P. and Ramirez, F. (1994) Structure and expression of fibrillin-2, a novel microfibrillar component preferentially located in elastic matrices *J. Cell Biol.* **124**: 855-863

APPENDICES



APPENDICES

Appendix 1. Sequencing Primers

APPENDIX 2

1R 5' TGC CTT TGC CGG TTT GTA CG 3'

3F 5' TCC AGG TGG CTA CGG TCT GC 3'

3R 5' GAG TAC CTA CGC CTG CGA TAC 3'

5R 5' GGA GTA CCA ACG CCG TAC TT 3'

6F 5' GGG TGT TGG CGT TGC ACC AG 3'

7R 5' TGC ACC TAC AAC ACC GCC CG 3'

8F 5' CAG CTC AGT TCG GTC TGG TT 3'

T7 forward 5' TAA TAC GAC TCA CTA TAG GG 3'

pET forward 5' GCA CTC ACT ATA GGG AGA CC 3'

pET reverse 5' GCC AAC TCA GCT TCC TTT CG 3'

APPENDIX 2

DNA Sequence and Protein Translation of SHELΔmod

1/1 31/11
 ATG GGT GGC GTT CCG GGT GCT GTT CCG GGT GGC GTT CCG GGT GGT GTA TTC TAC CCA GGC
 M G G V P G A V P G G V P G G V F Y P G
 61/21 91/31
 GCG GGT TTC GGT GCT GTT CCG GGT GGC GTT GCA GAC GCA GCT GCT GCG TAC AAA GCG GCA
 A G F G A V P G G V A D A A A A Y K A A
 121/41 151/51
 AAG GCA GGT GCG GGT CTG GGC GGG GTA CCA GGT GTT GGC GGT CTG GGT GTA TCT GCT GGC
 K A G A G L G G V P G V G G L G V S A G
 181/61 211/71
 GCA GTT GTT CCG CAG CCG GGT GCA GGT GTA AAA CCG GGC AAA GTT CCA GGT GTT GGT CTG
 A V V P Q P G A G V K P G K V P G V G L
 241/81 271/91
 CCG GGC GTA TAC CCG GGT TTC GGT GCT GTT CCG GGC GCG CGT TTC CCA GGT GTT GGT GTA
 P G V Y P G F G A V P G A R F P G V G V
 301/101 331/111
 CTG CCG GGC GTT CCG ACC GGT GCA GGT GTT AAA CCG AAG GCA CCA GGT GTA GGC GGC GCG
 L P G V P T G A G V K P K A P G V G G A
 361/121 391/131
 TTC GCG GGT ATC CCG GGT GTT GGC CCG TTC GGT GGT CCG CAG CCA GGC GTT CCG CTG GGT
 F A G I P G V G P F G G P Q P G V P L G
 421/141 451/151
 TAC CCG ATC AAA GCG CCG AAG CTT CCA GGT GGC TAC GGT CTG CCG TAC ACC ACC GGT AAA
 Y P I K A P K L P G G Y G L P Y T T G K
 481/161 511/171
 CTG CCG TAC GGC TAC GGT CCG GGT GGC GTA GCA GGT GCT GCG GGT AAA GCA GGC TAC CCA
 L P Y G Y G P G G V A G A A G K A G Y P
 541/181 571/191
 ACC GGT ACT GGT GTT GGT CCG CAG GCT GCT GCG GCA GCT GCG GCG AAG GCA GCA GCA AAA
 T G T G V G P Q A A A A A A A K A A A K
 601/201 631/211
 TTC GGC GCG GGT GCA GCG GGT TTC GGT GCT GTT CCG GGC GTA GGT GGT GCT GGC GTT CCG
 F G A G A A G F G A V P G V G G A G V P
 661/221 691/231
 GGT GTT CCA GGT GCG ATC CCG GGC ATC GGT GGT ATC GCA GGC GTA GGT ACT CCG GCG GCC
 G V P G A I P G I G G I A G V G T P A A
 721/241 751/251
 GCT GCG GCT GCG GCA GCT GCG GCG AAA GCA GCT AAA TAC GGT GCG GCA GCA GGC CTG GTT
 A A A A A A A K A A K Y G A A A G L V
 781/261 811/271
 CCG GGT GGT CCA GGC TTC GGT CCG GGT GTT GTA GGC GTT CCG GGT TTC GGT GCT GTT CCG
 P G G P G F G P G V V G V P G F G A V P
 841/281 871/291
 GGC GTA GGT GTT CCA GGT GCG GGC ATC CCG GTT GTA CCG GGT GCA GGT ATC CCG GGC GCT
 G V G V P G A G I P V V P G A G I P G A
 901/301 931/311
 GCG GGT TTC GGT GCT GTA TCC CCG GAA GCG GCA GCT AAG GCT GCT GCG AAA GCT GCG AAA
 A G F G A V S P E A A A K A A A K A A K
 961/321 991/331
 TAC GGA GCT CGT CCG GGC GTT GGT GTT GGT GGC ATC CCG ACC TAC GGT GTA GGT GCA GGC
 Y G A R P G V G V G G I P T Y G V G A G

APPENDIX 3

DNA Sequence and Protein Translation of SHELΔ26A

4089/1
 ATG GGT GGC GTT CCG GGT GCT ATC CCG GGT GGC GTT CCG GGT GGT GTA TTC TAC CCA GGC
 M G G V P G A I P G G V P G G V F Y P G
 4149/21
 GCG GGT CTG GGT GCA CTG GGC GGT GGT GCG CTG GGC CCG GGT GGT AAA CCG CTG AAA CCG
 A G L G A L G G G A L G P G G K P L K P
 4209/41
 GTT CCA GGC GGT CTG GCA GGT GCT GGT CTG GGT GCA GGT CTG GGC GCG TTC CCG GCG GTT
 V P G G L A G A G L G A G L G A F P A V
 4269/61
 ACC TTC CCG GGT GCT CTG GTT CCG GGT GGC GTT GCA GAC GCA GCT GCT GCG TAC AAA GCG
 T F P G A L V P G G V A D A A A A Y K A
 4329/81
 GCA AAG GCA GGT GCG GGT CTG GGC GGG GTA CCA GGT GTT GGC GGT CTG GGT GTA TCT GCT
 A K A G A G L G G V P G V G G L G V S A
 4389/101
 GGC GCA GTT GTT CCG CAG CCG GGT GCA GGT GTA AAA CCG GGC AAA GTT CCA GGT GTT GGT
 G A V V P Q P G A G V K P G K V P G V G
 4449/121
 CTG CCG GGC GTA TAC CCG GGT GGT GTT CTG CCG GGC GCG CGT TTC CCA GGT GTT GGT GTA
 L P G V Y P G G V L P G A R F P G V G V
 4509/141
 CTG CCG GGC GTT CCG ACC GGT GCA GGT GTT AAA CCG AAG GCA CCA GGT GTA GGC GGC GCG
 L P G V P T G A G V K P K A P G V G G A
 4569/161
 TTC GCG GGT ATC CCG GGT GTT GGC CCG TTC GGT GGT CCG CAG CCA GGC GTT CCG CTG GGT
 F A G I P G V G P F G G P Q P G V P L G
 4629/181
 TAC CCG ATC AAA GCG CCG AAG CTT CCA GGT GGC TAC GGT CTG CCG TAC ACC ACC GGT AAA
 Y P I K A P K L P G G Y G L P Y T T G K
 4689/201
 CTG CCG TAC GGC TAC GGT CCG GGT GGC GTA GCA GGT GCT GCG GGT AAA GCA GGC TAC CCA
 L P Y G Y G P G G V A G A A G K A G Y P
 4749/221
 ACC GGT ACT GGT GTT GGT CCG CAG GCT GCT GCG GCA GCT GCG GCG AAG GCA GCA GCA AAA
 T G T G V G P Q A A A A A A A K A A A K
 4809/241
 TTC GGC GCG GGT GCA GCG GGT GTT CTG CCG GGC GTA GGT GGT GCT GGC GTT CCG GGT GTT
 F G A G A A G V L P G V G G A G V P G V
 4869/261
 CCA GGT GCG ATC CCG GGC ATC GGT GGT ATC GCA GGC GTA GGT ACT CCG GCG GCC GCT GCG
 P G A I P G I G G I A G V G T P A A A A
 4929/281
 GCT GCG GCA GCT GCG GCG AAA GCA GCT AAA TAC GGT GCG GCA GCA GGC CTG GTT CCG GGT
 A A A A A A K A A K Y G A A A G L V P G
 4989/301
 GGT CCA GGC TTC GGT CCG GGT GTT GTA GGC GTT CCG GGT GCT GGT GTT CCG GGC GTA GGT
 G P G F G P G V V G V P G A G V P G V G
 5049/321
 GTT CCA GGT GCG GGC ATC CCG GTT GTA CCG GGT GCA GGT ATC CCG GGC GCT GCG GTT CCA
 V P G A G I P V V P G A G I P G A A V P

5109/341
GGT GTT GTA TCC CCG GAA GCG GCA GCT AAG GCT GCT GCG AAA GCT GCG AAA TAC GGA GCT
G V V S P E A A A K A A A K A A K Y G A

5169/361
CGT CCG GGC GTT GGT GTT GGT GGC ATC CCG ACC TAC GGT GTA GGT GCA GGC GGT TTC CCA
R P G V G V G G I P T Y G V G A G G F P

5229/381
GGT TTC GGC GTT GGT GTT GGT GGC ATC CCG GGT GTA GCT GGT GTT CCG TCT GTT GGT GGC
G F G V G V G G I P G V A G V P S V G G

5289/401
GTA CCG GGT GTT GGT GGC GTT CCA GGT GTA GGT ATC TCC CCG GAA GCG CAG GCA GCT GCG
V P G V G G V P G V G I S P E A Q A A A

5349/421
GCA GCT AAA GCA GCG AAG TAC GGC GTT GGT ACT CCG GCG GCA GCA GCT GCT AAA GCA GCG
A A K A A K Y G V G T P A A A A A K A A

5409/441
GCT AAA GCA GCG CAG TTC GGA CTA GTT CCG GGC GTA GGT GTT GCG CCA GGT GTT GGC GTA
A K A A Q F G L V P G V G V A P G V G V

5469/461
GCA CCG GGT GTT GGT GTT GCT CCG GGC GTA GGT CTG GCA CCG GGT GTT GGC GTT GCA CCA
A P G V G V A P G V G L A P G V G V A P

5529/481
GGT GTA GGT GTT GCG CCG GGC GTT GGT GTA GCA CCG GGT ATC GGT CCG GGT GGC GTT GCG
G V G V A P G V G V A P G I G P G G V A

5589/501
GCT GCT GCG AAA TCT GCT GCG AAG GTT GCT GCG AAA GCG CAG CTG CGT GCA GCA GCT GGT
A A A K S A A K V A A K A Q L R A A A G

5649/521
CTG GGT GCG GGC ATC CCA GGT CTG GGT GTA GGT GTT GGT GTT CCG GGC CTG GGT GTA GGT
L G A G I P G L G V G V G V P G L G V G

5709/541
GCA GGG GTA CCG GGC CTG GGT GTT GGT GCA GGC GTT CCG GGT TTC GGT GCT GTT CCG GGC
A G V P G L G V G A G V P G F G A V P G

5769/561
GCG CTG GCT GCT GCG AAA GCG GCG AAA TAC GGT GCA GCG GTT CCG GGT GTA CTG GGC GGT
A L A A A K A A K Y G A A V P G V L G G

5829/581
CTG GGT GCT CTG GGC GGT GTT GGT ATC CCG GGC GGT GTT GTA GGT GCA GGC CCA GCT GCA
L G A L G G V G I P G G V V G A G P A A

5889/601
GCT GCT GCT GCG GCA AAG GCA GCG GCG AAA GCA GCT CAG TTC GGT CTG GTT GGT GCA GCA
A A A A A K A A A K A A Q F G L V G A A

5949/621
GGT CTG GGC GGT CTG GGT GTT GGC GGT CTG GGT GTA CCG GGC GTT GGT GGT CTG GGT GGC
G L G G L G V G G L G V P G V G G L G G

6009/641
ATC CCG CCG GCG GCG GCA GCT AAA GCG GCT AAA TAC GGT GCA GCA GGT CTG GGT GGC GTT
I P P A A A A K A A K Y G A A G L G G V

6069/661
CTG GGT GGT GCT GGT CAG TTC CCA CTG GGC GGT GTA GCG GCA CGT CCG GGT TTC GGT CTG
L G G A G Q F P L G G V A A R P G F G L

6129/681
TCC CCG ATC TTC CCA GGC GGT GCA TGC CTG GGT AAA GCT TGC GGC CGT AAA CGT AAA TAA
S P I F P G G A C L G K A C G R K R K *

6189/701
TGA TAG

* *